DISSERTATION

POSTNATAL EPIGENETIC ALTERATIONS OF CATTLE FOLLOWING FETAL INFECTION WITH BOVINE VIRAL DIARRHEA VIRUS

Submitted by

Jessica Nicole Kincade

Department of Biomedical Sciences

In partial fulfillment of the requirements

For the Degree of Doctor of Philosophy

Colorado State University

Fort Collins, Colorado

Summer 2025

Doctoral Committee:

Advisor: Thomas R. Hansen
Co-advisor: Angela Bosco-Lauth

Hana Van Campen
Marcela Henao-Tamayo

ABSTRACT

POSTNATAL EPIGENETIC ALTERATIONS OF CATTLE FOLLOWING FETAL INFECTION WITH BOVINE VIRAL DIARRHEA VIRUS

Bovine viral diarrhea virus (BVDV) remains a costly disease despite extensive research, vaccine usage, and the implementation of control strategies. While it is difficult to approximate the overall profit loss due to BVDV infections, the global estimation is in the billions annually. As the main reservoir of the virus, persistently infected (PI) cattle that are infected early in gestation are the main targets for management of the disease and cost analysis. In contrast, infections that occur late in gestation and generate a transiently infected (TI) calf have generally been regarded as inconsequential even though research suggests an increased susceptibility to disease and decreased weight gain. Per the developmental origins of health and disease theory (DOHaD), environmental cues such as nutrition, stress, or pathogen exposure have the potential to alter epigenetic regulation of gene expression and lead to postnatal disease. In fact, alterations of the methylome have been demonstrated in fetal spleen of PIs at gestational day 245. It was hypothesized that these epigenetic changes in PI fetuses persist into the postnatal period and continue to correspond to observed pathologies. To this end, whole blood was collected from 4-month-old PI heifers at a local, cooperating ranch and age-matched control heifers housed at Colorado State University (CSU). Zoetis Inc. utilized whole blood to determine complete blood counts (CBCs). Peripheral WBCs were isolated from whole blood and subjected to spectral cytometry analysis in

collaboration with Zoetis Inc. The DNA was extracted from peripheral WBCs for reduced representation bisulfite sequencing (RRBS) to assess alterations of the methylome. The CBC analysis identified elevated monocytes, microcytic anemia, and elevated platelets with decreased mean platelet volume in PI heifers. Spectral cytometry revealed increased intermediate monocytes, B cells, $CD4^{+}/CD8b^{+}$ T cells, and $CD25^{+}/CD127^{-}$ T cells; the analysis also identified decreased $\gamma\delta^{+}$, $CD4^{+}$, and $CD4^{-}/CD8b^{-}$ T cells in PI heifers. Comparison of the methylome in PI heifers to that of control heifers revealed 8,367 differentially methylated CpG sites (DMSs) contained within genes associated with postnatal pathologies of the immune system, cardiac system, and skeletal system, similar to the methylome of PI fetal spleen. The identified list of genes containing differential methylation in PI fetal spleen was compared to those containing differential methylation in 4-month-old PI peripheral white blood cells. A total of 797 genes contained differential methylation in both the PI fetal spleen and 4-month-old peripheral WBCs. It was concluded that epigenetic alterations in PI fetuses persist into the postnatal period and continue to correspond to observed pathologies.

It was subsequently hypothesized that epigenetic alterations occur in calves due to transient infection with BVDV in late gestation. It was further postulated that these alterations would be present in the postnatal period and correspond to altered expression of transcripts within peripheral WBCs. To study this effect, 12 control and 11 TI calves were generated through maternal inoculation with non-cytopathic BVDV2 type 96B2222 on gestational day 175. Whole blood was collected from generated calves at 4 months of age and 17 months of age; these samples were used to isolate peripheral WBCs, extract DNA, and perform RRBS to quantify and compare the methylation of

CpG sites throughout the genome. Concurrently, peripheral WBCs were isolated for CBC and flow cytometry analysis in collaboration with Zoetis Inc. Peripheral WBCs from whole blood were also collected for single cell RNA sequencing at 17 months of age in collaboration with Zoetis Inc. The CBCs at 4 months of age demonstrated elevated lymphocyte percentage in TI heifers. Spectral cytometry analysis at 4 months of age revealed increased intermediate monocytes, B cells, and $CD25^{+}/CD127^{-}$ T cells; TI heifers also had decreased $CD4^{+}/CD8b^{+}$ T cells. Comparison of 4-month-old TI methylomes to that of age-matched controls identified a total of 3,047 DMSs contained in genes related to inflammation, metabolism, and growth. Identified DMSs were compared to those identified in TI heifers at birth. A total of 205 genes, 5 promoters, and 10 CpG islands were found to contain differential methylation at birth and 4 months of age. Moreover, genes containing differential methylation in TI heifers at 4 months of age were compared to those containing differential methylation in PI heifers at 4 months of age and revealed 1,098 genes, 34 CpG islands, and 18 promoters in common.

At 17 months of age, no differences were identified in CBCs. Flow cytometry once again demonstrated a decrease in $CD4^{+}/CD8b^{+}$ T cells in addition to a decrease in natural killer T cells in TI heifers. A total of 5,508 DMSs were identified when comparing the epigenome of TIs to that of controls and Ingenuity Pathway Analysis (IPA) predicted inhibition of pathways related to the immune system. Single cell RNA sequencing identified 25 unique cell clusters; TIs had greater proportions of B cell population 5 and smaller proportions of myeloid population 5. Four genes were identified as differentially expressed. The TI heifers demonstrated increased expression of *PDE4D* in a B cell population, increased expression of *SFMBT2* in a second B cell population, increased

expression of *ARHGEF18* in a myeloid cell population, and decreased expression of *HNRNPLL* in a population of natural killer T cells. While *SFMBT2* was found to contain hypomethylation at 17 months and corresponds to the observed increase in expression, neither *ARHGEF18* nor *HNRNPLL* contained differential methylation. Interestingly, *PDE4D,* as well as other phosphodiesterase genes, contained hypermethylation at 17 months. Comparison of differential methylation at birth, 4 months of age, and 17 months of age in TI heifers revealed that 347 genes that contained differential methylation compared to controls at all 3 timepoints. One gene contained differential methylation within a promoter region and 6 contained differential methylation within a CpG island. Of those 347 genes, only 64 maintained the same differential methylation status at all three timepoints; for example, leukemia inhibitory factor (*LIF*) contained at least one hypermethylated CpG site in TI heifers at birth, 4 months, and 17 months of age. Together, this data demonstrates that epigenetic alterations due to fetal infection with BVDV persist in the postnatal period and at least partially correspond to differences in gene expression.

ACKNOWLEDGEMENTS

I would not be here if not for the incredible amount of support I have found in every direction. First, to my mother, this would not be a true academic achievement without mentioning the person who fed my craving for knowledge after her three-year-old cried due to her inability to read her own bedtime stories. I also see this craving, and love it very dearly, in the daughter my sister is raising. To my sister, who has taken up her position as a second mother to me in times of need. To my grandmothers, Lillian, who cherished the achievements of her doppelgänger, Linda, who continues to celebrate the fighting spirit of the West that she gifted to me.

To Dr. Hansen, who was not taking students when I interviewed, you have a kind heart and *always* mean well. I am *so* glad to have met the 'academic grandfather' of Dr. Amanda Patterson, a student of Dr. Jim Pru. To Dr. Hana Van Campen, a truly unique individual with the most intriguing stories and an absolute wealth of knowledge. To Dr. Aydin Guzeloglu, who has been a fantastic sounding board for all my questions and concerns, especially as of recent. To Jeanette Bishop, who I adore for her special brand of honesty and genuine care, the lab would not function without you. To Dr. Marcela Henao-Tamayo, you are an incredible role model; you are proof that women in research can have it all. To Dr. Angela Bosco-Lauth, you are ultimately what brought me to Colorado State University. You have a fire in your heart that I hope never dims. Thank you all for changing my life.

To those who have helped make this project possible, at Zoetis: Jordan Eder, Erin McDonald, Darcy Deines, Brie Wright, Lex Bally, Reyes Murietta, and Jamie Pack;

at Colorado State: Terry Engle and all of the ARDEC crew; for bioinformatic support: Dilyara Murtazina, Stu Field, Andrew Kuppinger, Richie Castillo, and Erin Nishimura. Thank you for all the time you've dedicated to teaching me and helping me grow.

To my support system of incredibly talented individuals: Rachel Maison, Audrey Walker, Marissa Quilici, Jeffrey Marano, Airn Hartwig-Tolnay, Jenny Buczek, Dallas Lokey, Jen Appelman, Steph Porter, Hannah Braun, Jess Wittenstein, Sarah Singleton, Brandi Dunn, Tori Kennedy, Liv Carroll, Jasmin Twiggs, and so many more. To my soul-dog, Darlin, the most persistent and perhaps most distracting study buddy. And last, but never ever least, thank you to my partner, Alex Arellano, who has cooked, cleaned, and wholeheartedly supported me through nearly the entirety of this degree, but especially in the last few months. You are the best and I am lucky to have you.

My heart is full of wonderful people.

DEDICATION

To the ‘rough stock’ women before me:

i stand

on the sacrifices

of a million women before me

thinking

what can i do

to make this mountain taller

so the women after me

can see farther

- legacy

Rupi Kaur

TABLE OF CONTENTS

CHAPTER 1: LITERATURE REVIEW

Economic Impact

Bovine viral diarrhea virus (BVDV) remains one of the costliest diseases in the cattle industry. It is currently estimated that a producer loses anywhere from $20 to $103 per head during an outbreak, which culminates to an estimated global profit loss of $1.5 to $2.5 billion each year [1-3]. Acute infections with BVDV induce decreases in average daily weight gain and milk production [3-5]. Approximately 70-100% of non-vaccinated cattle become infected following exposure to a persistently infected (PI) animal [6, 7]. Immunosuppression due to BVDV infection contributes to the development of bovine respiratory disease (BRD), especially in calves. One study indicated a 43% increase in the risk of morbidity due to BRD in cattle that had direct contact with a PI [3]. This study also goes as far as to say that 16% of the observed BRD cases were directly attributable to exposure to a PI animal [3]. A single PI in an adjacent pen can directly expose 60% of a herd in less than 2 months [3]. In 2001, it was estimated that BRD in the US leads to economic losses of $800 to $900 million [8]. Accounting for a 2.51% inflation rate, those estimates are equivalent to losses of $1.5 to $1.6 billion today.

A large proportion of monetary loss due to BVDV manifests in the form of reproductive losses including decreased conception rates, abortions, stillbirths, and the production of weak, non-viable calves that have been infected *in utero* [9-11]. Dams that were infected with BVDV around the time of artificial insemination demonstrated a 44% decrease in conception rate, while dams infected during mid-gestation with non-

cytopathic (ncp) BVDV experienced a 10% increase in abortion rate [12]. Broadly, cattle producers in the U.S. lose approximately $1 billion due to reproductive diseases [13]. Infertility is reported to lead to the loss of $137 million in dairy herds and $249 million in beef herds [13]. Infertility due to BVDV likely contributes to these numbers, although the impact is difficult to quantify.

Calves that survive BVDV infection early in gestation develop immunotolerance to the infection and shed viral particles the entirety of their life. The global prevalence of PIs by animal was found to be approximately 1.85% from 1980 to 1991, 0.9% from 1992-2001, and 0.36% from 2002-2016 [14]. An estimated 42.36% of all cattle herds globally had at least one PI animal from 1980-2001 while 18.88% of herds contained a PI from 2002-2016 [14]. A 2023 information brief from the United States Department of Agriculture (USDA) lists that the prevalence of PIs in US beef herds is estimated to 0.13% per animal and approximately 1 in 15 feedlots (6.7%) have at least one PI animal [15].

A meta-analysis of published studies concerning BVDV determined that approximately 2.82% of cattle were viremic at any given time [14]. From 1992-2001, that number rose to 7.78% and from 2002-2017, it was approximated that 3.04% of cattle across the globe were shedding viral particles at any given time [14]. However, viremia rates only measure the number of *current* infections. Global antibody prevalence was 48.73% from 1980-1991, 46.83% from 1992-2001, and 46.23% from 2002-2016 [14]. The caveat with *these* measurements is found in the fact that antibodies are produced in response to natural infection as well as vaccination.

Interestingly, it was estimated in 2018 that nearly 80% of all cattle in the US were vaccinated against some form of BVDV [14]. However, the most recent information brief from the USDA found that only 57.4% of beef operations vaccinate for BVDV [15]. By region, data indicated a vaccination rate of 54.1% for the western states, 66.8 for the central states, and 54.1 for eastern states [15]. Additionally, 15.3% of beef operations had never heard of BVDV, 26.9% of operations recognized the name but not much else, 33.3% knew some basics of BVDV, and only 24.4% were considered ‘fairly knowledgeable’ when it came to BVDV [15].

History of BVDV

In March of 1946, an outbreak of a previously undocumented cattle disease surfaced in New York dairy farms [16]. Upon inspection, afflicted cattle presented with gastro-enteritis and severe diarrhea. When the autopsy of a diseased cow failed to reveal a conclusive diagnosis, researchers turned to feed analysis for answers. The feed was discovered to contain one percent of ammonium nitrate and was initially blamed for the outbreak. However, the outbreak continued. Large scale feed analyses failed to produce further ammonium nitrate contamination, clinical presentation of this new disease was inconsistent with ammonium nitrate poisoning, and laboratory trials of ammonium nitrate supplementation failed to produce the disease. Researchers also failed to isolate infectious bacteria from infected cattle, suggesting that the responsible pathogen was of viral origin. As such, the agent responsible for this outbreak was termed viral diarrhea (VD). Field reports noted that some infected cattle displayed no clinical symptoms, while other cattle were off feed, depressed, scouring, and febrile.

Severe cases displayed ulceration of the mucosal membranes, complete cessation of milk production and rumination, leukopenia, and hemorrhage in various tissues. Mortality rates were estimated at 4 to 8%. Interestingly, this outbreak also appeared to cause abortions in bred cattle. By July of 1946, the disease had spread to 6 herds in the US and by August it had disseminated to Canadian herds [16].

A Canadian researcher immediately began following the outbreaks. ‘X Disease’ was observed in July and August of 1946, although it was estimated that the disease had been present for 1-2 years prior. This disease was reported to occur in acute and sub-acute forms. Interestingly, young cattle with the acute form of the disease experienced symptoms for 7 to 10 days before fatality, while adult cattle often succumbed to the disease after 3 to 4 days of severe symptoms. Recorded symptoms were similar to those noted previously: sudden onset of fever, depression, recumbency, anorexia, inflammation and granular lesions of the mucosal membrane, and diarrhea. Postmortem findings reported extreme abdominal distension, erosive lesions of the mucosal membrane, and most interestingly, these cattle were found to have low blood volume and thrombosis of the spleen. Sub-acute cases of the disease were milder in presentation of symptoms that include skin lesions, recumbency, anorexia, and loss of body condition [17].

In 1953, during an outbreak of disease in Iowa that presented with mucopurulent nasal discharge, mild fever, as well as severe ulceration and hemorrhage of the oral and intestinal mucosa. However, presentation of clinical disease remained distinct between VD and the new outbreak. VD was associated with high morbidity and low mortality, while this new outbreak was associated with low morbidity but extremely high mortality,

especially in young cattle. This condition was reported as a separate entity from VD and termed fatal mucosal disease (MD) [18].

In 1957, virus was isolated from a cytopathic (cp) strain of MD and a non-cytopathic strain (ncp) of VD [19, 20]. Ncp viruses can be cultured *in vitro* without cellular destruction, while cp viruses cause cell death in culture. In 1960, a cp virus isolated from a case of VD in Oregon, named Oregon C24V, was used to generate experimental cases of VD. The antibodies produced by these experimentally infected cattle neutralized cp and ncp strains of VD [21]. This discovery led to the generation of the very first vaccine against VD [22]. However, this vaccine came with various problems: vaccine induced mucosal disease, reproductive failures, the induction of congenital abnormalities [23].

By the 1960's, researchers were working towards characterizing the pathogenic agents of both VD and MD. As these studies progressed, similarities began to emerge between VD and MD as well as classical swine fever virus [24, 25]. Moreover, experimental infection with MD yielded cases with symptoms consistent with VD. These discoveries led to the idea that VD and MD were, in fact, variations of the same viral infection. This virus was classified as a bovine enterovirus [26] and became known as bovine viral diarrhea-mucosal disease complex (BVD-MD) [27].

In 1984, the first experimental case of MD was produced by inoculating an animal that had been fetally infected with a ncp strain of BVDV, known as a persistently infected (PI), with a similar, cp strain of BVDV [28]. It was understood at this time that MD was generated through co-infection with both a ncp and cp strain of BVDV, which can also arise in PI cattle through mutation of the endogenous ncp strain [29]. The

pathogen known presently as BVDV was originally classified as a pestivirus, within the family of *Togaviridae,* along with hog cholera virus and border disease virus [30]. However, by the late 1980's differences between alphaviruses and flaviviruses were becoming evident and the pathogens were reclassified within the *Flaviviridae* family [31].

The clinical presentation of BVDV has continued to evolve with the occurrence of outbreaks. The observation or more severe disease in outbreaks of ncp BVDV subsequently altered the assumption that only MD caused severe clinical signs. For example, an outbreak in the 1980's of ncp BVDV was largely associated with hemorrhagic syndrome, fever, thrombocytopenia, bloody diarrhea, and inability to clot [32]. Another outbreak affecting North America and Europe in the 1990's demonstrated the wide variance in ncp BVDV clinical signs; hemorrhagic syndrome, respiratory disease, diarrhea, oral lesions, and abortions were reported with an average herd mortality rate of 25% [33]. It has since become evident that the clinical signs of BVDV infections vary with the genotype and subtype [34].

Control Programs

Due to significant antigenic diversity between genotypes and subtypes of BVDV, most BVDV control strategies depend on the implementation of a vaccine program in combination with identification and elimination of PIs. The first voluntary control program was introduced in Germany in the 1980's [35]. This program provided monetary support for producers who were encouraged to identify and remove PIs followed by vaccination of their herd [36]. Newborn calves are tested for BVDV, and positives are retested after

approximately 40 days to distinguish between PI and TI. The identified PI calves are culled to prevent further exposure to the herd, but participation in vaccination programs remained voluntary. Prevalence of PIs in Germany has been on the decline in recent years, demonstrating success of the control program [37]. Similarly, England, Wales, and Switzerland have more recently implemented structured but voluntary BVDV elimination strategies utilizing elimination of PIs in combination with vaccination [38]. However, other countries have eventually moved towards compulsory programs for BVDV control; these countries include Germany, Switzerland, Ireland, and Scotland [38]. Some countries have implemented control strategies without the aid of vaccination; Norway, Austria, and Switzerland utilize strategies entirely dependent on the identification and elimination of PI cattle followed by severe biosecurity measures [38-40]. Currently there is no structured BVDV control program in the United States. Control programs in the US are voluntary and often in collaboration with quality assurance programs that offer product certifications with the potential for increased profit [41]. Disappointingly, only 57.4% of beef operations in the U.S. in 2017 were found to vaccinate routinely for BVDV; only 3.7% of all beef operations had tested for PIs in the last 3 years [15].

Methods of Detection

To effectively control an infectious disease, it must be possible to identify and detect infections as they occur. Currently, there are a variety of tests that can be performed to identify current cases of BVDV including viral isolation, immunofluorescence, immunohistochemistry (IHC), antigen-capture ELISA, and reverse

transcriptase (RT) polymerase chain reaction (PCR). Serum neutralization can also detect past infections or vaccination by the quantification of antibodies.

Historically, the ‘gold standard’ for BVDV identification has been viral isolation. Viral isolation often begins with culture of cells, bovine turbinate (BT) or Madin-Darby Bovine Kidney (MDBK) are commonly used, which are then inoculated with serum samples in triplicate. These cellular cultures are incubated and monitored for cytopathogenicity, meaning it could not detect ncp BVDV. If viral isolation is being utilized for comparable quantification, the same cell culture system must be utilized each time; the cell type that the culture is grown in can influence the resulting titer [42]. Moreover, it was later determined that fetal bovine serum (FBS), which is used as a growth supplement for cell culture, is frequently contaminated with BVDV, producing false positives [43]. Likewise, the presence of BVDV antibodies in serum could also produce a false negative. This test can be paired with fluorescent staining using a monoclonal or polyclonal antibody specific for BVDV to identify ncp viruses.

Direct use of fluorescently labeled monoclonal antibodies is also a common detection method for BVDV. In this case, tissues from suspected cattle can be fixed in formalin and embedded in paraffin to perform IHC. Testing for BVDV this way allows for storage of samples for a brief period, but extended storage can result in failure of the monoclonal antibody to bind to antigen upon staining [44]. Due to its wide cellular tropism, many tissues from infected cattle can be isolated and tested using IHC including the liver, gastrointestinal tract, uterus, ovary, and mammary gland [45, 46]. It has become common to utilize an ‘ear notch’ for IHC testing, particularly due to high

expression of BVDV in epithelium but lower expression in the epithelium of acutely infected cattle [47, 48].

Panels of monoclonal antibodies are also used for antigen-capture ELISA testing. This test depends on the binding of monoclonal antibodies to antigen present in tissue or serum. The NS3 and E^{rns} viral antigens are highly conserved among BVDV strains and thus antigens against the two are frequently used to identify BVDV infected cattle [49, 50]. These tests have been modified for producer use, as per the IDEXX SNAP® BVDV antigen test (IDEXX, Westbrook, ME, USA) and provide the producer with all components necessary to test large numbers of easily obtainable samples (such as ear notches or serum). A single SNAP test can also be performed quickly, with readable results ready in as little as 20 minutes. While these tests are user friendly, fast, and cost-effective, the sensitivity is comparatively low; SNAP tests depend on high levels of antigen and are most appropriate for the identification of PIs, not acute infections [50].

Extraction of nucleic acids from any cell containing solution can also be used to identify BVDV infections. Because BVDV is a positive single stranded RNA virus, it must be treated with RT prior to detection. Treatment with RT produces double stranded DNA that can then be paired with a BVDV engineered primer to amplify only viral DNA. Varying sets of primers have even been designed to isolate specific genotypes of BVDV [51]. Due to high antigenic diversity, most BVDV engineered primers target the 5’ untranslated region of the virus. More recently, a pan-pestivirus primer has been more recently developed for use to detect strains of pestivirus in cattle as they continue to change genetically [52]. While this method of detection provides high sensitivity and

more descriptive results, it also requires time, expertise, and expensive laboratory equipment [50].

Serum neutralization tests do not specifically identify current, acute infections, but they can determine whether an animal is producing antibodies against BVDV. This might occur by maternal passive transfer of antibodies, natural exposure and infection, or intentional vaccination against BVDV. This method again requires the culture of cells prior to collection of serum from cattle suspected of infection. The serum potentially containing antibodies is then added to several wells containing cultured cells at several serial dilutions. A standardized concentration of cytopathic virus is then added to each well and allowed to incubate. If the sample contains antibodies, the virus will be neutralized, and no cytopathic effect will be seen [53]. The serial dilutions allow for quantification of antibody titer according to cytopathic effect.

Each method depicted has positive and negative aspects to its use, but each serves a specific purpose or services a need. Producers require a fast, easy, and reliable test for field use, which they find in commercially available SNAP tests. Identification of the specific genotype and subtype may be a necessity during outbreaks, monitoring, or consideration of vaccine formulations; this is made possible by RT-PCR. Quantification of antibody response is also vital for the development of vaccines against BVDV, which is possible through serum neutralization testing. However, all BVDV testing currently requires dual testing with approximately 3 weeks or more between testing times, to confirm the identification of a PI versus acute infection.

Vaccines

Recent outbreaks have been at least partially mitigated by the use of preventative vaccination. The first BVDV vaccine utilized a modified live virus developed using the Oregon C24V strain [22]. Modified live vaccines (MLVs) are often most effective in disease prevention and offer fast protection. However, early BVDV vaccines were occasionally associated with negative outcomes such as immunosuppression or the inadvertent induction of vertical infection by vaccination. In fact, fetal calf serum used to grow cells for viral vaccine culture is often contaminated with BVDV and can lead to unintended infections [54, 55]. Due to its inability to induce a persistent infection, most MLVs presently use cp strains of BVDV. Another strategy to MLVs is to alter the N^{pro} gene of an ncp strain of BVDV and eliminate the endoribonuclease activity of the E^{rns} protein, rendering the virus unable to cross the placenta and induce fetal infection [56]. As of 2017, MLV vaccines were the sole protection against BVDV for 38.1% of U.S. beef operations [15].

Killed vaccines (KVs) offer a vaccination option with application dates independent of pregnancy. While KVs are unable to induce accidental vertical infection, the level of protection is significantly lower than that generated by MLV vaccines and often requires additional vaccinations to achieve protection [57-59]. In recent years, adjuvants added to the vaccine formulation have boosted the efficacy and protection provided by KVs [60, 61]. However, at least one KV containing powerful adjuvants meant to sensitize and stimulate the immune system has led to fetal production of alloantibodies when used during gestation [62, 63]. In other words, overstimulation of the immune response caused the generation of antibodies against innate bovine cellular

components implicit in viral replication. Presently, it is estimated that 51.3% of beef operations in the U.S. utilized killed vaccinations for BVDV protection [15].

Antigenic diversity introduces additional obstacles in the development of BVDV vaccines. There is considerable antigenic diversity between the two BVDV genotypes and subtypes within each genotype; antigenic differences even exist between BVDV type 1a and type 1b [64]. These antigenic differences translate to differences in virus neutralizing antibody titers following vaccination [34] and can indicate varying levels of cross protection [65, 66]. For this reason, BVDV type 1a and 2a are added to US based vaccine formulations even though the most common strain of BVDV in the US continues to be type 1b [67-69]. However, the debate continues as to whether the strains included in US based vaccines offer an appropriate amount of protection against circulating strains [70, 71].

Virology

Pestiviruses such as BVDV, border disease, and classical swine fever were originally classified into the *Togaviridae* family [30]. However, further advancements in technology have led to its re-classification and current identification within the *Flaviviridae* family [31]. The *Flaviviridae* family consists of 3 genera: *Flavivirus*, *Hepacivirus*, and *Pestivirus*. All viruses within the *Flavivirus* family have a positive sense, single-stranded, non-polyadenylated, RNA genome with one open reading frame (ORF) and a viral envelope. BVDV was further categorized into BVDV1 and BVDV2, currently known as Pestivirus A and Pestivirus B, respectively. Through the use of genomic sequencing of the 5’ untranslated region, N^{pro}, and E2, several sub-genotypes

of BVDV have been identified. BVDV1 contains at least 23 sub-genotypes (BVDV1a – BVDV1w) and BVDV2 contains 4 sub-genotypes (BVDV2a-BVDV2c, BVDV2d, BVDV2e) [72, 73].

Although the actual length of the genome can vary with BVDV genotype and subtype, ncp BVDV is approximately 12.3 kilobases in size and codes for 4 structural proteins (E1, E2, C, E^{rns}) and 8 non-structural proteins (N^{pro}, p7, NS2, NS3, NS4a, NS4b, NS5a, NS5b) [74-76]. Due to the single ORF, these proteins are transcribed as a long polypeptide and then cleaved into individual proteins by cellular and viral proteases [76]. Because BVDV proteins are encoded in the order N^{pro}-C-E^{rns}-E1-E2-p7-NS2-NS3-NS4a-NS4b-NS5a-NS5b, N^{pro} is transcribed first and, as a viral auto-protease, cleaves itself from the polypeptide following translation. Structural capsid (C) and envelope (E1, E2, E^{rns}) proteins are transcribed and translated next, followed by the non-structural proteins. *In vitro*, N^{pro} has been shown to block interferon production through proteasomal degradation of IRF-3 [77, 78]. E1 and E2 are necessary for viral entry into host cells and subsequent membrane fusion [79].

The E2 specifically binds to the host cell receptor, thus influencing cellular tropism, and is often the target for neutralizing antibodies [80], but it is the E1-E2 heterodimer that is necessary for viral entry into host cells [79]. The E^{rns} homodimerizes and utilizes its RNase activity to degrade single stranded and double stranded RNA, thereby preventing activation of the cellular immune response [81]. While E^{rns} is considered a structural protein, it can be found both on the viral particle and in a disassociated, soluble form [82-84]. The p7 protein, cleaved by a cellular peptidase, is necessary for the production of infectious virus but not for RNA replication [85-87]. It has

been speculated that the p7 protein in BVDV acts in a similar fashion as the hepatitis C p7 protein which is known to create ion channels between infected cells [88]. NS2 is an auto-protease capable of cleaving NS2-3 into NS2 and NS3; this is particularly interesting as NS2 auto-cleavage activity is present very early in both ncp and cp infections, but drops beyond detection hours after ncp infection while remaining comparatively high in cp infections [89, 90]. While the NS2 protein contains signals required for movement to the endoplasmic reticulum, the NS3 protein participates directly in RNA replication [91]. The NS3 protein contains a serine protease at its N-terminus for cleavage of viral products from the translated polyprotein as well as a C-terminus RNA helicase [92, 93]. NS4a is required by NS3 to initiate proteolytic activity and NS4b participates in RNA replication and manipulation of the infected cell membrane [94, 95]. Little is known about the function of NS5a, but NS5b serves as the necessary viral RNA-dependent RNA polymerase [96].

BVDV infection begins at a molecular level by initiation of clathrin-mediated endocytosis of the viral particle into a host cell (Figure 1.1) [97, 98]. The E2 protein on the viral membrane is known to interact with host membrane bound receptors while E^{rns} interacts with host cell glycosaminoglycans and heparan sulfate [99-101]. Currently, there are two known BVDV receptors, complement regulatory protein 46 (CD46) and low density lipoprotein receptor [102, 103]; CD46 is considered the main receptor for BVDV [103]. Because CD46 is expressed on nearly all cell types [104], BVDV has been identified in a wide variety of tissues. Cell lines in which CD46 has been knocked out using CRISPR/Cas9 demonstrate a significant reduction in BVDV susceptibility [105, 106]. However, in the absence of CD46, the BVDV is known to enter host cells through

heparan sulfate binding [105]. These *in vitro* results do not always translate well to *in vivo* demonstration, but in 2023, a calf was born bearing genetic alterations within the BVDV binding site encoded in CD46 [107]. This animal and cell lines derived from this animal do indeed demonstrate reduced, but not a lack of, susceptibility to BVDV infection [107]. More recently, the loss of disintegrin and metalloprotease 17 (ADAM17) was found to associate with pestivirus resistance, including resistance to BVDV [108].

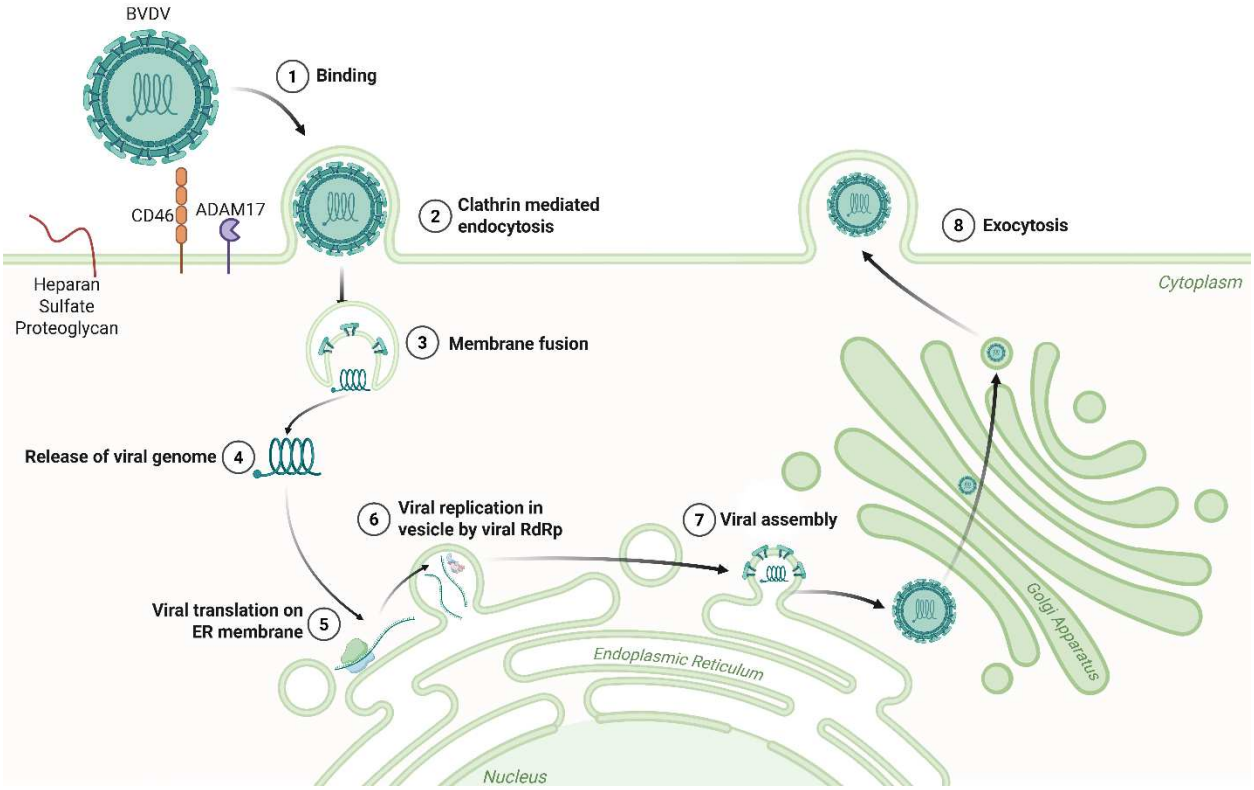

Figure 1.1 – Viral replication of bovine viral diarrhea virus. This schematic was created using BioRender.

After binding, the viral particle is slowly endocytosed into a vesicle coated in clathrin and delivered to an early endosome [109]. Within the endosome, a drop in pH triggers the fusion of the viral and endosome membrane, eventually uncoating and releasing the viral capsid into the host cytosol [109]. After disassembly of the viral capsid in the endoplasmic reticulum, the positive sense strand of viral RNA will be

immediately translated into a polyprotein and cleaved into individual proteins. From here, replication occurs in viral factories that are surrounded by vesicles. The virally encoded RNA dependent RNA polymerase (RdRp), NS5b, synthesizes the complementary negative sense RNA strand and subsequently provides the necessary template to create additional positive sense viral RNA. As viral products accumulate, new viral particles assemble and bud from the endoplasmic reticulum. The viral particle will move through the Golgi apparatus and leave the cell through exocytosis (in the case of ncp BVDV) [110].

If the BVDV is recognized by the host immune system, the antibodies produced by B cells mainly target the E2 and NS2-3 virally encoded proteins [111]. Antibodies are also produced against E^{rns} and E1, but in much lower quantity [111]. More specifically, the neutralizing epitopes for the E2 viral protein are dependent on cytosines at positions 4, 48, 104, 130, 140, and 168 which are conserved between BVDV1, BVDV2, and classical swine fever virus (CSFV) [112]. An immunodominant neutralizing epitope is also found in the E2 viral protein at amino acid positions 71-74 [113, 114]. While it is apparent that T cell epitopes are present within the viral proteins E2 and NS2-3 [115, 116], these epitopes remain unmapped.

Immune Evasion and Immunotolerance

The immune system is a complex system containing multiple branches of varying types of responses. The innate branch of immunity is initiated quickly in response to the detection of foreign antigens but employs broader tactics including the generation of inflammation. Briefly, pathogen-associated molecular patterns (PAMPs) within viral

transcripts or proteins can be recognized by pattern recognition receptors (PRRs) expressed on host cells. These PRRs include RIG-I-like receptors (RLRs), NOD-like receptors (NLRs), and toll-like receptors (TLRs) [117]. Once foreign antigen has been detected in host cells, molecular signals are released that promote inflammation and activation of innate immune cells such as macrophages, neutrophils, monocytes, natural killer cells, etc. [117]. Dendritic cells (DCs) then carry antigen to nearby lymph nodes and begin to initiate the adaptive immune response [117]. The adaptive immune response takes more time to initiate but utilizes more targeted methods of pathogen elimination such as antibody production [117]. Cells with epitopes specific to the foreign antigen presented on antigen presenting cells (APCs) such as DCs are then indicated to proliferate and reproduce [117]. Helper T cells aid B cells producing antibody specific to the presented epitope and cytotoxic T cells migrate to the site of infection to target and neutralize infected cells [117].

Two proteins encoded by the BVDV genome aid in the virus' evasion of the innate immune response. The E^{rns} protein degrades viral RNA amid replication of the viral genome, thereby preventing the detection of viral replication intermediates by the host [81, 118]. The N^{pro} protein targets interferon regulatory factor 3 (IRF3) for proteasomal degradation and effectively suppresses induction of interferon (IFN) β [78]. The N^{pro} protein also interacts with host S100A9 to prevent its homodimerization which is known to promote production of type I IFN [119]. It has also been recorded that *in vitro* infection of cells with ncp BVDV leads to decreased expression of antiviral IFN stimulated genes including ISG15, Mx1, and OSA1Y [120]. This likely dampens the

immune response but fails to inhibit it entirely, as *in vivo* infections demonstrate production of IFN stimulated genes in all types of ncp infection [121, 122].

Proteins specific to cytopathic (cp) strains of BVDV also manipulate the innate immune response. The NS4b protein prevents detection of viral double stranded DNA by inhibiting RIG-I-like receptors (RLRs) and reducing MDA5 mRNA levels which would normally initiate the production of interferons [123]. More recently, a cp strain of BVDV was found to induce production of the DNA damage-inducible transcript 3 (DDIT3) protein. Increased expression of DDIT3 indirectly leads to increased degradation of mitochondrial antiviral signaling (MAVS) protein, which would otherwise initiate production of interferons [124]. Moreover, *in vitro* infection of cells with cp BVDV led to the upregulation of IER3 and TNFAIP3, which negatively regulate expression of NFκB [125].

Infection of adaptive immune cells with BVDV produces varying impacts upon their function. Alveolar macrophages, when infected with cp BVDV, demonstrate reduced expression of the Fc receptor and complement receptor [126]. This likely decreases their phagocytic ability and decreases the cellular opportunities for antigen uptake and presentation [126]. Monocytes that have been infected with ncp BVDV are unable to stimulate helper T cell responses [127]; downregulation of 9 major histocompatibility complex (MHC) class I proteins and 6 MHC class II proteins was observed in monocytes infected with cp BVDV [128]. Monocyte derived dendritic cells (DCs) also demonstrate decreased expression of MHC class I and II as well as CD86 in response to infection with ncp BVDV [129]. Without appropriate presentation of antigen by MHCs, the immune system cannot identify and remove pathogens to its full capacity.

Fetuses infected with BVDV prior to gestational day 125 demonstrate the activation of the innate immune response [122]. However, these fetuses mount only a weak adaptive immune response [122]. This is likely due to the fact that in the case of PIs, BVDV infection is introduced prior to the maturity of the adaptive immune response (Figure 1.2). The current working theory of immunotolerance establishment describes that if the antigen is present during T cell education in the thymus, the resulting T cells are inappropriately instructed that BVDV antigen is actually 'self' and should not initiate an immune response [122]. The virus can then replicate in host cells and evade detection by host cells. By the time T cells become present in the periphery, as is seen later in gestation [130], the circulating T cells have already been 'educated' by thymic selection and are able to identify BVDV antigen as 'non-self' [122].

Similarly, the epigenome is yet determined for fetuses during gestation; as such, they are susceptible to long-term dysregulation of gene expression due to inappropriate epigenetic programming.

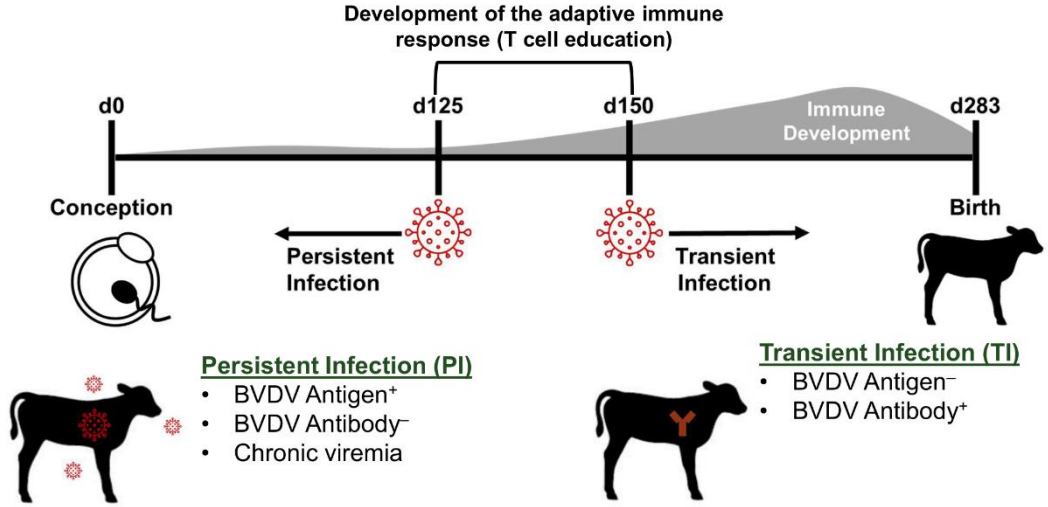

Figure 1.2 – Education of T cells: the difference between persistent and transient infection. Persistently infected (PI) calves are antigen positive, antibody negative, and experience chronic viremia. Transiently infected (TI) calves are antigen negative and antibody positive at birth.

Epigenetic Programming

Often plainly called “Barker’s Hypothesis”, the Developmental Origins of Health and Disease (DOHaD) theory was identified perhaps inadvertently. Following his research investigating the potential links between nutrition in the perinatal period and postnatal heart disease [131-133], Dr. David Barker theorized that variations in early life nutrition had a marked impact on the presence of pathology later in life [134]. The hypothesis has grown over time to indicate that variations in both the macro and micro environment during gestation can induce alterations that impact the health and presence of disease postnatally [134]. This phenomenon has since been demonstrated numerous times. Children born to obese mothers are more likely to experience metabolic dysfunction and also be obese toddlers [135, 136]. The method of delivery affects the immune system of human children, as does breast feeding status, and antibiotic use [137-139]. Gestational malnutrition can even lead to transgenerational deficits in fertility [140].

This ‘developmental programming’ occurs through epigenetic regulation of gene expression. Epigenetics is an area of study that concerns the heritable and stable changes in gene expression that do not directly alter the sequence of the genome [141]. The genome is organized around proteins called histones; how tightly or loosely the genome is packaged around these histones can influence the access of transcription binding machinery [142]. Phosphorylation, ubiquitination, methylation, and acetylation of histone tails can alter the packaging and thus alter transcriptional regulation. A methyl group (CH_3) can also be added to the DNA of the genome itself. In mammals, a vast majority (98%) of these additions occur on cytosine nucleotides which are immediately

followed by a guanine nucleotide within the genome [143]. Specific regions of the genome that are rich in cytosine-phosphate-guanine (CpG) motifs are termed ‘CpG islands.’ These regions are often found within promoter regions [144, 145]. When they lack methylation, they promote gene expression [146]; however, heavy methylation of CpG islands effectively silences gene expression [147].

Methylation is controlled by enzymes called DNA methyltransferases (DNMTs). The DNMT1 is responsible for maintenance of methylation throughout cellular division, while DNMT3a and DNMT3b establish *de novo* additions of methylation [146]. The DNMT enzymes are most active during embryonic development; expression subsequently decreases with postnatal age [148]. However, some level of DNMT must be maintained, as variations in the methylome have been documented across age; global methylation decreases with age but increases at CpG islands [148-154]. While it is recognized that the fetal and perinatal environment can influence the epigenetic landscape, puberty or infection in adulthood can also [155].

Viral infections have been documented as impacting the epigenetic regulation of gene expression. In some cases, a virally encoded protein directly interacts with the host to induce alterations, as in the case of hepatitis B. The HBx protein encoded within the viral genome of hepatitis B virus has transcriptional transactivation activity and can upregulate DNMT1 and DNMT3a [156, 157]. Kaposi’s sarcoma herpesvirus employs a similar mechanism in producing a virally encoded version of interleukin-6 (IL6), which binds to the signaling receptor subunit gp130 and induces DNMT1 expression via STAT3 activation [158]. In other cases, the impact on epigenetic regulation is indirect and is instead instigated by the inflammatory response to viral infection rather than the

virus itself. Tissue damage and infection leads to the production of IL6, which has implications within the immune response as well as gene regulation [159-161]. In fact, IL6 is capable of inducing DNMT1 expression via microRNA [162]. Other viruses known to induce epigenetic alterations include Epstein-Barr virus, hepatitis C, human immunodeficiency virus, human papillomavirus, human rhinovirus, Middle East respiratory syndrome coronavirus, severe acute respiratory syndrome coronavirus 1 and 2, and H5N1 influenza (reviewed in [163]).

Contributions to Fetal Infection Research

The collaborative efforts of Dr. Thomas R. Hansen and Dr. Hana Van Campen have produced an experimental model for the generation and study of transient and persistent fetal infection with BVDV. The strain utilized for experimental infections, ncp BVDV type 2 96B2222, was originally isolated from an outbreak characterized by abortions, stillbirths, and the generation of weak calves [164]. To produce PI or TI calves, pregnant dams are inoculated with BVDV on gestational day 75 or 175, respectively. This model of infection allows for the examination of acute, transient infection in the dams as well as investigation of the resulting fetuses or calves, whether they be PI or TI.

The first large-scale implementation of this model included 3 separate groups: maternal infection in early gestation on day 75 (generating a PI fetus), maternal infection in late gestation on day 175 (generating a TI fetus), or uninfected controls. All generated fetuses were collected on gestational day 190 via cesarean section (C-section) surgery. Historically, the establishment of immunotolerance in PI fetuses was

thought to be a result of innate immune evasion. This study was the first to demonstrate that the dams, TI fetuses, *and* PI fetuses demonstrate initiation of an innate immune response as evidenced by an increase in ISG expression in blood following infection with ncp BVDV [165]. The response mounted in PI fetuses was milder than that mounted in TI fetuses but present nonetheless [166]. A separate study performed by the lab analyzed adult PI steers and reported an ongoing but minimal innate immune response in WBCs to chronic infection, citing upregulation of ISG15, OAS1, and MX2 mRNA [166]. The upregulation of MDA5 and RIG-I WBC mRNA identified in BVDV infected dams as well as both TI and PI fetuses, demonstrated for the first time that BVDV is recognized through both cellular mechanisms of detection (MDA5 *and* RIG-I), rather than one or the other [167]. One finding led to more questions: CXCR4 mRNA was rapidly downregulated in WBCs from dams of PI fetuses and remained downregulated for approximately 90 days following maternal BVDV inoculation on gestational day 75 [165]. This led to the speculation that CXCR4, in addition to other biomarkers, may be present in the peripheral blood and aid in identification of PIs during gestation.

The second implementation of this experimental model included the generation of control and PI fetuses (infected on gestational day 75) that were collected via C-section on gestational days 82, 89, 97, 192, and 245. This study demonstrated that maternal viremia can be detected 7 days after infection but resolves by 22 days post infection ; concurrently, fetal viremia can be detected 14 days and peaks at 22 days post maternal infection [168]. Due to the lack of fetal immune development, peak viremia in the PI fetus was dramatically higher than that of the dam [168]. This study

was also the first to demonstrate an adaptive immune response to BVDV infection in fetuses, although at a diminished level in PIs [169]. However, the adaptive immune response, as evidence by increased transcription of STAT1, IFI16, CXCR6, CXCL10, and CXCL16 in PIs, subsequently waned and completely dissipated by gestational day 245 [169]; the viral titers of PIs also decreased in accordance [170]. Additionally, PI fetuses appeared to respond differentially to fetal BVDV infection, some PIs maintain high viremia while others can at least partially mitigate viremia [171].

These studies also demonstrate that γδ T cells, while not present in the spleen at day 82 or 87, begin to colonize the spleen around day 97 of gestation [169]. These T cells display the suppressive, tolerance promoting functions typically displayed by regulatory T cells in humans and mice [172]. Microarray analysis of splenic RNA from PI fetuses on gestational day 82, 97, 190, and 245 revealed a decrease in expression of genes involved with the adaptive immune response beginning at gestational day 190 and continuing to day 245 [173]. Because regulatory T cells are the predominate type of T cell during the first half of gestation and promote tolerance to self-antigens in humans, it was theorized that the presence of BVDV antigen during this period is inherently treated as though it is ‘self’ rather than foreign antigen [173]. Infection in late gestation when tolerance to self is no longer being promoted by regulatory T cells instead results in recognition of BVDV antigen as foreign and initiation of the adaptive immune response [122].

From here, the focus began to shift towards postnatal implications of fetal viral infections. Dr. Van Campen first demonstrated that maternal infection with influenza A in the peri-implantation period led to intrauterine growth restriction as well as differential

expression of genes by the thymus [174]. This led to the hypothesis that a similar phenomenon may occur in fetuses infected with BVDV. Alterations of the methylome and transcriptome were identified in DNA from gestational day 245 PI splenic tissue [175]. These alterations were found to affect genes associated with postnatal pathologies previously documented by the Hansen/Van Campen lab such as neural lesions [176], leukocyte infiltration [177], decreased osteoclasts, and perturbed bone formation in trabecular and cortical bone [178].

It was further hypothesized that these epigenetic alterations persist into the postnatal period and continue to correspond to postnatal pathologies. Analysis of the methylome of DNA isolated from peripheral WBCs from PI calves at 4 months of age allowed for investigation as to whether these alterations in the epigenome persist into the postnatal period and whether these alterations are conserved to any degree between splenic tissue and peripheral WBCs. Complete blood counts and flow cytometry were performed to provide context for epigenetic alterations identified in peripheral WBCs. Identification of persistent epigenetic markers in an easily obtainable sample such as peripheral blood may allow for the selection of a biomarker and development of a faster, more cost-effective test to identify and manage PI cattle without the necessity of dual timed testing.

Moreover, if epigenetic alterations occur in PI cattle due to fetal infection, it stands to reason that this phenomenon would also occur in calves that have been fetally infected with BVDV in late gestation. Epigenetic alterations were, in fact, identified in DNA isolated from peripheral WBCs derived from TIs at birth [179]. These alterations suggested impaired growth, development, and immune responses in TIs [179]. The TI

calves also demonstrated lighter body weight at birth compared to controls [179]. the TI heifers generated by a third iteration of this experimental model of BVDV infection were subjected to a feeding trial. Not only are TI calves lighter in body weight at birth, but they maintain a lower body weight compared to controls throughout their life and at harvest [180]. The TI heifers additionally demonstrated a decreased average daily gain in weight as well as increased indicators of inflammation including ceruloplasmin and the oxidized form of glutathione [180].

Herein, to investigate how the epigenome of fetal TIs changes or accumulates in the postnatal period following late gestational BVDV infection, analysis of the WBC methylome was completed at 4 months of age and 17 months of age. Complete blood counts and flow cytometry were performed to provide context for epigenetic alterations identified in peripheral WBCs. Alterations of the methylome in TI cattle may provide a map of sorts for postnatal pathologies and aid in understanding predisposition to disease. At 17 months of age, single cell RNA sequencing of peripheral WBCs was performed to determine whether these epigenetic alterations translate to differential expression of transcripts.

CHAPTER 2: FETAL PERSISTENT INFECTION WITH BOVINE VIRAL DIARRHEA VIRUS CAUSES POSTNATAL EPIGENETIC ALTERATIONS IN WBC DNA[1]

Short Summary

Bovine viral diarrhea virus (BVDV) is a globally prevalent pathogen that causes severe detriment within the commercial cattle industry. Vertical infection occurring before the development of the fetal adaptive immune response, before 125 days of gestation, results in an immunotolerant, persistently infected (PI) calf. Epigenetic and proteomic changes have been observed in the spleen of PI fetuses at 245 days of gestation and correspond to known pathologies. It was hypothesized that epigenetic alterations established in the prenatal period due to BVDV PI would persist into the postnatal period. White blood cell DNA from 5 PI and 5 control heifers at 4 months of age was subjected to reduced representation bisulfite sequencing and interpreted within the context of complete blood count and flow cytometry data herein. Analysis revealed 8,367 differentially methylated sites contained within genes associated with the immune and cardiac system as well as hematopoiesis. Differences observed in the complete blood counts of PI heifers include in-creased monocytes, microcytic anemia, and elevated platelets with decreased mean platelet volume. Flow cytometry revealed increased classical monocytes, B cells, $CD4^{+}/CD8B^{+}$ and $CD25^{+}/CD127^{-}$ T cells as well as decreased $\gamma\delta^{+}$, $CD4^{+}$, and $CD4^{-}/CD8B^{-}$ T cells.

---

[1]Kincade JN, Murtazina DA, Georges HM, Gonzalez-Berrios CL, Bishop JV, Engle TE, Henao-Tamayo M, Eder JM, McDonald EM, Deines DM, et al. Postnatal Epigenetic Alterations in Calves Persistently Infected with Bovine Viral Diarrhea Virus. *Viruses.* 2025; 17(5):708. https://doi.org/10.3390/v17050708

Introduction

Bovine viral diarrhea virus (BVDV) is an economically important pathogen of the cattle industry [181]. There are two biotypes and two genotypes of BVDV: non-cytopathic (ncp), cytopathic, BVDV1, and BVDV2, respectively. Cytopathic BVDV infections arise from mutated ncp strains in persistently infected (PI) cattle, cause cell death, and are mostly associated with fatal mucosal disease [19, 21]. Of the two biotypes, ncp is most common and does not result in death of the infected cells. Instead, ncp infections are more often associated with reproductive losses incurred through decreased conception rates, abortions, stillbirths, and the production of weak, non-viable cattle infected in utero [3, 182-185]. The fate of a calf infected in utero depends largely on the stage of gestation and the development of the fetal adaptive immune response [182, 186, 187]. The bovine adaptive immune response develops between 125 and 150 days of gestation. Infections occurring prior to 125 days of gestation can result in resorption of the fetus, mummification, stillbirth, or the birth of a live, PI calf [28, 188, 189]. These PI fetuses are known to mount a partial, albeit weak, immune response to BVDV infection, as evidenced by the diminished secretion of type I and II interferons (IFNs) [122, 167, 169, 173, 186]. However, PI fetuses ultimately fail to produce antibodies specific to the strain of BVDV that they are infected with during gestation. As a result, they are unable to clear the viral infection and shed viral particles for the entirety of their life. At birth, PI calves often have congenital defects of the brain, skeleton, heart, and thymus [178, 186-188, 190, 191]. Moreover, PIs experience severe immunosuppression that predisposes them to the development of secondary diseases

[192]. Many PI cattle succumb to disease early in life, but some survive into adulthood and go on to expose all cattle they contact [3]. Most BVDV management strategies focus on the identification and elimination of PI cattle. To differentiate PI cattle from transiently infected cattle within a herd, they must test positive for BVDV twice, with an interval of 3 weeks or greater in between the two [193]. Another component of BVDV management strategies focuses on the vaccination and prevention of BVDV infection. However, high antigenic diversity between the 24 BVDV1 and 4 BVDV2 subtypes renders vaccination only partially effective in BVDV mitigation [194] and produces varied clinical signs [195].

The developmental origin of health and disease theory indicates that environmental factors can have lasting effects on an organism and its associated phenotype [134]. Phenotypic plasticity is particularly high during gestation, making environmental factors including nutrition, stress, and pathogenic exposure during pregnancy particularly influential. One mode of action through which this influence is exerted occurs through chemical modifications upon the organism's epigenome, more specifically through methylation of DNA. Methylation patterns are relatively stable and heritable to subsequent cells [196]. Within mammalian species, DNA methylation occurs on cytosines; 98% of these methylated cytosine nucleotides are immediately followed by a guanine nucleotide [143]. Regions of the genome rich in cytosines and guanines are known as CpG islands and are not often found outside of promoter regions in mammalian genomes [144, 145]. Methylation of CpG islands located within the promoter region effectively silences gene transcription, while removal of methylation allows for increased transcriptional binding of these sites [147]. Epigenetic data

collected from PI fetal spleen revealed alterations in the methylation patterns of genes associated with the immune, neural, skeletal, and cardiac systems. These alterations within the methylome could result in the induction of postnatal defects [175]. Similarly, other vertical infections are known to induce both direct and indirect impacts on the epigenome. For example, the core protein of hepatitis C virus binds to *AURKB* and reduces subsequent transcription [197]. Other infections, as in the case of BVDV, induce epigenetic alterations through the generation of inflammation [198]. As de novo DNA methylation and chronic infection of PIs continues into the postnatal period, we hypothesized that the epigenome of PI calves at 4 months of age compared to controls would contain more differential methylation than the epigenome of PI fetuses at gestational day 245.

In this study, four-month-old PI heifers infected with a non-cytopathic BVDV1b isolate were assessed for differential methylation of DNA in comparison to control heifers. Differential analysis of the epigenome suggested that various physiological systems were impacted. Comparison of DNA methylation to complete blood counts (CBCs) and flow cytometry from the same calves infected with the same subtype of BVDV ensures compatibility of data and elimination of variability. The CBCs were consistent with chronic infection and altered hematopoiesis, such as elevated monocytes (which was corroborated by flow cytometry) and microcytic anemia. Flow cytometry results were correlated with differential methylation of the immune system genes through abnormal percentages of T cell sub-populations. A compelling argument is proposed that postnatal defects associated with PI heifers are maintained by epigenetic mechanisms. In addition, previously undocumented alterations in white blood

cell DNA from PI heifers have been discovered that have the potential to contribute to loss of monetary value and premature death.

Materials and Methods

Animals and PI Identification

Eleven Angus cross PI heifers were identified at a local, cooperating ranch at approximately two months of age. Ear notches were collected from calves suspected to be infected with BVDV by the High Plains Veterinary Clinic in Limon, Colorado. Ear notch samples were tested using a BVDV antigen capture ELISA and RT-PCR at the Colorado State University (CSU) Veterinary Diagnostic Laboratory (Rocky Ford, CO, USA). Calves with samples that returned positive for BVDV were retested 1 month later to distinguish persistent infections and transient infections. Twelve age-matched Hereford-Angus heifers were generated at CSU and seronegative status was confirmed at birth.

Blood Collection and Complete Blood Counts (CBCs)

Whole blood was collected from the jugular in K_2EDTA tubes (Becton, Dickinson, and Company, Franklin Lakes, NJ, USA cat # 07417). A separate blood sample was obtained for each analysis including viral neutralization testing, RRBS, flow cytometry, and complete blood counts. Blood samples utilized for analyses were collected from all control heifers at a single time. Blood samples from all PI heifers were collected at a single time separate from the control heifers, due to housing distance. Blood samples were held on ice until transport to the Animal Reproduction and Biotechnology

Laboratory (ARBL) at CSU. Hematological parameters for total white blood cells (WBCs), absolute cell counts and percentages of neutrophils, basophils, eosinophils, monocytes, and lymphocytes were measured using an Element HT5 (Heska, Lovaland, CO, USA. Red blood cell (RBC) count, hematocrit, hemoglobin, mean corpuscular hemoglobin, mean corpuscular hemoglobin concentration, mean corpuscular volume, red cell distribution width, and platelets (including mean platelet volume) were also measured.

Isolation of White Blood Cells

The WBCs were isolated through density centrifugation. Blood samples were centrifuged at 1500 x g for 15 minutes at 4°C (Eppendorf 5804R). The buffy coat was aspirated, transferred to a tube containing 5 mL of ammonium-chloride-potassium lysing buffer (ACK; KD Medical, Columbia, MD, USA cat#TGF-3015), and incubated for 5 minutes at room temperature. The WBCs were pelleted using centrifugation at 300 x g for 10 minutes at 4°C. After decanting the supernatant, the pellet was resuspended in 2.5 mL of ACK and incubated for 5 minutes at room temperature. Following centrifugation, pelleting, and decanting of the supernatant, the WBC pellet was resuspended in 1X PBS with a pH of 7.4 for washing. The sample was centrifuged at 300 x g for 10 minutes at 4°C. The supernatant was discarded, and WBCs were resuspended in either 1 mL of PBS for DNA extraction or 1 mL of TRIzol™ (Invitrogen, Carlsbad, CA, USA cat#15596018) for RNA extraction.

Confirmation of PI Status by RT-PCR

Control heifers were tested to confirm BVDV seronegative status, while PI heifers were tested to determine the infecting strain of BVDV. The RNA was extracted from WBCs using TRIzol™ reagent (Invitrogen, Carlsbad, CA, USA cat#15596018) and treated with 6.8 units of RNase-free DNase I (Qiagen, Germantown, MD, USA cat#79254) per sample. Each sample was then purified using the RNeasy MinElute Cleanup Kit (Qiagen, Germantown, MD, USA cat#74204) according to manufacturer's instructions. The RNA quantity and quality was determined using a nanodrop ND-1000 spectrophotometer (ThermoFisher Scientific, Waltham, MA, USA). All DNA samples had 260/280 ratios of 1.8 or greater. The cDNA was created from the extracted RNA using Bio-Rad iScript Reverse Transcription Supermix (Bio-Rad, Hercules, CA, USA cat#1708840). Using a thermocycler (Mastercycler, Eppendorf, Hamburg, Germany), the RNA/RT Supermix was held at 46°C for 1 hour before being heated to 94°C for 4 minutes, according to manufacturer's instructions. The cDNA (1.5 µL) was combined with 0.5 µL of the forward and reverse primers and 22.5 µL of Invitrogen PCR Supermix (Thermo Fisher Scientific, Walkham, MA, USA). Primers used to detect all BVDV isolates [21] were as follows: forward 5'- CAT GCC CAT AGT AGG AC-3' and reverse 5'-CCA TGT GCC ATG TAC AG-3'. Following 41 cycles of 10 seconds at 94°C, 15 seconds of 50°C, 30 seconds at 72°C, cDNA samples were held at 72°C for 10 minutes before an infinite hold at 4°C. Amplified samples were separated on a 2% agarose gel containing Gel Red (Biotium, Freemont, CA, USA cat#41003) and visualized using a Molecular Imager ChemDoc XRS+ with Image Lab software (Bio-Rad, Hercules, CA,

USA). Samples from PI heifers were then sequentially tested for BVDV1a, BVDV1b, and BVDV2 according to Ridpath et al. [51].

Viral Neutralization Test:

Whole blood was centrifuged at 500 x g for 10 min at 4°C (Eppendorf 5804R). The separated serum was placed into microcentrifuge tubes and stored at -20°C for serology. Serum neutralizing antibody titers were determined in a microtiter plate format using cytopathic (cp) BVDV2 (296c) and bovine turbinate (BT) cells as an indicator [16]. Each serum dilution was tested in duplicate and 100 TCID50/25 µL of the test virus was added to each well. The plates were incubated for 1 hour at 37°C, 5% CO_2 before adding 1 x 10^4 BT/well. The BTs in each well were scored for cytopathic effect after an additional 72 hours of incubation. Each titration assay included duplicates of the control calf sample, a positive control serum of known titers, cell controls, and the inoculum.

Reduced Representation Bisulfite Sequencing (RRBS)

The DNA was isolated from WBCs using the Qiagen DNeasy Blood and Tissue Kit (Qiagen, Germantown, MD, USA) according to the manufacturer's instructions. Extracted DNA from 5 randomly selected control heifers and 5 randomly selected PI heifers was sent to Zymo Research (Irvine, CA, USA) for genome-wide classic RRBS. The following methods were completed by Zymo Research. Samples were digested with 30 units of MspI (NEB; Ipswich, MA, USA) and purified with DNA Clean & Concentrator-5 (Zymo Research). Fragments were ligated to pre-annealed adapters with cytosine replaced with 5'-methyl-cytosine according to Illumina's guidelines.

Ligated fragments greater than 50 base pairs were recovered with the DNA Clean & Concentrator-5 (Zymo Research) then bisulfite treated with the EZ DNA Methylation-Lightning Kit (Zymo Research). Samples were subjected to PCR with Illumina indices and products were then purified with DNA Clean & Concentrator-5 (Zymo Research). Size and concentration of samples were confirmed with the Agilent 2200 TapeStation and libraries were sequenced on an Illumina platform.

Methylation Bioinformatics and Pathway Analysis

DNA samples from 5 randomly selected control and PI calves were submitted to Zymo Research for Reduced Representation Bisulfite Sequencing (RRBS). Raw binary alignment and map (BAM) files were received from Zymo Research. Using the 'methylKit' package in R [199], these files were aligned to the most recent bovine genome available through the University of California, Santa Cruz (ARS-UCD1.2/bosTau9). Quality control and gene ontology data and plots were generated with the 'clusterProfiler' and 'org.Bt.eg.db' packages in R [200, 201]. The package methylKit selects only the CpG sites identified in all samples for comparison. Data was normalized by median coverage, filtered by a standard deviation of 2 to remove sites that did not include variation, and assessed for outliers. Clustering and was performed at this stage to demonstrate differences in methylation between groups. Correlation was also performed here, with all Pearson correlation coefficients ≥ 0.95. Differentially methylated sites (DMSs), CpG islands, and promoter regions were identified using the 'methylKit' package in R using logistic regression. Per 'methylKit' default, read coverage is weighted during differential comparison to remove variation due to sample

heterogeneity. Methylation sites were identified as DMSs if they satisfied the qualifications of q <0.01 and the methylation was varied in at least 25% of the treatment sample population (|meth.diff| > 25). The CpG islands and promoter regions were identified if they satisfied the qualifications of q < 0.01 and |meth.diff| > 15. Gene identifications were associated using the 'genomation' package in R [202]. Deconvolution was not necessary for this analysis, as methylation of specific cell types were not compared. Raw files are available in the NCBI GEO Database (GSE271244). Pathway analysis for methylation data was performed using Ingenuity Pathway Analysis (IPA; Qiagen, Germantown, Maryland, USA). The IPA software houses genes contained within the human, mouse, and rat genomes for analysis.

Flow Cytometry

Additional wWhole blood samples were collected in K_2EDTA tubes and processed by Zoetis Inc. (Kalamazoo, MI, USA). The RBCs were lysed using 1X RBC lysis buffer (eBioscience, San Diego, CA, USA cat# 00-4300-54). Samples were centrifuged at 500 x g for 5 minutes. The WBCs were resuspended in 1 mL of DPBS (ThermoFisher, Waltham, MA, USA cat# 14190-136). Another 10 mL of DPBS was added to the suspension before centrifugation at 500 x g for 5 minutes. The supernatant was aspirated, and the cell pellet resuspended in 1 mL of DPBS and pipetted through a cell-strainer cap into a 5 mL round bottom tube (Corning, Corning, NY, USA cat# 352235). The cell suspension was diluted 1:20 into DPBS and counted using a Vi-CELL BLU (Beckman Coulter, Loveland, CO, USA). Viable cells were seeded into a 96-well V-bottom cell culture plate (Corning, Corning, NY, USA cat# 3894) at a concentration of

$1x10^6$ cells per well. The remaining cells were suspended in Serum Free Cell Freezing Medium (ATCC, Manassas, VA, USA cat# 30-2600) and stored at -80°C. The total volume of each well was brought up to 200-300 µL using DPBS prior to centrifugation of the plate. The supernatant was discarded. Cells were resuspended in 100 µL of Fixable Viability Stain 620 (BD Biosciences, Franklin Lakes, NJ, USA cat# 564996) at a concentration of 1:1000 and allowed to incubate on ice in the dark for 10 minutes. Afterwards, 200 µL of FACS buffer (BD Biosciences, Franklin Lakes, NJ, USA cat# 554657) was added to each well. Samples were centrifuged and the supernatant was discarded. Cells were resuspended in 100 µL of the staining master mix (Table 2.1) and incubated for 20 minutes on ice in the dark. Following incubation, 200 µL of FACS buffer was added, cells were centrifuged, and the supernatant was discarded. Cells were washed in 300 µL of FACS buffer and centrifuged. The supernatant was discarded before resuspension in 100 µL of diluted stabilizing fixative (1:3, BD Biosciences, Cat# 338036). After a 5-minute incubation at room temperature, 100 µL of FACS buffer was added prior to centrifugation and discarding of the supernatant. Cells were resuspended in a final 200 µL of FACS buffer and held at 4°C in the dark until transfer to the CSU Flow Cytometry Core for analysis using a 4L 16V-14B-10YG-8R Cytek Aurora spectral cytometer.

Data was gated using FlowJo (BD Biosciences, Franklin Lakes, NJ, USA). Flow cytometry data in the form of frequency relative to the parent population was compared in GraphPad Prism 10 (GraphPad Software, San Diego, CA, USA).

Table 2.1 - Flow Cytometry Fluorophore Panel.
From left to right, the first column indicates the laser utilized to detect the fluorophore and associated marker. The second column lists the intended molecular antigen for identification. The third column indicates what species the antibody was intended to target. The fourth column indicates the manufacturer the antibodies were obtained from. The fifth column denotes the fluorophore or fluorochrome that the antibodies were stained or conjugated with. The final column on the right indicates the wavelength necessary to excite the fluorophore or fluorochrome and the wavelength at which light is emitted.

Flow Cytometry Fluorophore Panel

Laser	Marker	Species (clone)	Manufacturer	Fluorophore (conjugate)	Ex/Em
405	CD11b	Anti-bovine (CC126)	BioRad	DyLight405 (conjugate)	400/420
	CD4	Anti-bovine (CC8)	BioRad	CF405 (conjugate)	408/452
	CCR7	Anti-human (3D12)	BD Horizon	BV480	436/478
	CD25	Anti-bovine (IL-A111)	BioRad	PacOrange	400/551
	CD44	Anti-mouse/human (IM7)	BioLegend	BV570	405/570
	CD127	Anti-mouse (A7R34)	BioLegend	BV605	405/605
	CD11c	Anti-human (HL3)	BD Horizon	BV650	405/645
	CD27	Anti-human (M-T271)	BD Horizon	BV711	405/711
	CD69	Anti-mouse (HI.2F3)	BioLegend	BV785	405/785
488	CD45	Anti-bovine (CC1)	BioRad	FITC	495/519
	CD14	Anti-human (M5E2)	BD	BB700	485/693
561	CD5	Anti-bovine (CC17)	BioRad	AF555 (conjugate)	553/568
	CD8b	Anti-bovine (CC58)	BioRad	PE	566/574
	CD21	Anti-bovine (CC21)	BioRad	AF568 (conjugate)	578/603
	Viability	Live/Dead	BD	FVS620	523/617
	CD335	Anti-bovine	BioRad	AF594 (conjugate)	590/618
	CD172a	Anti-bovine (CC149)	BioRad	PECy5	561/665
	MM20A	Anti-bovine	WSU	PECy7 (conjugate)	565/778
637	CD16	Anti-bovine (KD1)	BioRad	AF647	650/671
	δ chain	Anti-bovine (TCR1-N24 δ)	WSU	AF680 (conjugate)	684/707
	CD3	Anti-bovine (MM1A)	BioRad	AF750 (conjugate)	752/776

Statistical Analysis

Statistical analyses of CBCs and flow cytometry values were performed in GraphPad Prism 10 (GraphPad Software, San Diego, CA, USA). Grouped values were tested for normality using the Shapiro-Wilk test. Outliers were identified using the ROUT test with a false discovery rate (q-value) of 1%. Outliers were removed prior to calculation of mean and significance. Data with normal distribution was subjected to an unpaired, parametric T-test. Due to differing sample numbers (control n=12, PI n=11),

Welch's correction was applied. In cases where the data was not normally distributed, a nonparametric Mann-Whitney test was utilized. Differences between controls and PI heifers were considered significant if $p < 0.05$. Data are presented as mean ± standard error of the mean (SEM).

Results

BVDV Identification and Serology

Eleven PI heifers were confirmed positive for BVDV1b through RT-PCR genotyping at branding and 1 month following branding [51]. Twelve age matched control heifers housed at CSU facilities were tested to confirm seronegative status upon birth.

DNA Methylation

The methylation of CpG sites in the DNA of WBCs isolated from 4-month-old PI heifer calves were compared to those from a group of age-matched control calves. Of the bisulfite converted sequence reads, an average of 32.4% were aligned to a single location within the reference genome and 51.4% were aligned at more than one location within the reference genome. The average rate of bisulfite conversion for all samples was 99.1% and the average CpG coverage was 9X. Mean quality Phred scores were above 30 at all base positions, indicating high accuracy of sequencing. Using methylKit, CpG sites with coverage in the epigenome of all control and PI samples were selected and stored for comparison. Clustering of CpG methylation demonstrated overall similarity between control and PI heifers (Figure 2.1A). Pearson correlation coefficients

for all samples were greater than or equal to 0.95. A total of 8,367 differentially methylated CpG sites (DMSs) were identified throughout the PI epigenomes when compared to control epigenomes (Figure 2.1B). Of the identified DMSs, 5,349 (64%) sites were hypomethylated and 3,018 (36%) sites were hypermethylated. Sites identified as significant had differential methylation (meth.diff) of greater than 25% and a false discovery rate of less than 0.01 (Figure 2.1C). When the genome was analyzed by CpG islands, 317 differentially methylated regions (DMRs) were identified in PI cattle compared to controls. Similarly, when the epigenomic data was compared based on promoter regions, 182 DMRs were identified in PI cattle.

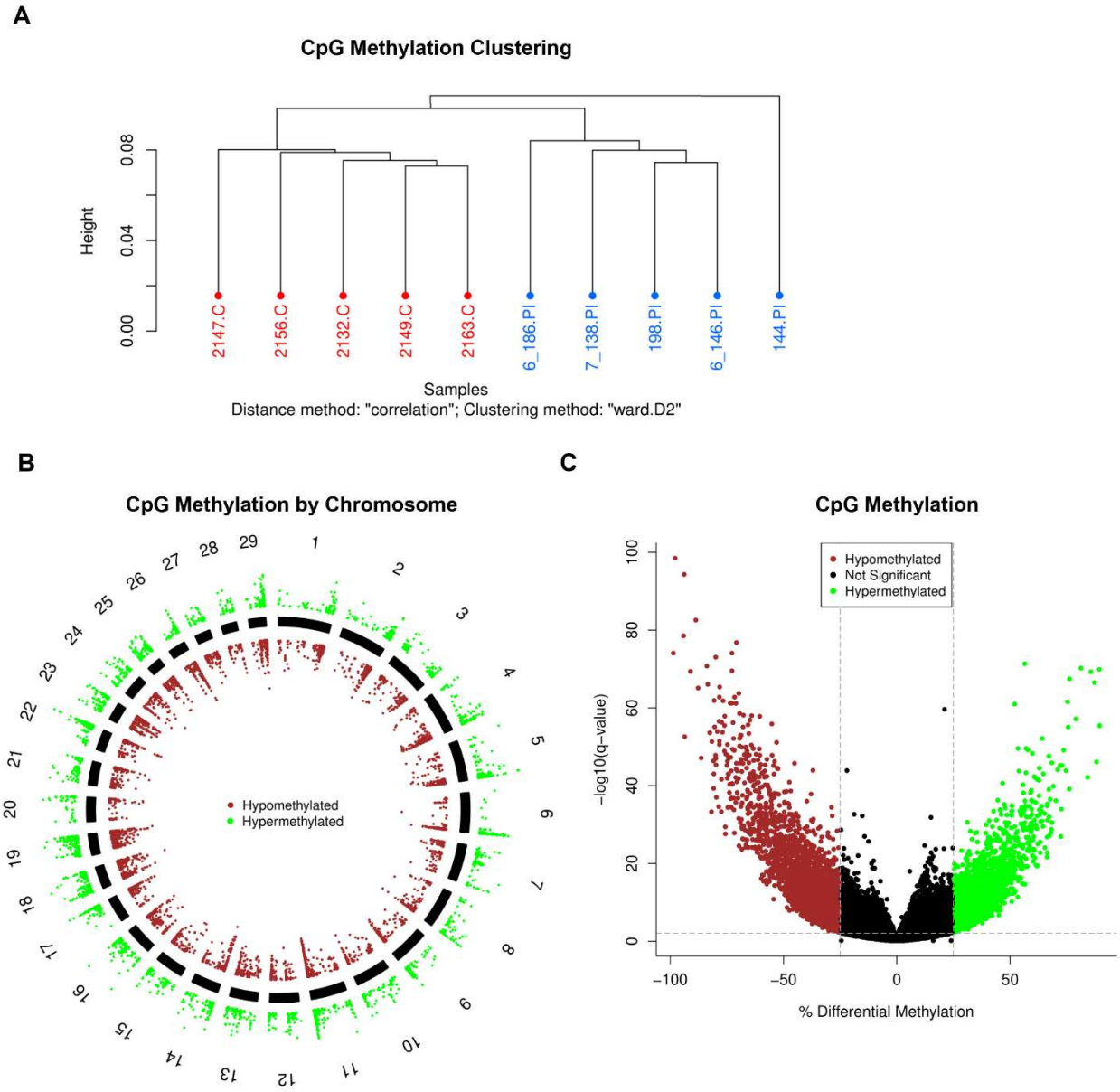

Figure 2.1 - Differential methylation of CpG sites in PI calves.
The CpG sites are defined as sites containing a 'CCGG' motif within the genome. (A) Clustering of samples based on percent methylation per base. Control heifers are denoted in red and heifer ID numbers are followed by '.C'. Persistently infected (PI) heifers are denoted in blue and animal ID numbers are followed by '.PI'. (B) Visualization of differentially methylated CpG sites identified in PI heifers compared to controls by chromosome. Each data point represents a differentially methylated CpG site in respect to its location on the chromosome. Hypermethylated CpG sites are denoted in green and are positioned outside of the solid chromosome bars. Hypomethylated CpG sites are denoted in red and are positioned within the solid chromosome bars. (C) Visualization of the hypermethylated and hypomethylated CpG sites identified in PI cattle compared to controls. The –log10(q-value) Y axis threshold was set at 2 and denoted as a horizontal, grey dashed line. The % differential methylation X axis threshold was set at -25 and 25 and is denoted as vertical, grey dashed line. Hypermethylated CpG sites are denoted in green and hypomethylated CpG sites are denoted in red.

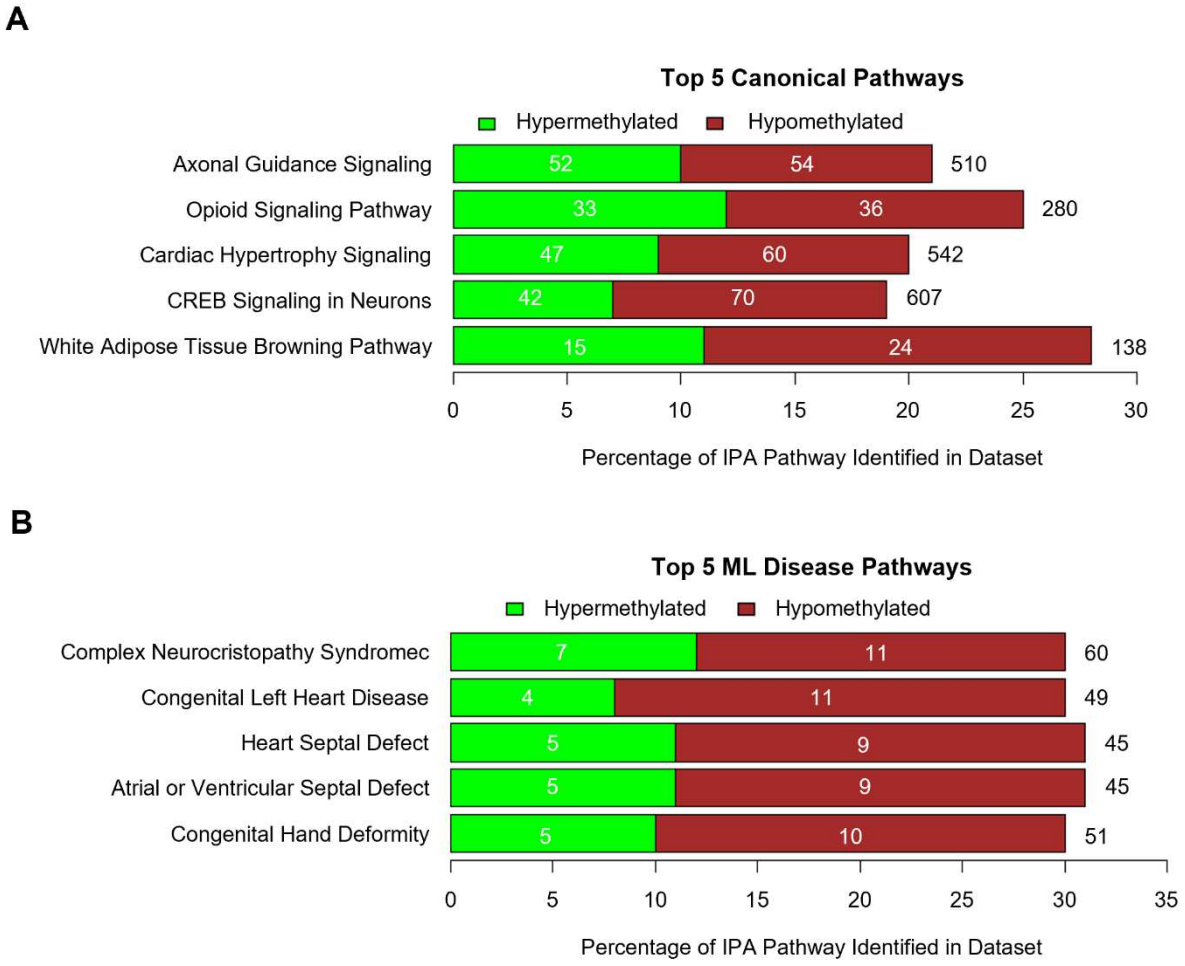

Figure 2.2 - IPA predicted impacts on PIs through utilization of differentially methylated CpG sites.
(A,B) Top 5 canonical pathways and ML disease pathways as determined by Ingenuity Pathway Analysis using genes contained with the human, mouse, or rat genome. Green denotes hypermethylation while red denotes hypomethylation. The total number of genes included in the IPA pathway is denoted to the right of each stacked bar. The number of hypo- or hyper-methylated genes identified in the dataset are denoted within each stacked bar.

Data collected from differential analysis of the methylome of PI and control heifers was analyzed through IPA software. The IPA analysis summarized the most significant findings within the dataset and predicted the most affected molecules, pathways, and disorders. By comparing the number of genes identified within a dataset to the number of total genes in a pathway (defined ‘overlap’), IPA identified pathways

that are likely to be altered in PI heifers. Canonical pathways in the IPA database are well-characterized and human curated. Machine learning (ML) was utilized to generate pathways of phenotypic disease and their associated genes within the IPA database. It was predicted through IPA that several canonical pathways and ML disease pathways would be affected by methylation of the genome. The top five canonical pathways identified include axonal guidance signaling (106/510), opioid signaling (69/280), cardiac hypertrophy signaling [enhanced] (107/542), CREB signaling in neurons (112/607), and white adipose tissue browning (39/138; Figure 2.2A).

The top ML disease pathways include complex neurocristopathy syndrome (18/60), congenital left heart disease (15/49), heart septal defect (14/45), atrial or ventricular septal defect (14/45), and congenital hand deformity (15/51; Figure 2.2B). Moreover, IPA demonstrated that a majority of the CpG DMSs identified were located on genes associated with neurotransmitters and nervous system signaling, organismal growth and development, cardiovascular signaling, cellular growth, proliferation, and development, and cancer, in order from most to least significant. Genes with a strong relationship to pathologies identified in PI cattle were also grouped manually (Table 2.2).

Table 2.2 - Pathology Related Genes Containing Differential Methylation in PI Calves. The left column contains the probable impact of the genes in the center column and the perspective methylation contained within each gene. The central column contains color coordinated gene symbols. Red coloring indicates that the gene contained overall hypomethylation while green coloring indicates that the gene contained overall hypermethylation. References detailing the relationship between the listed genes and associated impact are listed on the far right.

Pathology Related Genes Containing Differential Methylation in PI Calves

Associated Impact	Gene Names	References
Increased monocyte survival	*STAT6, IRF7*	[203, 204]
Decreased T cell development	*GATA3, NOTCH1, CD3, CD8a, ZAP70, BCL11b*	[122, 205-207]
Improper *de novo* methylation	*DNMT3A, DNMT3B*	[175, 208]
Impaired macrophage phagocytosis	*EZR*	[209]
Macrophage induced crusting dermatitis	*PLD4*	[210, 211]
Increased inflammation	*C1r, C2, C8*	[117]
Increased inflammasome activation	*NLRP6, NEK7, GSDMD, CASP4, PANX1*	[212-216]
Cardiac hypertrophy	*PPP3R2, CALM1, NFATc1, NFATc2*	[217-219]

Hypomethylated Hypermethylated

Complete Blood Counts

The whole blood collected from 4-month-old PI and control heifers was subjected to CBC analysis (Zoetis, Inc., Kalamazoo, MI, USA; Figure 2.3 and Table 2.3). Absolute basophil count (BAS), absolute neutrophil count (NEU), and RBC were not different between PI and control heifers. Absolute eosinophil count (EOS) was found to be increased in PI heifers (0.07 ± 0.01 vs 0.1 ± 0.01 x 10^9/L; $p < 0.05$). However, the average absolute monocyte count (MONO) observed in PI heifers was approximately 2-fold higher than the average observed in control heifers (0.38 ± 0.04 vs 0.78 ± 0.08 x 10^9/L; $p < 0.001$). Similarly, the average percentage of monocytes (MONO%) was significantly higher in PI heifers compared to controls (3.53 ± 0.41 % vs 6.8 ± 0.71 %; $p < 0.01$). Hemoglobin (HGB; 14.28 ± 0.23 vs 12.05 ± 0.39 g/dL; $p < 0.001$) and hematocrit (HCT; 41.33 ± 0.72 % vs 35.29 ± 1.1 %; $p < 0.001$) were significantly lower in PI heifers, while RBC distribution width (RDW; 22.96 ± 0.34% vs 27.15 ± 1.23 %; p <

0.05) was greater. Mean corpuscular volume (MCV; 33.99 ± 0.44 vs 29.86 ± 0.6 fL; $p < 0.0001$) and mean corpuscular hemoglobin (MCH; 11.76 ± 0.15 vs 10.2 ± 0.21 pg; $p < 0.0001$) were significantly decreased in PI heifers compared to controls, demonstrating microcytic anemia. The WBC count, absolute lymphocyte (LYM), and percent lymphocyte (LYM%) were not different between PI and control heifers. An increased platelet count (PLT; 462.8 ± 51.5 vs 768.2 ± 60.5 $x10^9$/L; $p < 0.01$) was found in PI heifers, while mean platelet volume was decreased (MPV; 4.93 ± 0.06 vs 4.35 ± 0.05 fL; $p < 0.0001$).

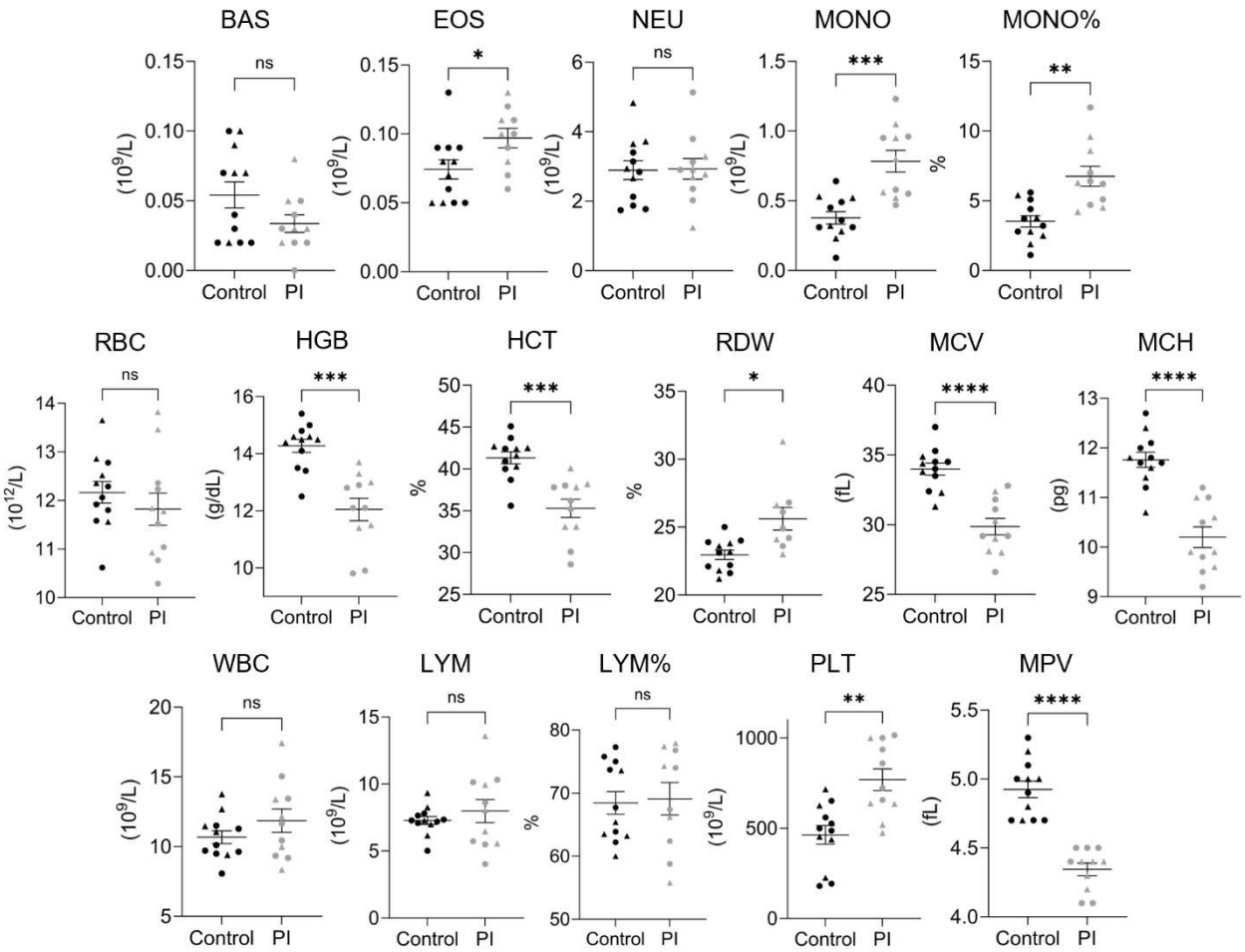

Figure 2.3 - PI cattle demonstrate elevated monocytes, microcytic anemia, and abnormal platelets.
Quantification of the average complete blood count values of control and persistently infected (PI) cattle. From left to right: absolute basophil count, absolute eosinophil count, absolute neutrophil count, absolute monocyte count, monocyte percentage, red blood cell count, hemoglobin, hematocrit, red cell distribution width, mean corpuscular volume, mean corpuscular hemoglobin, white blood cell count, absolute lymphocyte count, lymphocyte percentage, platelet count, mean platelet volume. Outliers were identified using the ROUT method and were excluded from calculation of the mean and significance. Two outliers were identified in the PI group for RDW% (34 and 34.1, one of which was derived from a PI submitted for RRBS), one of which was utilized for RRBS (34.1). A single outlier within the PI group was identified in LYM% and EOS count, 38.6 and 0.28, respectively. The 5 control and 5 PI heifers utilized for RRBS are denoted as triangles. Data are displayed as mean ± standard error of the mean (SEM). Asterisks denote significance between groups, * $P < 0.05$; ** $P < 0.01$; *** $P < 0.001$; **** $P < 0.0001$.

Table 2.3 - Complete Blood Counts in 4-Month-Old Heifer Calves.
Data in which outliers removed are denoted using the dagger†. Data are displayed as mean ± standard error of the mean (SEM). Asterisks denote significance between groups, * P < 0.05; ** P < 0.01; *** P < 0.001; **** P < 0.0001. Reference values were derived from the Element HT5 Veterinary Hematology Analyzer (Heska, Lovaland, CO, USA).

Complete Blood Counts in 4-Month-Old Heifer Calves

	Control		PI			
Population	**Average**	**SEM**	**Average**	**SEM**	**Reference**	**Unit**
Basophil Count	0.05	± 0.01	0.03	± 0.01	0 – 0.35	10^9/L
Eosinophil Count †*	0.07	± 0.01	0.10	± 0.01	0 – 1.3	10^9/L
Neutrophil Count	2.89	± 0.27	2.93	± 0.30	0.60 – 4.9	10^9/L
Monocyte Count ***	0.38	± 0.04	0.78	± 0.08	0 – 1.02	10^9/L
Monocyte Percentage **	3.53	± 0.41	6.80	± 0.71	0 – 9.5	%
Red Blood Cell Count	12.17	± 0.22	11.82	± 0.33	5.0 – 10.1	10^{12}/L
Hemoglobin ***	14.28	± 0.23	12.05	± 0.39	8.0 – 14.2	g/dL
Hematocrit ***	41.33	± 0.72	35.29	± 1.10	23.0 – 42.5	%
Red Cell Distribution Width †*	22.96	± 0.34	25.62	± 0.84	17.5 – 26.5	%
Mean Corpuscular Volume ****	33.99	± 0.44	29.86	± 0.60	37.0 – 55.0	fL
Mean Corpuscular Hemoglobin ****	11.76	± 0.15	10.20	± 0.21	12.5 – 18.2	pg
White Blood Cell Count	10.68	± 0.46	11.86	± 0.84	4.6 – 15.8	10^9/L
Lymphocyte Count	7.28	± 0.30	7.99	± 0.86	1.5 – 11.8	10^9/L
Lymphocyte Percentage †	68.44	± 1.79	69.10	± 2.57	52.3 – 85.6	%
Platelet Count **	462.8	± 51.5	768.2	± 60.5	100 – 720	10^9/L
Mean Platelet Volume ****	4.93	± 0.06	4.35	± 0.05	4.8 – 7.6	fL

Flow Cytometry

To examine the effect of BVDV PI upon the postnatal immune system, flow cytometry analysis was performed on WBCs isolated from whole blood. A 20-fluorophore panel (Zoetis Inc., Kalamazoo, MI, USA) and a gating strategy were developed to identify bovine immune cell types (Figure 2.4A). The entire sample was first gated to remove debris, doublet cells, and dead cells. Live cells were gated on staining for CD45, a pan leukocyte marker. All flow cytometric comparisons were made based on the frequency of the population in relation to the $CD45^+$ population unless otherwise stated (Figure 2.4B and Table 2.4).

Hematopoietic cells ($CD45^+$) were selected and gated for CD11b and CD172a expression to define myeloid cells. Monocyte populations were identified according to CD14 and CD16 expression. Classical monocytes ($CD45^+/CD11b^+/CD172a^+/CD14^+/CD16^-$) were increased in PI heifers (5.67% ± 0.43 vs 9.21% ± 0.86; $p < 0.01$). Intermediate monocytes ($CD45^+/CD11b^+/CD172a^+/CD14^+/CD16^+$) and non-classical monocytes ($CD45^+/CD11b^+/ CD172a^+/CD14^-/CD16^+$) were not different between the control and PI group. Granulocytes were identified within the myeloid population by gating for MM20A expression but were not different between groups.

To identify B cells ($CD45^+/CD3^-/CD21^+$), $CD45^+/CD3^-$ cells were gated based on CD21 expression. A significant increase in B cell percentage was discovered in PI heifers (18.28% ± 1.09 vs 23.95% ± 2.44; $p < 0.05$). Cells expressing CD3 were then gated based on expression of the gamma delta (γδ) chain. Comparison of γδ T cells ($CD45^+/CD3^+/γδ^+$) revealed a significantly lower percentage of $γδ^+$ T cells in PI heifers (15.85% ± 1.13 vs 12.67% ± 0.9; $p < 0.05$). Cells expressing CD45 and CD3, but not the γδ chain, were gated based on expression of CD335. Natural killer T (NKT) cells were not different between groups. Cells not expressing CD335 were further gated according to CD4 and CD8b expression to define cytotoxic T cells ($CD45^+/CD3^+/ γδ^-/CD335^-/CD4^-/CD8b^+$), helper T cells ($CD45^+/CD3^+/γδ^-/CD335^-/CD4^+/CD8b^-$), and double positive T cells ($CD45^+/CD3^+/ γδ^-/CD335^-/CD4^+/CD8b^+$). Comparison of population frequency in relation to the parent population of $CD45^+$ cells revealed no differences in cytotoxic T cells between groups. Helper T cells were significantly decreased in PI heifers (13.6% ± 0.61 vs 10.18% ± 0.90; $p < 0.01$). Double positive T cells were increased in PI heifers (0.07% ± 0.01 vs 0.13% ± 0.01; $p < 0.01$), while cells negative for CD4 and CD8b were

decreased in PI heifers (2.63% ± 0.2 vs 1.21% ± 0.09; $p < 0.0001$). Helper T cells were gated for CD25 and CD127 expression, but no difference was identified between groups concerning $CD25^{+}/CD127^{-}$ T cells. Total T lymphocytes (the summation of $\gamma\delta^{+}$ T cells, NK T cells, $CD4^{+}/CD8b^{-}$ T cells, cytotoxic T cells, and helper T cells) were lower in PI heifers than in controls (36.48% ± 1.53 vs 29.84% ± 1.57; $p < 0.01$).

Subpopulations of T cells were also compared based on frequency relative to their parent $CD3^{+}$ cell population (Figure 2.4C and Table 2.4). Neither $\gamma\delta^{+}$ T cells nor NK T cells within the $CD3^{+}$ gate were different between groups. Cells positive for CD4 and CD8b were significantly increased in PI cattle within the $CD3^{+}$ gate (6.7% ± 0.43 vs 3.9% ± 0.21; $p < 0.0001$). Cells negative for CD4 and CD8b were significantly decreased in PI heifers (6.7% ± 0.43 vs 3.9 % ± 0.21; $p < 0.0001$). Cytotoxic T cells and helper T cells were not different between groups. However, a significant increase was identified in PI cattle when the frequency of $CD25^{+}/CD127^{-}$ cells in relation to helper T cells was compared to controls (3.63% ± 0.21 vs 5.58% ± 0.25; $p < 0.01$). Cell population markers and results have been summarized in Figure 2.5.

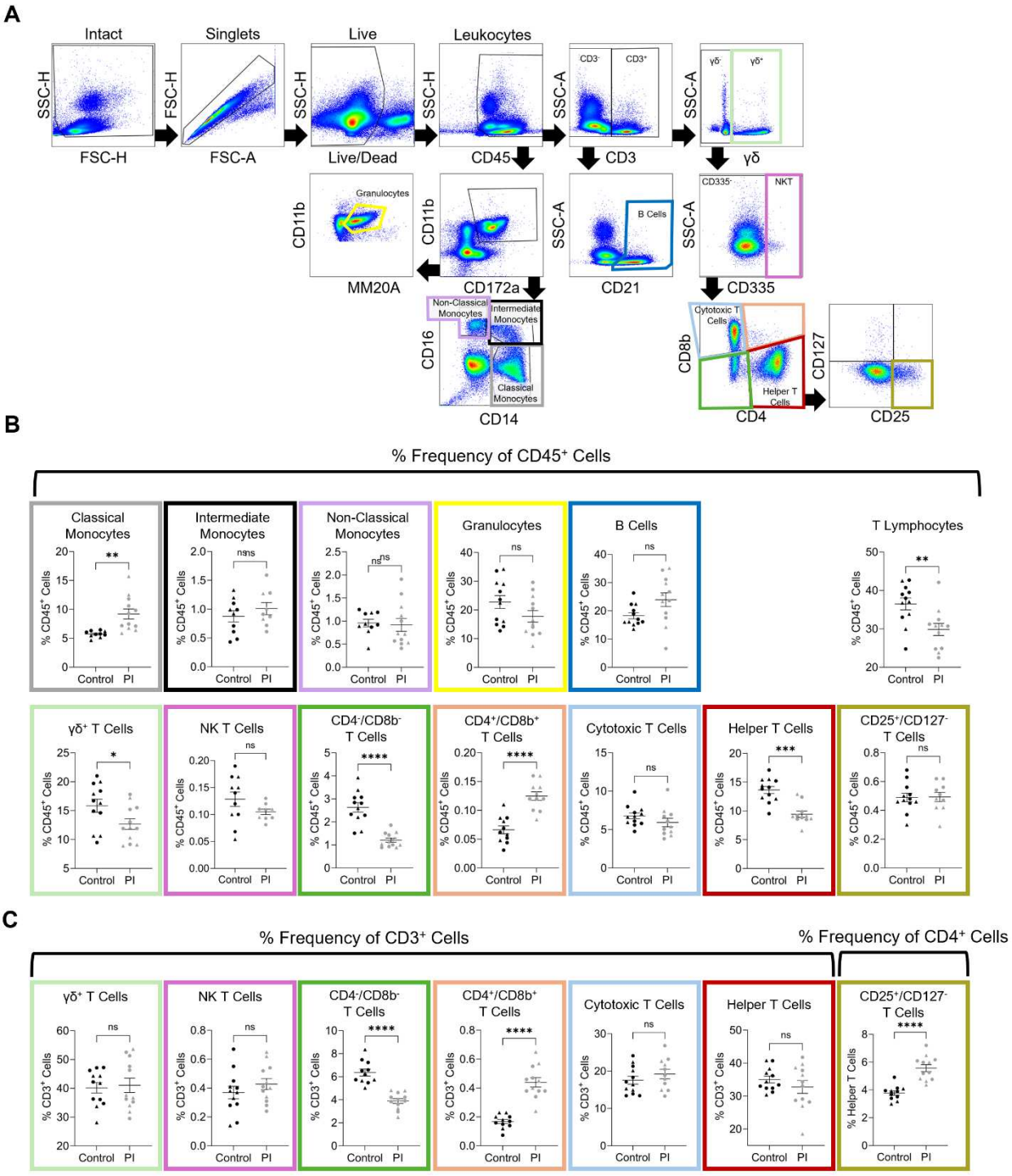

Figure 2.4 Decreased total T cells and increased subpopulations in PI heifers.
(A) Gating strategy for identification of T cells, B cells, monocytes, and granulocytes. Natural killer T cells are denoted 'NK' cells. (B) Quantification of cell population frequency in relation to the $CD45^+$ parent population. (C) Quantification of cell population frequency in relation to the $CD3^+$ cell parent population. Outliers were identified using the ROUT method and removed prior to calculation of mean and significance. The following outliers were identified in comparisons of CD45 frequency: classical monocytes (*2.13* in the control and 8.59 in the PI group), intermediate monocytes (2.59 & *2.76* in the control and *2.65*, 2.74, & *3.37* in the PI group), non-

classical monocytes (0.17 & 2.95 in the control group), NK T cells (0.31 in the control and *0.2*, *0.23*, & 0.24 in the PI group), $CD4^+/CD8b^+$ T cells (0.17 in the control and 0.24 in the PI group), cytotoxic T cells (*15.7* in the PI group), helper T cells (18.4 in the PI group), and $CD25^+/CD127^-$ T cells (*0.84* & 1.1 in the PI group). The following outliers were identified in comparisons of CD3 frequency: $CD4^-/CD8b^-$ T cells (*10.4* in the control group), $CD4^+/CD8b^+$ T cells (0.42 in the control group), and cytotoxic T cells (*44* in the PI group). An outlier was also found in the comparison of $CD25^+/CD127^-$ T cells in the context of helper T cell frequency (*1.93* in the control group). Italicized outliers belong to heifers utilized for RRBS. Data are displayed as mean ± standard error of the mean (SEM). Asterisks denote significance between groups, * P < 0.05; ** P < 0.01; *** P < 0.001; **** P < 0.0001. Non-significance is denoted by 'ns'.

Table 2.4 - Flow Cytometry Populations in 4-Month-Old Heifer Calves.
Data are displayed as mean ± standard error of the mean (SEM). Asterisks denote significance between groups, * P < 0.05; ** P < 0.01; **** P < 0.0001.

Flow Cytometry in 4-Month-Old Heifer Calves

	Control		PI		
Population	**Average (%)**	**SEM**	**Average (%)**	**SEM**	**Freq. of**
Classical Monocytes **	5.73	± 0.18	9.21	± 0.86	CD45
Intermediate Monocytes	0.88	± 0.10	1.01	± 0.10	CD45
Non-Classical Monocytes	0.96	± 0.08	0.92	± 0.14	CD45
Granulocytes	22.76	± 2.24	17.75	± 2.01	CD45
B Cells *	18.28	± 1.09	23.95	± 2.44	CD45
T Lymphocytes **	36.48	± 1.53	29.84	± 1.57	CD45
$\gamma\delta^+$ T Cells *	15.85	± 1.13	12.67	± 0.09	CD45
NK T Cells	0.13	± 0.01	0.10	± 0.01	CD45
$CD4^-/CD8b^-$ T Cells ****	2.63	± 0.2	1.21	± 0.09	CD45
$CD4^+/CD8b^+$ T Cells **	0.07	± 0.1	0.12	± 0.1	CD45
Cytotoxic T Cells	6.78	± 0.39	5.91	± 0.55	CD45
Helper T Cells	13.64	± 0.61	9.43	± 0.54	CD45
$CD25^+/CD127^-$ T Cells	0.49	± 0.03	0.49	± 0.03	CD45
$\gamma\delta^+$ T Cells	40.17	± 1.79	41.04	± 2.49	CD3
NK T Cells	0.37	± 0.04	0.43	± 0.04	CD3
$CD4^-/CD8b^-$ T Cells ****	6.36	± 0.30	3.9	± 0.21	CD3
$CD4^+/CD8b^+$ T Cells ****	0.17	± 0.01	0.44	± 0.03	CD3
Cytotoxic T Cells	17.55	± 1.06	19.22	± 1.26	CD3
Helper T Cells	35.02	± 1.02	32.76	± 1.93	CD3
$CD25^+/CD127^-$ T Cells **	3.79	± 0.16	5.58	± 0.25	CD4

Figure 2.5 - Molecular markers for cellular populations in flow cytometry.
Rows indicate cellular populations. Columns indicate molecular markers. Light grey indicates that a molecular marker was not present in the population. Black shaded boxes indicate positivity for a molecular marker within a given cellular population.

Discussion

The cattle industry experiences billions of dollars in profit loss each year due to BVDV infections [3, 220]. The cost of a BVDV outbreak ranges from $20 to $103 per head, which culminates to an estimated $1.5 to $2.5 billion dollars in loss each year [1]. Current disease mitigation strategies focus on the elimination of the main reservoir of the virus, PI calves, as they are responsible for infecting 70% - 100% of cattle they encounter [7]. Once PIs have been eliminated, BVDV prevention strategies depend on herd vaccination. However, due to the high antigenic diversity of BVDV, even herds that are routinely vaccinated can experience acute transient infections or fetal infections that produce PIs [194]. Routine testing is often performed in conjunction with vaccination, identifying any transient infections occurring in the herd. To identify a PI, testing must be performed twice. The cost of routine testing and vaccination is significantly lower than

the costs incurred by an outbreak of BVDV [1]; however, the period between initial testing and secondary testing for PI confirmation allows for additional infections and profit loss to occur. Investigation and increased understanding of potential biomarkers may provide a faster identification time for PIs and further mitigate profit loss for producers.

Relationships Between PI CBCs, Flow Cytometry, and DNA Methylation

An increase in monocytes in PI cattle has been previously documented and is likely a result of chronic, ongoing infection [221]. The finding of elevated monocytes in PI calves was reinforced by flow cytometry analysis, which identified the specific population of classical monocytes to be elevated. It has been noted that monocytes infected with ncp BVDV1b upregulate proteins associated with cell survival [203]. It is possible that hypomethylation within *STAT6* and *IRF7* (Table 2.2), which is associated with the potential for increased expression, contributes to increased monocyte development and subsequent elevation of monocytes in PI calves [204]. The increase of eosinophils seen in PI cattle is likely due to an increased parasite load, although this remains unconfirmed.

The PI calves in this study were also found to be anemic, demonstrating decreased hemoglobin, hematocrit, mean corpuscular volume, and mean corpuscular hemoglobin as well as increased red cell distribution width. Extramedullary hematopoiesis (EMH), a condition in which the production of blood cells occurs outside of the bone marrow, has previously been observed in PI cattle [175, 191]. In fact, PI fetuses experience osteopetrosis, which may be a driving factor in the observed EMH,

anemia, and platelet disturbances [178, 190]. While it is uncommon to see increased platelets in BVDV infected cattle, it is likely that the circulating platelets are smaller in size due to increased age [222, 223]. Moreover, BVDV infects megakaryocytes, which are responsible for platelet production [224, 225].

Flow cytometry revealed that PI calves have elevated B cells. This could be explained by the fact that the PIs have been exposed to more foreign antigen compared to controls, but no additional infections were observed.. The PI calves were also found to have decreased percentages of total T lymphocytes, $\gamma\delta^+$ T cells, $CD4^-/CD8b^-$ T cells, and $CD4^+$ Helper T cells. Acute cytopathic BVDV infections have been shown to decrease T cells [226, 227], but PIs are not often associated with diminished T cells [228]. In accordance with publications demonstrating decreased transcription of T cell genes CD4, CD8a, and CD8b [122], several genes associated with T cell development were found to contain hypermethylation. These genes include *GATA3, NOTCH1, CD3, CD8a, ZAP70,* as well as *BCL11b*, and potentially contribute to the observed decreases in T cell subpopulations (Table 2.2). Hypermethylation, which is associated with decreased expression, of genes necessary for T cell development may play a role in suppression of T cell subpopulations in PI calves as identified by flow cytometry.

Interestingly, PI calves were found to have increased percentages of $CD4^+/CD8b^+$ T cells and $CD25^+/127^-$ T cells. Cells positive for both CD4 and CD8b display memory and high anti-viral activity [229]. Increases in double positive T cells have been associated with immune stimulation by vaccination or infection; a recent study demonstrated that double positive T cells are increased in bovine following foot-and-mouth vaccination and that the increase was dependent upon vaccine potency

[230]. In humans, $CD25^{+}/CD127^{-}$ T cells are defined as regulatory T cells that function to suppress the immune response. However, this sub-population of T cells is neither anergic nor suppressive of the immune system in bovine [231]. Neither of these bovine T cell sub-populations are well characterized, leaving much to be investigated.

Epigenetic Findings in PI Calves are Supported by Previous Research

The enzymes responsible for de novo methylation are most active during the development of the embryo and fetus but have been shown to remain active into the postnatal period [208]. The genes encoding these enzymes, known as DNA methyltransferases (DNMTs), were found to contain hypomethylation in a previous study utilizing DNA from splenic tissue collected from PI fetuses at gestational day 245 [175]. At 4 months of age, we also identified hypomethylation contained within *DNMT3A* and *DNMT3B* in PI heifers (Table 2.2). Moreover, 797 genes were found to contain differential methylation in both the DNA isolated from fetal spleen and DNA isolated from postnatal WBCs (Figure 2.6) [175]. Pathways associated with previous and current studies include the immune and cardiovascular system, as well as hematopoiesis [175].

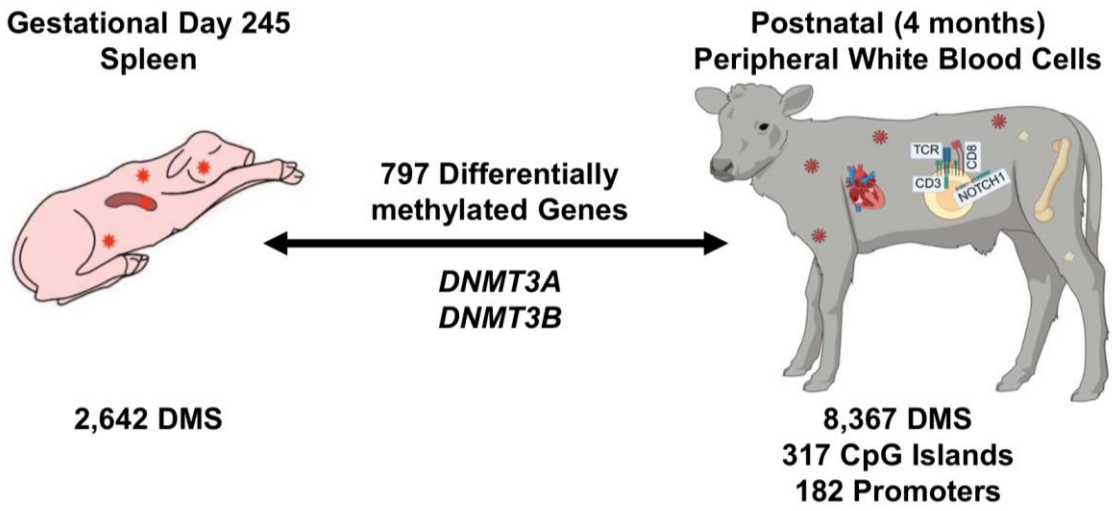

Figure 2.6 – Comparison of differentially methylated genes identified in PIs using gestational day 245 spleen and 4-month postnatal peripheral white blood cells. The red symbols represent BVDV. The spleen is indicated within the fetus at gestational day 245. The heart, a T cell, and femur are indicated in the 4-month-old calf.

Monocytes infected with ncp BVDV have an altered profile of protein expression [232], which may cause their reduced ability to stimulate T cell responses [233]. A 2010 study identified 137 proteins that were differentially expressed in monocytes infected with the ncp BVDV1b NY strain [232]. Comparing the gene name from the 137 differentially expressed proteins to the differentially methylated genes in our dataset revealed 24 genes in common. Of the 24 genes in common, 8 genes displayed differential methylation in accordance with differential expression observed previously. The 8 genes with corroborative methylation include *SH3GL1, MCM4, IGF2R, ECE1, RANBP3, MAN2B1, PDXK,* and *ANXA2* (Table 2.5). For example, *MAN2B1* was found to be hypomethylated at 3 different CpG sites and was previously observed to be upregulated in monocytes infected with ncp BVDV1b [232].

Table 2.5. Differentially Expressed Genes in PI Derived Monocytes Containing Differential Methylation in PI WBC DNA.
The left most column contains gene symbol for those identified to contain differential methylation in PI cattle in correspondence with those differentially expressed in PI derived monocytes. The central column contains indication of whether the gene was found to contain a hyper- or hypo- methylated CpG site. In cases where the gene contained more than one differentially methylated CpG site, xN indicates the number of sites identified. The differential expression of genes identified in PI derived monocytes listed in the right column was derived from [232].

Differentially Expressed Genes Containing Differential Methylation

Gene Symbol	Methylation	Expression
SH3GL1	Hyper	Decreased
MCM4	Hyper	Decreased
RANBP3	Hyper x3 / Hypo x1	Decreased
IGF3R	Hypo	Increased
MAN2B1	Hypo x3	Increased
PDXK	Hypo x3 / Hyper x 1	Increased
ANXA2	Hypo x2	Increased

It has been reported that PI cattle have lower amounts of macrophages and that macrophages derived from PI cattle show diminished reactivity in vitro [29, 147, 232]. While we were unable to identify and quantify macrophages in this study, we were able to identify genes specifically associated with macrophage function that contained differential methylation in PIs. For example, the gene encoding the F-actin binding protein *EZR* was found to contain 5 hypermethylated DMSs (Table 2.2). In vitro, macrophages lacking *EZR* demonstrated impaired phagocytosis [209]. The endosomal endonuclease encoded by *PLD4* was found to contain hypermethylation of a CpG site (Table 2.2). Under normal conditions, the PLD4 endonuclease acts to degrade foreign genetic material that would otherwise initiate a signaling cascade to promote pro-inflammatory macrophages [210]. Perhaps the most intriguing is the similarity between PI cattle and those with deficient PLD4. Calves with insufficient PLD4 present with severe crusting dermatitis, increased vacuolated macrophages, and anemia [211].

Similarly, PI cattle are known to develop crust-like dermatosis, macrophage vacuolization, and even the PI calves identified herein suffered from anemia [187].

Previous research also indicates that PI cattle often suffer from inflammatory disorders such as myocarditis, arthritis, non-suppurative gut inflammation, and respiratory tract inflammation [234-238]. Consistent with these reports, several genes associated with inflammatory processes were found to contain differential methylation. Two different mechanisms that work to generate inflammation appear to be altered by PI with BVDV: the complement cascade and the activation of inflammasomes. Components of the complement cascade found to contain hypomethylation in PI calves include *C1r, C2*, and *C8*. Upon initiation, the complement cascade creates by-products called anaphylatoxins which promote acute inflammation [117]. In addition, multiple inflammasome components were found to contain hypomethylation and include *NLRP6, NEK7, GSDMD, CASP4,* and *PANX1* (Table 2.2). Pro-inflammatory cytokines are also produced as a result of inflammasome activation [117]. Because PIs are continuously circulating viral particles throughout the body, chronic activation of processes involving hypomethylated genes could result in over-promotion of inflammation and the development of secondary inflammatory diseases.

Reports of aborted PI fetuses having an ‘enlarged, flabby heart’ and an adult PI steer with myocarditis, microscopic fibrotic lesions, and necrotic cardiomyocytes indicate the involvement of the heart in chronic BVDV infections [239, 240]. Epigenetic data herein further validate these reports as IPA predicted an increase in hypertrophic response, inflammation, and altered cardiac signaling. Cardiac associated genes including *PPP3R2, CALM1, NFATc1*, and *NFATc2* were found to contain differential

methylation in PI heifers (Table 2.2). A regulatory subunit of calcineurin, encoded by *PPP3R2* was hypomethylated in PI calves. A surplus of NFATs has been implicated in the development of vascular disease and pathological cardiac hypertrophy [217, 218]. Moreover, a total of 47 CpG sites, 3 CpG islands, and a single promoter were found contained within the 31 different genes encoding for potassium channels. Of the 47 DMS, 35 were hypomethylated and 12 were hypermethylated; all CpG islands and promoters were hypomethylated. Improper amounts of potassium within the heart are known to induce arrhythmia [219, 241], as potassium is critically important within the heart during cardiac repolarization.

Potential Confounders and Future Research

While the results of this study show similarity to previous research and documented pathologies of PI cattle, it is important to note the caveats within this dataset. The average CBC values obtained for RBCs, hemoglobin, mean corpuscular hemoglobin, and mean platelet volume are outside of the reference ranges provided with the Element HT5 Veterinary Hematology Analyzer (Heska, Loveland, CO, USA). The ranges provided by the analyzer are similar to those published by the University of California, Davis [242]. However, these references were established using mid-lactation dairy cattle with an average age of 5 years. As the calves in this study are a mere 4 months of age, the reference ranges provided are not entirely suitable for comparison; rather, the control calves generated for this study provide a more accurate comparison. While PI calves exhibit increased $CD4^{+}/CD8b^{+}$ T cells and decreased $CD4^{-}/CD8b^{-}$ T cells, as determined by flow cytometry analysis, it is important to note that we were

unable to definitively identify true double positive or double negative T cell populations in peripheral blood. These populations likely include true ‘double positive’ and ‘double negative’ T cells but may also include other cell types.

The control and treatment group utilized in this study were of similar, but not identical cattle breed. Indeed, the control group generated consisted of Hereford-Angus cross cattle, while the PI calves identified were Angus. During analysis, only CpG sites identified in all control and PI samples were selected for comparison of methylation. Thus, any variation induced by structural variance or single nucleotide polymorphisms associated with breed were excluded from analysis. The perinatal environment also has the potential to influence the epigenome Rather than utilizing a difference in methylation $\geq$ 10%, as is standard in other publications [243], this study opted to increase the threshold to $\geq$ 25% to identify DMSs. The increased threshold for significance was applied to mitigate individual variation and increase reliability of results in the face of differing environments. While steps were taken during analysis to address these potentially confounding variables, it is possible that a percentage of the genes containing differential methylation identified in this study are due to difference in breed or environment [244].

The identification of differential methylation within a gene, while capable of influencing transcription, is not guaranteed to induce pathology. For example, the gene encoding ZAP70 was found to contain hypermethylation. Canonically, the introduction of methylation within the gene could prevent the binding of transcriptional machinery and thus decrease expression. However, not all genes are being actively transcribed all the time. Because ZAP70 is involved in T cell receptor activation[117], it is most likely that

this epigenetic mark would influence the ability of the calf to react to foreign antigen. The same epigenetic mark may not induce a marked impact on the heifer in the absence of immune stimulation. Additional research is required not only to confirm and validate the identification of differential methylation within specific genes, but to evaluate the impact of all identified differential methylation upon the transcription and function of potentially impacted cells in PI cattle.

Conclusions

Research on BVDV PIs remains necessary to minimize losses in the global cattle industry. As the main reservoir of the virus, it is critical to understand how these persistent infections are established and maintained. In this study, 4-month-old PI heifers infected with a BVDV1b isolate were found to contain differential methylation of genes within the immune system, generation of blood cells, and the heart. Concurrently, complete blood count analysis at 4 months of age revealed microcytic anemia, an overabundance of small platelets, and elevated monocytes. Through flow cytometry, we determined that the PI heifers also displayed decreased populations of T lymphocytes, specifically $\gamma\delta^+$, $CD4^-/CD8b^-$, and helper T cells while also exhibiting increased percentages of $CD4^+/CD8b^+$ T cells (Figure 2.7). The data herein supports the narrative of immunosuppression in PI heifers through the perspective of compounding epigenetic alteration through methylation of genes. This work provides potential translatability to other vertically transmitted viruses such as hepatitis C, Zika virus, HIV, and Oropouche virus. With continued research and comparison, it may one day be possible to differentiate between the direct and indirect consequences of gestational viral infections.

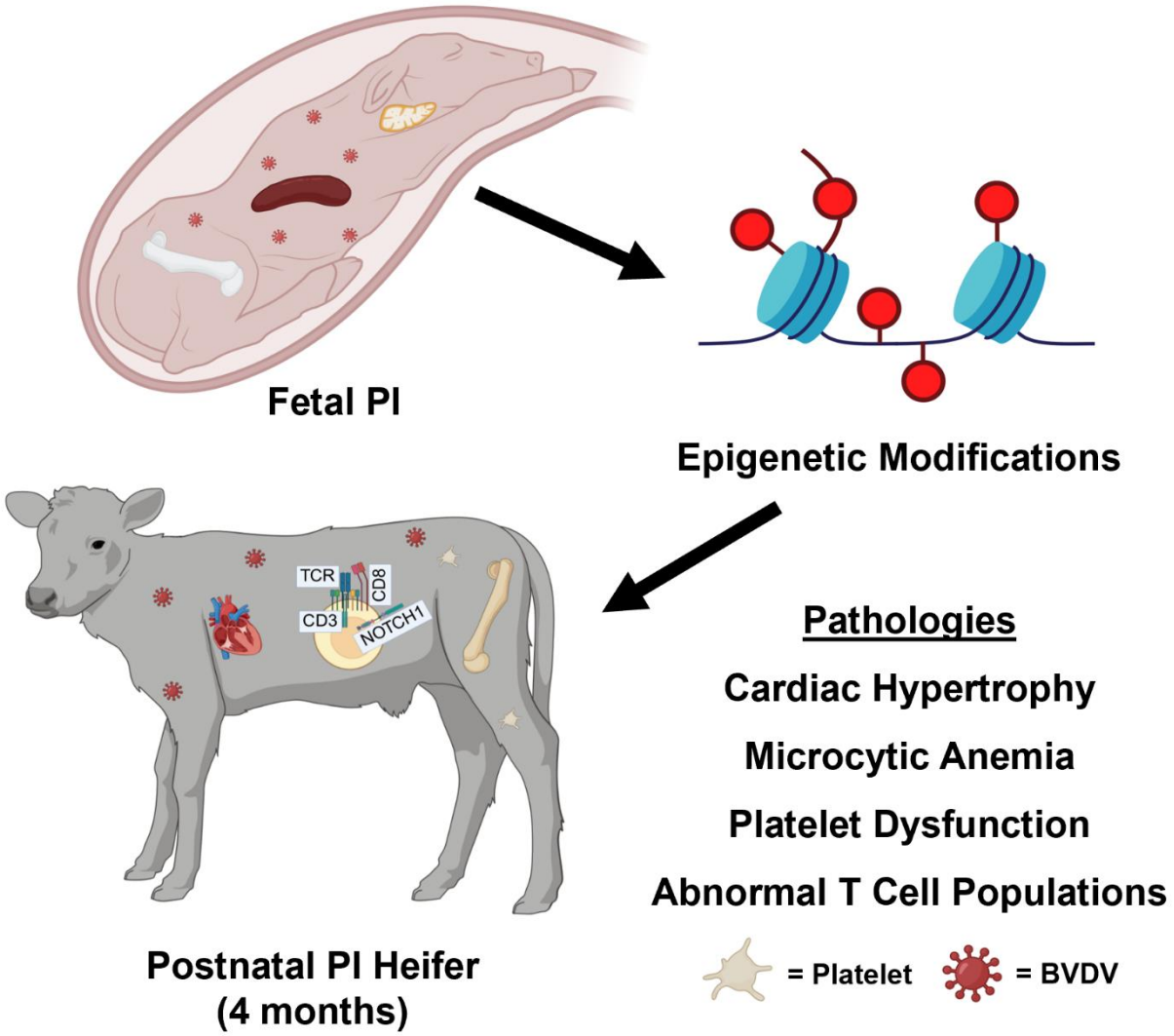

Figure 2.7. Graphical Summary of Results.
Fetal infection with BVDV leads to epigenetic modifications that persist to the postnatal period and correspond with observed pathologies that include cardiac hypertrophy, microcytic anemia, platelet dysfunction, and abnormal T cell populations.

CHAPTER 3: FETAL TRANSIENT INFECTION WITH BOVINE VIRAL DIARRHEA VIRUS INDUCES POSTATAL EPIGENETIC DIFFERENCES IN WBC DNA[2]

Short Summary

Bovine viral diarrhea virus (BVDV) is the most detrimental pestivirus within the cattle industry. Infection with vertically transmissible BVDV prior to 125 days of gestation results in the generation of a persistently infected (PI) calf. These PI calves are unable to clear the virus *in utero*, due to an incomplete immune response. However, when infection with BVDV occurs after 150 days of gestation, the fetus clears the transient infection (TI) *in utero* and is born with antibodies specific to the infecting strain of BVDV. Variations in DNA methylation have been identified in white blood cells (WBC) from TI heifers at birth. It was hypothesized that epigenomic alterations persist into the postnatal period and contribute to previously undocumented pathologies. To study these possible effects, DNA was isolated from the WBCs of 5 TI heifers and 5 control heifers at 4 months of age and subjected to reduced representation bisulfite sequencing (RRBS). Differential analysis of the methylome revealed a total of 3,047 differentially methylated CpG sites (DMSs), 1,349 of which were hypermethylated and the other 1,698 were hypomethylated. Genes containing differential methylation were associated with inflammation, reactive oxygen species (ROS) production, and metabolism. Complete blood count (CBC) data identified a higher lymphocyte percentage in TI

[2]Kincade JN, Engle TE, Henao-Tamayo M, Eder JM, McDonald EM, Deines DM, Wright BM, Murtazina DA, Bishop JV, Hansen TR, et al. Postnatal epigenetic differences in calves following transient fetal infection with bovine viral diarrhea virus. *BMC Genomics.* 2025; 26(1): p. 441. https://doi.org/10.1186/s12864-025-11562-5

heifers. When compared in the context of the $CD45^+$ parent population, spectral flow cytometry revealed increased intermediate monocytes, B cells, and $CD25^+/CD127^-$ T cells, and decreased $CD4^+/CD8b^+$ T cells. Comparative analysis revealed differential methylation of CpG sites contained in 205 genes, 5 promoters, and 10 CpG islands at birth that were also present at 4 months of age. Comparison of differential methylation in TI heifers and PI heifers at 4 months of age showed 465 genes, 18 promoters, and 34 CpG islands in common. Differential methylation of WBC DNA persists to 4 months of age in TI heifers and is associated with dysregulation of inflammation, metabolism, and growth. Analysis of differential methylation in TI heifers contributes to the understanding of how fetal infection with BVDV induces postnatal detriments related to profit loss.

Introduction

Bovine viral diarrhea virus (BVDV) is a globally prevalent virus that causes billions of dollars in loss to the cattle industry. It is estimated that an outbreak of BVDV costs a cattle producer anywhere from $20 to $103 per infected animal [3, 220]. Acute infections resulting from horizontal transmission not only decrease the average daily weight gain and milk production but cause reproductive losses as well [3, 40, 182-185, 245]. Additionally, BVDV is one of the few viruses capable of crossing the placenta and infecting the fetus during gestation. The outcome of a fetal calf infected in utero depends largely on the developmental progress of the adaptive immune response [182, 186, 187]. If the infection occurs early in gestation, after 30 days of gestation but prior to 125 days of gestation, the fetus mounts an incomplete immune response and is unable to clear the virus [122, 167, 169, 173, 178, 186]. These calves, termed persistently

infected (PI), are immunotolerant and serve as the primary reservoir for the virus due to their chronic shedding of the virus.

If fetal infection occurs after 150 days of gestation, the fetus mounts a more robust immune response. The generated immune response induces both innate and adaptive immunity, as evidenced by transcriptional activation of genes associated with inflammation and viral immunity (DDX58, NFκB, IRF7, IFNβ, and ISG15) as well as those associated with T and B cells (PSMB9, IFI30, CD4, CD8A, CD8B, and CD79B) [122]. These calves, termed transiently infected (TI), produce antibodies specific to the infecting strain of BVDV and clear the virus prior to birth. Currently, there is no way to distinguish calves with BVDV TI in utero from those that experience TI with BVDV in the early postnatal period.

Environmental influences such as nutrition, stress, and disease can affect the postnatal health and development of an organism, per the developmental origin of health and disease (DOHaD) theory. One study of postnatal effects following fetal TI found calves to be 2.3 times more likely to develop an illness requiring treatment [246], while another demonstrated lower body weight in suspected TI calves [247]. It has recently been shown by our laboratory that during a feed trial, heifers infected with BVDV during late fetal development (TIs) have a lower entry and exit body weight as well as decreased average daily gain [180]. During the feedlot trial, TI heifers also exhibited signs of increased inflammation which include decreased glutathione, increased oxidized glutathione, and increased plasma ceruloplasmin concentrations [180]. We have previously demonstrated that TI heifers have lower mean body weight and differential methylation of white blood cell (WBC) DNA in genes associated with the

immune system, growth, and development at birth [179]. However, little remains known about the postnatal epigenetics of TI calves.

Methylation of DNA in mammals occurs most often on cytosines that are immediately followed by guanines [143]. These cytosine-phosphate-guanine (CpG) motifs are known to enhance transcriptional binding when not methylated, but in striking contrast, methylation of these sites is known to effectively silence gene transcription [147]. Other viruses within Flaviviridae such as hepatitis c virus and Zika virus are known to evade immune detection through manipulation of epigenetic mechanisms [248, 249]. Differential methylation of splenic tissue and WBCs has been demonstrated in PI calves at day 245 of gestation and 4 months of age, respectively [175, 250]. Moreover, differential methylation has been identified in TI calves at birth [179]. Because gestation is a time of high fetal epigenetic plasticity, it is possible that normal fetal epigenetic programming is disrupted by fetal BVDV infection. Per the DOHaD theory, it was then hypothesized that epigenetic alterations in TI fetal DNA due to fetal BVDV infection persist into the postnatal period and continue to impact immune function and growth. In this study, fetal TI and control heifers were generated by inoculating seronegative pregnant heifers on day 175 of gestation with a non-cytopathic (ncp) strain of BVDV type 2 or sham-inoculated with phosphate buffered saline. The methylation of WBC DNA in four-month-old heifers born from dams infected with BVDV during pregnancy was compared to that of uninfected controls. Complete blood counts (CBCs), flow cytometry analysis, and body weight demonstrate the state of the immune system and growth.

Materials and Methods

Animals

Twenty-eight yearling, Hereford heifers were purchased from a private Montana ranch that does not vaccinate for BVDV. These heifers were housed at the Animal Research, Development, and Education Center (ARDEC) at Colorado State University (CSU) where they were vaccinated with Ultrabac 7 (Zoetis, Kalamazoo, MI, USA) upon arrival and one month later. Heifers were then moved to the Animal Reproduction and Biotechnology Laboratory (ARBL) at CSU for breeding. Estrous cycles were synchronized in yearling heifers using 14-day intravaginal progesterone devices (EAZI-BREED, Zoetis) and an intramuscular injection of prostaglandin F2α (Lutalyse HighCon, Zoetis). Estrus was detected using heat-detection patches (Estrotect, Spring Valley, WI, USA) and visual observation. Upon detection of estrus, heifers were artificially inseminated with X-bearing sperm from a single Angus bull (Select Sires MidAmerica, Logan, UT, USA). The pregnant dams were inoculated with BVDV or sham inoculated with phosphate buffered saline on day 175 of gestation. Pregnant heifers were vaccinated with ScourGuard 4KC (Zoetis) at 6 and 3 weeks prior to the expected calving date. The dams of the calves generated were sold at auction after weaning. Control and TI heifer calves were maintained on a standard finishing ration at ARDEC until 4 months of age. Upon completion of the longitudinal study, heifers were euthanized humanely at 17 months of age using penetrative captive bolt followed by exsanguination at the JBS Global Food Innovation Center (GFIC) at CSU.

Study Design

To study the postnatal impact of fetal TI with BVDV, 12 of the heifers seronegative for BVDV were randomly selected for inoculation with 4.0 $\log_{10}TCID_{50}$/mL of non-cytopathic BVDV 2 type 96B2222 at day 175 of pregnancy (Figure 3.1) [179]. The separately housed treatment groups were confirmed by serum neutralization testing; all BVDV inoculated dams seroconverted and all sham inoculated dams remained seronegative. The other twelve dams were sham inoculated with phosphate buffered saline. Twelve female control pregnancies were carried to term. Twelve TI pregnancies were carried to term and resulted in the generation of our TI group; a single TI bull calf was excluded from the study to prevent skew of the data due to potential sex differences (n = 11). Treatment groups were again confirmed; all calves from BVDV inoculated cows were seropositive at birth and all sham inoculated calves were seronegative at birth. Heifers were assigned a number ID based on their birth date for the duration of the study. At 4 months of age, multiple blood samples from all heifers were collected. Two of which were analyzed for complete blood count and flow cytometry. The WBCs were isolated from whole blood samples for DNA extraction and subsequent reduced representation bisulfite sequencing (RRBS). A total of 10 samples were sent to Zymo Research for sequencing; 5 samples were selected at random from both the control and TI group.

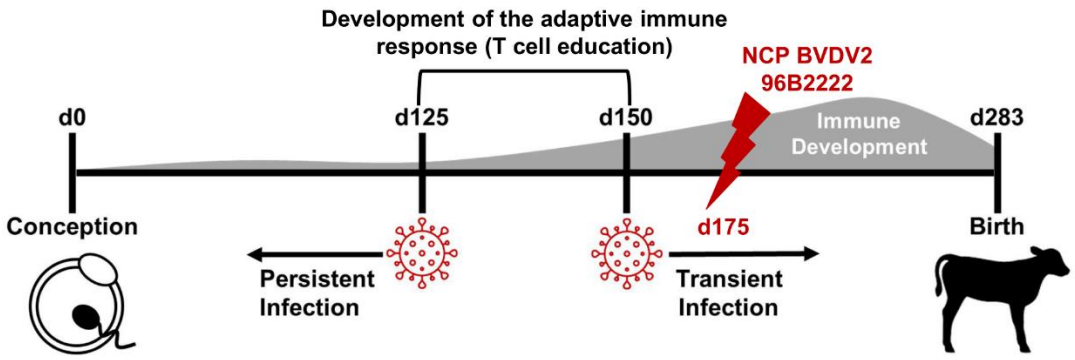

Figure 3.1 – Generation of calves transiently infected with BVDV *in utero.* Gestational day is indicated by 'd' followed by a number. The lightning bolt indicates the day of maternal infection with non-cytopathic BVDV.

Hematology

Whole blood samples were collected from 4-month-old calves in K_2EDTA tubes (Becton, Dickinson and Company, Franklin Lakes, New Jersey, USA cat# 07417) for DNA, RNA, flow cytometry, CBCs (Heska Elemental 5), and immunoglobulin concentration testing. Samples were stored on ice until processing. Upon arrival at the ARBL, the whole blood samples were centrifuged at 1500 x g for 15 minutes at 4°C to separate the serum, buffy coat, and red blood cells. The buffy coat was aspirated and transferred to a sterile 15mL tube containing 5 mL of ammonium-chloride-potassium lysing buffer (ACK; KD Medical, Columbia, MD, USA, cat # TGF-3015). Following a 5-minute incubation at room temperature, centrifugation at 300 x g for 10 minutes at 4°C was used to pellet the WBCs. The supernatant was discarded, and the pellet was resuspended in 2.5 mL of ACK lysing buffer. After another 5-minute incubation at room temperature, the pelleting of the WBCs via centrifugation, and decanting of the supernatant, the pellet was resuspended in phosphate buffered saline at a pH of 7.4. The sample was pelleted again by centrifugation at 300 x g for 10 minutes at 4°C, the supernatant was discarded, and the WBCs were resuspended in 1 mL of phosphate

buffered saline. The samples were snap-frozen using dry ice and stored until DNA extraction. These methods are previously described in [179].

Reduced Representation Bisulfite Sequencing

White blood cell samples for RRBS were processed according to manufacturer's instructions using the Qiagen DNeasy Blood and Tissue Kit (Qiagen, Germantown, Maryland, USA). Samples were shipped on dry ice to Zymo Research (Irvine, CA, USA) for paired end RRBS. Samples were digested using MspI (NEB; Ipswich, MA, USA) and purified with DNA Clean & Concentrator-5 (Zymo Research). Per Illumina's specifications, fragments were ligated to pre-annealed adapters with cytosine replaced with 5'-methyl-cytosine. Ligated fragments larger than 50 base pairs were recovered with DNA Clean & Concentrator-5 (Zymo Research) and bisulfite treated with EZ DNA Methylation-Lightning Kit (Zymo Research). Using Illumina indices, samples were subjected to PCR and purified using DNA Clean & Concentrator-5 (Zymo Research). Sample size and concentration were confirmed using the Agilent 2200 TapeStation and libraries were sequenced using a NovaSeq6000.

Zymo Research trimmed and filtered sequences shorter than 20 base pairs using TrimGalore (v0.6.4_dev). FastQC (v0.11.9) was used to determine quality Phred scores, per sequence GC content, and remove overrepresented sequences. Adapter contamination was below 0.1% in all samples. Samples were aligned to a bisulfite converted version of the most recent bovine reference genome from the University of California, Santa Cruz (UCSC; ARS-UCD1.2/bosTau9) using Bismark (v0.22.3). The average observed vs expected methylation level and the associated Pearson correlation

coefficients were found using MethylDackel (v0.5.0). Additional details pertaining to quality control performed by Zymo Research can be found on using GitHub username Zymo-Research within the 'service-pipeline-documentation' repository, folder 'docs', file 'how_to_read_methylseq_report.basic.'

The average CpG coverage was 8X, the average quantity of unique CpGs per sample was 7.9 million. The average total number of reads was approximately 40 million per sample. The percent bisulfite conversion rate was greater than 99% for both non-CpG and spike-in reads. All mean quality scores (Phred) were greater than 30 at all base pairs. An average of 33% of reads mapped uniquely to a single sequence within the genome, an average of 51% mapped ambiguously to more than a single sequence within the genome, and an average of 16% did not align at all. Pearson correlation coefficients for observed vs expected methylation level were greater than 0.95 for all samples.

Methylation Bioinformatics and Pathway Analysis

Files received by Zymo Research were processed as raw .bam files using the methylKit package in R [199]. These files were aligned to the most recent bovine genome available through the UCSC (ARS-UCD1.2/bosTau9). Data was initially filtered to remove sites containing less than 10 reads or reads greater than the 99.9th percentile. Data was normalized by median coverage, filtered by a standard deviation of 2, and assessed for outliers. To eliminate SNPs and potential genetic variance, only cytosines identified in all samples in both the treatment and control group were stored for analysis, as per methylKit. Logistic regression was used to identify singular CpG

sites containing hypermethylation (positive meth.diff values) or hypomethylation (negative meth.diff values). Singular CpG sites were classified as differentially methylated if the site varied in methylation in at least 25% of the treatment group (absolute value of meth.diff > 25) and the false discovery rate (FDR/q-value) was less than 0.01. Identified CpG sites containing differential methylation were annotated and mapped to genes using the most recent reference genome available from the UCSC (ARS-UCD1.2/bosTau9).

Subsequent analyses identified regions of the genome mapped either as promoters or CpG islands. Experimentally validated promoters included in the UCSC reference genome were mapped and analyzed for differential methylation. The UCSC also provides a publicly available reference track mapping areas likely to be CpG islands. These areas must have a length greater than 200 base pairs, a guanine-cytosine content of greater than 50%, and an observed-to-expected CpG ratio greater than 0.6. The methylKit package contains functions that summarize the methylation data contained within a specified region. The quantified summary of methylation within a specific region can then be compared between treatment groups to reveal differential methylation in regions with greater regulatory function. Logistic regression was utilized to compare the levels of methylation between control and treatment groups. The CpG islands and promoters were deemed differentially methylated if the absolute value of meth.diff > 15 and FDR/q-value < 0.01. Genes associated with differential methylation were annotated using commands from ‘genomation’, ‘clusterProfiler’, and ‘org.Bt.eg.db’ in R [200, 202]. Bioinformatic code is available online at GitHub user profile jnkincade repository Bovine-RRBS-Analysis.

Data resulting from differential analysis was analyzed using Ingenuity Pathway Analysis (IPA; Qiagen, Germantown, Maryland, USA). The IPA software contains pathways consisting of a list of genes pertaining to a specific function, disease, or process. The IPA software utilizes a fisher's exact test to assign a p-value to each pathway based on the probability that the observed overlap between genes in the dataset and predetermined pathways are due to random chance. The IPA software also calculates a predictive value, a z-score, to each pathway based on the input data [251]. The canonical pathways were then sorted according to the absolute value of the z-score, from largest to smallest, with positive z-scores indicating activation and negative z-scores indicating inhibition. The machine learning (ML) disease pathways do not have an associated z-score and were instead sorted according to the largest -log(p-value). Predicted upstream regulators are identified in IPA based on how many known downstream targets are identified within the dataset. A prediction of activation or inhibition is made according to the observed differential measures of the identified downstream activators.

Previously analyzed data utilized for comparisons herein can be found within publications titled "Epigenetic Modifications of White Blood Cell DNA Caused by Transient Fetal Infection with Bovine Viral Diarrhea Virus" (DOI: 10.3390/v1605721) and "Epigenetic Alterations in Calves Persistently Infected with Bovine Viral Diarrhea Virus." Details pertaining to the analysis of previously published datasets can be found within their respective publications but were identical to methods published herein. A file listing individual DMSs, along with promoter and CpG island differentially methylated regions (DMRs), was generated for the TI calves at 4 months of age and previously published

datasets. The file includes the chromosome, start position, end position, gene symbol, gene name, REFSEQ, and ENTREZID in which the identified DMS was contained. The associated p-value, q-value, and meth.diff value were also listed. These files were merged according to gene symbol in R, allowing for comparison of DMSs within the same gene body. A secondary comparison was made to yield only DMSs with similar methylation status at both timepoints (MIF contained hypermethylated DMSs at birth in TI heifers and at 4 months). Genes containing multiple DMSs with opposing methylation (hyper and hypomethylation of DMSs within a single gene) were excluded from this comparison.

Flow Cytometry

Whole blood samples were collected in K_2EDTA tubes and processed by Zoetis Inc. Red blood cells were lysed using 1X RBC lysis buffer (eBiosciences, San Diego, CA, USA cat # 00-4300-54). After centrifugation at 500 x g for 5 minutes, the supernatant was discarded and the pellet was resuspended in 1 mL of Dulbecco's phosphate buffered saline (DPBS; ThermoFisher, Waltham, MA, USA cat # 14190-136). After adding an additional 10 mL of DPBS to the solution, the samples were centrifuged at 500 x g for 5 minutes. The supernatant was discarded, and the pellet resuspended in 1 mL of DPBS before filtering through a cell-strainer cap (Corning, Corning, NY, USA cat # 352235). After a 1:20 dilution using DPBS, the concentration of viable cells was determined using a Vi-CELL (Beckman Coulter, Loveland, CO, USA). Viable cells were seeded into a 96 well plate at a concentration of 1 x 10^6 cells per well. Remaining cells were frozen in a solution of Serum Free Cell Freezing Medium (ATCC, Manassas, VA, USA cat # 30-2600) and stored at -80°C. Each well containing cells in the 96 well plate

was brought to a final volume of approximately 200-300 µL with DPBS. The plate was centrifuged, supernatant discarded, and the cell pellets resuspended in 100 µL of Fixable Viability Stain 620 (BD Biosciences, Franklin Lakes, NJ, USA cat # 564996) at a 1:1000 concentration. After a dark, 10-minute incubation on ice, 200 µL of fluorescence-activated cell sorting (FACS) buffer (BD Biosciences, cat # 554657) was added to each well. The plate was centrifuged, the supernatant discarded, and the cells were resuspended in 100 µL of the staining master mix. The cells were incubated in the staining solution for 20 minutes in the dark, on ice. Another 200 µL of FACS buffer was added before the plate was centrifuged and the supernatant was discarded. Cells were washed using 300 µL of FACS buffer, centrifuged, and the supernatant was discarded. Cells were resuspended in 100 µL of diluted stabilizing fixative (1:3; BD Biosciences, cat # 338036) and incubated at room temperature for 5 minutes. Lastly, 100 µL of FACS buffer was added to each well, the plate was centrifuged, the supernatant was discarded, and the cells were resuspended in 200 µL of FACS buffer. Samples were held in the dark at 4°C until analysis. Cell samples were run at the CSU Flow Cytometry Core using a 4L 16V-14B-10YG-8R Cytek Aurora spectral cytometer.

Data was gated using FlowJo (BD Biosciences, Franklin Lakes, NJ, USA). Flow cytometry data in the form of frequency relative to the parent population of either CD45 positive cells or CD3 positive cells was compared in GraphPad Prism 10 (GraphPad Software, San Diego, CA, USA).

Statistical Analysis

Statistical analyses were performed in GraphPad Prism 10 (GraphPad Software, San Diego, California, USA). Values within the control or treatment group were first tested for normality. Outliers were identified and removed prior to analysis but are denoted in figures as a hollow circle. Data with normal distribution was analyzed using an unpaired parametric t-test. Because the control group contained values from 12 heifers and the treatment group contained values from 11 heifers, Welch's correction was applied. Data that was not normally distributed was subjected to a non-parametric Mann-Whitney test. Differences between controls and TI heifers were considered significant if $p < 0.05$. Data are presented as mean ± standard error of the mean (SEM).

Results

Generation of TI calves and Body Weight

At 4 months of age, the average body weight of the TI heifers was lower than the average body weight of the control heifers (165.6 ± 2.918 kg vs 144 ± 7.53 kg; $p < 0.01$; Figure 3.2).

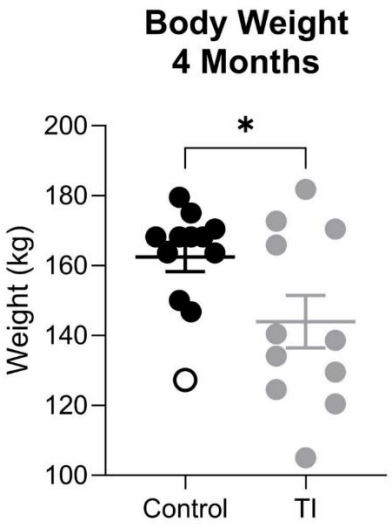

Figure 3.2 – Body weight is decreased in TI heifers at 4 months of age.
Quantification of body weight in kilograms of control and TI heifers at 4 months of age. A single outlier (Control - 127.27kg) was excluded from significance testing but is denoted within the figure as a hollow circle. Following removal of the outlier, the data passed a Shapiro-Wilk normality test. Data are displayed as mean ± standard error of the mean (SEM). Asterisks denote the significance between groups, ** $P < 0.01$.

DNA Methylation

Whole blood was collected from 4-month-old heifers and processed to extract DNA from WBCs. These DNA samples were subjected to classic RRBS to determine CpG methylation status. The epigenomes of 5 TI heifers were compared to the epigenomes of 5 control heifers. The average rate of bisulfite conversion for all samples was 99.2% for non-CpG sites and 99.4% for known DNA spike-ins, which serve as a quantifiable control. Within the control group, 32.74% of bisulfite converted sequences aligned uniquely to the most recent reference genome and 51.02% aligned ambiguously. Within the TI group, 33.14% of bisulfite converted reads aligned uniquely and 50.16% aligned ambiguously to the reference genome. The average CpG coverage was 8X. Phred scores were above 30 at all base positions, indicating the potential for an

incorrectly labeled nucleotide to be less than or equal to 1 in 1000 (99.9% accuracy). Hierarchical clustering of sample methylation profiles using 1 - Pearson's correlation distance demonstrated overall similarity between control and TI heifers (Figure 3.3A). Identified differentially methylated CpG sites DMSs had a differential methylation (meth.diff) of greater than 25% and a false discovery rate of less than 0.01, per the calculateMethDiff() default. The meth.diff values were identified through logistic regression that compared the fraction of methylation in TI heifers to that of control heifers at a specific CpG site [199]. A total of 3,047 DMS were identified throughout the genomes of TI heifers when compared to controls (Figure 3.3B). Of the DMSs, 1,698 sites were hypomethylated (56%; meth.diff > 25) and 1,349 sites were hypermethylated (44%; meth.diff < -25; Figure 3.3C).

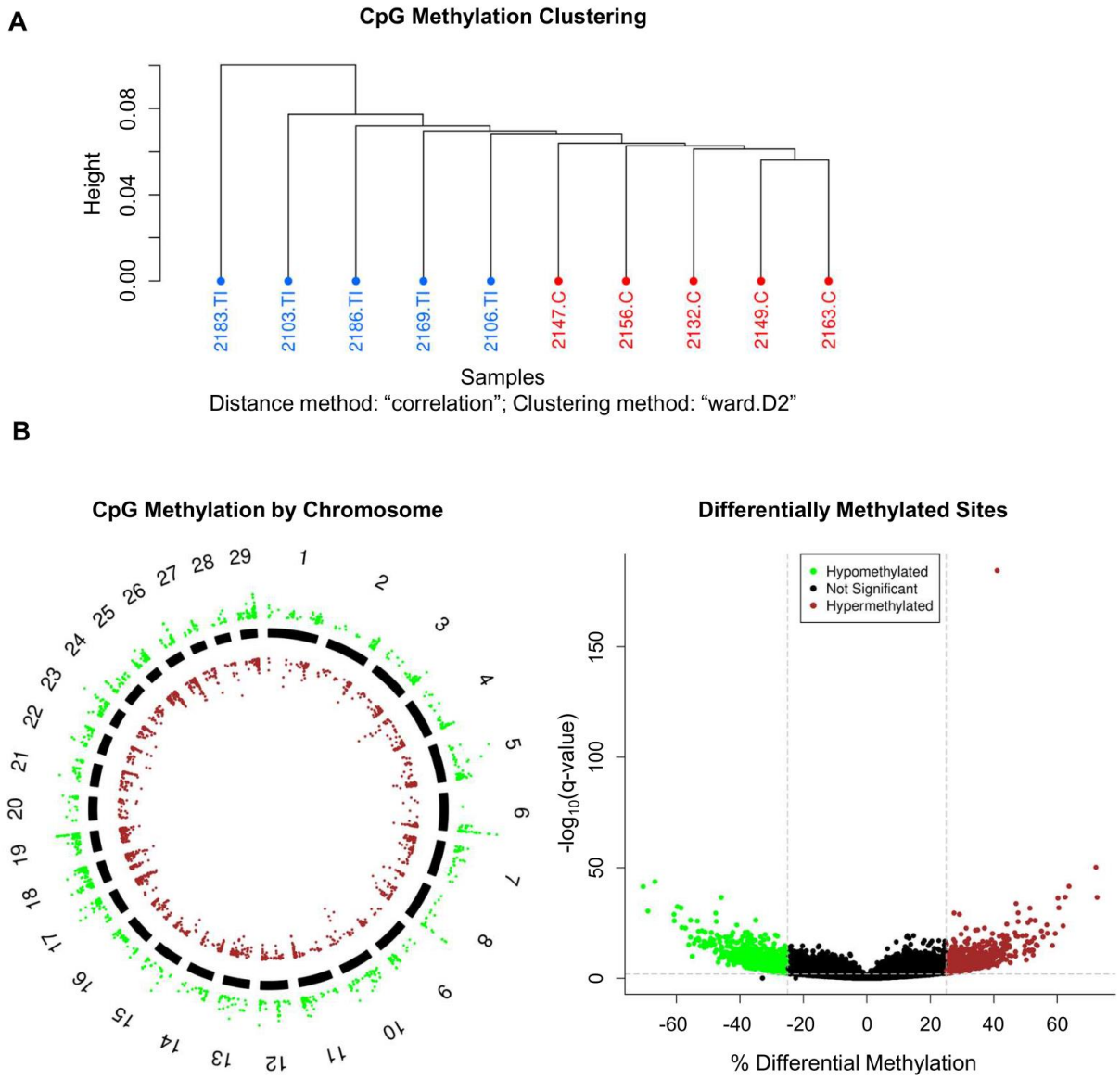

Figure 3.3 – Differential methylation of CpG sites in TI heifers.
The CpG sites are defined as sites containing a 'CCGG' motif within the genome. (A) Hierarchical clustering of sample methylation profiles based using 1 - Pearson's correlation distance. Control heifers are denoted in red and heifer ID numbers are followed by '.C'. Transiently infected (TI) heifers are denoted in blue and animal ID numbers are followed by '.TI'. (B) Visualization of differentially methylated CpG sites identified in TI heifers compared to controls by chromosome. Each data point represents a differentially methylated CpG site in respect to its location on the chromosome. Hypermethylated CpG sites are denoted in green and are positioned outside of the solid chromosome bars. Hypomethylated CpG sites are denoted in red and are positioned within the solid chromosome bars. (C) Visualization of the hypermethylated and hypomethylated CpG sites identified in TI cattle compared to controls. The –log10(q-value) Y axis threshold was set at 2 and denoted as a horizontal, grey dashed line. The % differential methylation X axis thresholds were set at -25 and 25 and are denoted as vertical, grey dashed lines. Hypermethylated CpG sites are denoted in green and hypomethylated CpG sites are denoted in red.

Once identified, DMSs were annotated according to which gene body the site was contained within. The DMSs were then categorized based on their location within the gene body according to the reference genome obtained from the UCSC, 40% of DMSs were found within introns, 36% within intergenic regions, 13% in exons, and 11% within promoters. A total of 1,562 genes contained a single DMS, while 518 genes were identified to contain multiple DMSs (Table 3.1).

Table 3.1 – Genes containing single or multiple differentially methylated CpG sites in TI heifers.
Column 1 contains the quantification of genes containing the corresponding number of differentially methylated sites (DMSs) as listed in column 2. The ranges of adjusted q-value and percent of differential methylation (meth.diff) for the total number of genes in column 1 are listed in column 3 and 4.

Genes containing single or multiple differentially methylated CpG sites in TI heifers

Genes Containing	# of DMS	Adj. Q Value	Meth.Diff
1,562	1	$4.28e^{-185}$ – $6.05e^{-3}$	-69.01 – 72.20
326	2	$2.55e^{-42}$ – $5.55e^{-3}$	-58.35 – 72.58
106	3	$3.29e^{-30}$ – $4.81e^{-3}$	-54.47 – 55.54
34	4	$1.10e^{-19}$ – $2.81e^{-4}$	-52.54 – 47.57
17	5	$1.84e^{-37}$ – $1.61e^{-3}$	-42.59 – 56.91
9	6	$1.91e^{-37}$ – $1.57e^{-3}$	-41.23 – 62.53
8	7	$3.30e^{-42}$ – $1.71e^{-3}$	-70.50 – 51.93
2	8	$1.29e^{-22}$ – $1.46e^{-5}$	25.85 – 44.01
4	9	$2.99e^{-19}$ – $5.73e^{-4}$	-51.29 – 39.33
5	10	$1.73e^{-21}$ – $5.22e^{-5}$	-47.84 – 37.85
5	11	$1.29e^{-21}$ – $9.07e^{-4}$	-50.97 – 41.51
1	13	$3.17e^{-16}$ – $1.62e^{-5}$	-25.90 – 37.66
1	14	$4.36e^{-27}$ – $8.17e^{-4}$	-55.56 – 51.62

To identify differentially methylated CpG islands and promoters, differential methylation was required to be greater than 15% and have a false discovery rate of less than 0.01. Both CpG islands and promoter regions were identified using the most recent bovine reference genome (bostau9, 2018) from the UCSC. The meth.diff threshold was

decreased when identifying regions to preserve potential true positives within the small sample size. Within TI heifers, 84 CpG islands were differentially methylated. Of the CpG Islands, 45 were hypomethylated (54%) and 39 were hypermethylated (46%). The TI heifers also exhibited differential methylation of 106 promoters, 62 of which were hypomethylated (58%) and 44 of which were hypermethylated (42%).

The DMSs identified during differential analysis of TI and control heifer epigenomes were further examined using IPA software (Qiagen, Germantown, MD, USA). The IPA software identified which canonical pathways and disease pathways were most likely to be altered in the TI heifers compared to controls. Pathways identified by IPA list the number of genes identified within the dataset over the number of genes within the IPA pathway database. Canonical pathways in the IPA software are curated to the current understanding of biological functions. Pathways identified in IPA were sorted according to the absolute value of the z-score, from largest to smallest. A positive z-score indicates activation of the pathway, while a negative z-score indicates inhibition. The canonical pathways with the top highest z-scores include White Adipose Tissue Browning Pathway (3.13), Integrin Signaling (2.82), Myelination Signaling Pathway (2.8), Ephrin Signaling Pathway (2.67), and Transcriptional Regulation by RUNX2 (2.6; Figure 3.4A). The IPA software includes pathways containing genes that are associated with specific diseases that have been generated by machine learning software. The top 5 ML disease pathways identified by IPA altered in TI heifers with the most significant p-value included heart septal defect (5.5), atrial or ventricular septal defect (5.5), ventricular septal defect (4.7), nephrosis (4.54), and familial nephrotic syndrome (4.54; Figure 3.4B).

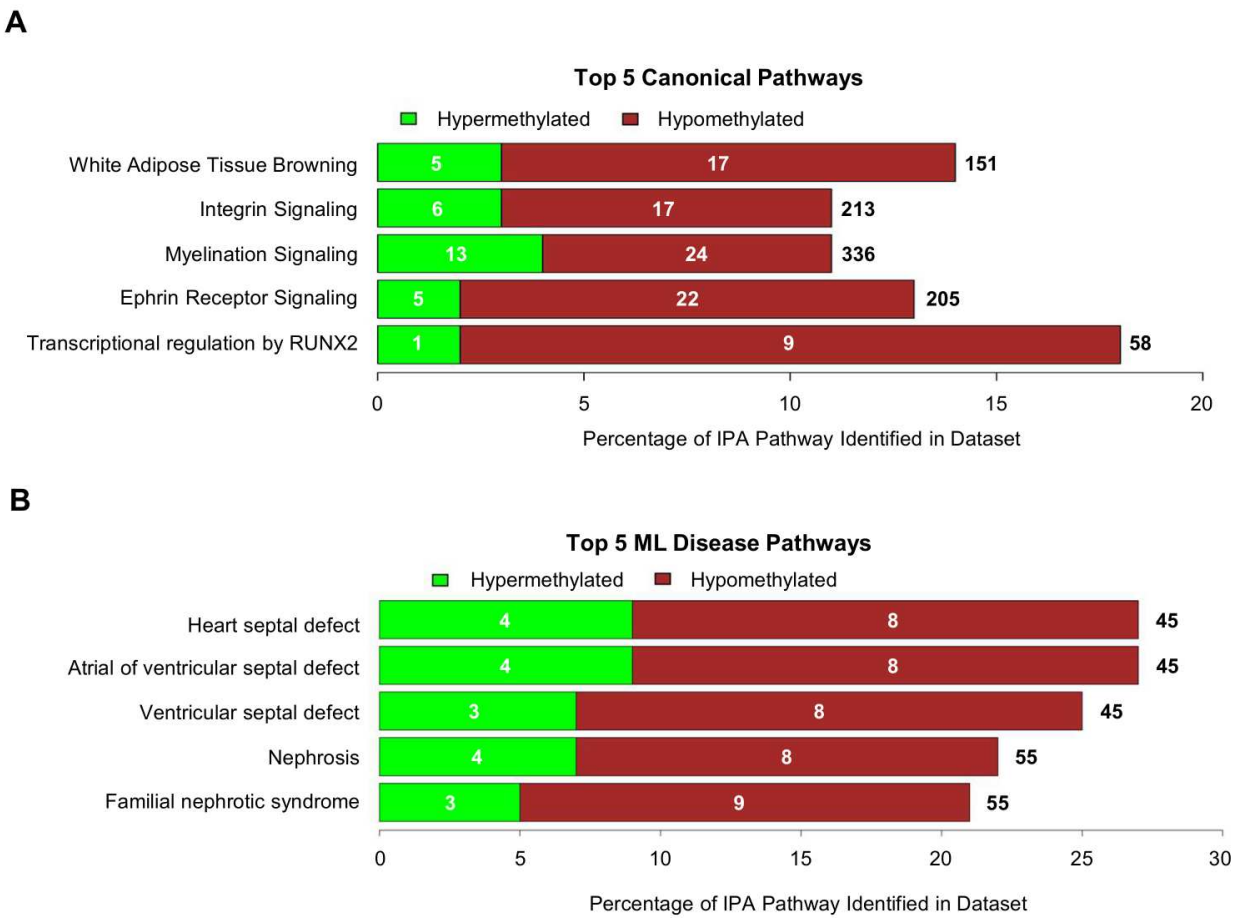

Figure 3.4 – IPA predicted impacts on TI cattle through utilization of differentially methylated CpG sites.
Top 5 canonical pathways and machine learning (ML) disease pathways as determined by IPA. Green denotes hypermethylation while red denotes hypomethylation. The total number of genes included in the IPA pathway is denoted to the right of each stacked bar. The number of hypo- or hyper- methylated genes identified in the dataset are denoted within each stacked bar. (A) Canonical pathways were sorted according to the absolute value of the predictive z-score determined by IPA. (B) Disease pathways were sorted according to the -log(p-value) determined by IPA.

Several genes contained multiple sites of differential methylation within their promoter regions (Table 3.2). Genes are listed in the following format: *GENENAME* (methylation status; number of DMS with denoted methylated status). These genes include *BREH1* (hypermethylated x4), *ABCA9* (hypermethylated x2), *RIPOR2* (hypermethylated x2), *BCKDK* (hypermethylated x2), *LOC613282* (hypermethylated x2), *LOC104974744* (hypermethylated x2), *PODNL1* (hypomethylated x5), *ILVBL*

(hypomethylated x4), *LOC112448525* (hypomethylated x4), *ASZ1* (hypomethylated x2), *SORBS1* (hypomethylated x2), *RUSC1* (hypomethylated x2), and *LOC112444767* (hypomethylated x2).

Table 3.2 – Genes containing multiple differentially methylated CpG sites within promoter regions in TI heifers.
Listing of genes containing multiple differentially methylated CpG sites within a promoter region in TI heifers. Information is presented in each row corresponds to the gene name, whether the promoter region within the gene contained hyper- or hypo- methylation, and the number of differentially methylated CpG sites contained within the promoter region.

Genes containing multiple differentially methylated CpG sites within promoter regions in TI heifers

Gene Name	Methylation Status	Number of CpG Sites
BREH1	Hyper	4
ABCA9	Hyper	2
RIPOR3	Hyper	2
BCKDK	Hyper	2
LOC613282	Hyper	2
LOC104974744	Hyper	2
ASZ1	Hypo	5
SORBS1	Hypo	4
RUSC1	Hypo	2
LOC112444767	Hypo	2

Comparison of WBC differential methylation in TI heifers compared to controls at birth and 4 months of age

The list of genes containing DMSs identified in the DNA of WBCs from TI heifers at 4 months of age was compared to those identified in the same TI heifers at birth [179]. At birth, 2,349 DMSs were identified within a total of 1,563 genes. Of these genes, 503 were identified to contain DMSs at 4 months of age. After removal of genes containing both a hypermethylated and hypomethylated DMS, 205 CpG sites were identified to contain the same differential methylation status in comparison to controls at birth and 4 months of age (S file 1 ‘d0TI vs 4moTI – DMS’). At birth and 4 months of age, 5 genes contained differentially methylated promoters, and 10 genes contained a

differentially methylated CpG island. Genes that contained differentially methylated promoters at birth and 4 months of age include *UBXN11, MMP9, VWA3B, LOC520626,* and *LOC112449328* (Table 3.3). Genes containing a differentially methylated CpG island include *EIF2S2, CACNG1, CELA3B, RAB20, UBAC1, LOC107131849, LOC101904842,* and *LOC112448374* (Table 3.3).

Table 3.3 – Comparison of differential methylation in TI heifers at birth and 4 months of age.
Listing of genes containing a differentially methylated promoter or CpG island at birth and 4 months of age (M.O.A.) in TI heifers. The list of genes containing differential methylation in TI calves compared to controls at 4 M.O.A. was generated herein. The list of genes containing differential methylation in TI calves compared to controls at birth was generated in (19). The methylation status (hypermethylated or hypomethylated) is denoted at birth and 4 M.O.A. Genes containing more than one site of differential methylation list the methylation status of both sites. If multiple sites within a promoter or island have the same methylation status, xN is used to denote multiple sites, as in (x2).

Comparison of differential methylation in TI heifers at birth and 4 months of age (M.O.A.)

Promoters

	Methylation Status	
Gene Symbol	Birth	4 M.O.A.
MMP9	hypo	hypo
UBXN11	hyper	hypo
VWA3B	hypo	hyper
LOC520626	hypo	hypo
LOC112449328	hypo	hypo

CpG Islands

	Methylation Status	
Gene Symbol	Birth	4 M.O.A.
CACNG1	hypo	hyper
CELA3B	hyper	hyper
EIF2S2	hyper	hypo
RAB20	hypo	hypo
UBAC1	hypo	hypo
LOC107131849	hypo	hypo
LOC101904842	hyper	hyper
LOC101907146	hyper	hypo
LOC112448374	hyper/hypo	hypo x2

Genes that were identified to contain differential methylation at birth and 4 months of age in TI heifers were extracted from their retrospective datasets and utilized to perform a comparative analysis in IPA. Canonical pathways identified to be altered in TI heifers at birth and 4 months of age include epithelial adherens junction signaling (activated), atherosclerosis signaling (activated), Signaling by Rho family GTPases (activated), cardiac conduction (inhibited), and L1CAM interactions (inhibited). Using

IPA, it was predicted that TI heifers experience decreased growth of lymphoid tissue (Figure 3.5A), decreased growth of muscle tissue (Figure 3.5B), as well as increased differentiation of keratinocytes, development of hematopoietic progenitor cells, differentiation of helper T lymphocytes, and maturation of T lymphocytes. It was also predicted through IPA that TI heifers would suffer from increased bleeding and longer clotting times following injury (Figure 3.5C). Toxicological pathways identified indicate increased levels of alkaline phosphatase, risk of arrhythmia (Figure 3.5D), and proliferation of cardiomyocytes. The IPA software utilizes input data to infer and identify upstream regulators that, if altered, may explain the input data. Upstream regulators identified by IPA include *FGFR1, FGF2, DICER1, FOXC2, INHBA, SOX2, SOX3, SOX9, KLF5, LIF, PTH, cyclic AMP, GLI1,* and *IL6,* among others (S file 2 ‘d0TI vs 4moTI – Upstream Regulators’).

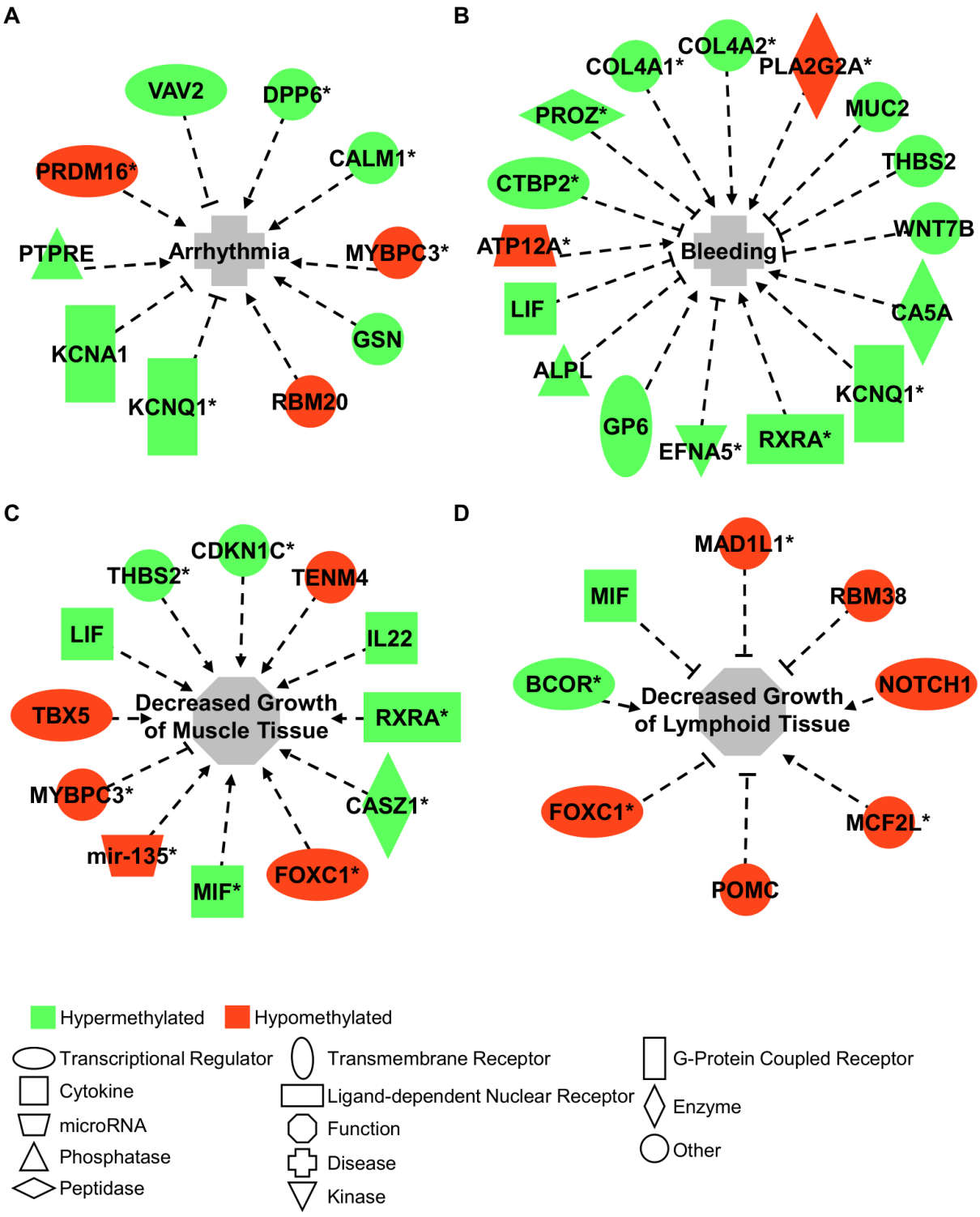

Figure 3.5 – IPA predicts increased risk of arrhythmia and bleeding, decreased growth of muscle and lymphoid tissue.
Modified IPA figures depict genes containing differential methylation that contribute to central diseases or altered functions. (A) Genes associated with arrhythmia. (B) Genes associated with increased bleeding. (C) Genes associated with decreased growth of muscle tissue. (D) Genes associated with decreased growth of lymphoid tissue. Green indicates hypermethylation, red

indicates hypomethylation. Dashed lines ending with a flat line end indicate inhibition. Dashed lines ending with an arrow indicate contribution to the central disease or altered state. Asterisks following a gene name indicate that multiple identifiers in the dataset map to a single gene or chemical in the Global Molecular Network.

Comparison of WBC methylation in TI and PI heifers

The list of genes containing DMSs in TI heifers at 4 months of age was also compared to the list of genes containing DMSs in PI heifers at 4 months of age [250]. The 8,367 DMSs identified in PI heifers were found on a total of 3,812 genes. When compared, 1,098 genes containing at least 1 DMSs were found in both TI and PI heifers at 4 months of age. After removal of genes containing both a hypermethylated and hypomethylated DMS, 465 CpG sites were identified to contain the same differential methylation status in comparison to controls in TI and PI heifers (S file 3 ‘4moTI vs 4moPI – DMS’). Comparison of genes containing differentially methylated promoters revealed 18 genes in common between TI and PI heifers (Table 3.4). Comparison of differentially methylated CpG islands yielded 34 genes in common between TI and PI heifers at 4 months of age (Table 3.4).

Table 3.4 – Comparison of differential methylation in TI and PI heifers at 4 months of age. Listing of genes containing a differentially methylated promoter or CpG island in either TI or PI heifers at 4 months of age. The list of genes containing differential methylation in TI calves compared to controls was generated herein. The list of genes containing differential methylation in PI calves compared to controls was generated in (26). The methylation status (hypermethylated or hypomethylated) is denoted in TI calves and PI calves. Genes containing more than one site of differential methylation list the methylation status of both sites. If multiple sites within a promoter or island have the same methylation status, xN is used to denote multiple sites, as in (x2).

Comparison of differential methylation in TI and PI heifers

Promoters

	Methylation Status	
Gene Symbol	**TI**	**PI**
ABCA2	Hypo	Hypo
ABCA9	Hypo x2	Hyper x2
GBP4	Hypo	Hypo
KIFC3	Hyper	Hyper
LOC112444931	Hypo	Hypo
LOC112447841	Hypo	Hypo
LOC112448077	Hypo	Hypo
LOC112449328	Hypo	Hypo
LOC112449597	Hyper	Hypo
LOC522763	Hypo	Hypo
MMP9	Hypo	Hypo
NEDD4L	Hypo	Hyper
OR4C1J	Hyper	Hyper
P2RY11	Hyper	Hyper
PKNOX2	Hypo	Hypo
SPNS2	Hypo	Hypo
TKDP4	Hypo	Hypo
TNNC1	Hypo	Hypo

CpG Islands

	Methylation Status	
Gene Symbol	**TI**	**PI**
BOC	Hyper	Hyper
CACNG1	Hyper	Hypo
DTX2	Hypo	Hypo
EIF2S2	Hypo	Hypo
FOXS1	Hyper	Hyper
GATD3	Hypo	Hypo
GP9	Hypo	Hypo
IGSF22	Hyper	Hyper
INPP5A	Hypo	Hypo
IRF4	hypo	Hypo
LOC101906717	Hyper	Hypo
LOC101907140	Hypo	Hypo
LOC104972957	Hypo	Hypo
LOC104976302	Hypo	Hypo
LOC107131765	Hypo/Hyper	Hyper
LOC107131849	Hypo	Hypo
LOC107132967	Hypo	Hypo
LOC112443431	Hypo/Hyper	Hypo
LOC112443852	Hyper	Hyper
LOC112444931	Hypo	Hypo
LOC112448161	Hyper	Hyper
LOC112448374	Hypo	Hypo
LOC112449090	Hypo	Hypo
MEF2A	Hypo	Hypo
MX1	Hyper	Hyper
PES1	Hypo	Hypo
PITPNA	Hypo	Hypo
PRR18	Hyper	Hypo
SMYD2	Hyper	Hyper
SNTG2	Hypo	Hypo
SPTBN4	Hyper	Hyper
TMEM91	Hyper	Hyper
TRMU	Hyper	Hyper
UBE2T	Hypo	Hypo

The list of genes containing differential methylation at single or multiple CpG sites in TI heifers at 4 months of age was compared to those identified in PI heifers at 4 months of age. Canonical pathways identified by IPA include the role of osteoclasts in rheumatoid arthritis signaling, GP6 signaling, GPVI-mediated activation cascade, wound healing signaling, Rho GTPase cycle, signaling by Rho family GTPases, and G-protein coupled receptor signaling, and others (S file 4 '4moTI vs 4moPI – Canonical Pathways). Upstream regulators predicted to be altered include *EGLN2, BDNF, NOTCH1, SOX2, BMPR1A, SAMD8, BACH2, SPP1,* and *LAMP2.* A full list of upstream regulators predicted to be altered in both TI and PI heifers can be found in S file 5 '4moTI vs 4moPI – Upstream Regulators.'

Complete Blood Counts

Whole blood was collected from the jugular vein of control and TI heifers at 4 months of age. Blood samples were then analyzed for Complete Blood Counts (Table 3.5). The percentage of lymphocytes was higher in TI heifers at 4 months of age compared to controls (68.44 ± 1.79% vs 73.25 ±1.41%; p-value ≤ 0.05). Other CBC measurements that were not different between control and TI heifers include the absolute basophil count, absolute eosinophil count, absolute neutrophil count, absolute monocyte count, monocyte percentage, absolute red blood cell count, hemoglobin, hematocrit, red cell distribution width, mean corpuscular volume, mean corpuscular hemoglobin, mean corpuscular hemoglobin concentration, absolute white blood cell count, absolute lymphocyte count, absolute platelet count, and mean platelet volume.

Table 3.5 – Increased lymphocyte percentage in TI heifers.
Quantification of the average complete blood count values in TI and control heifers at 4 months of age. Data were first assessed using the Shapiro-Wilk normality test. Outliers were removed prior to significance testing. The dagger (†) was utilized to indicate which cell measures contained outliers that were removed. Data that were normally distributed were compared using an unpaired, parametric Student's T test. Welch's correction was applied to all T test comparisons due to unequal sample populations (Control n = 12, TI n = 11; prior to outlier removal). Data that was not normally distributed were compared using a nonparametric Mann-Whitney test. Data are displayed as mean ± standard error of the mean (SEM). Asterisks indicate significant differences between groups, * P ≤ 0.05.

Complete Blood Counts (CBCs)

	Control		TI			
Complete Blood Count Parameter	**Average**	**SEM**	**Average**	**SEM**	**Unit**	**p-value**
Basophil Count †	0.05	± 0.01	0.04	± 0.01	10^9/L	0.98
Eosinophil Count	0.07	± 0.01	0.09	± 0.02	10^9/L	0.27
Neutrophil Count	2.89	± 0.27	2.31	± 0.36	10^9/L	0.21
Monocyte Count	0.38	± 0.04	0.35	± 0.06	10^9/L	0.69
Monocyte Percentage	3.53	± 0.41	3.2	± 0.39	%	0.57
Red Blood Cell Count	12.17	± 0.22	12.03	± 0.43	10^{12}/L	0.78
Hemoglobin	14.28	± 0.23	13.73	± 0.47	g/dL	0.31
Hematocrit	41.33	± 0.72	40.12	± 1.33	%	0.44
Red Cell Distribution Width	22.96	± 0.34	23.42	± 0.45	%	0.68
Mean Corpuscular Volume	33.99	± 0.44	33.41	± 0.6	fL	0.44
Mean Corpuscular Hemoglobin	11.76	± 0.15	11.44	± 0.24	pg	0.28
Mean Corpuscular Hemoglobin Concentration	34.59	± 0.16	34.22	± 0.16	g/dL	0.12
White Blood Cell Count	10.68	± 0.46	10.09	± 1.28	10^9/L	0.67
Lymphocyte Count	7.28	± 0.3	7.28	± 0.89	10^9/L	0.99
Lymphocyte Percentage *	68.44	± 1.79	73.25	± 1.41	%	0.05
Platelet Count	462.8	± 51.53	332.5	± 78.92	10^9/L	0.18
Mean Platelet Volume	4.93	± 0.06	4.74	± 0.12	fL	0.18

Flow Cytometry

Peripheral WBCs were isolated from whole blood collected from the jugular vein of control and TI heifers at 4 months of age. Flow cytometry was utilized to investigate the impact of fetal TI on postnatal immune cell populations (Figure 3.6 and Table 3.6). Gating was performed to remove debris, doublet, and dead cells. General populations of cells were first compared based on their frequency within total leukocytes ($CD45^+$

cells). Subpopulations of T cells were also compared according to their frequency within total T cells ($CD3^+$). As a subset of Helper T cells, the $CD25^+/CD127^-$ population frequency within $CD4^+$ was compared to mitigate external bias.

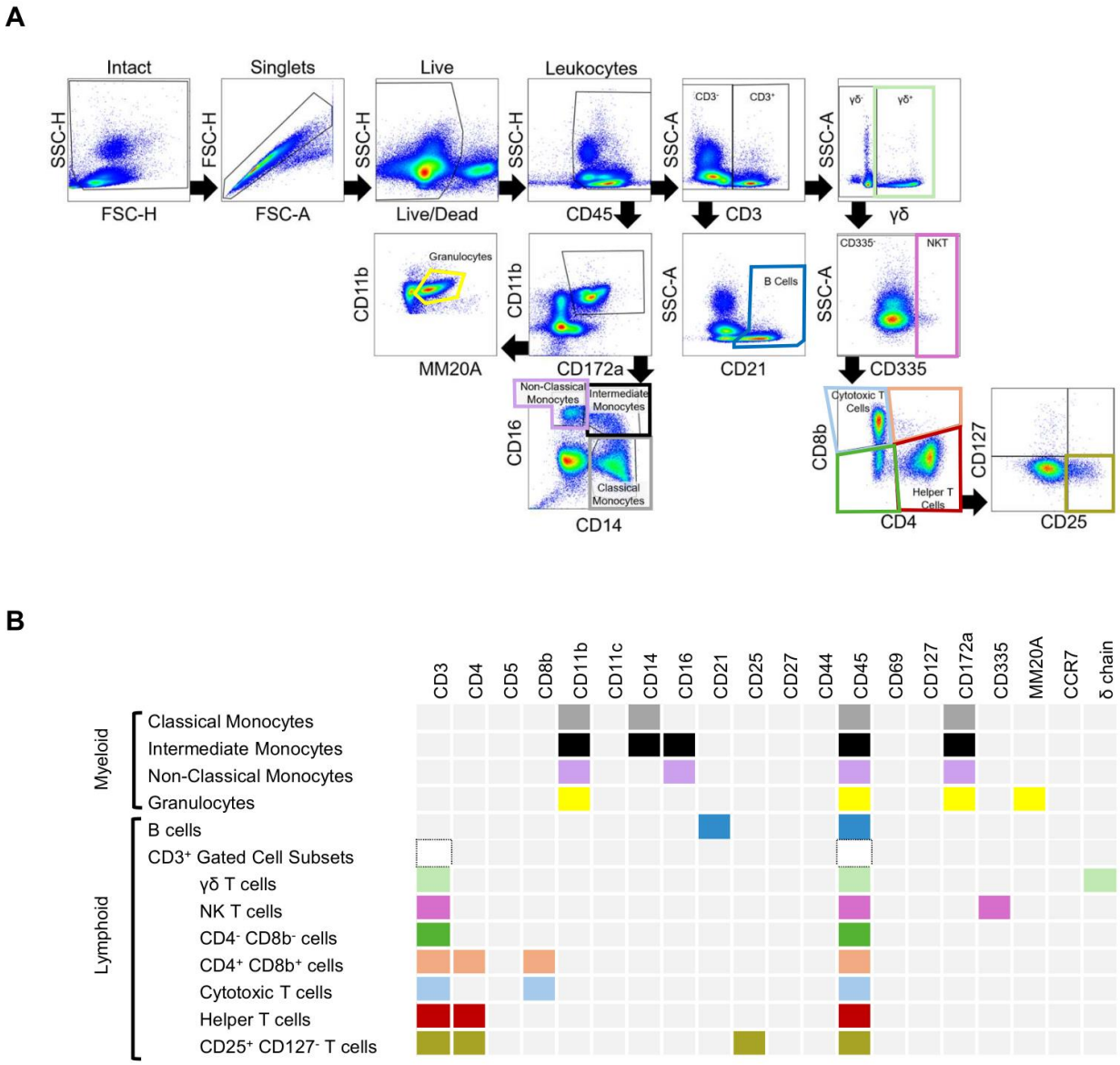

Figure 3.6 – Markers utilized to identify immune cell populations.
(A) A schematic depicting the fluorescent markers used to identify various immune cell populations through flow cytometry. Colors used here correspond to those utilized in Table 3.4. Boxes shaded in light grey were not identified in populations, while boxes shaded in various colors (including white) indicate positive fluorescence in a cellular population. (B) Schematic representation of the gating strategy used to identify various immune cell populations. Colors here correspond to colors representing various populations in Table 3.6.

When comparing frequency of $CD45^+$ cells, intermediate monocytes (0.5 ± 0.14% vs 0.95 ± 0.44%; p-value ≤ 0.05) and B cells (16.65 ± 1.08% vs 20.64 ± 1%; p-value ≤ 0.01) were higher in TI heifers than in controls. Identified T cells positive for both $CD4^+$ and $CD8^+$ were decreased in TI cattle (0.26 ± 0.06% vs 0.07 ± 0.01%; p-value < 0.05). When $CD25^+/CD127^-$ cells were compared using frequency of $CD4^+$ cells, they were found to be increased in TI heifers (3.94 ± 0.24% vs 5.53 ± 0.68%; p-value < 0.05). Frequency of classical monocytes, non-classical monocytes, granulocytes, T lymphocytes, gamma delta ($\gamma\delta^+$) T cells, natural killer (NK) T cells, $CD4^-/CD8^-$ T cells, cytotoxic T cells, helper T cells, and $CD25^+/CD127^-$ T cells within total leukocytes ($CD45^+$) were not different between groups. Subpopulations of T cells were not different when frequency of $CD3^+$ cells was compared.

Table 3.6 – TI heifers display elevated intermediate monocytes and B cells but decreased $CD4^+/CD8b^+$ and $CD25^+/CD127^-$ T cells.
Quantification of cell population frequency in relation to the indicated parent population. Shading color corresponds to cell population markers in Figure 3.3. Data was first assessed using the Shapiro-Wilk normality test. Outliers were removed prior to significance testing. The dagger (†) was utilized to indicate which cell measures contained outliers that were removed. Data that were normally distributed were compared using an unpaired, parametric Student's T test. Welch's correction was applied to all T test comparisons due to unequal sample populations (Control n = 12, TI n = 11; prior to outlier removal). Data that was not normally distributed were compared using a nonparametric Mann-Whitney test. Data are displayed as mean ± standard error of the mean (SEM). Asterisks indicate significant differences between groups, * P ≤ 0.05.

Flow Cytometry

		Control		TI			
Population		**Average (%)**	**SEM**	**Average (%)**	**SEM**	**p-value**	**Freq. of**
Classical Monocytes †		5.93	± 0.14	6.74	± 0.44	0.28	CD45
Intermediate Monocytes * †		0.5	± 0.07	0.95	± 0.13	0.02	CD45
Non-Classical Monocytes †		0.97	± 0.13	1.45	± 0.24	0.14	CD45
Granulocytes		22.14	± 2.01	17.08	± 1.59	0.6	CD45
B Cells *		16.65	± 1.08	20.64	± 1.00	0.01	CD45
T Lymphocytes		40.14	± 1.62	37.46	± 2.29	0.35	CD45
$\gamma\delta^+$ T Cells		16.83	± 1.22	17.04	± 1.61	0.60	CD45
NK T Cells		0.14	± 0.01	0.19	± 0.03	0.25	CD45
$CD4^-/CD8b^-$ T Cells †		1.69	± 0.90	1.70	± 0.17	0.65	CD45
$CD4^+/CD8b^+$ T Cells * †		0.26	± 0.06	0.07	± 0.01	0.05	CD45
Cytotoxic T Cells		7.07	± 0.38	5.90	± 0.54	0.09	CD45
Helper T Cells		14.02	± 0.63	11.84	± 1.14	0.11	CD45
$CD25^+/CD127^-$ Cells		0.55	± 0.04	0.64	± 0.09	0.36	CD45
$\gamma\delta^+$ T Cells		41.48	± 1.88	45.21	± 2.58	0.26	CD3
NK T Cells		0.36	± 0.03	0.47	± 0.06	0.13	CD3
$CD4^-/CD8b^-$ T Cells †		4.59	± 0.39	4.29	± 0.29	0.86	CD3
$CD4^+/CD8b^+$ T Cells †		0.64	± 0.15	0.44	± 0.12	0.19	CD3
Cytotoxic T Cells		17.83	± 1.07	15.97	± 1.28	0.28	CD3
Helper T Cells		35.07	± 1.07	31.87	± 2.54	0.27	CD3
$CD25^+/CD127^-$ Cells *		3.94	± 0.24	5.53	± 0.68	0.05	CD4

Discussion

Billions of dollars in potential profit are lost each year due to BVDV infections [3, 220]. Currently, TI cattle generated through fetal infection cannot be distinguished from uninfected cattle and may induce additional loss of potential profit through decreased weight gain and increased susceptibility to severe morbidity [179, 180, 246]. The TI heifers in this study were generated through gestational infection with ncp BVDV type 2. Differentially methylated genes identified in TI heifers are associated with inflammation, ROS production, and insulin secretion. These findings are supported by increased concentrations of inflammatory markers found in TI heifers [180]. The CBC values identified in TI and control heifers do not often fall within reference ranges for cattle, likely due to differences in age, breed, and lactation status [252]. The CBC values identified in TI calves were not different from those of controls, except for the case of lymphocyte percentage, which is corroborated by flow cytometry. Spectral flow cytometry maintains increased resolution and sensitivity in comparison to CBC analysis, allowing for the observation of differences in lymphocyte subsets. As such, flow cytometry revealed that TI heifers had increased cellular populations of B cells and $CD25^{+}/CD127^{-}$ T cells. By analyzing individual monocyte subpopulations, rather than monocytes as a sum, intermediate monocytes were observed to be increased in TI heifers compared to controls. The TI heifers were also found to have decreased cellular populations of $CD4^{+}/CD8b^{+}$ T cells. This study sheds light on potential pathologies associated with TI heifers and provides foundational knowledge for the development of management strategies to mitigate profit loss.

Differential methylation of genes associated with observed clinical pathologies in PI cattle has been described [250]. Moreover, differential methylation has been identified in TI heifers at birth [179]. Analysis of WBC DNA of TI and control heifer calves at birth revealed 2,349 DMSs with the potential to influence growth, development, and the immune system [179]. A study by Munoz-Zanzi et al. [246] describes calves positive for BVDV antibodies at birth, termed congenitally infected (CI; synonymous with TI), as having 2.3 times the risk of a severe morbid episode in comparison to non-CI calves. A severe morbid episode is defined as an illness requiring 3 or more days of treatment followed by recovery, or death without record of previous[246]. Of the 41 CI calves, 9 experienced a severe morbid episode [246].

Many of the pathways identified by IPA using the DNA methylation data obtained from 4-month-old TI heifers contained genes within the human genome that are associated with an increased risk of cancer. Activation of integrin signaling is often associated with tumorigenesis and tumor invasion [253-255], as is ephrin signaling [256], GTPase signaling [257], and the predicted activated upstream regulator *SOX9* [258]. If a TI calf developed cancer, it is possible that other epigenetic alterations could enhance the development and metastasis of cancer, as is demonstrated by predicted activation of the transcriptional regulation by RUNX2 pathway which can promote tumor growth and metastasis [259]. Increases in cardiac defects or nephrosis, as predicted by IPA, may ultimately lead to loss of profit due to premature death of TI calves. However, the impact would depend on the severity of the defect or progression of disease.

At 4 months of age, lymphocyte percentage was elevated in TI heifers compared to controls. However, the average absolute lymphocyte count was identical between

groups. The highest lymphocyte percentage identified in the TI group was 80.8%, which is within the normal range for cattle under the age of 2 years [260]. Using spectral cytometry, TI heifers were identified to have increased percentages of B cells and $CD25^{+}/CD127^{-}$ T cells. A larger circulating B cell population in TI calves compared to controls could be explained by fetal exposure to BVDV, causing an expansion in circulating memory B cells [261].

The $CD4^{+}$ subpopulation of cells defined by expression of $CD25^{+}$ and lack of $CD127^{-}$ expression is defined as T regulatory cells in humans. However, these cells do not exert immunosuppressive activity in the bovine [231]. Little is known about $CD4^{+}$ $CD25^{+}/CD127^{-}$ T cells in bovine. The $CD4^{+}/CD8b^{+}$ T cell population was decreased in TI heifers compared to controls. It has been speculated that the $CD4^{+}/CD8b^{+}$ T cell population may be an uncharacterized population of peripheral T helper cells, as an increase in $CD4^{+}/CD8^{+}$ T cells was observed in accordance with B cell proliferation following vaccination for foot and mouth disease in cattle [230]. In humans, an increased amount of $CD4^{+}/CD8^{+}$ T cells has been observed in cases of viral infection and chronic disease (reviewed in [262]). This observation is in accordance with observed increases of $CD4^{+}/CD8^{+}$ T cells in PI heifers, which experience chronic BVDV infection [250]. However, neither TI nor control calves displayed any clinical signs of illness at the time of sample collection. Additional research characterizing this cell population is necessary to determine the global impact of their elevation.

Flow cytometry also revealed increased intermediate monocytes in TI heifers compared to controls. Several genes known to be enriched in intermediate monocytes were found to contain hypomethylated CpG sites in TI heifers, including *CCL5, C1QA,*

IRF4, GBP4, and *MAFB [263].* Additionally, *GBP4* was also found to contain hypomethylation within a promoter region and *IRF4* contained hypomethylation within a CpG island. Increased expression of *IRF4* and *GBP4*, which is associated with hypomethylation, could push TI calves towards T cell exhaustion and an inability to appropriately respond to infection [264, 265]. Intermediate monocytes in the bovine express the highest amount of MHCII on their cell surface, as well as produce the largest amount of reactive oxygen species and pro-inflammatory cytokines such as CXCL8, CXCL1, IL1B and TNF [266]. An increase in absolute count of intermediate monocytes in TI calves may indicate stimulation of the immune system prior to data collection at 4 months of age, as treatment of classical monocytes *in vitro* with IFNγ resulted in expansion of the intermediate monocyte population [266]. However, no clinical signs were noted in TI heifers at the time of blood collection.

A cascade of aberrant methylation

The DNA methyltransferase 3 (DNMT3) family contains DNMT3A, DNMT3B, and DNMT3L [267, 268]. The DNMT3L protein is catalytically inactive regulatory factor for DNMT3A and DNMT3B [269]. Interestingly, *DNMT3L* contained hypermethylated DMSs at birth in TI heifers, but was not differentially methylated at 4 months of age. The DNMT3L protein is highly expressed during gametogenesis [270]. Mice lacking DNMT3L produce oocytes with defects in maternal imprinting, leading to death of offspring [269, 270]. The maternal imprinting process is dependent on oocyte growth in bovine [271] and only primordial follicles are present in pre-pubertal heifers. Differential methylation of *DNMT3L* may impact fertility of these TI calves following pubertal development. The

DNMT3L protein is known to enhance the activity of DNMT3A and DNMT3B [272]. As such, it is possible that hypermethylation of *DNMT3L*, associated with decreased expression, could lead to a decrease in DNMT3A and DNMT3B activity and *de novo* methylation in the perinatal period.

Expression of DNA methyltransferases is markedly decreased in adult tissues and decreases overall as organisms age [148]. A study by Zhenhua Li et al. recently demonstrated that overexpression of DNMT3A in rats leads to variation of gene expression, specifically within the brain and testis [273]. It is possible that the scenario is similar in the present TI calf study; hypomethylation of *DNMT3A* in TI calves could lead to overexpression and alteration of methylation and expression of other genes. This suggestion is supported by the identification of hypomethylation within *DNMT3A* and *DNMT3B* in PI heifers, who are infected earlier in gestation and present with more clinical abnormalities [250].

Differential methylation of genes associated with inflammation and ROS production

Inflammation and ROS production are linked processes with the potential to induce damage if not regulated appropriately. Increased inflammation can lead to increased ROS production and vice versa. Typically, this self-amplifying cycle is mediated by cellular antioxidant systems, but these systems can be overwhelmed and lead to oxidative stress. Analysis of DMSs by IPA predicted an increase in oxidative stress, citing hypermethylation of CpG sites within genes encoding *GSTA3, SOD1, MAFK,* and *PGC1A.*

During a feedlot trial, TI calves were found to exhibit signs of increased inflammation including elevated levels of oxidized glutathione and plasma ceruloplasmin concentrations [180]. No clinical signs of illness were observed in the heifers during the trial. If TI calves maintain a higher base level of inflammation, it is possible that immune activation would lead to oxidative stress. The CCL5 chemokine, containing a hypomethylated DMS in TI calves at 4 months of age, has been implicated in several inflammatory diseases in humans (reviewed in [274]) and is transcriptionally regulated by KLF13 [275]. The KLF13 gene also contained at least one hypomethylated CpG site in TI calves at birth and at 4 months of age [179]. Similarly, CCL24 is associated with inflammatory or fibrotic disease and contained a hypomethylated CpG site in TI calves [276, 277]. Another gene, *LIF*, which is known to have immunomodulatory effects[179], contained hypermethylated CpG sites; 1 site was identified within the gene at birth and 3 sites were identified at 4 months of age in TI heifers. The IPA software also predicted LIF to be an activated upstream regulator. Human T regulatory cells are stimulated to proliferate in the presence of LIF, while Th17 cell proliferation is inhibited by LIF [278]. Dendritic and macrophage inflammatory responses are also mitigated by *LIF* expression [279, 280]. Hypomethylation of inflammatory-associated genes in TI heifers along with hypermethylation of immunosuppressive genes may indicate chronic inflammation.

Immune stimulated inflammation can also lead to the upregulation of IL17 receptors [281]. The IL17 receptor A (IL17RA) was found to contain a hypomethylated CpG site in TI heifers and is one of five IL17 receptors and is required for the proinflammatory activity of IL17A [282]. The activation of IL17RA induces inflammation through chemokine and cytokine expression, but also recruits neutrophils, activates T

cells, and enhances migration of monocytes (reviewed in [283]) [284, 285]. Activation of the immune response leads to proliferation and activation of phagocytic cells that are known to produce high amounts of ROS through respiratory burst [286, 287]. Specifically, lipopolysaccharide stimulated inflammation can lead to the release of redox molecules from both macrophages and monocytes [288]. Phagocytic cells produce ROS through NADPH oxidases, specifically through NOX2 [286, 287]. A cytosolic subunit encoded by *Rac1* is required for activation of NOX2 and was identified to contain a hypomethylated CpG site in TI heifers. Intermediate monocytes were identified to be increased in TI heifers at 4 months of age. While the phagocytic activity of intermediate monocytes is lower than that of classical monocytes and higher than that of non-classical monocytes, they generate the highest amount of ROS in response to stimulation [266]. Together, these findings suggest that TI cattle may have higher risk of oxidative stress upon immune activation. Moreover, it has been noted that lipoprotein lipase (LPL) upregulates macrophage activation, and inflammation, in the presence of increased ROS [289]. The *LPL* gene was found to contain a hypomethylated CpG site in TI heifers, which may indicate increased expression and perpetuation of the inflammation-ROS cycle leading to oxidative stress.

A recent study described 66 CpG sites associated with markers of oxidative stress [290], 4 of which were identified to contain a differentially methylated CpG site in TI heifers. The genes *LRIG1, FAM20C,* and *EPHB1* contained a hypomethylated CpG site and *CBFA2T3* contained a hypermethylated CpG site. Additionally, the glutathione S-transferase alpha 3 gene, GSTA3, contained a hypermethylated CpG site in TI heifers and has been shown to increase ROS production when knocked down in cell culture

[291]. The superoxide dismutase, SOD1, was found to contain a hypermethylated CpG site in TI heifers at 4 months of age. It has been described that a deficiency of SOD1 can lead to decreased weight at a young age, increased oxidative stress, and decreased DNA methylation in the prostate of mice [292]. While SOD1 is an important antioxidant enzyme, it has been suggested that other anti-oxidant systems can compensate for loss of *SOD1* [293].

Hypomethylation of a CpG site within *NDOR1, SDHB,* and *GSTK1* suggests the need for increased expression of alternative antioxidant genes as the physiological systems attempt to mediate abnormal levels of ROS production [294-298]. However, the gene encoding MAFK contained a hypermethylated CpG site and is required for induction of antioxidant and detoxification enzymes [299]. The peroxisome proliferator-activated receptor γ coactivator 1-alpha, PCG1A, which is directly regulated by NFκB, was found to contain a hypermethylated CpG site in 4-month-old TI calves. During infection, an increase in NFκB would inversely lead to a decrease in PGC1A, which further leads to a transcriptional decrease of antioxidant genes [300]. Calves affected by fetal TI maintain differential methylation indicative of increased inflammation, ROS production, and a potentially stunted ability to manage ROS imbalances, which are likely to contribute to increased oxidative stress.

Methylation and metabolic dysfunction

Inflammation and oxidative stress have also been implicated in metabolic dysfunction. Oxidative stress plays a role in downregulation of the transcription factor MAFA, which influences insulin secretion by pancreatic beta cells [301]. Interestingly,

MAFA contained a hypermethylated CpG site in TI heifers, which may impair insulin secretion, as mice lacking MAFA display reduced expression of insulin in beta cells [302]. The gene encoding *PGC1A* contained a hypermethylated CpG site in TI heifers and is involved in redox balancing, inflammation, and metabolic disease (reviewed in [303]). Downregulation of PGC1A can enhance the inflammatory response, increase ROS production, and lead to insulin resistance and glucose intolerance [304].

In accordance with suggested metabolic dysfunction, hypermethylation of a CpG site within *DGKD, TRPC3,* and two CpG sites within *KCNB1* may contribute to abnormal insulin secretion. The diacylglycerol (DAG) kinase is responsible for the conversion of DAG into phosphatidic acid [305]. Elevated levels of DAG have been associated with the development of insulin resistance in type 2 diabetes (reviewed in [306]). Inhibition of *TRPC3,* whether through pharmacologic inhibition or knockout, results in decreased insulin secretion and glucose intolerance in mice [307]. The voltage-dependent potassium channel *KCNB1* is involved in exocytosis of insulin from pancreatic beta cells [308]. Additionally, the retinoid X receptor alpha (*RXRA*) was hypomethylated at 10 different CpG sites and hypermethylated at a single CpG site in TI heifers. One study described that RXRs act to inhibit insulin secretion in response to high glucose levels [309].

While IPA predicted overall activation of the White Adipose Tissue Browning pathway with a z-score of 3.13, it was predicted that there would be a decrease in mitochondrial biogenesis, differentiation of white adipocytes, and transdifferentiation of white adipose tissue to beige adipose tissue. The *ADCY* gene was identified by IPA to contain hypomethylation, but upon further investigation, it was actually the gene

encoding *ADCY6* which contained a hypomethylated CpG site in the gene body and a hypomethylated CpG island. Upregulation of ADCY6 is associated with increased hepatic glucose production, which can contribute to high blood glucose and overall glucose intolerance [310]. The gene encoding for positive regulatory domain containing 16, PRDM16, contained 4 hypomethylated CpG sites and a single hypermethylated CpG site. Due to decreased methylation within *PRDM16*, one would expect the potential for increased expression. As such, overexpression of PRDM16 would inhibit differentiation of white adipocytes and conversely encourage the formation of brown and beige adipocytes which expend energy as heat [311]. Brown and/or beige adipose tissue are not favorable in cattle, as expense of energy as heat decreases the average daily gain, which was observed in TI heifers [180]. The *DICER1* gene, which was predicted to be a possibly inhibited upstream regulator, is also known to impact weight gain. In fact, mice lacking DICER1 expression were found to maintain a lower body weight than controls [312]. Decreased average daily gain and decreased muscle growth, as predicted by IPA, translate to increased input costs and decreased profit return for cattle producers.

Persistence of methylation in TI heifers

It is important to note that while DNA methylation is stable and heritable, this statement refers to the ability of such to remain throughout the cellular replication process. More recently it has been reported that DNA methylation does vary over time within individuals [149]. Specifically, DNA methylation decreases globally with age [148, 150], but simultaneously increases in CpG islands [151-154]. Because RRBS

specifically identifies methylation at CpG sites, the increase from 2,349 DMSs at birth to 3,047 DMSs at 4 months of age demonstrates the site-specific increase in methylation, but not the global decrease in methylation (Figure 3.7).

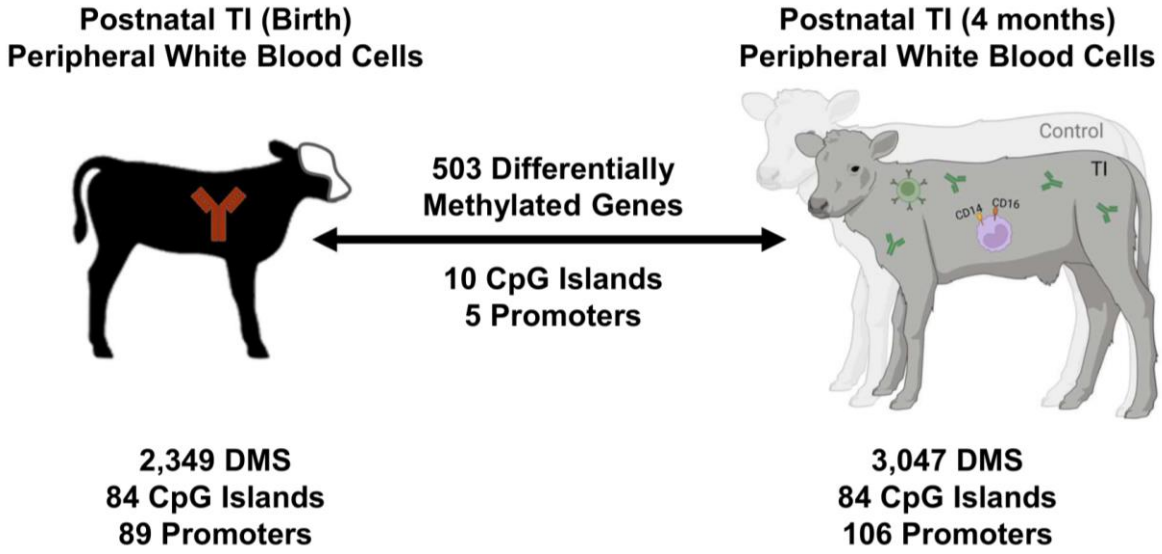

Figure 3.7 – Comparison of differential methylation in peripheral white blood cells from TI heifers at birth and 4 months of age. The green symbols on the 4-month-old calf represent antibodies against BVDV. The shadow of a control calf behind the 4-month-old TI calf represents a decreased body weight in TIs. A monocyte expressing CD14 and CD16 is also indicated.

Not only does the percentage of methylation change over time, but the methylation status of genes can change. For example, hormonal changes in puberty have been associated with changes in DNA methylation in humans [155]. More recently, even SARS-CoV-2 infection has been noted to lead to variation in DNA methylation [155]. In theory, access to genetic material may be dependent upon the physiological need indicated by the organism. As TI heifers continue to develop, it is likely that the genes containing differential methylation will also change.

Variations in DNA methylation have been identified to play a role in inducing postnatal disease in organisms exposed to sub-optimal conditions *in utero*, which

indicates some level of persistence epigenetic marks of DNA methylation. For example, differential methylation of genes corresponding to observed pathologies was identified in humans following prenatal exposure to malnutrition [313, 314]. The methylation status of DNA may also indicate the risk of occurrence or severity of disease, as in the case of type 2 diabetes and cardiovascular disease [315, 316]. It is possible that variations in DNA methylation in TI heifers indicate dysfunction of various physiological systems. Both at birth and 4 months of age, TI heifers were predicted to experience decreased growth of lymphoid tissue. This may support the claim that TI heifers mount an abnormal immune response, as lymphoid tissue is critical to appropriate immune response [317]. As this longitudinal study continues, variation in DNA methylation may prove critical in identification of cattle affected by late gestation BVDV infection.

Commonalities between TI and PI heifers

It is evident that exposure to environmental stressors *in utero* can influence DNA methylation and there are time periods during gestation in which the fetus is especially susceptible to these factors. One study denotes that the changes in DNA methylation appear to be dependent upon sex of the fetus and gestational timing of exposure, and that exposure in late gestation resulted in fewer significant variations in DNA methylation of targeted genes (Figure 3.8) [313]. All control, TI, and PI cattle utilized in this study were heifers, to eliminate the potential of sex differences. It is also well documented that the gestational timing of BVDV infection leads to vastly different outcomes for infected fetuses. The findings of differential methylation in TI and PI

heifers agree with the concept that fetuses in early gestation are more ‘sensitive’ to DNA methylation variation than those in late gestation.

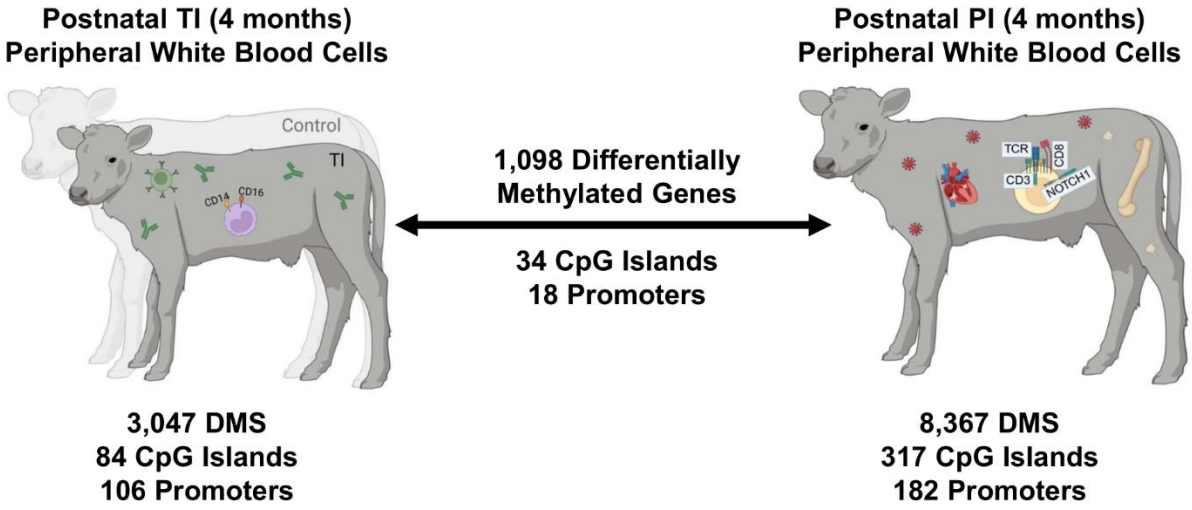

Figure 3.6 – Comparison of differential methylation in 4-month-old TI and PI heifers. Antibodies against BVDV are represented by the Y-shaped icons on the 4-month-old TI in addition to a monocyte expressing CD14 and CD16. The 4-month-old PI schematic contains red BVDV antigen as well as the heart, femur, and a T cell to indicate alterations of the methylome in relation to each system.

Many commonalities were identified in the variations of DNA methylation in TI and PI heifers. For example, *IL22* contained a hypermethylated CpG site in both TI and PI heifers. Interestingly, methylation of *IL22* increased in TI heifers from birth to 4 months of age (meth.diff = 26.22 at birth, 72.2 at 4 months) and even surpassed the level of hypermethylation in PI heifers at 4 months of age (meth.diff = 31.1 at 4 months). The IL22 signaling pathway was predicted to be inhibited by IPA, citing the identification of hypermethylation of a CpG site within *IL22* and *MAPK11.* The software predicted a decrease in negative feedback control of IL22 signaling and JNK. Additionally, mice lacking IL22 expression experience increased severity of colitis infections following chemical or bacterial induction [318-320]. On the other hand, macrophage migration inhibitor factor (MIF) contained a hypermethylated CpG site in TI and PI heifers. Mice

lacking MIF were at least partially protected from the development of chemical induced colitis [321, 322]. Not all genes identified in TI and PI heifers are as contradictory as *IL22* and *MIF.*

Genes that are similarly methylated in TI and PI heifers may support the predisposition of PI cattle to bacterial infections and support the previous study denoting more severe illness in TI cattle [246]. Myxovirus resistance protein 1 (*MX1*) was found to contain 3 hypermethylated CpG sites in TI calves and 7 hypermethylated CpG sites in PI heifers. This protein acts as a cellular defense against viral infection. As such, a lack of MX1 has been shown to increase susceptibility of mice to influenza [323]. Mice without MPEG1, which contained a single hypermethylated CpG site in TI calves and two hypermethylated CpG sites in PI heifers, are also more susceptible to infection by inhibiting early transcription and replication of viral RNA [324, 325]. Lack of adequate MX1 and MPEG1 in TI and PI heifers may contribute to an immunocompromised state, which has at least been documented in PI cattle [326].

At 4 months of age, PI heifers display differential methylation of genes inv olved in blood coagulation [250]. It has also been suggested that PI cattle may suffer from platelet dysfunction; a presumed PI steer died of a fatal hemorrhage following castration [240]. Similarly, TI heifers display differential methylation of genes associated with bleeding and clotting time, although the genes altered in TI heifers are different from those altered in PI heifers. Alterations in the DNA of TI heifers at 4 months of age that indicate increased bleeding time include a hypermethylated CpG site within *CTBP2,* two within *EFNA5,* three within *GP6,* three within *KCNQ1,* three within *LIF ,* two within *MUC2,* one within *PROZ,* eleven within *RXRA,* one within *THBS2,* four within *WNT7B,*

one within *ALPL,* one within *CA5A,* one within *COL4A1,* one within *COL4A2,* and a single hypomethylated CpG site within *ATP12A* (Fig 4A). Differential methylation indicating altered clotting time in PI heifers was identified primarily in coagulation factors. No coagulation factors were differentially methylated in TI heifers. Further research will be necessary to conclude whether TI heifers suffer from disturbances to the coagulation cascade.

Potential Confounders and Future Research

As with all research, it is important to note potentially confounding variables related to the data. While peripheral WBCs are not the canonical choice to observe potentially pathological differences in DNA methylation, primary and secondary lymphoid tissue is unobtainable from a live animal. Peripheral WBCs were chosen for this study, not because they best represent the immune response, but because they represent a facet of the immune system that can be obtained without the need for euthanasia. By doing so, the monetary value of the experimental subject is preserved and the data produced is more suitable for application in production settings. Peripheral WBCs can be heterogeneous in cellular composition, which was verified by the finding of elevated intermediate monocytes and B cells by flow cytometry. As such, it is possible that a portion of the identified DMSs or DMRs were biased by increased concentrations of specific cell types. However, multiple steps were taken to assess and minimize the potential for bias within this study. Pearson correlation coefficients between all samples were greater than 0.94, coverage values between samples were normalized by the

median, and the threshold for the identification of DMSs was set to 25% to mitigate potential sources of bias.

It is also important to note that the identification of increased methylation within a gene body, promoter, or CpG island is only associated with decreased expression, the impact is not implicit; the same is especially true for sites with decreased methylation, indicative of increased expression potential. Not all genes are always being actively transcribed. For example, hypermethylation within *MX1* may have no impact upon a calf that is not actively responding to an infection. If the same calf *were* to be infected with a pathogen, it is more possible that hypermethylation within *MX1* would decrease the calf's ability to mount an effective immune response. Additional research is required to validate and confirm whether the differential methylation identified herein is truly translational to observed pathologies.

Conclusions

At 4 months of age, TI heifers exhibit increased circulating lymphocyte percentage, intermediate monocytes, B cells, $CD4^{+}/CD8b^{+}$ T cells, and $CD25^{+}/CD127^{-}$ T cells in comparison to 4-month-old control heifers. Analysis of differential methylation in WBC DNA indicates abnormal regulation of genes involved in inflammation, ROS production, and insulin secretion (Figure 3.9). Increased ROS production and inflammation are complementary responses to tissue injury and are related to the development of cancers, arthritis, as well as cardiac and metabolic disease. Further research concerning postnatal aberrations identified in TI cattle is crucial to the development of an accurate estimate of profit loss to BVDV which demonstrates the

continued importance of the virus. A better understanding of how late gestation BVDV infections influence postnatal metabolism could allow for the application of therapeutics or management strategies to mitigate profit loss incurred by TI calves through decreased weight gain. Comparison of differential methylation identified in TI heifers to that found in PI heifers indicates some similarity in immunosuppression. The immunocompromised state of PIs is likely driven by constant infection, while immunosuppression in TI calves appears to be more related to chronic inflammation and over-responsiveness of facets of the immune system. Comparison of genes containing differentially methylated CpG sites indicates the persistence of methylation variation from birth to 4 months of age. If specific CpG sites are persistently differentially methylated over time, epigenetic marks may have the potential to serve as a biomarker for the identification of TI calves. If late gestation TI calves can be identified, the profit loss they induce can be managed through intervention strategies.

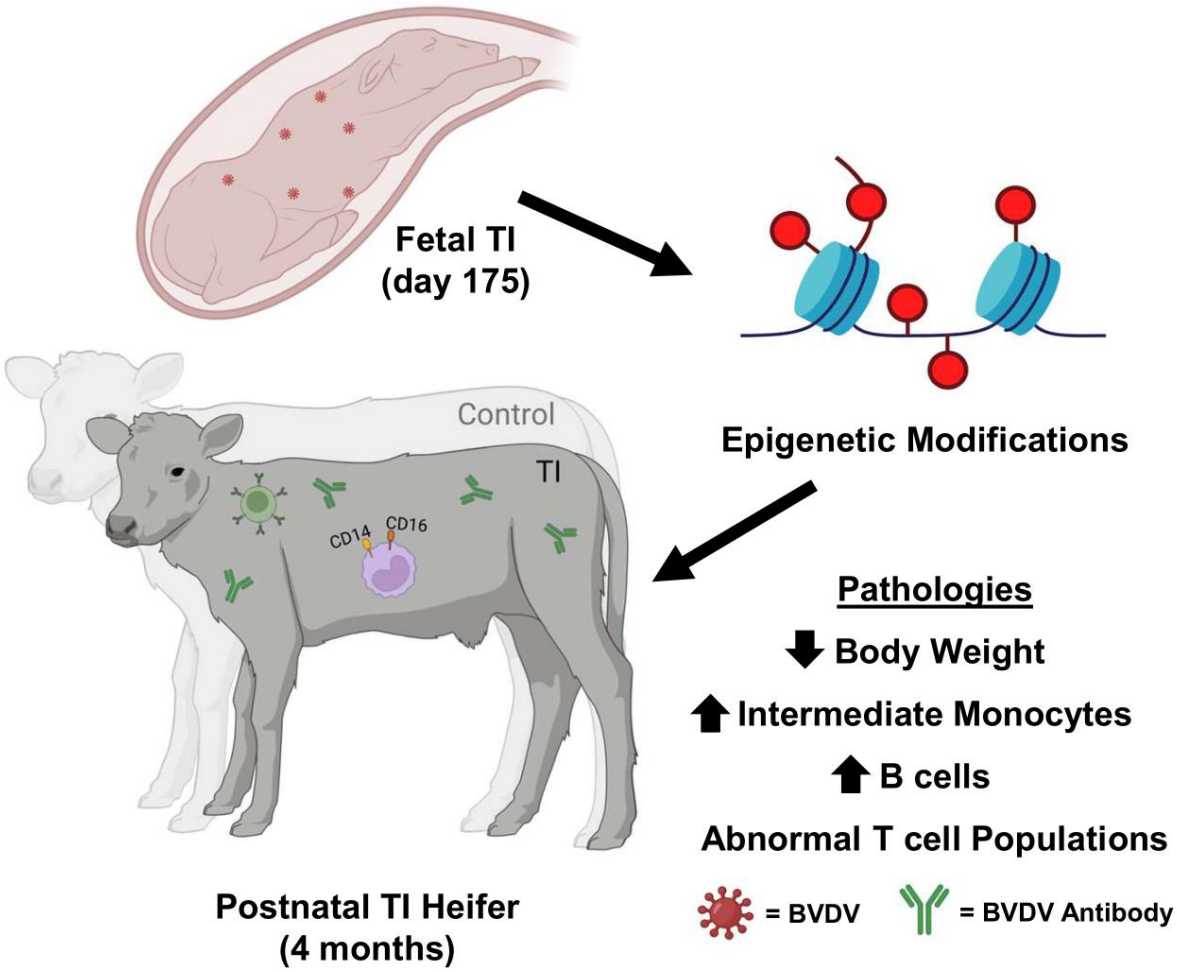

Figure 3.9 – Transient fetal infection with BVDV results in epigenetic alterations and differences in intermediate monocytes, B cells, and body weight.
A graphical summary of the findings identified in postnatal heifers following transient fetal infection with BVDV. The findings include decreased body weight as well as elevated intermediate monocytes and B cells.

CHAPTER 4: TRANSIENT FETAL INFECTION WITH BOVINE VIRAL DIARRHEA VIRUS GENERATES MULTI-OMIC ALTERATIONS IN PERIPHERAL WBCS

Short Summary

Fetuses that have been transiently infected (TI) with bovine viral diarrhea virus (BVDV) in the late gestational period mount an immune response including the production of BVDV specific antibodies. Analysis of profit loss due to BVDV may be incomplete, as epigenetic alterations with the capacity to affect genetic expression of growth and immune related genes were identified in TI heifers at birth and 4 months of age. We hypothesized that these epigenetic alterations would persist, accumulate, and lead to differential gene expression in peripheral immune cells of TI heifers. To this end, seronegative pregnant cows were infected with BVDV on day 175 of gestation to generate fetal TIs. Blood was collected from postnatal control and TI heifers at 17 months of age for complete blood counts (CBCs) and isolation of peripheral white blood cells (WBCs) for flow cytometry analysis (immune cell populations), reduced representation bisulfite sequencing (RRBS; methylome), and single cell RNA sequencing (scRNA-seq; transcriptome). The TIs demonstrated decreased proportions of natural killer T cells (NKT) and $CD4^{+}/CD8b^{+}$ T cells compared to controls. Comparative analysis of the methylome in TI WBCs revealed a total of 5,508 differentially methylated CpG sites predicted to impact the immune system. The scRNA-seq analysis revealed an increased frequency of a B cell population decreased frequency of a myeloid cell population TI heifers. The *PDE4D* gene was overexpressed in cluster B1, *SFMBT2* was increased in cluster B5, *ARHGEF18* was overexpressed in

myeloid cluster 3, and *HNRNPLL* expression was decreased in NKT cell population 1. Differential methylation of peripheral WBC DNA does persist to 17 months of age in TI heifers. It remains to be confidently determined whether differential methylation corresponds to differential expression of genes in immune cell populations. This research continues to contribute to the identification of a potential biomarker for the identification of fetal TIs compared to postnatal TIs.

Introduction

Bovine viral diarrhea virus (BVDV) remains one of the costliest diseases in the cattle industry [3, 193, 220]. Acute transient infections with BVDV are known to decrease average daily gain and milk production in adult cattle [183, 185]. Arguably, the most detrimental effects of BVDV manifest in the form of reproductive losses. These effects include decreased conception rates or increased rates of abortions and stillbirths [183, 184]. The BVDV is vertically transmissible from an infected dam to the fetus. If a fetus is infected prior to 125 days of gestation and survives the infection, they develop immunotolerance and thus fail to produce antibodies in response to the viral infection [182, 186, 187]. These persistently infected (PI) calves remain infectious for the entirety of their life. The congenital defects of PI calves are well documented and often contribute to the development of secondary disease and premature death [186-188, 190]. These PI calves also demonstrate alterations of the epigenome that correspond to the observed pathologies both in fetal spleen at gestational day 245 and in peripheral white blood cells (WBCs) at 4 months of age [175, 250].

If BVDV infection occurs after 150 days of gestation, the calf mounts a more complete immune response which includes the production of antigen specific antibodies [122]. These calves are termed transiently infected (TI) and are born having cleared the infection. However, as demonstrated with PI calves, infections *in utero* can lead to alterations of the epigenomic control of gene regulation. This has been similarly demonstrated in TI cattle at birth and 4 months of age [179, 327]. Moreover, CpG sites are often located within promoter regions of genes [144, 145]. The addition of methylation can effectively prevent normal transcription and silence gene expression while removal or the lack of methylation at a CpG site can enhance the binding of transcription machinery and increase gene expression [147]. At birth and 4 months of age, TI calves demonstrate decreased methylation of *de novo* DNA methyltransferases (DNMTs) 3A and 3B, which is associated with increased expression [179, 327]. As CpG specific methylation increases with age [148], it is possible that aberrations observed in the TI epigenome continue to compound in the postnatal period and to the end of life. While a TI can be identified by the detection of serum neutralizing antibodies, there is currently no way to determine whether a TI occurred in the prenatal or postnatal period. As such, it is impossible to determine which calves may need additional management for mitigation of profit loss.

It was hypothesized that not only would alterations in the epigenome persist and compound in the late postnatal period, but that cellular expression of peripheral WBCs would be altered in TI heifers as a result. Complete blood counts (CBCs) and spectral cytometry of immune cells isolated from whole blood at 17 months of age were analyzed to provide enhanced context for alterations in the methylome. The DNA was

extracted from peripheral WBCs and submitted to Zymo Research for paired end reduced representation bisulfite sequencing (RRBS).

Single cell RNA sequencing (scRNA-seq) detected differential expression of four genes in peripheral WBCs, potentially altering the immune response to pathogens. Two of the four identified genes were not differentially methylated; one gene was hypomethylated in accordance with observed increased expression and another gene was hypermethylated in contrast to the finding of increased expression. The findings herein demonstrate that 17-month-old heifers infected with BVDV *in utero* have fewer T cells positive for both CD4 and CD8b and fewer natural killer cells in comparison to controls. Greater proportions of a B cell subset and decreased proportions of a myeloid cell subset were identified in TI compared to control heifers. Differential analysis of the methylome indicates inhibition of immune related processes that could contribute to immunosuppression in postnatal TI heifers.

Materials and Methods

Animals

Hereford heifers seronegative for BVDV were purchased from a private ranch in Montana, USA. The heifers were housed at the Animal, Research, Development, and Education Center (ARDEC) at Colorado State University (CSU) for approximately one month; during this month, the heifers were vaccinated twice with Ultrabac7 (Zoetis, Kalamazoo, MI, USA) with an interval of 1 month. After being transported to the Animal Reproduction and Biotechnology Laboratory (ARBL) at CSU, the heifers were synchronized using EASI-BREED (Zoetis) inserts for 14 days followed by an

intramuscular injection of Lutalyse HighCon (Zoetis). Upon detection of heat via Estrotect patches (Spring Valley, WI, USA) and visual observation, the heifers were artificially inseminated with female sexed sperm from a single bull (Select Sires MidAmerica, Logan, UT, USA). All dams were vaccinated with ScourGuard 4KC (Zoetis) 6 and 3 weeks prior to the expected calving date. Twenty-four live calves were generated. All calves were vaccinated for rabies (IMRAB, Boehringer-Ingelheim, Ingelheim am Rhein, Germany) at birth. All cow-calf pairs were transported to ARDEC and maintained on irrigated pasture from 2-7 months of age, per the national Cattleman's Beef Association Beef Quality Assurance guidelines. All calves were vaccinated with Bovilis® Covexin® (Merck, Rahway, NJ USA) at 4 and 5.5 months of age. Calves were weaned at 7 months of age and entered a feed trial study [180]. Dams were sold at auction. At 17 months of age, all generated heifers were humanely euthanized via penetrative bolt and exsanguination at the JBS Global Food Innovation Center at CSU. These methods are published previously [179, 180, 327]. All experiments were approved by the Institutional Animal Care and Use Committee at Colorado State University (Protocol approval number: 1656, 27 April 2021).

Study Design

To study the impact of fetal TI with BVDV in the late postnatal period, thirteen of the dams with confirmed pregnancy were intranasally inoculated with 4.0 $\log_{10}TCID_{50}$/mL of non-cytopathic BVDV 2 (96B2222) on day 175 of pregnancy to generate TI fetuses. Twelve dams confirmed to be pregnant were sham inoculated with Dulbecco's Modified Eagle Medium (DMEM) + 2% horse serum to generate control fetuses. All TI dams seroconverted within 14 days of inoculation, and all control dams

remained seronegative [179]. Twenty-four live calves were generated and consisted of n = 12 control heifers, n = 11 transiently infected heifers, and a single TI bull which was excluded from analysis. Control and TI status was confirmed via serum neutralization prior to calf ingestion of colostrum [179]. Calves were randomly assigned an identification number based on date of birth rather than their treatment status. Whole blood was collected from all 23 heifers for CBCs and flow cytometry analysis in collaboration with Zoetis, Inc. at the Research Innovation Center (Fort Collins, CO, USA). Extracted DNA from 5 randomly selected control and 5 randomly selected TI heifers was subjected to RRBS. A subset of collected samples was utilized for scRNA-seq (5 controls and 9 TIs) Zoetis, Inc.

Hematology

Whole blood was collected in K_2EDTA tubes (Becton, Dickinson and Company, Franklin Lakes, NJ, USA cat # 07417). The whole blood samples were held on ice until they could be transported to the laboratory for processing. Complete blood counts were obtained using whole blood (Heska Element 5, Heska Corporation, Loveland, Colorado, USA). Density centrifugation was utilized to isolate the buffy coat prior to incubation with ammonium-chloride-potassium lysing buffer (ACK; KD Medical, Columbia, MD, USA, cat # TGF-3015). The peripheral WBCs were washed in phosphate buffered saline and snap frozen and stored at -80°C until DNA extraction. These methods have been published previously with greater detail [179, 327].

In Vitro Embryo Production

Reduced Representation Bisulfite Sequencing (RRBS)

The DNA was extracted from WBCs using the Qiagen DNeasy Blood and Tissue Kit (Qiagen, Germantown, MD, USA) according to manufacturer's instructions. Extracted DNA was snap frozen using dry ice and shipped to Zymo Research for paired end RRBS. The samples were digested using the restriction endonuclease enzyme MspI (New England Biolabs, Inc.; Ipswitch, MA, USA) and purified with DNA Clean & Concentrator-5 (Zymo Research) prior to ligation to pre-annealed adapters in which cytosines were replaced with 5'-methyl-cytosines, per Illumina specifications. Ligated fragments greater than 50 base pairs were recovered with DNA Clean & Concentrator-5, bisulfite treated with the EZ DNA Methylation-Lightning Kit (Zymo Research), subjected to PCR using Illumina indices, and purified using DNA Clean & Concentrator-5. Sample size and concentration was determined using the Agilent 2200 TapeStation (Agilent; Santa Clara, CA, USA). Libraries were sequences using a NovaSeqX.

The R package TrimGalore (v0.6.4_dev) was used to trim and filter sequences shorter than 20 base pairs in length. FastQC (v0.11.9) was utilized to determine quality Phred scores, per sequences GC content, and remove overrepresented samples. No samples were found to contain adapter contamination greater than 0.1%. Samples were aligned to a bisulfite converted version of the most recent bovine reference genome available from the University of California, Santa Cruz (UCSC; ARS-UCD1.2/bosTau9) using Bismark (v0.22.3). MethylDackel (v0.5.0) was used to determine the average observed vs expected methylation level and the associated Pearson correlation coefficients. Additional details pertaining to the quality control performed by Zymo

Research can be found on their GitHub within the repository titled ‘service-pipeline-documentation’, the folder ‘docs’, and file ‘how_to_read_methylseq_report.basic.’

Flow Cytometry

Whole blood samples in K_2EDTA tubes were transported on ice and processed by Zoetis, Inc. at the Research Innovation Center (RIC) in Fort Collins, CO. Samples were treated with 1X red blood cell (RBC) lysing buffer (eBiosciences, San Diego, CA, USA cat # 00-4300-54) and centrifuged at 500 x g for 5 minutes. The resulting supernatant was discarded, and the pellet resuspended in 1 mL of Dulbecco’s phosphate buffered saline (DPBS; ThermoFisher, Waltham, MA, USA cat # 14190-136) before adding an additional 10 mL of DPBS to the sample. The samples were centrifuged again at 500 x g for 5 minutes, the supernatant was discarded, and the pellet was resuspended in 1 mL of DPBS prior to filtering through a cell-strainer cap (Corning, Corning, NY, USA cat # 352235). The sample was diluted in DPBS at a rate of 1:20 and the concentration of viable cells was determined using a Vi-CELL BLU cell viability analyzer (Beckman Coulter, Loveland, CO, USA). Viable cells were seeded into a 96 well plate at a concentration of 1 x 10^6 cells per well. Remaining cells were snap frozen in Serum Free Cell Freezing Medium (ATCC, Manassass, VA, USA cat # 30-2600) and stored at -80°C. Each well of the 96 well plate was brought to an approximate final volume of 200-300 µL with DPBS before the plate was centrifuged and the supernatant was discarded. The pelleted cells were resuspended in 100 µL of Fixable Viability Stain 620 (BD Biosciences, cat # 564996) at a concentration of 1:1000. The plate was incubated in the dark, on ice, for 10 minutes before adding 200 µL of fluorescence-activated cell sorting (FACS) buffer (BD Biosciences, cat # 554657). The

plate was again centrifuged, the supernatant discarded, and the pelleted cells resuspended in 100 µL of the cell staining master mix (Table 4.1). The plate was incubated in the dark, on ice for 20 minutes before 200 µL of FACS buffer was added to each well and the plate was centrifuged and the supernatant discarded. Cells were washed in 300 µL of FACS buffer, centrifuged, the supernatant was discarded, and the pelleted cells were resuspended in 100 µL of diluted stabilizing fixative (1:3; BD Biosciences, cat # 338036). The plate was incubated at room temperature for 5 minutes before 100 µL of FACS buffer was added to each well, the plate was centrifuged, and the supernatant was discarded. The cells were resuspended for a final time in 200 µL of FACS buffer and held in the dark until analysis at the CSU Flow Cytometry Core using a 4L 16V-14B-10YG-8R Cytek Aurora spectral cytometer. FlowJo (BD Biosciences) was used to gate the resultant flow cytometry data. The frequency of each population in relevance to either all CD45 positive cells or CD3 positive cells was exported for comparison in GraphPad Prism 10 (GraphPad Software, San Diego, CA, USA).

Table 4.1 - Flow Cytometry Fluorophore Master Mix Panel.
From left to right, the first column lists the wavelength of the laser used to detect the associated fluorophore and marker. The second column lists the molecular target. The third column lists the intended target species. The fourth column indicates the manufacturer of the antibody. The fifth column lists the fluorochrome associated with the antibody and the sixth column indicates the excitation wavelength and emission wavelength of the fluorochrome. This table has been published previously [250, 327].

Flow Cytometry Fluorophore Panel

Laser	Marker	Species (clone)	Manufacturer	Fluorophore (conjugate)	Ex/Em
405	CD11b	Anti-bovine (CC126)	BioRad	DyLight405 (conjugate)	400/420
	CD4	Anti-bovine (CC8)	BioRad	CF405 (conjugate)	408/452
	CCR7	Anti-human (3D12)	BD Horizon	BV480	436/478
	CD25	Anti-bovine (IL-A111)	BioRad	PacOrange	400/551
	CD44	Anti-mouse/human (IM7)	BioLegend	BV570	405/570
	CD127	Anti-mouse (A7R34)	BioLegend	BV605	405/605
	CD11c	Anti-human (HL3)	BD Horizon	BV650	405/645
	CD27	Anti-human (M-T271)	BD Horizon	BV711	405/711
	CD69	Anti-mouse (HI.2F3)	BioLegend	BV785	405/785
488	CD45	Anti-bovine (CC1)	BioRad	FITC	495/519
	CD14	Anti-human (M5E2)	BD	BB700	485/693
561	CD5	Anti-bovine (CC17)	BioRad	AF555 (conjugate)	553/568
	CD8b	Anti-bovine (CC58)	BioRad	PE	566/574
	CD21	Anti-bovine (CC21)	BioRad	AF568 (conjugate)	578/603
	Viability	Live/Dead	BD	FVS620	523/617
	CD335	Anti-bovine	BioRad	AF594 (conjugate)	590/618
	CD172a	Anti-bovine (CC149)	BioRad	PECy5	561/665
	MM20A	Anti-bovine	WSU	PECy7 (conjugate)	565/778
637	CD16	Anti-bovine (KD1)	BioRad	AF647	650/671
	δ chain	Anti-bovine (TCR1-N24 δ)	WSU	AF680 (conjugate)	684/707
	CD3	Anti-bovine (MM1A)	BioRad	AF750 (conjugate)	752/776

Methylation Bioinformatics and Pathway Analysis

Data from this project can be found within the NCBI GEO database under the identifier GSEpending. Raw .bam files from Zymo Research were processed according to the R package *methylKit* [199]. The files were aligned to the most recent bovine reference genome ARS-UCD1.2/bosTau9 [328]. Filtering was performed to remove CpG sites containing less than 10 reads or greater than the 99.9th percentile of reads. The data was normalized by the median coverage and filtered by a standard deviation of 2 prior to removal of outliers. Per *methylKit,* only CpG sites identified in all samples are stored for analysis; this removes potential bias due to single nucleotide polymorphisms or genetic variance. Logistic regression was used to identify singular CpG sites containing differential methylation in at least 25% of the treatment group (absolute value of meth.diff > 25) and a s (FDR; q-value) of less than 0.01. Identified CpG sites were annotated according to the gene in which the site was contained, per the bosTau9 reference genome.

The UCSC website provides a reference genome that includes annotation of experimentally validated promoter regions and areas likely to be CpG islands. The CpG islands were identified based on the criteria that they must be greater than 200 base pairs in length, have a guanine-cytosine content of greater than 50%, and an observed-to-expected CpG ration greater than 0.6. Logistic regression was performed on predefined regions by summarizing the level of methylation within the region in the weighted context of coverage, as per *methylKit.* Regions were considered to be differentially methylated if they demonstrated a difference in 15% of the treatment group (absolute value of meth.diff > 15) and a FDR/q-value less than 0.01. Regions and sites

were annotated using *genomation, clusterProfiler,* and *org.Bt.eg.db* [200, 202]. Bioinformatic code is available online at GitHub user profile jnkincade within the repository labeled ‘Bovine-RRBS-Analysis.’

The list of genes containing differentially methylated sites (DMSs) as well as the associated p-value, q-value, and meth.diff value were entered into Ingenuity Pathway Analysis (IPA; Qiagen). The IPA software contains canonical pathways that have been curated according to the scientific community’s understanding of specific functions, diseases, or processes. The number of genes within a specific pathway that were identified within the dataset is compared to the overall number of genes contained within the known, curated pathway and is called overlap. A Fisher’s exact test is used to estimate the probability of the overlap occurring due to random chance. The software also utilizes the meth.diff values to calculate a z-score and predict whether the pathway is likely to be activated or inhibited in the context of the entered data [251]. The canonical pathways and machine learning (ML) disease pathways were sorted according to z-score; positive z-scores indicate predicted activation of a pathway, and negative z-scores indicate predicted inhibition of a pathway.

The generated list of genes containing DMSs at 17 months of age (presented herein) was compared to those generated by previous analysis of the methylome at 4 months of age and birth (NCBI GEO Identifiers GSE255721 and GSE288374, respectively). Analysis of previous datasets was identical to the analysis performed and described here; alternatively, methods for analysis can be found in previous publication [250, 327]. To identify genes that contained only hyper- or hypo- methylation from birth until harvest, genes containing both a hypermethylated CpG and a hypomethylated

CpG at any one time were removed. The three datasets were then compared against one another to extract only genes containing consistent hyper- or hypo- methylation at all 3 timepoints.

Single Cell RNA Sequencing

FASTQ files returned from Parse Biosciences (Seattle, Washington, USA) were loaded into the Alpine high performance computing environment supported by the University of Colorado Boulder, the University of Colorado Anschutz, and CSU. An indexed reference genome was generated using the most recent reference genome mapped by the UCSC (ARS-UCD1.2/bostau9) downloaded from Ensembl. The proprietary *split-pipe* workflow was used to process sub-libraries and combine sub-libraries into a single expression matrix. The resulting expression matrix for all samples contained from 17 months of age were loaded into R using *Seurat* [329, 330]. Sample 2149 was removed due to severe overrepresentation that could not be mitigated by normalization methods. Sample 2156 was removed due to accidental vaccination against BVDV at approximately 9 months of age. Cells containing less than 500 features or greater than 5000 features were removed. Contamination with mitochondrial RNA was quantified by expression of NADH dehydrogenases (*ND1, ND2, ND3, ND4, ND4L, ND5,* and *ND6),* cytochrome c oxidase subunits 1 through 3 (*COX1, COX2,* and *COX3*), cytochrome B (*CYB*), cytochrome c oxidase II (*CO2*), as well as ATP synthase complex subunits 6 and 8 (*ATP6* and *ATP8*). Cells with greater than 2% mitochondrial contamination were removed. Cells likely to be doublets were removed using the R package *scDblFinder* [331]. Features were normalized according to Pearson residuals, variable features were identified, and the top 2000 were scaled using the R package

SCTransform [332, 333]. A principal component (PC) analysis dimensionality reduction was performed and plotted on an elbow plot to determine the number of PCs necessary to adequately describe the variation in the data. The nearest neighbors were calculated using 30 dimensions and clusters identified using a resolution of 2. A Uniform manifold approximation and projection (UMAP) dimensional reduction was performed and visualized using UMAP reduction. Markers for each cluster were identified using Seurat::FindMarkers with default settings. Clusters were annotated manually according to bovine cell type markers. The R package *scCustomize* was utilized to make figures demonstrating marker expression by cluster. The frequency of each cluster within each sample was extracted and compared in GraphPad Prism (Boston, Massachusetts, USA).

Seurat::AggregateExpression was used to pseudobulk the data prior to differential expression analysis of each cluster by treatment. In summary, sample level counts are aggregated to create a single counts matrix which is converted to a DESeq2 object. The object was filtered according to the above specifications. Differential analysis was performed using the DESeq2 test option. The WBCs derived from control and TI heifers were compared within each annotated cluster to reveal genes that were differentially expressed due to late gestational BVDV infection. Differentially expressed genes (DEGs) had an FDR of 0.05 or less and a $\log_2$fold change in expression of 1 or greater. Genes with a $\log_2$fold change in expression greater than 1 but an FDR of 0.05 to 0.1 were considered as ‘tendencies.’ Code used to perform the above analysis can be found on GitHub user ‘jnkincade’ in the repository titled ‘Bovine-pWBC-scRNAseq.’

The raw files for this analysis can be found in the NCBI GEO database under the identifier (GSE pending).

Statistical Analysis

The CBC values and frequencies obtained from flow cytometry analysis were imported and compared in GraphPad Prism 10 (GraphPad Software). Values were tested for normality using the Shapiro-Wilk test and outliers were identified using the ROUT method with an FDR/q-value of 10%. Outliers were removed prior to calculation of descriptive statistics and significance. An unpaired, parametric T-test was used to detect differences between the control and treatment group when the data was normally distributed. Welch's correction was applied due to unequal sample numbers. When the data was not normally distributed after the removal of outliers, a non-parametric Mann-Whitney rank test was utilized to detect significance. Differences between the control and treatment group were considered significant if the p-value was less than 0.05. Data are presented as mean ± standard error of the mean (SEM). One asterisk (*) indicates that the p-value was less than 0.05. Two asterisks (**) indicates that the p-value was less than 0.01. Three asterisks (***) indicates that the p-value was less than 0.001. Four asterisks (****) indicates that the p-value was less than 0.0001. Comparisons resulting in a p-value of less than 0.1 but greater than 0.05 were considered 'tendencies.'

Results

Complete Blood Counts

No differences in CBCs were detected between TI and control heifers at 17 months of age (Table 4.2).

Table 4.2 – Complete blood counts in 17-month-old TI heifers.
Parameters in which outliers were removed are indicated by the presence of the dagger†. Outliers removed include a neutrophil TI value of 4.02, a mean corpuscular volume TI value of 38.0, a lymphocyte percent TI value of 49.6 and 58.7, and a red cell distribution width TI value of 27.1 and 26.7. Data are displayed as mean ± standard error of the mean (SEM). Reference values were derived from the Element HT5 Veterinary Hematology Analyzer (Heska).

Complete Blood Counts in 17-Month-Old Heifer Calves

	Control		TI			
Population	**Average**	**SEM**	**Average**	**SEM**	**Reference**	**Unit**
Basophil Count	0.02	± 0.00	0.02	± 0.00	0 – 0.35	10^9/L
Eosinophil Count†	0.08	± 0.01	0.14	± 0.03	0 – 1.3	10^9/L
Neutrophil Count†	1.52	± 0.17	1.72	± 0.22	0.60 – 4.9	10^9/L
Monocyte Count	0.16	± 0.02	0.19	± 0.03	0 – 1.02	10^9/L
Monocyte Percentage	1.06	± 0.19	1.81	± 0.42	0 – 9.5	%
Red Blood Cell Count	8.47	± 0.25	8.24	± 0.20	5.0 – 10.1	10^{12}/L
Hemoglobin	14.26	± 0.34	13.35	± 0.40	8.0 – 14.2	g/dL
Hematocrit	40.83	± 0.92	38.30	± 1.11	23.0 – 42.5	%
Red Cell Distribution Width†	23.01	± 0.79	21.85	± 0.30	17.5 – 26.5	%
Mean Corpuscular Volume†	48.34	± 0.72	47.33	± 0.56	37.0 – 55.0	fL
Mean Corpuscular Hemoglobin	16.90	± 0.25	16.55	± 0.19	12.5 – 18.2	pg
White Blood Cell Count	8.84	± 0.42	8.94	± 0.33	4.6 – 15.8	10^9/L
Lymphocyte Count	7.07	± 0.29	6.63	± 0.28	1.5 – 11.8	10^9/L
Lymphocyte Percentage†	80.25	± 1.48	79.03	± 1.61	52.3 – 85.6	%
Platelet Count	323.2	± 29.86	365.0	± 31.62	100 – 720	10^9/L
Mean Platelet Volume	6.25	± 0.16	6.12	± 0.11	4.8 – 7.6	fL

Flow Cytometry

Collaborators at Zoetis Inc. developed a 20-fluorophore panel to identify bovine immune cell types (Table 4.1). A gating strategy (Figure 4.1A) was developed using the 20-fluorophore panel to identify subsets of myeloid and lymphoid immune cell types (Figure 4.1B). All samples were initially gated on the forward and side scatter to remove debris and doublets. Samples were then gated to remove dead cells. Hematopoietic cells were selected based on the expression of CD45.

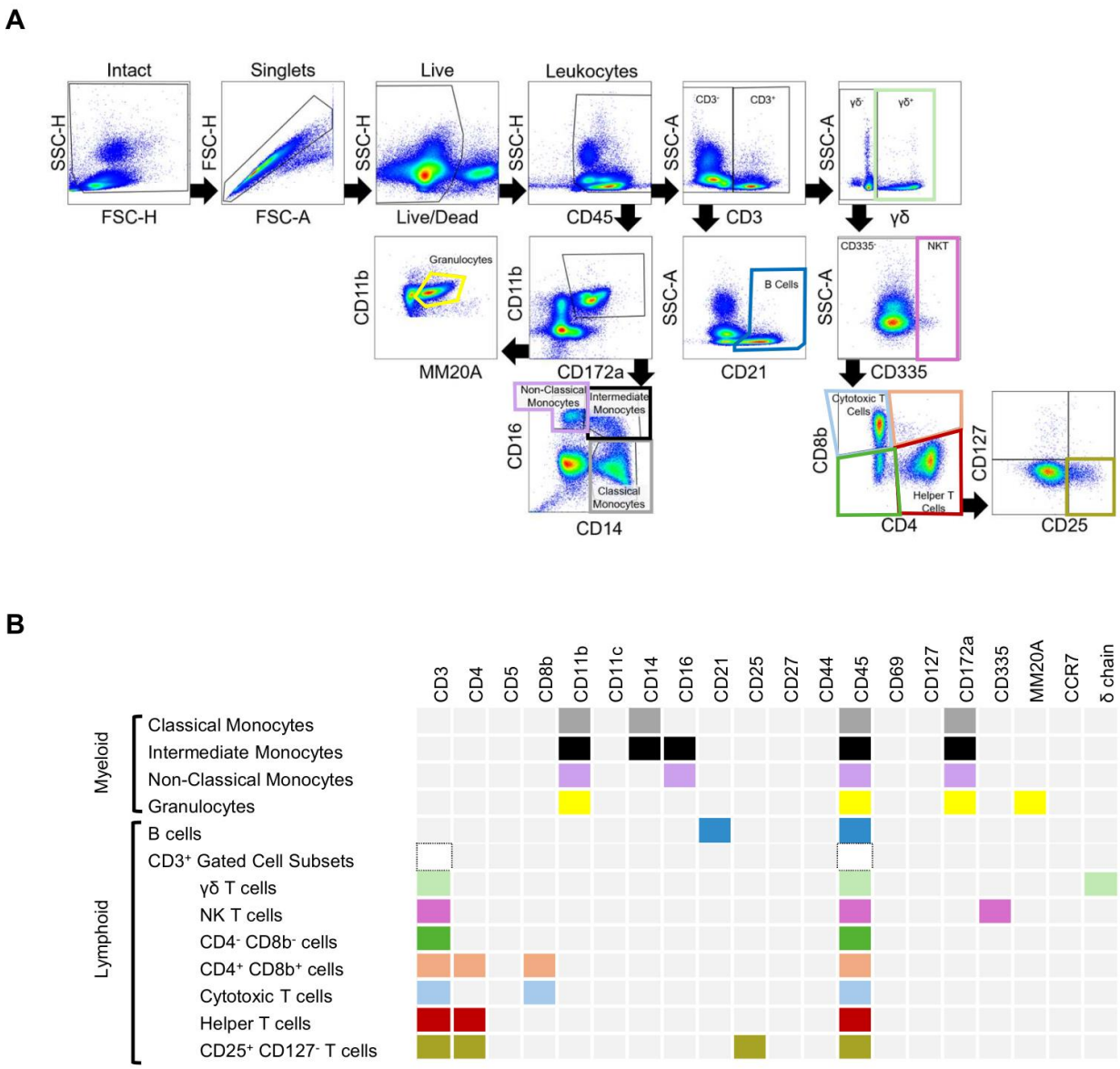

Figure 4.1 – Identifying immune cell populations in cattle.
(A) Gating strategy to identify immune cell populations in bovine. This schematic was generated using FlowJo. (B) Molecular markers for immune cell populations. Each row is color coded according to the gating strategy and indicates which markers (column IDs) were present in each population. Light grey indicates that the population was *not* present in the population (row). This figure is reprinted with permission from previous publication within this laboratory [250, 327].

To determine whether there was any impact of fetal TI with BVDV on the frequency of immune cell populations in the late postnatal period, spectral cytometry was performed on WBCs isolated from whole blood. The frequency of each cell population in relation to the total number of $CD45^+$ cells was quantified for comparison. Additionally, the frequency of T cell subpopulations in relation to the total number of $CD3^+$ cells was quantified for comparison. A subset of helper T cells, $CD25^+/CD127^-$ was compared based on the frequency in relation to the total number of $CD4^+$ T cells.

No differences were detected in myeloid populations including classical monocytes, intermediate monocytes, non-classical monocytes, granulocytes, B cells, γδ T cells, helper T cells, or cytotoxic T cells. Differences were detected in NKT cells and T cells positive for both CD4 and CD8b (Table 4.3). Natural killer cells were found to be decreased in TI heifers at 17 months of age when the frequency in the context of total CD45 positive cells was compared (0.47% ± 0.5 vs 0.26% ± 0.23). The frequency of T cells positive for CD4 and CD8b was found to be decreased in TI heifers both in the context of total $CD45^+$ cells (0.23% ± 0.03 vs 0.15% ± 0.02) and $CD3^+$ cells (0.53% ± 0.06 vs 0.37 ± 0.4).

Table 4.3 – Decreased NKT and CD4$^+$/CD8b$^+$ T cells in TI heifers at 17 months of age. Quantification of immune cell population frequency in relation to the parent frequency of either CD45$^+$ cells or CD3$^+$ cells. The shading color corresponds to the gating strategy and molecular markers in Figure 4.1. Outliers were identified using the ROUT test set at 10%. Identified outliers include an intermediate monocyte/CD45 control value of 1.13, NKT/CD45 TI values of 0.65 and 0.54, and CD25$^+$/CD127$^-$ of CD4 frequency TI values of 17.4 and 19.9. Parameters containing outliers are marked with a dagger†. After the removal of outliers, a Shapiro-Wilk test was performed to assess normality. Normally distributed data were compared using an unpaired, parametric T-test. Data that were not normally distributed were compared using a non-parametric Mann Whitney test. Data are displayed as the mean ± standard error of the mean (SEM). Asterisks indicate a significant difference between the control and treatment group, * $p < 0.05$, *** $p < 0.001$. This figure is derived from a format published previously from this laboratory [250, 327].

	Immune Cell Populations via Flow Cytometry					
	Control		TI			
Population	Average (%)	SEM	Average (%)	SEM	p-value	Freq. of
Classical Monocytes	4.60	± 0.28	5.01	± 0.39	0.40	CD45
Intermediate Monocytes†	0.56	± 0.06	0.76	± 0.10	0.07	CD45
Non-Classical Monocytes	0.85	± 0.06	0.87	± 0.12	0.90	CD45
Granulocytes	22.47	± 1.50	21.65	± 2.48	0.78	CD45
B Cells	15.21	± 0.72	16.85	± 0.95	0.18	CD45
T Lymphocytes	43.54	± 1.50	41.77	± 2.96	0.60	CD45
γδ$^+$ T Cells	14.38	± 0.76	13.25	± 1.46	0.50	CD45
NK T Cells† ***	0.47	± 0.50	0.26	± 0.23	0.0009	CD45
CD4$^-$/CD8b$^-$ T Cells	3.08	± 0.15	2.78	± 0.18	0.22	CD45
CD4$^+$/CD8b$^+$ T Cells *	0.23	± 0.03	0.15	± 0.02	0.04	CD45
Cytotoxic T Cells	9.49	± 0.58	8.75	± 0.77	0.45	CD45
Helper T Cells	14.29	± 1.07	14.93	± 0.86	0.49	CD45
CD25$^+$/CD127$^-$ T Cells	1.60	± 0.13	1.59	± 0.16	0.97	CD45
γδ$^+$ T Cells	34.59	± 2.13	32.40	± 1.77	0.44	CD3
NK T Cells	1.12	± 0.10	0.82	± 0.12	0.06	CD3
CD4$^-$/CD8b$^-$ T Cells	7.34	± 0.30	6.97	± 0.23	0.34	CD3
CD4$^+$/CD8b$^+$ T Cells *	0.53	± 0.06	0.37	± 0.4	0.04	CD3
Cytotoxic T Cells	22.56	± 1.25	21.73	± 1.37	0.66	CD3
Helper T Cells	33.76	± 1.64	37.71	± 1.25	0.07	CD3
CD25$^+$/CD127$^-$ T Cells†	11.49	± 0.96	9.20	± 0.55	0.06	CD4

Methylome

An average of 48 million reads were processed from each sample and an average of 7.4 million unique CpGs were identified within each sample. The average CpG coverage was 10X. The bisulfite conversion rate for spike-ins was greater 99.3% or greater for all samples. The bisulfite conversion rate for non-CpGs was 99.2% or greater for all samples. All mean quality scores (Phred) were greater than 30 at all base pairs, indicating that the likelihood of labeling an incorrect base to be less than or equal to 1 in 1000 (99.9% accuracy or greater). An average of 31.9% of reads mapped uniquely to the reference genome, an average of 53.6% mapped ambiguously to one or more region in the reference genome, and approximately 14.5% did not map to the reference genome. Pearson correlation coefficients were 0.97 or greater for all samples. The samples were clustered according to 1 – the Pearson correlation coefficient to demonstrate overall similarity between control and TIs (Figure 4.2A).

A total of 5,508 differentially methylated CpG sites (DMSs) were identified when comparing the methylome of TI heifers to that of control heifers at 17 months of age (Figure 4.2B). Of the total 5,508 DMSs identified, 2,986 demonstrated hypermethylation (54%; meth.diff > 25) and 2,522 demonstrated hypomethylation (46%; meth.diff < -25; Figure 4.2C).

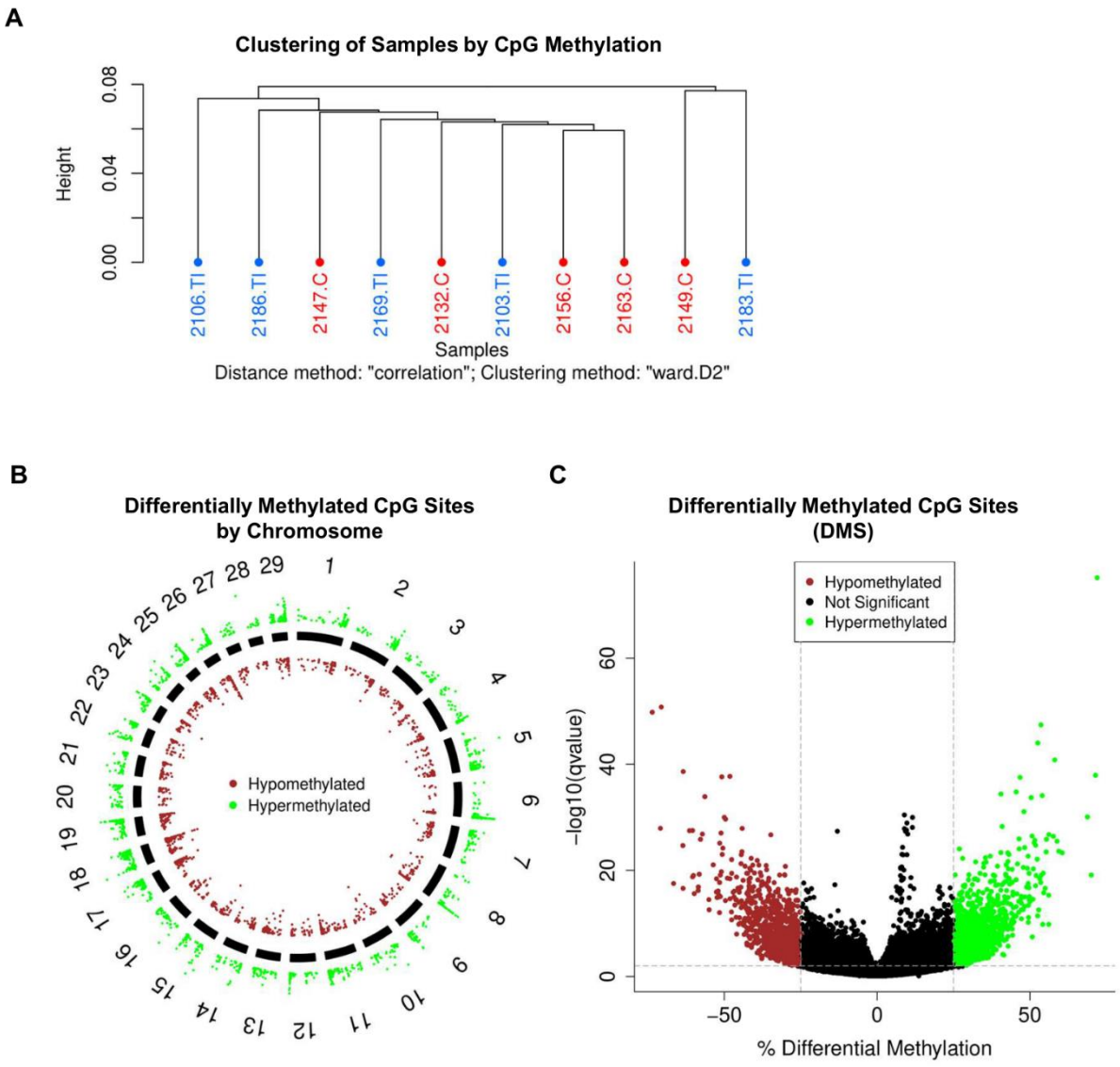

Figure 4.2 – Differential methylation of CpG sites in TI heifers at 17 months of age.
(A) Hierarchical clustering of the samples according to 1 – Pearson's correlation coefficient. The ID numbers of control heifers are labeled in red and followed by '.C' while the ID numbers of TI heifers is labeled in blue and followed by '.TI'. (B) Each dot represents a differentially methylated CpG site. The color indicates whether the site was found to contain increased methylation (hypermethylated; green) or decreased methylation (hypomethylation; red) in TI heifers compared to controls. The numbers and black lined track indicate the chromosome number containing the differentially methylated CpG site. (C) Each dot denotes a differentially methylated CpG site (DMS). These DMSs were required to have a false discovery rate of less than 0.01 and an absolute meth.diff value greater than 25%. DMSs with negative meth.diff values indicate hypomethylation (red) and those with positive meth.diff values indicate hypermethylation (green).

A total of 3,177 genes contained at least 1 DMS. The retinoid X receptor alpha (*RXRA*) gene was found to contain 34 DMS, the eukaryotic translation initiation factor 2 subunit beta (*EIF2S2*) contained 24, and the synaptonemal complex central element protein 1 (*SYCE1*) contained a total of 22 DMS. Approximately 66% of the genes identified to contain differential methylation contained a single DMS; an additional 19% contained 2 DMSs. The remaining 15% of genes identified to be differentially methylated contained 3 or more DMS. It was determined that 10% of the DMSs were in a promoter region, 13% were in an exon, 41% were found in an intron, and 36% were in an intergenic region.

A list of the genes containing DMSs identified during differential analysis of TI and control heifers at 17 months of age were exported and entered into IPA software (Qiagen). The top 5 canonical pathways predicted to be activated in TI heifers (and the associated z-score) include smooth muscle contraction (3.16), mitochondrial division signaling (3.13), mitotic G1 phase and G1/S transition (2.53), eukaryotic translation initiation factor 2 (EIF2) signaling (2.53), and Huntington's disease signaling (2.31; Figure 4.3A). The top 5 canonical pathways predicted to be inhibited in TI heifers include stress activated protein kinase/c-Jun N-terminal kinase (SAPK/JNK) signaling (-2.65), leukocyte extravasation signaling (-2.54), HIPPO signaling (-2.45), extracellular signal-regulated kinase/mitogen-activated protein kinase (ERK/MAPK) signaling (-2.24), and transcriptional regulation by VENT homeobox (VENTX; -2.24; Figure 4.3B). The top 5 ML disease pathways predicted to affect TI heifers include familial autoimmune disease, withdrawal syndrome, prostatic intraepithelial tumor, thyroid gland tumor, and stenosis of the cardiac valve (Figure 4.3C).

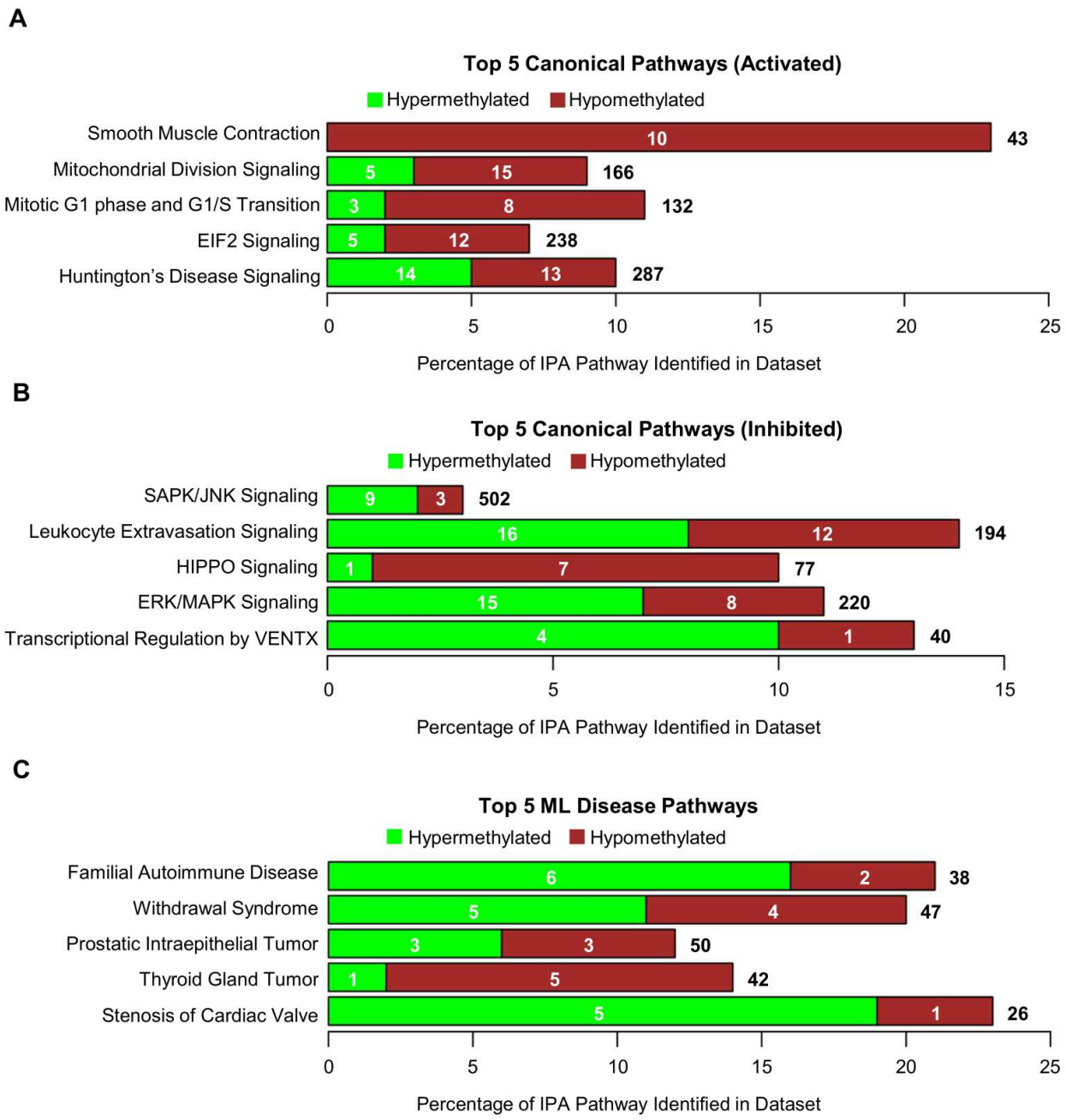

Figure 4.3 – Pathways predicted by IPA software to be altered in TI heifers.
The white numbers included within green regions of the bar graph indicate the number of genes found to contain hypermethylation in TI heifers. The white numbers included within red regions of the bar graph indicate the number of genes found to contain hypomethylation in TI heifers. The black number to the right of each bar denotes the total number of genes contained in that IPA pathway.

In addition to identification of singular DMSs, the level of methylation was summarized within known promoter regions and CpG islands and compared between treatment groups. A total of 81 DMS were identified within mapped promoter regions contained within a total of 61 genes. Of the identified 81 DMS within promoter regions, 47 were hypermethylated (58%) and 34 were hypomethylated (42%). The gene encoding intracellular adhesion molecule 2 (*ICAM2*) was found to contain 7 hypomethylated DMS within promoter regions. Within TI heifers, a total of 73 DMSs were found within CpG islands of 72 genes. Of the DMSs within CpG islands, 52 were hypermethylated (71%) and 21 were hypomethylated (29%). Only the potassium inwardly rectifying channel subfamily J member 8 (*KCNH8*) gene was found to contain 2 DMSs in CpG islands.

The list of genes identified to contain DMSs at 17 months of age were compared to those identified by our lab at 4 months (chapter 3) of age and birth [179, 334]. The comparison between all 3 timepoints resulted in the identification of 26 genes containing consistently hypermethylated DMSs, 35 genes containing hypomethylated DMSs, 2 genes containing hypermethylation in CpG islands, and 1 gene containing a hypomethylation within the promoter region of the gene.

Single Cell Transcriptome

Peripheral WBCs isolated from the whole blood of TI and control heifers at 17 months of age were subjected to scRNA-seq using the Evercode® platform produced by Parse Biosciences (Seattle, WA). A total of 5 control samples and 9 TI samples were barcoded and sequenced. A total of 40,346 cells were recovered and mapped to the most recent bovine reference genome ARS-UCD1.2/bosTau9. Following quality control

filtering, a total of 37,214 cells remained for downstream analysis, 13,767 of which were derived from control samples and 23,447 of which were derived from TI samples. The average number of genes contained within a single cell across both groups was 2,116; the average number of unique gene identifiers expressed by a single cell was 2,026 and 2,169 for control and TI derived cells, respectively. The overall average expression of mitochondrial RNA was found to be approximately 0.2% of the total RNA expression per cell (Figure 4.4).

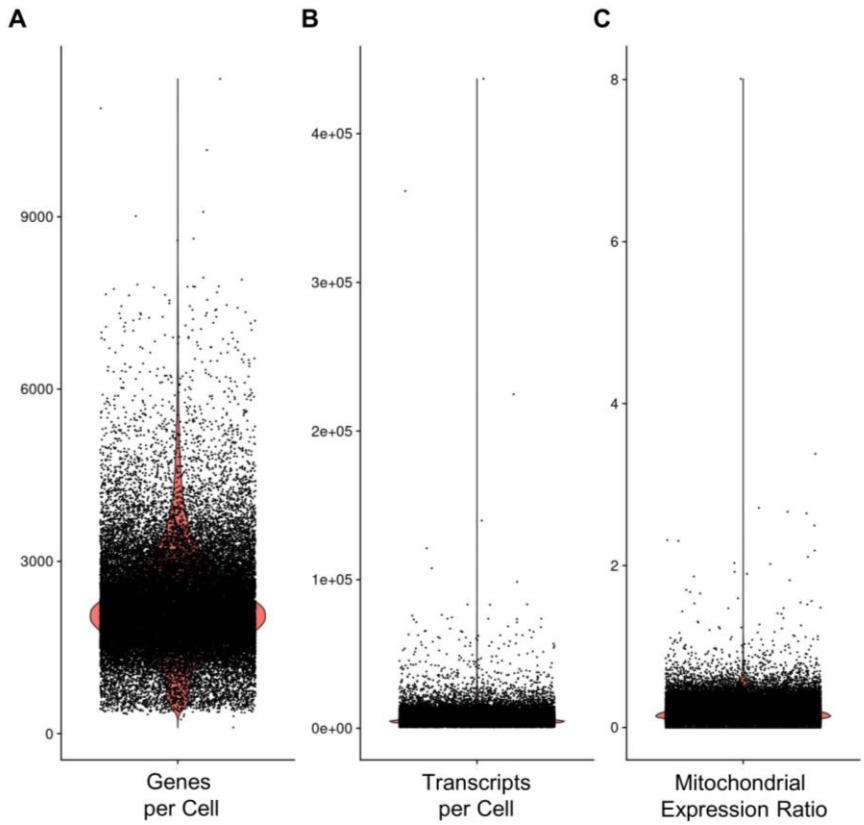

Figure 4.4 – Filtering of single cell RNA sequencing (scRNA-seq) data.

Each dot within the figure represents a single cell. Thresholds were set to filter out any cells with less than 500 or greater than 5000 genes. A threshold was also set to remove any cells in which the ratio of mitochondrial gene expression was greater than 2% of the total gene expression.

Guided clustering was performed using Seurat (v5.2.1) and resulted in 25 unique cell clusters (Figure 4.5A). The cell clusters were manually annotated according to cellular expression (Figure 4.5B) and current literature Identification of B cells was performed based on cellular expression of *CD19, CD20, CD21, CD79a,* and *CD79b.* Expression of *CD335* allowed for identification of populations of cells as natural killer (NK)*;* NKT cells expressed *CD335* in addition to *CD3e.* Myeloid cells (MYE) were identified according to expression of *CD11a, CD11b, CD172a,* and *CD115* in combination with or without *CD14* and *CD16.* Dendritic cells (DCs) were the only cell populations with enriched expression of *FLT3.* Helper T cells expressed *CD3e* and *CD4* while cytotoxic T cells (CTLs) expressed *CD3e* in combination with *CD8a* and *CD8b.* Populations of γδ T cells were identified by expression of *CD3e* and any variant of *WC1.*

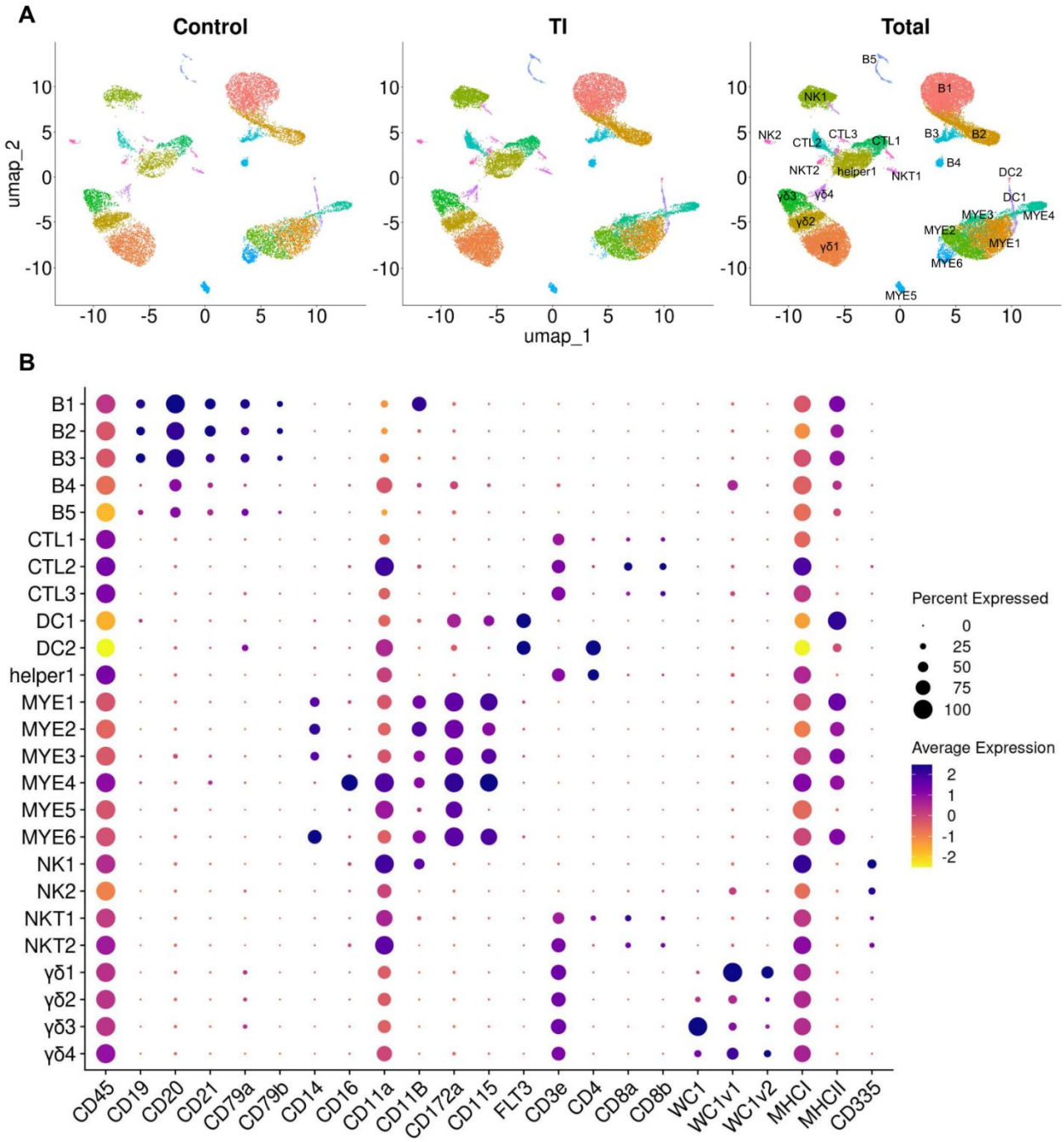

Figure 4.5 – Identification of cell clusters in bovine peripheral WBCs via scRNA-seq. (A) Uniform Manifold Approximation and Projection (UMAP) reduction of cell populations in bovine peripheral WBCs. Twenty-five distinct clusters were identified in both control and TI heifers. (B) Expression of molecular markers used to annotate cellular populations. The size of the dot indicates the proportion of cells within the population found to express the marker. The darker value color indicates greater expression. B cells (B1-B5) were identified according to expression of CD19, CD20, CD21, CD79a, and CD79b. Cytotoxic T cells (CTL1 – CTL3) and helper T cells (helper1) were identified by expression of CD3e and either CD8a and CD8b or CD4, respectively. Clusters were identified as dendritic cells (DC1 and DC2) if expressing FLT3. Cell clusters were classified as myeloid (MYE1 – MYE6) when expressing CD172a in combination with CD11a and CD11b. Natural killer cells (NK1 and NK2) were identified by

expression of CD335; cells expressing CD335 and CD3e were classified as natural killer T cells (NKT1 and NKT2). T cells expressing any variant of WC1 were classified as γδ T cells (γδ1 – γδ4).

The proportion of each cell type within each sample was compared by treatment to detect any differences in cellular representation. The TI heifers had smaller proportions of myeloid population 5 (MYE5; 1.6% ± 0.2 vs 0.8% ± 0.2) compared to controls. The TI heifers were also found to have a greater proportion of B cell population 5 (B5; 0.7% ± 0.1 vs 1.3% ± 0.00; Figure 4.6). Each cell type cluster was also analyzed for differential expression of genes. Four differentially expressed genes (DEGs) were identified when TI derived cells were compared to control derived cells by cell type cluster. The B1 cells derived from TI samples expressed a higher proportion of *PDE4D* (log_2fold of 1; p-value < 0.0001) and B5 cells expressed higher proportions of *SFMBT2* (1.5; 0.0001). The myeloid population, MYE3, was found with increased expression of *ARHGEF18* (1.7; 0.01) in TI heifers, respectively. The NKT1 cells derived from TI heifers were also found to express less *HNRNPLL* (-1.2; 0.02) when compared to those derived from control heifers (Figure 4.7). An additional 8 genes were found to display a tendency for difference in cell clusters derived from TI heifers. The γδ2 population in TIs expressed lower proportions of *DPP6* (-1.5; 0.06) and the helper1 population in TIs expressed less *FAM184A* (-1.2; 0.09). The NKT1 TI population expressed smaller proportions of *TSPAN13* (-1.5; 0.09). The B2 population expressed greater amounts of *RPS4Y1* (-1.06; 0.06) and the B5 population expressed higher amounts *ENSBTAG00000048268* (2.5; 0.09).

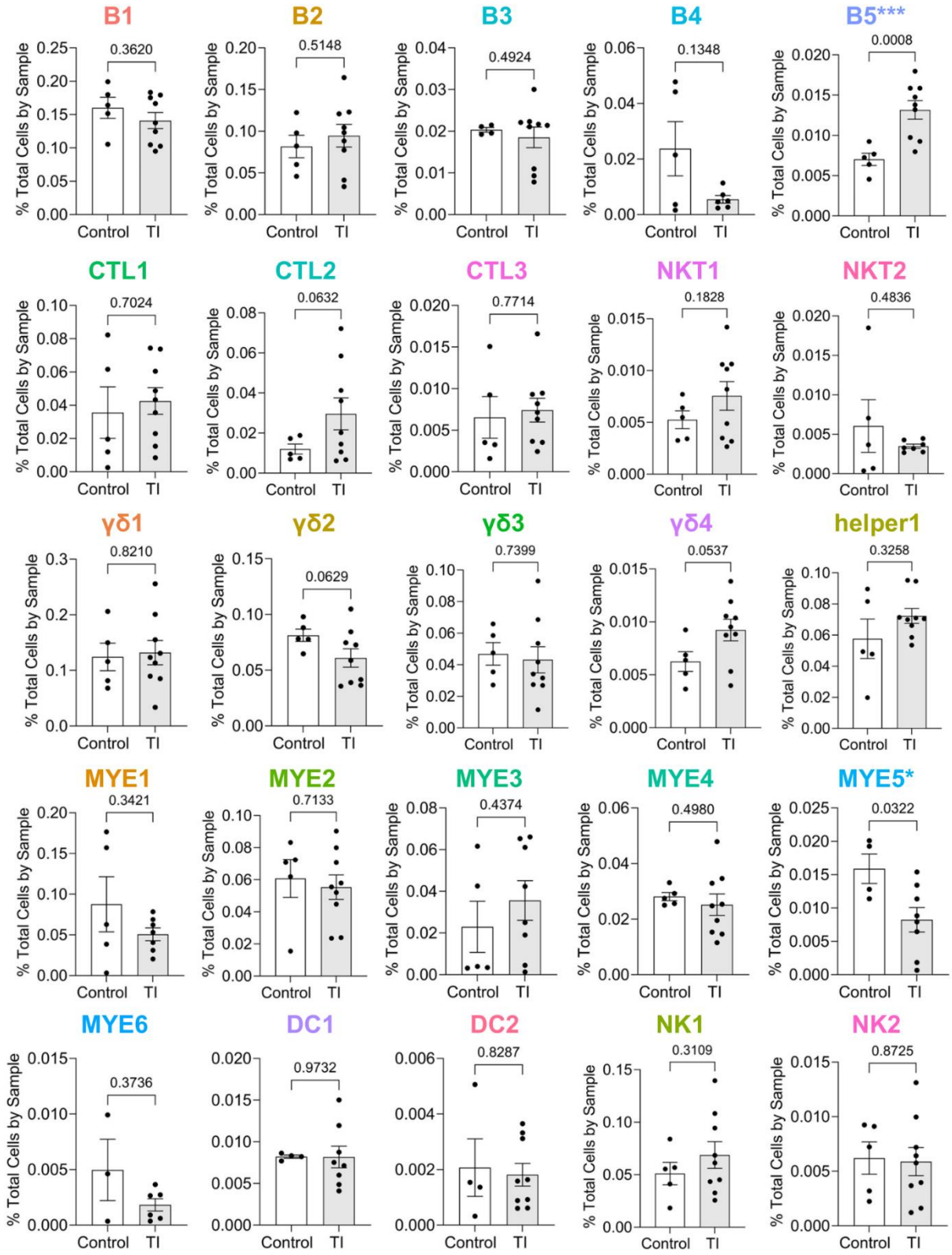

Figure 4.6 – Cellular frequencies in TI heifers compared to controls.
The color of the label corresponds to the color of the population within the UMAP in Figure 4.4A. P-value is indicated above the bracket within each graph. Outliers were removed prior to assessing normality and application of the appropriate comparative test.

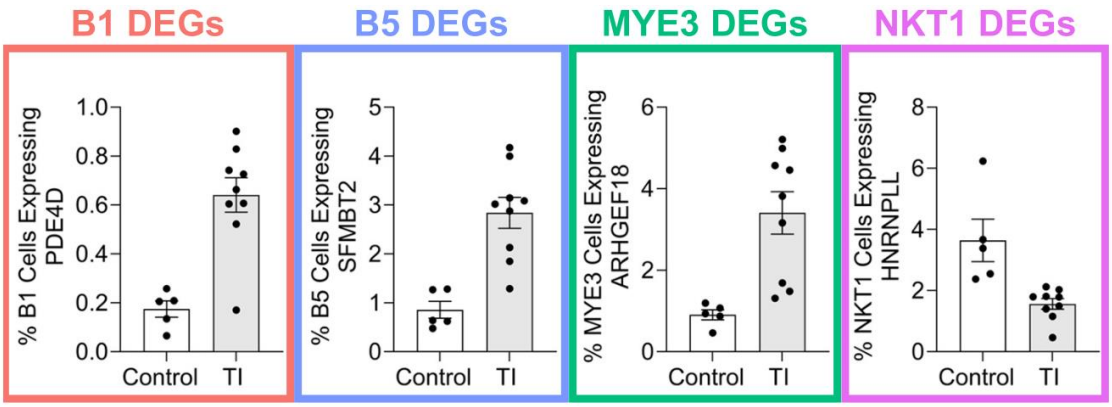

Figure 4.7 – Differentially expressed genes (DEGs) in cell type clusters derived from TI heifers.
The color of the box surrounding each graph corresponds to the color of the population within the UMAP in figure 4.4A. All DEGs demonstrated an adjusted p-value of 0.05 or less and a log_2fold change in expression.

Discussion

It was hypothesized that the methylation and transcription of DNA in immune cells would be modified in 17-month-old heifers following fetal TI with BVDV and subsequently indicate decreased profitability in a production setting due to increased risk of disease. The TI heifers were infected with ncp BVDV type 2 at gestational day 175, generated specific antibodies in response, and cleared the virus prior to birth. Facets of the immune system were analyzed via CBCs, spectral cytometry, RRBS, and scRNA-seq. The TI heifers had smaller proportions of T cells positive for both CD4 and CD8b, at 4 months of age and 17 months of age in comparison to controls [327]. This population of cells is not well studied in humans and is even less characterized in cattle. However, an increase in this 'double positive' population has been observed following vaccination to foot and mouth disease, suggesting that $CD4^+/CD8b^+$ T cells may function more like helper T cells [230, 262]. Similarly, CD4/CD8b+ T cells have been reported to increase in response to infection and express interleukin (IL) 10, interferon-γ

(IFNγ), and transforming growth factor-β, indicating a role in pathogen clearance and stimulation of inflammation (reviewed in [262, 335]). A decrease in NKT cells was also identified in 17-month-old TI heifers. The NKT cells demonstrate cytotoxic abilities when exposed to glycolipid antigens presented by CD1d but are also known to express cytokines most associated with helper T cells such as IL-4 and IFNγ (reviewed in [336]). At 4 months of age, TI heifers demonstrated differential methylation of WBC DNA indicative of increased inflammation [327]; during a feedlot trial, TI heifers were found to have increased indicators of inflammation including elevated ceruloplasmin and oxidized glutathione [180]. Inflammation can lead to a decrease in NKT cells, as demonstrated in humans with rheumatoid arthritis or inflammatory bowel disease [337, 338]. Mice lacking NKT cells demonstrate reduced weight gain, metabolic dysfunction, and exacerbated viral, parasite, bacterial, and fungal infections [339, 340].

Analysis of differential methylation of genes in TI heifers compared to controls largely supports the theory of immunosuppression in TI heifers. One study describes TI heifers as being 2.3 times more likely to require treatment for morbid episodes compared to their non-TI counterparts [246]. Similarly, IPA predicted activation of the familial autoimmune disease pathway, citing hypomethylation within ATPase plasma membrane Ca^{2+} transporting 4 (*ATP2B4*) and collagen type 6 alpha 2 chain (*COL6A2*) as well as hypermethylation within collagen type 6 a 3 chain (*COL6A3*), forkhead box protein 3 (*FOXP3*), interleukin 2 receptor subunit alpha (*IL2RA*), interleukin 3 receptor subunit beta (*IL3RB*), and T-box transcription factor 21 (*TBX21*). Using these genes, IPA predicts that TI heifers are likely to experience a decrease in the following: activation of peripheral blood lymphocytes, stimulation of natural killer cells, differentiation of effector

helper T lymphocytes, and cellular infiltration by regulatory T cells. Specifically, loss of FOXP3 expression leads to autoimmunity in mice due to disruption of regulatory T cell function [341]. Decreases in *IL2RB* in humans have been shown to lead to decreased regulatory T cells and altered populations of NK cells [342]. Regulatory T cells are classically identified as alpha beta T cells positive for CD4 and CD25 but negative for CD127. It is important to note that while these cells can be identified in cattle, they do not demonstrate typical regulatory behaviors; in fact, they are anergic and not suppressive [231]. While $CD25^{+}/CD127^{-}$ T cells cells were identified in TI heifers, no differences were detected via spectral cytometry.

The IPA software also predicted leukocyte extravasation to be inhibited in TI heifers. Mice lacking P-selectin demonstrate decreased leukocyte extravasation, partially recapitulating the human disease known as leukocyte adhesion deficiency (LAD) [343]. These mice demonstrate increased morbidity, higher bacterial load, and elevated inflammation as a result [344]. Similarly, humans with LAD are known to experience recurrent bacterial infections, impaired wound healing, and persistent leukocytosis (reviewed in [345]).

The *PDE4D* gene was found to be expressed at a greater proportion in B1 cells derived from TI heifers compared to control heifers. The PDE4D enzyme hydrolyzes cyclic AMP [346]. A reduction of PDE4D and subsequent increase in cyclic AMP is necessary for activation as well as stimulated proliferation [347]. As such, it is possible that overexpression of PDE4D may be an obstacle to B cell activation and proliferation in the case of infection. The B5 population is likely a population of peripheral memory B cells, as they lack expression of CD138 but retain expression of other memory B cell

markers such as CD27, CD40, CD80, and CD86 in addition to low expression of canonical B cell markers CD19 and CD20 [348, 349]. The explanation as to why TI heifers have a greater proportion of circulating memory B cells is implicit; TI heifers have been inherently exposed to BVDV type 2 *in utero,* whereas the controls were not, and thus would have built a greater repertoire of antibody memory. However, this could also be due to exposure and contraction of other infections, but no clinical signs were observed. The gene encoding Scm-like-with-four-Mbt-domains-2 (SFMBT2), which was found to be overexpressed in TI derived B5 cells, is involved in histone binding activity and negative regulation of gene expression [350]. Its impact on B cell function remains unclear; most of its known functions are associated with tumor suppression in humans or mice [351, 352].

Myeloid population 3 (MYE3) was found to overexpress the Rho guanine nucleotide exchange factor 18 (ARHGEF18) in WBCs derived from TI heifers compared to controls. This protein was recently found to interact directly with the BVDV viral nonstructural protein 5 (NS5) and promote immune activation through NFκB signaling [353]. This protein is a RhoGEF, which facilitates the conversion of GDP to GTP and thus activate Rho GTPases [354], which are critical to both adhesion and migration of myeloid cells [355]. The fifth myeloid population, MYE5, which was found to be decreased in TI heifers, potentially consists of macrophages with an expression profile more similar to that of M2 macrophages [356]. The MYE5 subset expresses low levels of CD80 and CD86, which are expressed in M1 macrophages, but expresses higher amounts of CD163 and IL10 [356]. Circulation of macrophages in peripheral blood is uncommon but has been demonstrated to occur [357]. Canonically, M2 macrophages

promote anti-inflammatory responses, wound healing, and angiogenesis [358]. A decrease in MYE5, which appear similar to M2 macrophages, corresponds to previous findings indicating increased inflammation in TI heifers.

The NKT cell 1 population was also found to express lower proportions of *HNRNPLL* (heterogenous nuclear ribonucleoprotein L-like). This protein is necessary for alterative splicing of CD45 in T cells but does not impact the development of differentiation of NKT cells [359]. However, partial loss of function mutations affecting HNRNPLL can reduce T cell accumulation in lymphoid tissues [360]. A decrease in T cell expansion in lymphoid tissue may impair the immune response [361]. The differentially expressed genes discovered by scRNA-seq analysis support the hypothesized immunosuppression in TI heifers. Further research is required to characterize their effects on the immune system.

Moreover, only one other study has performed scRNA-seq using peripheral WBCs in cattle [362]. While the other study opted to use an automated cell type identification platform *ScType,* we chose to categorize cells according to current literature and understanding of cell type markers in bovine. The creation of a transcriptomic atlas of peripheral WBCs in cattle would aid in cellular characterization and interpretation of findings.

Transcriptomic data must be presented with a few specific caveats. Not all transcripts are expressed at a single time; the immune response was not stimulated or challenged in these heifers and therefore transcription of immune related genes remained at a minimum. It is possible that more differences in expression may become evident between TI and control heifers during an immune challenge. Similarly,

differential expression of immune associated genes during an immune response may have a greater impact on immune cell expansion. Additional research is required for complete characterization of the immune response in TI heifers.

Conclusion

The findings herein demonstrate that TI heifers exhibit differences within the immune system compared to controls from birth to 17 months of age. The TI heifers in this study demonstrated decreased proportions of T cells positive for both CD4 and CD8b as well as natural killer cells. Moreover, scRNA-seq identified greater proportions of a B cell subpopulation, likely memory B cells, and decreased proportions of a myeloid population with an expression profile like that of M2 macrophages. Analysis of the methylome revealed numerous genes related to the immune system which contained differential methylation predicted to inhibit immune efficacy. Four genes were identified to be differentially expressed in cell clusters from TI heifers and have the potential to impact the TI immune response to pathogens. As the discovery of BVDV induced profit loss due to fetal TI is relatively new, it is critical to continue to characterize and determine the extent of impact. Only then can a proper estimate of BVDV related profit loss be calculated and utilized to encourage control strategies for profit preservation. Additionally, the identification of a biomarker in which to differentiate fetal TI heifers from postnatal TIs would allow for the application of targeted management strategies or increased biosecurity protocols that may allow for mitigation of profit loss.

Preliminary Data – Potential Reproductive Impacts

At 4 months of age, TI heifers demonstrated hypermethylation contained within several genes relating to the meiotic process and cytoskeletal remodeling. Genes including *TERB2, HORMAD2, SMC1A,* and *RBBP8* were found to contain hypermethylated CpG sites, which are associated with decreased expression, and demonstrate roles in the fidelity of the meiotic process [363-366]. The genes encoding *HES1* and *NLRP5* also contained a hypermethylated CpG site. These genes play critical roles in embryonic development [367, 368]. At 17 months of age, hypermethylated CpG sites were identified within *NR5A2, KLF2, LIF, SOX2, ESRRB,* and *MYC*. Decreased transcription of these genes, which play various roles in embryo development [369-374], may contribute to a decrease in fertility and pregnancy rate in TI heifers. Based on these alterations of the methylome, it was hypothesized that embryos from TI heifers would demonstrate higher rates of degeneration and lower rates of successful development.

Preliminary data was collected using 2 control heifers and 4 TI heifers at 17 months of age. Upon harvest of the heifers, ovaries were utilized for *in vitro* production of embryos. Ovaries were washed in ethanol and saline prior to aspiration of follicular contents and manual oocyte collection. Comparison of the average number of oocytes collected from 2 control heifers (48.5 ± 17.5) to the average number of oocytes collected from 4 TI heifers (25.75 ± 2.75) did not demonstrate a significant difference between treatments (Figure 4.8). Oocytes were matured in CSU chemically defined medium, fertilized, and observed for cleavage and blastocyst formation. The cleavage rate of TI heifers (43.59 ± 5.57) was not different from that of control heifers (59.58 ± 11.2; Figure

4.8). However, the blastocyst rate was decreased in TI heifers at 17 months of age (3.18 ± 1.22) in comparison to controls (10.3 ± 2.6; Figure 4.8).

The sample number for this preliminary data is not sufficient to demonstrate significant differences between embryos derived from TI heifers and controls at 17 months of age in terms of oocytes collected or cleavage rate. However, with an increased sample size, these differences may become more evident. Even so, a decrease in blastocyst rate due to maternal fetal TI with BVDV demonstrates once again that profit loss due to BVDV is largely underestimated. Further research is necessary to fully elucidate the reproductive impact of late gestational BVDV infection and determine whether transgenerational influences exist.

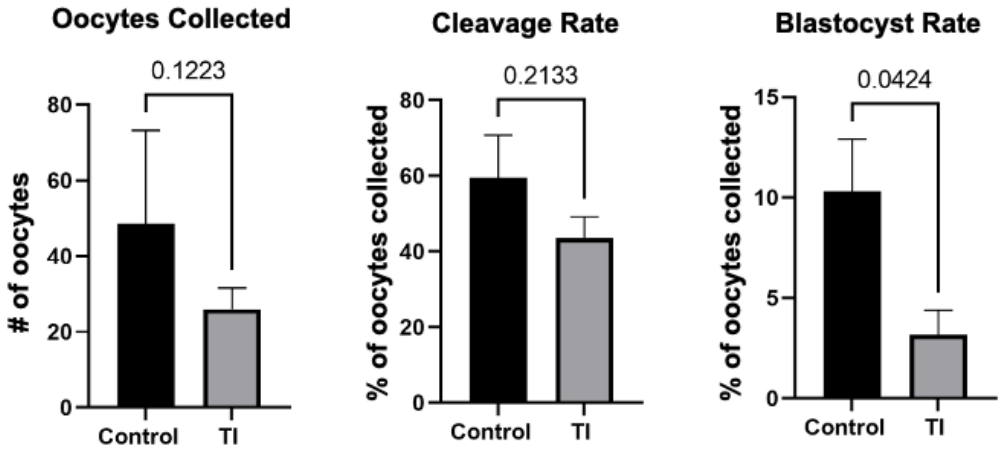

Figure 4.8 – Development of in vitro produced embryos is reduced in TI heifers.
This preliminary data is derived from 2 control and 4 TI heifers at 17 months of age. The number above each panel denotes the p-value calculated between treatment groups after applying a Shapiro-Wilk test and a Student's T-test with a Welch's correction.

CHAPTER 5: CONCLUSIONS

Fetal development is a complex process that can be impacted by alterations of the environment *in utero* or the external, maternal environment. These alterations of the environment can program responses that are inappropriate to the postnatal environment through epigenetic marks such as methylation. The studies herein present important insight as to fetal programming of the immune system and the postnatal consequences of fetal viral infection in early and late gestation.

Viral infections occurring during the gestational period are known to negatively impact the development of the fetus. Some viruses impact the fetus directly by crossing the placenta to infect the fetus, as in the case of Zika virus [375], cytomegalovirus, or rubella virus (reviewed in [376]). Other gestational viral infections activate the maternal immune response and impact developmental programming of the fetus via expression of cytokines such as IL6 which induce DNMTs (reviewed in [377]). Infection with BVDV at gestational day 75 induces similar epigenetic alterations, as observed by comparison of the splenic methylome in PI and control fetuses collected at gestational day 245 [175]. Activation of the human maternal immune response during gestation can lead to fetal metabolic, cardiovascular, neurodevelopmental, and immune disorders in the postnatal period [378]. Similarly, postnatal PI cattle are characterized by congenital defects of the brain, heart, skeletal system, and experience chronic immunosuppression [178, 187, 240]. Identification of epigenetic and proteomic alterations in the late prenatal period, at gestational day 245, led to the question as to whether these epigenetic

alterations were detectable in the postnatal period. If these epigenetic marks can be identified in the postnatal period and confirmed through comparison of those identified at gestational day 245, it may be possible to develop a cost-effective test panel for the identification of PI cattle. Current testing methods only identify current infections, meaning that the identification of a PI requires testing twice with a period of approximately 4 weeks in between.

As viral infections in late gestation in humans and mice continue to impact fetal development, it is feasible that the same would also occur in cattle. A fetus is more susceptible to epigenetic influence in the early periods of gestation but maintain some level of epigenetic plasticity even in the early postnatal period [313]. As such, it was hypothesized that fetuses subjected to fetal TI with BVDV would demonstrate alterations of the epigenome. Moreover, it was hypothesized that fetal infection with BVDV, even in late gestation, would result in undescribed postnatal pathologies.

Infection with influenza A in the pre-implantation period decreases placental weight, infection in the peri-implantation period decreases fetal and placental weight, and infection in the post-implantation period reduces fetal weight in mice [174]. In fact, a common theme of gestational viral infections is the occurrence of an intrauterine growth restriction phenotype; this phenotype is presented as a result of gestational infection with human cytomegalovirus [379] and Zika virus [380]. Per the longitudinal studies partially describe herein, it was demonstrated that calves born following infection with BVDV on gestational day 175 have decreased body weight at birth, 4 months of age, throughout the feedlot period, and even at harvest [179, 180, 327]. Analysis of the TI methylome at 4 months of age in comparison to the methylome of controls revealed

differential methylation suggestive of metabolic dysfunction, increased inflammation, and increased oxidative stress [327]. In accordance with these findings, the TI heifers also demonstrated decreased dry matter digestibility and increased indicators of inflammation including elevated ceruloplasmin and the oxidized form of glutathione [180]. Human children exposed to maternal activation of the immune response *in utero* display a similar metabolic dysfunction in the form of diabetes mellitus type 1 [381], thus indicating that the activation of the immune response rather than the viral infection itself, impacts postnatal metabolism.

In humans, exposure to maternal activation of the immune response results in offspring with increased occurrence of allergies and asthma [378]. Fetal exposure to BVDV at gestational day 175 did not result in overt differences in CBCs aside from an increased lymphocyte percentage at 4 months of age, but did induce alterations in immune cell populations that were detectable via spectral cytometry. At both 4 and 17 months of age, TI heifers had decreased proportions of $CD4^+/CD8b^+$ T cells in comparison to controls. While these findings do not demonstrate an increased occurrence of disease, they do suggest that TI heifers suffer from an impairment of the immune system. Specifically, because $CD4^+/CD8b^+$ T cells have been implicated in the response to immunization against foot and mouth disease [230], they may not respond to vaccination appropriately or require additional immunizations. However, the lack of functional characterization of bovine immune cells leaves an opportunity for continued future research.

At 17 months of age, four differentially expressed genes were identified in 4 separate immune cell populations identified by scRNA-seq. Two of the four genes were

also identified to contain at least one DMS at 17 months of age. One gene, *SFMBT2*, was hypomethylated at 17 months of age and was found to be overexpressed in a subset of B cells (B5) derived from TI heifers. The other gene, *PDE4D*, was instead hypermethylated in contradiction to the observed overexpression in a TI B cell subset (B1). While methylation of CpG sites can influence the expression of genes, it is critical to note a few reasons that the two may not directly correspond. Methylation of DNA is only one of three epigenetic mechanisms of transcriptional control; expression is also influenced by long non-coding RNAs and histone modifications. It is possible that the gene *PDE4D* is influenced by other epigenetic control mechanisms. Additionally, it is possible that the lack of differential expression in TI heifer immune cell populations is due to a lack of immune stimulation. Not all genes are transcribed at the same rate; differential expression in immune cells may fail to demonstrate appropriate statistical power, thereby making them undetectable, in the absence of immune activation.

The identification of fewer DMSs in TI heifers at 4 months of age in comparison to DMSs identified in PI heifers at 4 months of age demonstrates well that the impact upon the epigenome is dependent on gestational exposure. However, it is also possible that the ongoing, chronic infection observed in PI heifers is responsible for the increased number of DMSs, as viral infections in adulthood can also alter the epigenome [382]. Because the epigenome continues to be altered in response to the environment in the postnatal period, the methylomes of heifers exposed to fetal TI with BVDV were compared to those of control heifers at 17 months of age. Moreover, 4-month-old TI heifers demonstrated decreased methylation, which is associated with increased expression, of DNMTs responsible for the implementation of new epigenetic

marks. Longitudinal comparison of DMSs identified in heifers exposed to fetal TI with BVDV demonstrates an interesting, compounding influence of epigenetic alteration. Typically, global methylation decreases with age while CpG specific methylation increases [148]. However, these studies demonstrate that while the former may hold true, the divergence in CpG methylation between TI and control heifers increases with age (Figure 5.1).

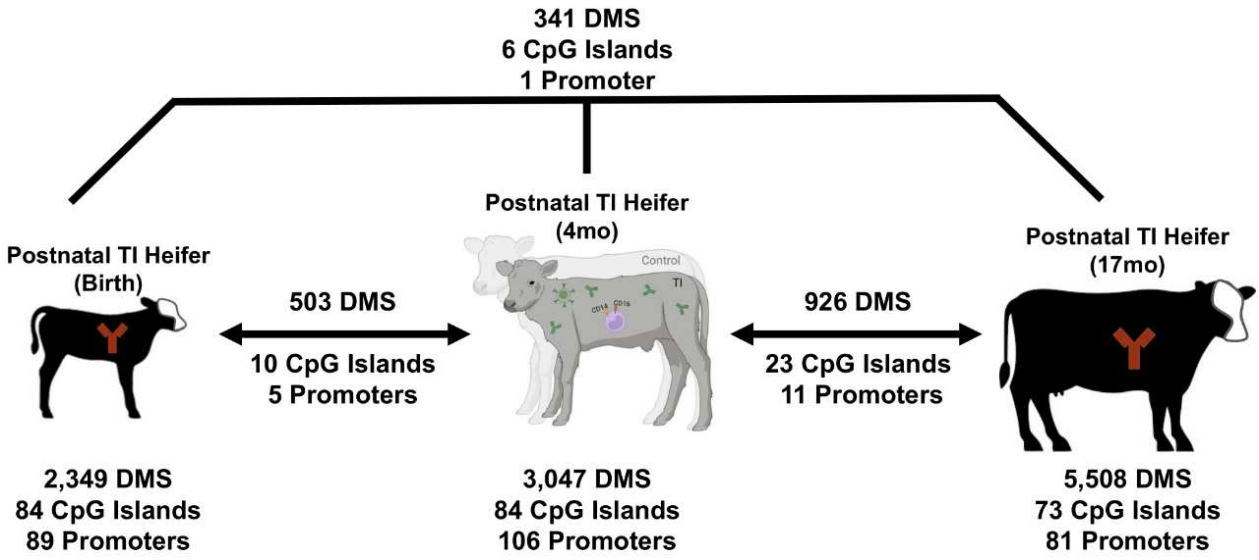

Figure 5.1 – Differential methylation of genes in peripheral white blood cells from TI heifers at birth, 4 months of age, and 17 months of age.

The data presented herein provides a foundation for the development of methylation-based biomarkers for PI and TI cattle and characterizes postnatal deficits in TI cattle that contribute to BVDV induced profit loss. These findings are critical for an accurate calculation of BVDV induced profit loss which demonstrates the importance of BVDV control strategies. The identification of cattle that have been infected with BVDV *in utero* would allow for targeted increases of biosecurity, vaccination, or other

preventative disease measures that might mitigate profit loss. Moreover, TI heifers provide a research model for the epigenetic influence of gestational viral infection in alternative to collection of clinical human data.

REFERENCES

1. Riley, J.M., *Economic consequences of beef cow-calf disease mismanagement: Bovine viral diarrhea virus.* Applied Animal Science 2019. **35**(6): p. 606-614.
2. Ishmael, W., *How much money have you lost to BVD? .* Beef Editor's Blog 2016.
3. Hessman, B.E., et al., *Evaluation of economic effects and the health and performance of the general cattle population after exposure to cattle persistently infected with bovine viral diarrhea virus in a starter feedlot.* Am J Vet Res, 2009. **70**(1): p. 73-85.
4. Runyan, C.A., et al., *Feed Intake and Weight Changes in Bos indicus-Bos taurus Crossbred Steers Following Bovine Viral Diarrhea Virus Type 1b Challenge Under Production Conditions.* Pathogens, 2017. **6**(4).
5. Basqueira, N.S., et al., *An Assessment of Secondary Clinical Disease, Milk Production and Quality, and the Impact on Reproduction in Holstein Heifers and Cows from a Single Large Commercial Herd Persistently Infected with Bovine Viral Diarrhea Virus Type 2.* Viruses, 2020. **12**(7).
6. Fulton, R.W., et al., *Challenge with Bovine viral diarrhea virus by exposure to persistently infected calves: protection by vaccination and negative results of antigen testing in nonvaccinated acutely infected calves.* Can J Vet Res, 2006. **70**(2): p. 121-7.
7. Fulton, R.W., et al., *Transmission of bovine viral diarrhea virus 1b to susceptible and vaccinated calves by exposure to persistently infected calves.* Can J Vet Res, 2005. **69**(3): p. 161-9.
8. Chirase, N.K., *Dietary zinc and manganese sources administered from the fetal stage onwards affect immune response of transit stressed and virus infected offspring steer calves.* Animal Feed Science and Technology, 2001. **93**(3-4): p. 217-228.
9. Houe, H., *The effect of bovine virus diarrhoea virus infection on conception rate.* Preventetive Veterinary Medicine, 1993. **15**(2-3): p. 117-123.
10. Kendrick, J.W., *Bovine viral diarrhea virus-induced abortion.* Theriogenology, 1976. **5**(3): p. 91-93.
11. Houe, H. and A. Meyling, *Surveillance of cattle herds for bovine virus diarrhoea virus (BVDV)-infection using data on reproduction and calf mortality.* Arch Virol Suppl, 1991. **3**: p. 157-64.
12. Wathes, D.C., et al., *Importance of Viral Disease in Dairy Cow Fertility.* Engineering (Beijing), 2020. **6**(1): p. 26-33.
13. Bellows, D.S., *Review: Cost of Reproductive Diseases and Conditions in Cattle.* The Professional Animal Scientist, 2002. **18**(1): p. 26-32.
14. Scharnbock, B., et al., *A meta-analysis of bovine viral diarrhoea virus (BVDV) prevalences in the global cattle population.* Sci Rep, 2018. **8**(1): p. 14420.
15. United States Department of Agriculture, A.a.P.H.I.S., *Bovine Viral Diarrhea on U.S. Beef Cow-calf Operations NAHMS Beef 2017 Study.* 2023.
16. Olafson, P., C.A. Mac, and F.H. Fox, *An apparently new transmissible disease of cattle.* Cornell Vet, 1946. **36**: p. 205-13.

17. Childs, T., *X Disease of Cattle - Saskatchewan.* Can J Comp Med Vet Sci, 1946. **10**(11): p. 316-9.
18. Ramsey, F., *Mucosal disease of cattle. .* North American Veterinarian, 1953. **34, 629-633**.
19. Underdahl, N.R., O.D. Grace, and A.B. Hoerlein, *Cultivation in tissue-culture of cytopathogenic agent from bovine mucosal disease.* Proc Soc Exp Biol Med, 1957. **94**(4): p. 795-7.
20. Lee, K.M. and J.H. Gillespie, *Propagation of virus diarrhea virus of cattle in tissue culture.* Am J Vet Res, 1957. **18**(69): p. 952-3.
21. Gillespie, J.H., J.A. Baker, and K. McEntee, *A cytopathogenic strain of virus diarrhea virus.* Cornell Vet, 1960. **50**: p. 73-9.
22. Coggins, L., et al., *Attenuation of virus diarrhea virus (strain Oregon C24V) for vaccine purposes.* Cornell Vet, 1961. **51**: p. 539-45.
23. Bolin, S.R., *Control of bovine viral diarrhea infection by use of vaccination.* Vet Clin North Am Food Anim Pract, 1995. **11**(3): p. 615-25.
24. Darbyshire, J., *Agar gel diffusion studies with a mucosal disease of cattle. II. A serological relationship between mucosal disease and swine fever. .* Res Vet Sci 1962. **3**: p. 125-128.
25. Pritchard, W.R., D. B. Taylor, H. E. Moses, and L. P. Doyle, *A Transmissible Disease Affecting the Mucosae of Cattle.* J Am Vet Med Assoc, 1956. **128**: p. 1-4.
26. Hermodsson, S. and Z. Dinter, *Properties of bovine virus diarrhoea virus.* Nature, 1962. **194**: p. 893-4.
27. Huck, R.A., *Mucosal disease complex.* J Comp Pathol, 1957. **67**(3): p. 267-76.
28. Brownlie, J., M.C. Clarke, and C.J. Howard, *Experimental production of fatal mucosal disease in cattle.* Vet Rec, 1984. **114**(22): p. 535-6.
29. Sopp, P., et al., *Detection of bovine viral diarrhoea virus p80 protein in subpopulations of bovine leukocytes.* J Gen Virol, 1994. **75 (Pt 5)**: p. 1189-94.
30. Westaway, E.G., et al., *Togaviridae.* Intervirology, 1985. **24**(3): p. 125-39.
31. Westaway, E.G., et al., *Flaviviridae.* Intervirology, 1985. **24**(4): p. 183-92.
32. Corapi, W.V., et al., *Thrombocytopenia and hemorrhages in veal calves infected with bovine viral diarrhea virus.* J Am Vet Med Assoc, 1990. **196**(4): p. 590-6.
33. Carman, S., et al., *Severe acute bovine viral diarrhea in Ontario, 1993-1995.* J Vet Diagn Invest, 1998. **10**(1): p. 27-35.
34. Fulton, R.W., et al., *Bovine viral diarrhoea virus antigenic diversity: impact on disease and vaccination programmes.* Biologicals, 2003. **31**(2): p. 89-95.
35. Stahl, C., et al., *[Control measures for BVD virus infections in cattle breeding herds].* Dtsch Tierarztl Wochenschr, 1987. **94**(10): p. 594-6.
36. Greiser-Wilke, I., B. Grummer, and V. Moennig, *Bovine viral diarrhoea eradication and control programmes in Europe.* Biologicals, 2003. **31**(2): p. 113-8.
37. Wernike, K., et al., *Six Years (2011-2016) of Mandatory Nationwide Bovine Viral Diarrhea Control in Germany-A Success Story.* Pathogens, 2017. **6**(4).
38. Moennig, V. and M.J. Yarnall, *The Long Journey to BVD Eradication.* Pathogens, 2021. **10**(10).
39. Marschik, T., et al., *A cost-benefit analysis and the potential trade effects of the bovine viral diarrhoea eradication programme in Styria, Austria.* Vet J, 2018. **231**: p. 19-29.

40. Valle, P.S., et al., *Ten years of bovine virus diarrhoea virus (BVDV) control in Norway: a cost-benefit analysis.* Prev Vet Med, 2005. **72**(1-2): p. 189-207; discussion 215-9.
41. Van Campen, H., *Epidemiology and control of BVD in the U.S.* Vet Microbiol, 2010. **142**(1-2): p. 94-8.
42. Laamanen, U.I., et al., *Comparison of RT-PCR assay and virus isolation in cell cultures for the detection of bovine viral diarrhoea virus (BVDV) in field samples.* Res Vet Sci, 1997. **63**(3): p. 199-203.
43. Bolin, S.R. and J.F. Ridpath, *Prevalence of bovine viral diarrhea virus genotypes and antibody against those viral genotypes in fetal bovine serum.* J Vet Diagn Invest, 1998. **10**(2): p. 135-9.
44. Leong, A.S. and P.N. Gilham, *The effects of progressive formaldehyde fixation on the preservation of tissue antigens.* Pathology, 1989. **21**(4): p. 266-8.
45. Grooms, D.L., K.V. Brock, and L.A. Ward, *Detection of bovine viral diarrhea virus in the ovaries of cattle acutely infected with bovine viral diarrhea virus.* J Vet Diagn Invest, 1998. **10**(2): p. 125-9.
46. Shin, T. and H. Acland, *Tissue distribution of bovine viral diarrhea virus antigens in persistently infected cattle.* J Vet Sci, 2001. **2**(2): p. 81-4.
47. Njaa, B.L., et al., *Diagnosis of persistent bovine viral diarrhea virus infection by immunohistochemical staining of formalin-fixed skin biopsy specimens.* J Vet Diagn Invest, 2000. **12**(5): p. 393-9.
48. Thur, B., K. Zlinszky, and F. Ehrensperger, *Immunohistochemical detection of bovine viral diarrhea virus in skin biopsies: a reliable and fast diagnostic tool.* Zentralbl Veterinarmed B, 1996. **43**(3): p. 163-6.
49. Saliki, J.T. and E.J. Dubovi, *Laboratory diagnosis of bovine viral diarrhea virus infections.* Vet Clin North Am Food Anim Pract, 2004. **20**(1): p. 69-83.
50. Dubovi, E.J., *Laboratory diagnosis of bovine viral diarrhea virus.* Biologicals, 2013. **41**(1): p. 8-13.
51. Ridpath, J.F. and S.R. Bolin, *Differentiation of types 1a, 1b and 2 bovine viral diarrhoea virus (BVDV) by PCR.* Mol Cell Probes, 1998. **12**(2): p. 101-6.
52. Monteiro, F.L., et al., *Detection of bovine pestiviruses in sera of beef calves by a RT-PCR based on a newly designed set of pan-bovine pestivirus primers.* J Vet Diagn Invest, 2019. **31**(2): p. 255-258.
53. Deregt, D., S. Smithson, and G.C. Kozub, *A short incubation serum neutralization test for bovine viral diarrhea virus.* Can J Vet Res, 1992. **56**(2): p. 161-4.
54. Makoschey, B., et al., *Bovine viral diarrhoea virus antigen in foetal calf serum batches and consequences of such contamination for vaccine production.* Biologicals, 2003. **31**(3): p. 203-8.
55. Bolin, S.R., P.J. Matthews, and J.F. Ridpath, *Methods for detection and frequency of contamination of fetal calf serum with bovine viral diarrhea virus and antibodies against bovine viral diarrhea virus.* J Vet Diagn Invest, 1991. **3**(3): p. 199-203.
56. Meyers, G., et al., *Bovine viral diarrhea virus: prevention of persistent fetal infection by a combination of two mutations affecting Erns RNase and Npro protease.* J Virol, 2007. **81**(7): p. 3327-38.

57. Rodning, S.P., et al., *Comparison of three commercial vaccines for preventing persistent infection with bovine viral diarrhea virus.* Theriogenology, 2010. **73**(8): p. 1154-63.
58. Newcomer, B.W., et al., *Efficacy of bovine viral diarrhea virus vaccination to prevent reproductive disease: a meta-analysis.* Theriogenology, 2015. **83**(3): p. 360-365 e1.
59. Zimmer, G.M., et al., *Failure of foetal protection after vaccination against an experimental infection with bovine virus diarrhea virus.* Vet Microbiol, 2002. **89**(4): p. 255-65.
60. Stevens, E.T., et al., *The induction of a cell-mediated immune response to bovine viral diarrhea virus with an adjuvanted inactivated vaccine.* Vet Ther, 2009. **10**(4): p. E1-8.
61. Platt, R., et al., *Humoral and T cell-mediated immune responses to bivalent killed bovine viral diarrhea virus vaccine in beef cattle.* Vet Immunol Immunopathol, 2008. **122**(1-2): p. 8-15.
62. Kasonta, R., et al., *Effect of the vaccination scheme on PregSure(R) BVD induced alloreactivity and the incidence of Bovine Neonatal Pancytopenia.* Vaccine, 2012. **30**(47): p. 6649-55.
63. Deutskens, F., et al., *Vaccine-induced antibodies linked to bovine neonatal pancytopenia (BNP) recognize cattle major histocompatibility complex class I (MHC I).* Vet Res, 2011. **42**(1): p. 97.
64. Jones, L., *Comparison of neutralizing antibodies to type 1a, 1b, and 2 bovine viral diarrhea virus from experimentally infected and vaccinated cattle. .* Bovine Practitioner 2001. **35**(2): p. 137-140.
65. Howard, C.J., M.C. Clarke, and J. Brownlie, *Protection against respiratory infection with bovine virus diarrhoea virus by passively acquired antibody.* Vet Microbiol, 1989. **19**(3): p. 195-203.
66. Bolin, S.R. and J.F. Ridpath, *Assessment of protection from systemic infection or disease afforded by low to intermediate titers of passively acquired neutralizing antibody against bovine viral diarrhea virus in calves.* Am J Vet Res, 1995. **56**(6): p. 755-9.
67. Brock, K.V. and V.S. Cortese, *Experimental fetal challenge using type II bovine viral diarrhea virus in cattle vaccinated with modified-live virus vaccine.* Vet Ther, 2001. **2**(4): p. 354-60.
68. Workman, A.M., et al., *Resolving Bovine viral diarrhea virus subtypes from persistently infected U.S. beef calves with complete genome sequence.* J Vet Diagn Invest, 2016. **28**(5): p. 519-28.
69. Fulton, R.W., et al., *Prevalence of bovine viral diarrhea virus (BVDV) in persistently infected cattle and BVDV subtypes in affected cattle in beef herds in south central United States.* Can J Vet Res, 2009. **73**(4): p. 283-91.
70. Mosena, A.C.S., et al., *Multivariate analysis as a method to evaluate antigenic relationships between BVDV vaccine and field strains.* Vaccine, 2020. **38**(36): p. 5764-5772.
71. Mosena, A.C.S., et al., *Multivariate analysis reveals that BVDV field isolates do not show a close VN-based antigenic relationship to US vaccine strains.* BMC Res Notes, 2023. **16**(1): p. 121.

72. Tian, B., et al., *Identification and genotyping of a new subtype of bovine viral diarrhea virus 1 isolated from cattle with diarrhea.* Arch Virol, 2021. **166**(4): p. 1259-1262.
73. Yesilbag, K., G. Alpay, and P. Becher, *Variability and Global Distribution of Subgenotypes of Bovine Viral Diarrhea Virus.* Viruses, 2017. **9**(6).
74. Collett, M.S., et al., *Proteins encoded by bovine viral diarrhea virus: the genomic organization of a pestivirus.* Virology, 1988. **165**(1): p. 200-8.
75. Deng, R. and K.V. Brock, *Molecular cloning and nucleotide sequence of a pestivirus genome, noncytopathic bovine viral diarrhea virus strain SD-1.* Virology, 1992. **191**(2): p. 867-9.
76. Colett, M.S., et al., *Molecular cloning and nucleotide sequence of the pestivirus bovine viral diarrhea virus.* Virology, 1988. **165**(1): p. 191-9.
77. Chen, Z., et al., *Ubiquitination and proteasomal degradation of interferon regulatory factor-3 induced by Npro from a cytopathic bovine viral diarrhea virus.* Virology, 2007. **366**(2): p. 277-92.
78. Hilton, L., et al., *The NPro product of bovine viral diarrhea virus inhibits DNA binding by interferon regulatory factor 3 and targets it for proteasomal degradation.* J Virol, 2006. **80**(23): p. 11723-32.
79. Ronecker, S., et al., *Formation of bovine viral diarrhea virus E1-E2 heterodimers is essential for virus entry and depends on charged residues in the transmembrane domains.* J Gen Virol, 2008. **89**(Pt 9): p. 2114-2121.
80. Liang, D., et al., *The envelope glycoprotein E2 is a determinant of cell culture tropism in ruminant pestiviruses.* J Gen Virol, 2003. **84**(Pt 5): p. 1269-1274.
81. Matzener, P., et al., *The viral RNase E(rns) prevents IFN type-I triggering by pestiviral single- and double-stranded RNAs.* Virus Res, 2009. **140**(1-2): p. 15-23.
82. Tews, B.A. and G. Meyers, *The pestivirus glycoprotein Erns is anchored in plane in the membrane via an amphipathic helix.* J Biol Chem, 2007. **282**(45): p. 32730-41.
83. Rumenapf, T., et al., *Processing of the envelope glycoproteins of pestiviruses.* J Virol, 1993. **67**(6): p. 3288-94.
84. Weiland, F., et al., *Localization of pestiviral envelope proteins E(rns) and E2 at the cell surface and on isolated particles.* J Gen Virol, 1999. **80 (Pt 5)**: p. 1157-1165.
85. Harada, T., N. Tautz, and H.J. Thiel, *E2-p7 region of the bovine viral diarrhea virus polyprotein: processing and functional studies.* J Virol, 2000. **74**(20): p. 9498-506.
86. Elbers, K., et al., *Processing in the pestivirus E2-NS2 region: identification of proteins p7 and E2p7.* J Virol, 1996. **70**(6): p. 4131-5.
87. Behrens, S.E., et al., *Characterization of an autonomous subgenomic pestivirus RNA replicon.* J Virol, 1998. **72**(3): p. 2364-72.
88. Griffin, S.D.C., et al., *A conserved basic loop in hepatitis C virus p7 protein is required for amantadine-sensitive ion channel activity in mammalian cells but is dispensable for localization to mitochondria.* J Gen Virol, 2004. **85**(Pt 2): p. 451-461.

89. Walther, T., et al., *Membrane Topology of Pestiviral Non-Structural Protein 2 and determination of the minimal autoprotease domain.* J Virol, 2021. **95**(11).
90. Lackner, T., et al., *Temporal modulation of an autoprotease is crucial for replication and pathogenicity of an RNA virus.* J Virol, 2004. **78**(19): p. 10765-75.
91. Guo, K.K., et al., *Identification of two internal signal peptide sequences: critical for classical swine fever virus non-structural protein 2 to trans-localize to the endoplasmic reticulum.* Virol J, 2011. **8**: p. 236.
92. Gu, B., et al., *The RNA helicase and nucleotide triphosphatase activities of the bovine viral diarrhea virus NS3 protein are essential for viral replication.* J Virol, 2000. **74**(4): p. 1794-800.
93. Grassmann, C.W., O. Isken, and S.E. Behrens, *Assignment of the multifunctional NS3 protein of bovine viral diarrhea virus during RNA replication: an in vivo and in vitro study.* J Virol, 1999. **73**(11): p. 9196-205.
94. Weiskircher, E., et al., *Bovine viral diarrhea virus NS4B protein is an integral membrane protein associated with Golgi markers and rearranged host membranes.* Virol J, 2009. **6**: p. 185.
95. Xu, J., et al., *Bovine viral diarrhea virus NS3 serine proteinase: polyprotein cleavage sites, cofactor requirements, and molecular model of an enzyme essential for pestivirus replication.* J Virol, 1997. **71**(7): p. 5312-22.
96. Zhong, W., L.L. Gutshall, and A.M. Del Vecchio, *Identification and characterization of an RNA-dependent RNA polymerase activity within the nonstructural protein 5B region of bovine viral diarrhea virus.* J Virol, 1998. **72**(11): p. 9365-9.
97. Lecot, S., et al., *Bovine viral diarrhea virus entry is dependent on clathrin-mediated endocytosis.* J Virol, 2005. **79**(16): p. 10826-9.
98. Helenius, A., et al., *On the entry of Semliki forest virus into BHK-21 cells.* J Cell Biol, 1980. **84**(2): p. 404-20.
99. Iqbal, M., H. Flick-Smith, and J.W. McCauley, *Interactions of bovine viral diarrhoea virus glycoprotein E(rns) with cell surface glycosaminoglycans.* J Gen Virol, 2000. **81**(Pt 2): p. 451-9.
100. Schelp, C., et al., *Identification of cell membrane proteins linked to susceptibility to bovine viral diarrhoea virus infection.* Arch Virol, 1995. **140**(11): p. 1997-2009.
101. Xue, W. and H.C. Minocha, *Identification of the cell surface receptor for bovine viral diarrhoea virus by using anti-idiotypic antibodies.* J Gen Virol, 1993. **74 (Pt 1)**: p. 73-9.
102. Agnello, V., et al., *Hepatitis C virus and other flaviviridae viruses enter cells via low density lipoprotein receptor.* Proc Natl Acad Sci U S A, 1999. **96**(22): p. 12766-71.
103. Maurer, K., et al., *CD46 is a cellular receptor for bovine viral diarrhea virus.* J Virol, 2004. **78**(4): p. 1792-9.
104. Seya, T., et al., *Human membrane cofactor protein (MCP, CD46): multiple isoforms and functions.* Int J Biochem Cell Biol, 1999. **31**(11): p. 1255-60.
105. Szillat, K.P., et al., *A CRISPR/Cas9 Generated Bovine CD46-knockout Cell Line-A Tool to Elucidate the Adaptability of Bovine Viral Diarrhea Viruses (BVDV).* Viruses, 2020. **12**(8).

106. Chen, H.W., et al., *Viral Traits and Cellular Knock-Out Genotype Affect Dependence of BVDV on Bovine CD46.* Pathogens, 2021. **10**(12).
107. Workman, A.M., et al., *First gene-edited calf with reduced susceptibility to a major viral pathogen.* PNAS Nexus, 2023. **2**(5): p. pgad125.
108. Zaruba, M., et al., *ADAM17 Is an Essential Factor for the Infection of Bovine Cells with Pestiviruses.* Viruses, 2022. **14**(2).
109. Marsh, M. and A. Helenius, *Virus entry into animal cells.* Adv Virus Res, 1989. **36**: p. 107-51.
110. Knipe, D.M. and P.M. Howley, *Fields virology*. 6th ed. 2013, Philadelphia, PA: Wolters Kluwer/Lippincott Williams & Wilkins Health. 2 volumes.
111. Bolin, S.R. and J.F. Ridpath, *Specificity of neutralizing and precipitating antibodies induced in healthy calves by monovalent modified-live bovine viral diarrhea virus vaccines.* Am J Vet Res, 1989. **50**(6): p. 817-21.
112. van Rijn, P.A., et al., *Antigenic structure of envelope glycoprotein E1 of hog cholera virus.* J Virol, 1994. **68**(6): p. 3934-42.
113. Paton, D.J., J.P. Lowings, and A.D. Barrett, *Epitope mapping of the gp53 envelope protein of bovine viral diarrhea virus.* Virology, 1992. **190**(2): p. 763-72.
114. Deregt, D., et al., *Monoclonal antibodies to the E2 protein of a new genotype (type 2) of bovine viral diarrhea virus define three antigenic domains involved in neutralization.* Virus Res, 1998. **57**(2): p. 171-81.
115. Young, N.J., et al., *Immune responses to non-structural protein 3 (NS3) of bovine viral diarrhoea virus (BVDV) in NS3 DNA vaccinated and naturally infected cattle.* Prev Vet Med, 2005. **72**(1-2): p. 115-20; discussion 215-9.
116. Nobiron, I., et al., *DNA vaccination against bovine viral diarrhoea virus induces humoral and cellular responses in cattle with evidence for protection against viral challenge.* Vaccine, 2003. **21**(17-18): p. 2082-92.
117. Murphy, K. and C. Weaver, *Janeway's immunobiology*. 9th edition. ed. 2016, New York, NY: Garland Science/Taylor & Francis Group, LLC. xx, 904 pages.
118. Zurcher, C., K.S. Sauter, and M. Schweizer, *Pestiviral E(rns) blocks TLR-3-dependent IFN synthesis by LL37 complexed RNA.* Vet Microbiol, 2014. **174**(3-4): p. 399-408.
119. Darweesh, M.F., et al., *BVDV Npro protein mediates the BVDV induced immunosuppression through interaction with cellular S100A9 protein.* Microb Pathog, 2018. **121**: p. 341-349.
120. Liu, C., et al., *RNA-Seq based transcriptome analysis during bovine viral diarrhoea virus (BVDV) infection.* BMC Genomics, 2019. **20**(1): p. 774.
121. Muller-Doblies, D., et al., *Innate immune responses of calves during transient infection with a noncytopathic strain of bovine viral diarrhea virus.* Clin Diagn Lab Immunol, 2004. **11**(2): p. 302-12.
122. Knapek, K.J., et al., *Fetal Lymphoid Organ Immune Responses to Transient and Persistent Infection with Bovine Viral Diarrhea Virus.* Viruses, 2020. **12**(8).
123. Shan, Y., et al., *Bovine viral diarrhea virus NS4B protein interacts with 2CARD of MDA5 domain and negatively regulates the RLR-mediated IFN-beta production.* Virus Res, 2021. **302**: p. 198471.
124. Wang, S., et al., *DDIT3 Targets Innate Immunity via the DDIT3-OTUD1-MAVS Pathway To Promote Bovine Viral Diarrhea Virus Replication.* J Virol, 2021. **95**(6).

125. Villalba, M., et al., *Transcriptomic analysis of responses to cytopathic bovine viral diarrhea virus-1 (BVDV-1) infection in MDBK cells.* Mol Immunol, 2016. **71**: p. 192-202.
126. Welsh, M.D., B.M. Adair, and J.C. Foster, *Effect of BVD virus infection on alveolar macrophage functions.* Vet Immunol Immunopathol, 1995. **46**(3-4): p. 195-210.
127. Chase, C.C., *The impact of BVDV infection on adaptive immunity.* Biologicals, 2013. **41**(1): p. 52-60.
128. Lee, S.R., et al., *Bovine viral diarrhea virus infection affects the expression of proteins related to professional antigen presentation in bovine monocytes.* Biochim Biophys Acta, 2009. **1794**(1): p. 14-22.
129. Rajput, M.K., et al., *The effect of bovine viral diarrhea virus (BVDV) strains on bovine monocyte-derived dendritic cells (Mo-DC) phenotype and capacity to produce BVDV.* Virol J, 2014. **11**: p. 44.
130. Senogles, D.R., et al., *Ontogeny of T cells, B cells and monocytes in the bovine foetus.* Clin Exp Immunol, 1979. **36**(2): p. 299-303.
131. Barker, D.J., et al., *Fetal nutrition and cardiovascular disease in adult life.* Lancet, 1993. **341**(8850): p. 938-41.
132. Barker, D.J., et al., *Weight in infancy and death from ischaemic heart disease.* Lancet, 1989. **2**(8663): p. 577-80.
133. Barker, D.J. and C. Osmond, *Infant mortality, childhood nutrition, and ischaemic heart disease in England and Wales.* Lancet, 1986. **1**(8489): p. 1077-81.
134. Barker, D.J., *The origins of the developmental origins theory.* J Intern Med, 2007. **261**(5): p. 412-7.
135. Catalano, P.M. and H.M. Ehrenberg, *The short- and long-term implications of maternal obesity on the mother and her offspring.* BJOG, 2006. **113**(10): p. 1126-33.
136. Dodd, J.M., et al., *Limiting weight gain in overweight and obese women during pregnancy to improve health outcomes: the LIMIT randomised controlled trial.* BMC Pregnancy Childbirth, 2011. **11**: p. 79.
137. Gibson, M.K., T.S. Crofts, and G. Dantas, *Antibiotics and the developing infant gut microbiota and resistome.* Curr Opin Microbiol, 2015. **27**: p. 51-6.
138. Normia, J., et al., *Impact of intrauterine and post-natal nutritional determinants on blood pressure at 4 years of age.* J Hum Nutr Diet, 2013. **26**(6): p. 544-52.
139. Fall, C.H., et al., *Weight in infancy and prevalence of coronary heart disease in adult life.* BMJ, 1995. **310**(6971): p. 17-9.
140. Radford, E.J., et al., *In utero effects. In utero undernourishment perturbs the adult sperm methylome and intergenerational metabolism.* Science, 2014. **345**(6198): p. 1255903.
141. Berger, S.L., et al., *An operational definition of epigenetics.* Genes Dev, 2009. **23**(7): p. 781-3.
142. Li, B., M. Carey, and J.L. Workman, *The role of chromatin during transcription.* Cell, 2007. **128**(4): p. 707-19.
143. Lister, R., et al., *Human DNA methylomes at base resolution show widespread epigenomic differences.* Nature, 2009. **462**(7271): p. 315-22.
144. Bird, A.P., *DNA methylation and the frequency of CpG in animal DNA.* Nucleic Acids Res, 1980. **8**(7): p. 1499-504.

145. Coulondre, C., et al., *Molecular basis of base substitution hotspots in Escherichia coli.* Nature, 1978. **274**(5673): p. 775-80.
146. Moore, L.D., T. Le, and G. Fan, *DNA methylation and its basic function.* Neuropsychopharmacology, 2013. **38**(1): p. 23-38.
147. Mohn, F., et al., *Lineage-specific polycomb targets and de novo DNA methylation define restriction and potential of neuronal progenitors.* Mol Cell, 2008. **30**(6): p. 755-66.
148. Heyn, H., et al., *Distinct DNA methylomes of newborns and centenarians.* Proc Natl Acad Sci U S A, 2012. **109**(26): p. 10522-7.
149. Mulder, R.H., et al., *Epigenome-wide change and variation in DNA methylation in childhood: trajectories from birth to late adolescence.* Hum Mol Genet, 2021. **30**(1): p. 119-134.
150. Boks, M.P., et al., *The relationship of DNA methylation with age, gender and genotype in twins and healthy controls.* PLoS One, 2009. **4**(8): p. e6767.
151. Weidner, C.I., et al., *Aging of blood can be tracked by DNA methylation changes at just three CpG sites.* Genome Biol, 2014. **15**(2): p. R24.
152. Florath, I., et al., *Cross-sectional and longitudinal changes in DNA methylation with age: an epigenome-wide analysis revealing over 60 novel age-associated CpG sites.* Hum Mol Genet, 2014. **23**(5): p. 1186-201.
153. Horvath, S., et al., *Aging effects on DNA methylation modules in human brain and blood tissue.* Genome Biol, 2012. **13**(10): p. R97.
154. Rakyan, V.K., et al., *Human aging-associated DNA hypermethylation occurs preferentially at bivalent chromatin domains.* Genome Res, 2010. **20**(4): p. 434-9.
155. Almstrup, K., et al., *Pubertal development in healthy children is mirrored by DNA methylation patterns in peripheral blood.* Sci Rep, 2016. **6**: p. 28657.
156. Baidya, A., et al., *Hepatitis B virus suppresses complement C9 synthesis by limiting the availability of transcription factor USF-1 and inhibits formation of membrane attack complex: implications in disease pathogenesis.* J Biomed Sci, 2022. **29**(1): p. 97.
157. Zheng, D.L., et al., *Epigenetic modification induced by hepatitis B virus X protein via interaction with de novo DNA methyltransferase DNMT3A.* J Hepatol, 2009. **50**(2): p. 377-87.
158. Suthaus, J., et al., *Viral Interleukin-6: Structure, pathophysiology and strategies of neutralization.* Eur J Cell Biol, 2011. **90**(6-7): p. 495-504.
159. Brocke-Heidrich, K., et al., *Interleukin-6-dependent gene expression profiles in multiple myeloma INA-6 cells reveal a Bcl-2 family-independent survival pathway closely associated with Stat3 activation.* Blood, 2004. **103**(1): p. 242-51.
160. Mauer, J., J.L. Denson, and J.C. Bruning, *Versatile functions for IL-6 in metabolism and cancer.* Trends Immunol, 2015. **36**(2): p. 92-101.
161. Tanaka, T., M. Narazaki, and T. Kishimoto, *IL-6 in inflammation, immunity, and disease.* Cold Spring Harb Perspect Biol, 2014. **6**(10): p. a016295.
162. Braconi, C., N. Huang, and T. Patel, *MicroRNA-dependent regulation of DNA methyltransferase-1 and tumor suppressor gene expression by interleukin-6 in human malignant cholangiocytes.* Hepatology, 2010. **51**(3): p. 881-90.
163. Locatelli, M. and S. Faure-Dupuy, *Virus hijacking of host epigenetic machinery to impair immune response.* J Virol, 2023. **97**(9): p. e0065823.

164. Van Campen, H., et al., *A case report: evidence for type 2 bovine viral diarrhea virus (BVDV)-associated disease in beef herds vaccinated with a modified-live type 1 BVDV vaccine.* J Vet Diagn Invest, 2000. **12**(3): p. 263-5.
165. Smirnova, N.P., et al., *Acute non-cytopathic bovine viral diarrhea virus infection induces pronounced type I interferon response in pregnant cows and fetuses.* Virus Res, 2008. **132**(1-2): p. 49-58.
166. Shoemaker, M.L., et al., *Differential expression of the type I interferon pathway during persistent and transient bovine viral diarrhea virus infection.* J Interferon Cytokine Res, 2009. **29**(1): p. 23-35.
167. Smirnova, N.P., et al., *Persistent fetal infection with bovine viral diarrhea virus differentially affects maternal blood cell signal transduction pathways.* Physiol Genomics, 2009. **36**(3): p. 129-39.
168. Smirnova, N.P., et al., *Development of fetal and placental innate immune responses during establishment of persistent infection with bovine viral diarrhea virus.* Virus Res, 2012. **167**(2): p. 329-36.
169. Smirnova, N.P., et al., *Induction of interferon-gamma and downstream pathways during establishment of fetal persistent infection with bovine viral diarrhea virus.* Virus Res, 2014. **183**: p. 95-106.
170. Hansen, T.R., et al., *Maternal and fetal response to fetal persistent infection with bovine viral diarrhea virus.* Am J Reprod Immunol, 2010. **64**(4): p. 295-306.
171. Hansen, T.R., et al., *Innate and adaptive immune responses to in utero infection with bovine viral diarrhea virus.* Anim Health Res Rev, 2015. **16**(1): p. 15-26.
172. Guzman, E., et al., *Bovine gammadelta T cells are a major regulatory T cell subset.* J Immunol, 2014. **193**(1): p. 208-22.
173. Georges, H.M., et al., *Attenuated lymphocyte activation leads to the development of immunotolerance in bovine fetuses persistently infected with bovine viral diarrhea virusdagger.* Biol Reprod, 2020. **103**(3): p. 560-571.
174. Van Campen, H., et al., *Maternal Influenza A Virus Infection Restricts Fetal and Placental Growth and Adversely Affects the Fetal Thymic Transcriptome.* Viruses, 2020. **12**(9).
175. Georges, H.M., et al., *Epigenomic and Proteomic Changes in Fetal Spleens Persistently Infected with Bovine Viral Diarrhea Virus: Repercussions for the Developing Immune System, Bone, Brain, and Heart.* Viruses, 2022. **14**(3).
176. Montgomery, D.L., et al., *The fetal brain in bovine viral diarrhea virus-infected calves: lesions, distribution, and cellular heterogeneity of viral antigen at 190 days gestation.* Vet Pathol, 2008. **45**(3): p. 288-96.
177. Bielefeldt-Ohmann, H., et al., *Neuro-invasion by a 'Trojan Horse' strategy and vasculopathy during intrauterine flavivirus infection.* Int J Exp Pathol, 2012. **93**(1): p. 24-33.
178. Webb, B.T., et al., *Bovine viral diarrhea virus cyclically impairs long bone trabecular modeling in experimental persistently infected fetuses.* Vet Pathol, 2012. **49**(6): p. 930-40.
179. Van Campen, H., et al., *Epigenetic Modifications of White Blood Cell DNA Caused by Transient Fetal Infection with Bovine Viral Diarrhea Virus.* Viruses, 2024. **16**(5).

180. Engle, T.E., et al., *Late gestation maternal infection with bovine viral diarrhea virus impacts offspring feedlot performance, digestion, blood parameters, and hot carcass weights.* J Anim Sci, 2024.
181. Pinior, B., et al., *A systematic review of financial and economic assessments of bovine viral diarrhea virus (BVDV) prevention and mitigation activities worldwide.* Prev Vet Med, 2017. **137**(Pt A): p. 77-92.
182. Moennig, V. and B. Liess, *Pathogenesis of intrauterine infections with bovine viral diarrhea virus.* Vet Clin North Am Food Anim Pract, 1995. **11**(3): p. 477-87.
183. Moerman, A., et al., *Clinical consequences of a bovine virus diarrhoea virus infection in a dairy herd: a longitudinal study.* Vet Q, 1994. **16**(2): p. 115-9.
184. Dubovi, E.J., *Impact of bovine viral diarrhea virus on reproductive performance in cattle.* Vet Clin North Am Food Anim Pract, 1994. **10**(3): p. 503-14.
185. Brownlie, J., et al., *Pathogenesis and epidemiology of bovine virus diarrhoea virus infection of cattle.* Ann Rech Vet, 1987. **18**(2): p. 157-66.
186. Baker, J.C., *The clinical manifestations of bovine viral diarrhea infection.* Vet Clin North Am Food Anim Pract, 1995. **11**(3): p. 425-45.
187. Bielefeldt-Ohmann, H., *The pathologies of bovine viral diarrhea virus infection. A window on the pathogenesis.* Vet Clin North Am Food Anim Pract, 1995. **11**(3): p. 447-76.
188. Done, J.T., et al., *Bovine virus diarrhoea-mucosal disease virus: pathogenicity for the fetal calf following maternal infection.* Vet Rec, 1980. **106**(23): p. 473-9.
189. McClurkin, A.W., et al., *Production of cattle immunotolerant to bovine viral diarrhea virus.* Can J Comp Med, 1984. **48**(2): p. 156-61.
190. Scruggs, D.W., et al., *Osteopetrosis, anemia, thrombocytopenia, and marrow necrosis in beef calves naturally infected with bovine virus diarrhea virus.* J Vet Diagn Invest, 1995. **7**(4): p. 555-9.
191. Nuss, K., et al., *Transient benign osteopetrosis in a calf persistently infected with bovine virus diarrhoea virus.* Vet Comp Orthop Traumatol, 2005. **18**(2): p. 100-4.
192. Brodersen, B.W., *Bovine viral diarrhea virus infections: manifestations of infection and recent advances in understanding pathogenesis and control.* Vet Pathol, 2014. **51**(2): p. 453-64.
193. Fulton, R.W., et al., *Multiple diagnostic tests to identify cattle with Bovine viral diarrhea virus and duration of positive test results in persistently infected cattle.* Can J Vet Res, 2009. **73**(2): p. 117-24.
194. Antos, A., et al., *Vaccination Failure in Eradication and Control Programs for Bovine Viral Diarrhea Infection.* Front Vet Sci, 2021. **8**: p. 688911.
195. Kelling, C.L., et al., *Comparative virulence of isolates of bovine viral diarrhea virus type II in experimentally inoculated six- to nine-month-old calves.* Am J Vet Res, 2002. **63**(10): p. 1379-84.
196. McRae, A.F., et al., *Contribution of genetic variation to transgenerational inheritance of DNA methylation.* Genome Biol, 2014. **15**(5): p. R73.
197. Madejon, A., et al., *Hepatitis C virus-mediated Aurora B kinase inhibition modulates inflammatory pathway and viral infectivity.* J Hepatol, 2015. **63**(2): p. 312-9.
198. Claycombe, K.J., C.A. Brissette, and O. Ghribi, *Epigenetics of inflammation, maternal infection, and nutrition.* J Nutr, 2015. **145**(5): p. 1109S-1115S.

199. Akalin, A., et al., *methylKit: a comprehensive R package for the analysis of genome-wide DNA methylation profiles.* Genome Biol, 2012. **13**(10): p. R87.
200. Yu, G., et al., *clusterProfiler: an R package for comparing biological themes among gene clusters.* OMICS, 2012. **16**(5): p. 284-7.
201. Carlson, M., *org.Bt.eg.db: Genome wide annotation for Bovine.* . 2019, BioCore: Bioconductor.
202. Akalin, A., et al., *Genomation: a toolkit to summarize, annotate and visualize genomic intervals.* Bioinformatics, 2015. **31**(7): p. 1127-9.
203. Pinchuk, G.V., et al., *Bovine viral diarrhea viruses differentially alter the expression of the protein kinases and related proteins affecting the development of infection and anti-viral mechanisms in bovine monocytes.* Biochim Biophys Acta, 2008. **1784**(9): p. 1234-47.
204. Zhang, Z., et al., *Central gene transcriptional regulatory networks shaping monocyte development in bone marrow.* Front Immunol, 2022. **13**: p. 1011279.
205. Radtke, F., et al., *Deficient T cell fate specification in mice with an induced inactivation of Notch1.* Immunity, 1999. **10**(5): p. 547-58.
206. Avram, D. and D. Califano, *The multifaceted roles of Bcl11b in thymic and peripheral T cells: impact on immune diseases.* J Immunol, 2014. **193**(5): p. 2059-65.
207. Li, L., M. Leid, and E.V. Rothenberg, *An early T cell lineage commitment checkpoint dependent on the transcription factor Bcl11b.* Science, 2010. **329**(5987): p. 89-93.
208. Okano, M., et al., *DNA methyltransferases Dnmt3a and Dnmt3b are essential for de novo methylation and mammalian development.* Cell, 1999. **99**(3): p. 247-57.
209. Di Pietro, C., et al., *Ezrin links CFTR to TLR4 signaling to orchestrate anti-bacterial immune response in macrophages.* Sci Rep, 2017. **7**(1): p. 10882.
210. Gavin, A.L., et al., *PLD3 and PLD4 are single-stranded acid exonucleases that regulate endosomal nucleic-acid sensing.* Nat Immunol, 2018. **19**(9): p. 942-953.
211. Langenmayer, M.C., et al., *Macrophages in dermal disease progression of phospholipase D4-deficient Fleckvieh calves.* Vet Pathol, 2022. **59**(2): p. 319-327.
212. Elinav, E., et al., *NLRP6 inflammasome regulates colonic microbial ecology and risk for colitis.* Cell, 2011. **145**(5): p. 745-57.
213. Grenier, J.M., et al., *Functional screening of five PYPAF family members identifies PYPAF5 as a novel regulator of NF-kappaB and caspase-1.* FEBS Lett, 2002. **530**(1-3): p. 73-8.
214. Schmid-Burgk, J.L., et al., *Caspase-4 mediates non-canonical activation of the NLRP3 inflammasome in human myeloid cells.* Eur J Immunol, 2015. **45**(10): p. 2911-7.
215. Shi, J., et al., *Cleavage of GSDMD by inflammatory caspases determines pyroptotic cell death.* Nature, 2015. **526**(7575): p. 660-5.
216. Kayagaki, N., et al., *Caspase-11 cleaves gasdermin D for non-canonical inflammasome signalling.* Nature, 2015. **526**(7575): p. 666-71.
217. Wilkins, B.J., et al., *Calcineurin/NFAT coupling participates in pathological, but not physiological, cardiac hypertrophy.* Circ Res, 2004. **94**(1): p. 110-8.

218. Molkentin, J.D., et al., *A calcineurin-dependent transcriptional pathway for cardiac hypertrophy.* Cell, 1998. **93**(2): p. 215-28.
219. Yang, T. and D.M. Roden, *Extracellular potassium modulation of drug block of IKr. Implications for torsade de pointes and reverse use-dependence.* Circulation, 1996. **93**(3): p. 407-11.
220. Larson, R.L., *Bovine Viral Diarrhea Virus-Associated Disease in Feedlot Cattle.* Vet Clin North Am Food Anim Pract, 2015. **31**(3): p. 367-80, vi.
221. Bachofen, C., et al., *Clinical appearance and pathology of cattle persistently infected with bovine viral diarrhoea virus of different genetic subgroups.* Vet Microbiol, 2010. **141**(3-4): p. 258-67.
222. Karpatkin, S., *Heterogeneity of human platelets. II. Functional evidence suggestive of young and old platelets.* J Clin Invest, 1969. **48**(6): p. 1083-7.
223. Karpatkin, S. and N. Strick, *Heterogeneity of human platelets. V. Differences in glycolytic and related enzymes with possible relation to platelet age.* J Clin Invest, 1972. **51**(5): p. 1235-43.
224. Wood, R.D., et al., *Effect on hematopoietic tissue of experimental infection of calves with noncytopathic type 2 bovine viral diarrhea virus.* Can J Vet Res, 2004. **68**(1): p. 42-8.
225. Spagnuolo, M., et al., *Bovine viral diarrhoea virus infection in bone marrow of experimentally infected calves.* J Comp Pathol, 1997. **116**(1): p. 97-100.
226. Bolin, S.R., A.W. McClurkin, and M.F. Coria, *Effects of bovine viral diarrhea virus on the percentages and absolute numbers of circulating B and T lymphocytes in cattle.* Am J Vet Res, 1985. **46**(4): p. 884-6.
227. Ellis, J.A., et al., *Flow cytofluorimetric analysis of lymphocyte subset alterations in cattle infected with bovine viral diarrhea virus.* Vet Pathol, 1988. **25**(3): p. 231-6.
228. Brewoo, J.N., et al., *Leukocyte profile of cattle persistently infected with bovine viral diarrhea virus.* Vet Immunol Immunopathol, 2007. **115**(3-4): p. 369-74.
229. Kitchen, S.G., et al., *The CD4 molecule on CD8+ T lymphocytes directly enhances the immune response to viral and cellular antigens.* Proc Natl Acad Sci U S A, 2005. **102**(10): p. 3794-9.
230. Zhang, Z., et al., *Characterization of T-cell subsets in response to foot-and-mouth disease bivalent inactivated vaccine in Chinese Holstein cows.* Microbiol Spectr, 2023. **11**(6): p. e0102923.
231. Hoek, A., et al., *Subpopulations of bovine WC1(+) gammadelta T cells rather than CD4(+)CD25(high) Foxp3(+) T cells act as immune regulatory cells ex vivo.* Vet Res, 2009. **40**(1): p. 6.
232. Ammari, M., et al., *Analysis of Bovine Viral Diarrhea Viruses-infected monocytes: identification of cytopathic and non-cytopathic biotype differences.* BMC Bioinformatics, 2010. **11 Suppl 6**(Suppl 6): p. S9.
233. Glew, E.J., et al., *Differential effects of bovine viral diarrhoea virus on monocytes and dendritic cells.* J Gen Virol, 2003. **84**(Pt 7): p. 1771-1780.
234. Baule, C., et al., *Pathogenesis of primary respiratory disease induced by isolates from a new genetic cluster of bovine viral diarrhea virus type I.* J Clin Microbiol, 2001. **39**(1): p. 146-53.

235. Liebler-Tenorio, E.M., et al., *Incidence of BVDV1 and BVDV2 infections in cattle submitted for necropsy in Northern Germany.* J Vet Med B Infect Dis Vet Public Health, 2006. **53**(8): p. 363-9.
236. Khodakaram-Tafti, A., *The comparative evaluation of cellular localization of viral antigens with microscopic changes in the ileum of cattle infected with bovine viral diarrhea.* Comparative Clinical Pathology, 2006. **15**: p. 90-93.
237. Shahriar, F.M., et al., *Coinfection with bovine viral diarrhea virus and Mycoplasma bovis in feedlot cattle with chronic pneumonia.* Can Vet J, 2002. **43**(11): p. 863-8.
238. Haines, D.M., et al., *The immunohistochemical detection of Mycoplasma bovis and bovine viral diarrhea virus in tissues of feedlot cattle with chronic, unresponsive respiratory disease and/or arthritis.* Can Vet J, 2001. **42**(11): p. 857-60.
239. Kirkbride, C.A., *Viral agents and associated lesions detected in a 10-year study of bovine abortions and stillbirths.* J Vet Diagn Invest, 1992. **4**(4): p. 374-9.
240. Breshears, M.A. and B.J. Johnson, *Systemic reactive angioendotheliomatosis-like syndrome in a steer presumed to be persistently infected with bovine viral diarrhea virus.* Vet Pathol, 2008. **45**(5): p. 645-9.
241. Yang, J., et al., *Independent signals control expression of the calcineurin inhibitory proteins MCIP1 and MCIP2 in striated muscles.* Circ Res, 2000. **87**(12): p. E61-8.
242. Davis, U.o.C., *Clinical Diagnostic Laboratory CBC Reference Intervals* 2011: Veterinary Medical Teaching Hospital.
243. MacPhillamy, C., et al., *DNA methylation analysis to differentiate reference, breed, and parent-of-origin effects in the bovine pangenome era.* Gigascience, 2024. **13**.
244. Powell, J., et al., *Profiling the immune epigenome across global cattle breeds.* Genome Biol, 2023. **24**(1): p. 127.
245. Fritzemeier, J., et al., *The development of early vs. late onset mucosal disease is a consequence of two different pathogenic mechanisms.* Arch Virol, 1997. **142**(7): p. 1335-50.
246. Munoz-Zanzi, C.A., et al., *Quantification, risk factors, and health impact of natural congenital infection with bovine viral diarrhea virus in dairy calves.* Am J Vet Res, 2003. **64**(3): p. 358-65.
247. Waldner, C.L. and R.I. Kennedy, *Associations between health and productivity in cow-calf beef herds and persistent infection with bovine viral diarrhea virus, antibodies against bovine viral diarrhea virus, or antibodies against infectious bovine rhinotracheitis virus in calves.* Am J Vet Res, 2008. **69**(7): p. 916-27.
248. Hamdane, N., et al., *HCV-Induced Epigenetic Changes Associated With Liver Cancer Risk Persist After Sustained Virologic Response.* Gastroenterology, 2019. **156**(8): p. 2313-2329 e7.
249. Anderson, D., et al., *Zika Virus Changes Methylation of Genes Involved in Immune Response and Neural Development in Brazilian Babies Born With Congenital Microcephaly.* J Infect Dis, 2021. **223**(3): p. 435-440.
250. Kincade, J., Murtazina, DA, Georges, HM, Gonzalez-Berrios, CL, Bishop, JV, Engle, TE, Henao-Tamayo, M, Eder, JM, McDonald, EM, Deines, DM, Wright,

BM, Van Campen, H, Hansen, TR *Epigenetic Alterations in Calves Persistently Infected with Bovine Viral Diarrhea Virus.* submitted to Viruses, 2025.
251. Kramer, A., et al., *Causal analysis approaches in Ingenuity Pathway Analysis.* Bioinformatics, 2014. **30**(4): p. 523-30.
252. George, J.W., J. Snipes, and V.M. Lane, *Comparison of bovine hematology reference intervals from 1957 to 2006.* Vet Clin Pathol, 2010. **39**(2): p. 138-48.
253. Liu, B., et al., *Co-opted JNK/SAPK signaling in Wnt/beta-catenin-induced tumorigenesis.* Neoplasia, 2008. **10**(9): p. 1004-13.
254. Guo, Y.J., et al., *ERK/MAPK signalling pathway and tumorigenesis.* Exp Ther Med, 2020. **19**(3): p. 1997-2007.
255. Cooper, J. and F.G. Giancotti, *Integrin Signaling in Cancer: Mechanotransduction, Stemness, Epithelial Plasticity, and Therapeutic Resistance.* Cancer Cell, 2019. **35**(3): p. 347-367.
256. Pasquale, E.B., *Eph receptors and ephrins in cancer progression.* Nat Rev Cancer, 2024. **24**(1): p. 5-27.
257. Haga, R.B. and A.J. Ridley, *Rho GTPases: Regulation and roles in cancer cell biology.* Small GTPases, 2016. **7**(4): p. 207-221.
258. Panda, M., S.K. Tripathi, and B.K. Biswal, *SOX9: An emerging driving factor from cancer progression to drug resistance.* Biochim Biophys Acta Rev Cancer, 2021. **1875**(2): p. 188517.
259. Lin, T.C., *RUNX2 and Cancer.* Int J Mol Sci, 2023. **24**(8).
260. Weber, W.T., *Hematologic Aspects of Bovine Lymphosarcoma.* Ann N Y Acad Sci, 1963. **108**: p. 1270-83.
261. Forsthuber, T., H.C. Yip, and P.V. Lehmann, *Induction of TH1 and TH2 immunity in neonatal mice.* Science, 1996. **271**(5256): p. 1728-30.
262. Hagen, M., et al., *Legend or Truth: Mature CD4(+)CD8(+) Double-Positive T Cells in the Periphery in Health and Disease.* Biomedicines, 2023. **11**(10).
263. Talker, S.C., et al., *Monocyte biology conserved across species: Functional insights from cattle.* Front Immunol, 2022. **13**: p. 889175.
264. Man, K., et al., *Transcription Factor IRF4 Promotes CD8(+) T Cell Exhaustion and Limits the Development of Memory-like T Cells during Chronic Infection.* Immunity, 2017. **47**(6): p. 1129-1141 e5.
265. Tasiheng, Y., et al., *DNA hypo-methylation and expression of GBP4 induces T cell exhaustion in pancreatic cancer.* Cancer Immunol Immunother, 2024. **73**(10): p. 208.
266. Hussen, J., et al., *Phenotypic and functional heterogeneity of bovine blood monocytes.* PLoS One, 2013. **8**(8): p. e71502.
267. Aapola, U., et al., *Isolation and initial characterization of a novel zinc finger gene, DNMT3L, on 21q22.3, related to the cytosine-5-methyltransferase 3 gene family.* Genomics, 2000. **65**(3): p. 293-8.
268. Okano, M., S. Xie, and E. Li, *Cloning and characterization of a family of novel mammalian DNA (cytosine-5) methyltransferases.* Nat Genet, 1998. **19**(3): p. 219-20.
269. Hata, K., et al., *Dnmt3L cooperates with the Dnmt3 family of de novo DNA methyltransferases to establish maternal imprints in mice.* Development, 2002. **129**(8): p. 1983-93.

270. Bourc'his, D., et al., *Dnmt3L and the establishment of maternal genomic imprints.* Science, 2001. **294**(5551): p. 2536-9.
271. O'Doherty, A.M., L.C. O'Shea, and T. Fair, *Bovine DNA methylation imprints are established in an oocyte size-specific manner, which are coordinated with the expression of the DNMT3 family proteins.* Biol Reprod, 2012. **86**(3): p. 67.
272. Suetake, I., et al., *DNMT3L stimulates the DNA methylation activity of Dnmt3a and Dnmt3b through a direct interaction.* J Biol Chem, 2004. **279**(26): p. 27816-23.
273. Li, Z., et al., *Overexpression of human-derived DNMT3A induced intergenerational inheritance of DNA methylation and gene expression variations in rat brain and testis.* Epigenetics, 2020. **15**(10): p. 1107-1120.
274. Zeng, Z., et al., *CCL5/CCR5 axis in human diseases and related treatments.* Genes Dis, 2022. **9**(1): p. 12-27.
275. Ahn, Y.T., et al., *Dynamic interplay of transcriptional machinery and chromatin regulates "late" expression of the chemokine RANTES in T lymphocytes.* Mol Cell Biol, 2007. **27**(1): p. 253-66.
276. Mor, A., et al., *Blockade of CCL24 with a monoclonal antibody ameliorates experimental dermal and pulmonary fibrosis.* Ann Rheum Dis, 2019. **78**(9): p. 1260-1268.
277. Segal-Salto, M., et al., *A blocking monoclonal antibody to CCL24 alleviates liver fibrosis and inflammation in experimental models of liver damage.* JHEP Rep, 2020. **2**(1): p. 100064.
278. Gao, W., et al., *Treg versus Th17 lymphocyte lineages are cross-regulated by LIF versus IL-6.* Cell Cycle, 2009. **8**(9): p. 1444-50.
279. Hamelin-Morrissette, J., et al., *Leukemia inhibitory factor regulates the activation of inflammatory signals in macrophages and trophoblast cells.* Mol Immunol, 2020. **120**: p. 32-42.
280. Sesti-Costa, R., et al., *Leukemia Inhibitory Factor Inhibits Plasmacytoid Dendritic Cell Function and Development.* J Immunol, 2020. **204**(8): p. 2257-2268.
281. Barin, J.G., et al., *Macrophages participate in IL-17-mediated inflammation.* Eur J Immunol, 2012. **42**(3): p. 726-36.
282. Ye, P., et al., *Requirement of interleukin 17 receptor signaling for lung CXC chemokine and granulocyte colony-stimulating factor expression, neutrophil recruitment, and host defense.* J Exp Med, 2001. **194**(4): p. 519-27.
283. Iwakura, Y., et al., *The roles of IL-17A in inflammatory immune responses and host defense against pathogens.* Immunol Rev, 2008. **226**: p. 57-79.
284. Shahrara, S., et al., *IL-17-mediated monocyte migration occurs partially through CC chemokine ligand 2/monocyte chemoattractant protein-1 induction.* J Immunol, 2010. **184**(8): p. 4479-87.
285. Shahrara, S., et al., *IL-17 induces monocyte migration in rheumatoid arthritis.* J Immunol, 2009. **182**(6): p. 3884-91.
286. Sbarra, A.J. and M.L. Karnovsky, *The biochemical basis of phagocytosis. I. Metabolic changes during the ingestion of particles by polymorphonuclear leukocytes.* J Biol Chem, 1959. **234**(6): p. 1355-62.
287. Babior, B.M., *NADPH oxidase: an update.* Blood, 1999. **93**(5): p. 1464-76.

288. Salzano, S., et al., *Linkage of inflammation and oxidative stress via release of glutathionylated peroxiredoxin-2, which acts as a danger signal.* Proc Natl Acad Sci U S A, 2014. **111**(33): p. 12157-62.
289. Renier, G., et al., *Role of oxidant injury on macrophage lipoprotein lipase (LPL) production and sensitivity to LPL.* J Lipid Res, 1996. **37**(4): p. 799-809.
290. Hedman, A.K., et al., *DNA methylation patterns associated with oxidative stress in an ageing population.* BMC Med Genomics, 2016. **9**(1): p. 72.
291. Xiao, Y., et al., *GSTA3 Attenuates Renal Interstitial Fibrosis by Inhibiting TGF-Beta-Induced Tubular Epithelial-Mesenchymal Transition and Fibronectin Expression.* PLoS One, 2016. **11**(9): p. e0160855.
292. Bhusari, S.S., et al., *Superoxide dismutase 1 knockdown induces oxidative stress and DNA methylation loss in the prostate.* Epigenetics, 2010. **5**(5): p. 402-9.
293. Zhu, J.H. and X.G. Lei, *Lipopolysaccharide-induced hepatic oxidative injury is not potentiated by knockout of GPX1 and SOD1 in mice.* Biochem Biophys Res Commun, 2011. **404**(1): p. 559-63.
294. Costa, C.F., et al., *Functional Analysis of GSTK1 in Peroxisomal Redox Homeostasis in HEK-293 Cells.* Antioxidants (Basel), 2023. **12**(6).
295. Wang, S., et al., *Identification of key genes and biological pathways associated with vascular aging in diabetes based on bioinformatics and machine learning.* Aging (Albany NY), 2024. **16**(11): p. 9369-9385.
296. Goncalves, J., et al., *Loss of SDHB Promotes Dysregulated Iron Homeostasis, Oxidative Stress, and Sensitivity to Ascorbate.* Cancer Res, 2021. **81**(13): p. 3480-3494.
297. Besselink, N., et al., *The genome-wide mutational consequences of DNA hypomethylation.* Sci Rep, 2023. **13**(1): p. 6874.
298. Shan, P., et al., *RXR agonists inhibit oxidative stress-induced apoptosis in H9c2 rat ventricular cells.* Biochem Biophys Res Commun, 2008. **375**(4): p. 628-33.
299. Katsuoka, F., et al., *Genetic evidence that small maf proteins are essential for the activation of antioxidant response element-dependent genes.* Mol Cell Biol, 2005. **25**(18): p. 8044-51.
300. Abu Shelbayeh, O., et al., *PGC-1alpha Is a Master Regulator of Mitochondrial Lifecycle and ROS Stress Response.* Antioxidants (Basel), 2023. **12**(5).
301. Harmon, J.S., R. Stein, and R.P. Robertson, *Oxidative stress-mediated, post-translational loss of MafA protein as a contributing mechanism to loss of insulin gene expression in glucotoxic beta cells.* J Biol Chem, 2005. **280**(12): p. 11107-13.
302. Nishimura, W., S. Takahashi, and K. Yasuda, *MafA is critical for maintenance of the mature beta cell phenotype in mice.* Diabetologia, 2015. **58**(3): p. 566-74.
303. Rius-Perez, S., et al., *PGC-1alpha, Inflammation, and Oxidative Stress: An Integrative View in Metabolism.* Oxid Med Cell Longev, 2020. **2020**: p. 1452696.
304. Sczelecki, S., et al., *Loss of Pgc-1alpha expression in aging mouse muscle potentiates glucose intolerance and systemic inflammation.* Am J Physiol Endocrinol Metab, 2014. **306**(2): p. E157-67.
305. Kanoh, H., K. Yamada, and F. Sakane, *Diacylglycerol kinase: a key modulator of signal transduction?* Trends Biochem Sci, 1990. **15**(2): p. 47-50.

306. Erion, D.M. and G.I. Shulman, *Diacylglycerol-mediated insulin resistance.* Nat Med, 2010. **16**(4): p. 400-2.
307. Rached, G., et al., *TRPC3 Regulates Islet Beta-Cell Insulin Secretion.* Adv Sci (Weinh), 2023. **10**(6): p. e2204846.
308. Fu, J., et al., *Kv2.1 Clustering Contributes to Insulin Exocytosis and Rescues Human beta-Cell Dysfunction.* Diabetes, 2017. **66**(7): p. 1890-1900.
309. Miyazaki, S., et al., *Nuclear hormone retinoid X receptor (RXR) negatively regulates the glucose-stimulated insulin secretion of pancreatic ss-cells.* Diabetes, 2010. **59**(11): p. 2854-61.
310. Jia, L., et al., *Purbeta promotes hepatic glucose production by increasing Adcy6 transcription.* Mol Metab, 2020. **31**: p. 85-97.
311. Kajimura, S., et al., *Initiation of myoblast to brown fat switch by a PRDM16-C/EBP-beta transcriptional complex.* Nature, 2009. **460**(7259): p. 1154-8.
312. De Cauwer, A., et al., *Dicer1 deficient mice exhibit premature aging and metabolic perturbations in adipocytes.* iScience, 2022. **25**(10): p. 105149.
313. Tobi, E.W., et al., *DNA methylation differences after exposure to prenatal famine are common and timing- and sex-specific.* Hum Mol Genet, 2009. **18**(21): p. 4046-53.
314. Heijmans, B.T., et al., *Persistent epigenetic differences associated with prenatal exposure to famine in humans.* Proc Natl Acad Sci U S A, 2008. **105**(44): p. 17046-9.
315. Hamilton, O.K.L., et al., *An epigenetic score for BMI based on DNA methylation correlates with poor physical health and major disease in the Lothian Birth Cohort.* Int J Obes (Lond), 2019. **43**(9): p. 1795-1802.
316. McCartney, D.L., et al., *Epigenetic prediction of complex traits and death.* Genome Biol, 2018. **19**(1): p. 136.
317. Makris, S., et al., *Immune function and dysfunction are determined by lymphoid tissue efficacy.* Dis Model Mech, 2022. **15**(1).
318. Pham, T.A., et al., *Epithelial IL-22RA1-mediated fucosylation promotes intestinal colonization resistance to an opportunistic pathogen.* Cell Host Microbe, 2014. **16**(4): p. 504-16.
319. Zindl, C.L., et al., *IL-22-producing neutrophils contribute to antimicrobial defense and restitution of colonic epithelial integrity during colitis.* Proc Natl Acad Sci U S A, 2013. **110**(31): p. 12768-73.
320. Zheng, Y., et al., *Interleukin-22 mediates early host defense against attaching and effacing bacterial pathogens.* Nat Med, 2008. **14**(3): p. 282-9.
321. Ohkawara, T., et al., *Lack of macrophage migration inhibitory factor suppresses innate immune response in murine dextran sulfate sodium-induced colitis.* Scand J Gastroenterol, 2008. **43**(12): p. 1497-504.
322. de Jong, Y.P., et al., *Development of chronic colitis is dependent on the cytokine MIF.* Nat Immunol, 2001. **2**(11): p. 1061-6.
323. Verhelst, J., et al., *Interferon-inducible protein Mx1 inhibits influenza virus by interfering with functional viral ribonucleoprotein complex assembly.* J Virol, 2012. **86**(24): p. 13445-55.

324. McCormack, R., et al., *Perforin-2 Protects Host Cells and Mice by Restricting the Vacuole to Cytosol Transitioning of a Bacterial Pathogen.* Infect Immun, 2016. **84**(4): p. 1083-1091.
325. McCormack, R.M., et al., *Perforin-2 is essential for intracellular defense of parenchymal cells and phagocytes against pathogenic bacteria.* Elife, 2015. **4**.
326. Johnson, D.W. and C.C. Muscoplat, *Immunologic abnormalities in calves with chronic bovine viral diarrhea.* Am J Vet Res, 1973. **34**(9): p. 1139-41.
327. Kincade, J., Engle, TE, Henao-Tamayo, M, Eder, JM, McDonald, EM, Deines, DM, Wright, BM, Murtazina, DA, Bishop, JV, Hansen, TR, Van Campen, H *Postnatal epigenetic differences in calves following transient fetal infection with bovine viral diarrhea virus* BMC Genomics, 2025.
328. Perez, G., et al., *The UCSC Genome Browser database: 2025 update.* Nucleic Acids Res, 2025. **53**(D1): p. D1243-D1249.
329. Hao, Y., et al., *Dictionary learning for integrative, multimodal and scalable single-cell analysis.* Nat Biotechnol, 2024. **42**(2): p. 293-304.
330. Hao, Y., et al., *Integrated analysis of multimodal single-cell data.* Cell, 2021. **184**(13): p. 3573-3587 e29.
331. Germain, P.L., et al., *Doublet identification in single-cell sequencing data using scDblFinder.* F1000Res, 2021. **10**: p. 979.
332. Choudhary, S. and R. Satija, *Comparison and evaluation of statistical error models for scRNA-seq.* Genome Biol, 2022. **23**(1): p. 27.
333. Hafemeister, C. and R. Satija, *Normalization and variance stabilization of single-cell RNA-seq data using regularized negative binomial regression.* Genome Biol, 2019. **20**(1): p. 296.
334. Kincade, J.N., et al., *Postnatal epigenetic differences in calves following transient fetal infection with bovine viral diarrhea virus.* BMC Genomics, 2025. **26**(1): p. 441.
335. Alam, M.R., et al., *CD4(+)CD8(+) double-positive T cells in immune disorders and cancer: Prospects and hurdles in immunotherapy.* Autoimmun Rev, 2025. **24**(3): p. 103757.
336. Wu, L. and L. Van Kaer, *Natural killer T cells in health and disease.* Front Biosci (Schol Ed), 2011. **3**(1): p. 236-51.
337. Grose, R.H., et al., *Deficiency of invariant NK T cells in Crohn's disease and ulcerative colitis.* Dig Dis Sci, 2007. **52**(6): p. 1415-22.
338. Yanagihara, Y., et al., *Natural killer (NK) T cells are significantly decreased in the peripheral blood of patients with rheumatoid arthritis (RA).* Clin Exp Immunol, 1999. **118**(1): p. 131-6.
339. Ren, Y., et al., *A Novel Mouse Model of iNKT Cell-deficiency Generated by CRISPR/Cas9 Reveals a Pathogenic Role of iNKT Cells in Metabolic Disease.* Sci Rep, 2017. **7**(1): p. 12765.
340. Kinjo, Y. and M. Kronenberg, *V alpha14 i NKT cells are innate lymphocytes that participate in the immune response to diverse microbes.* J Clin Immunol, 2005. **25**(6): p. 522-33.
341. Tai, Y., et al., *Dysregulation of humoral immunity in Foxp3 conditional-knockout mice.* Biochem Biophys Res Commun, 2019. **513**(4): p. 787-793.

342. Fernandez, I.Z., et al., *A novel human IL2RB mutation results in T and NK cell-driven immune dysregulation.* J Exp Med, 2019. **216**(6): p. 1255-1267.
343. Mayadas, T.N., et al., *Leukocyte rolling and extravasation are severely compromised in P selectin-deficient mice.* Cell, 1993. **74**(3): p. 541-54.
344. Kum, W.W., et al., *Impaired innate immune response and enhanced pathology during Citrobacter rodentium infection in mice lacking functional P-selectin.* Cell Microbiol, 2010. **12**(9): p. 1250-71.
345. Almarza Novoa, E., et al., *Leukocyte adhesion deficiency-I: A comprehensive review of all published cases.* J Allergy Clin Immunol Pract, 2018. **6**(4): p. 1418-1420 e10.
346. Ong, W.K., et al., *The role of the PDE4D cAMP phosphodiesterase in the regulation of glucagon-like peptide-1 release.* Br J Pharmacol, 2009. **157**(4): p. 633-44.
347. Gantner, F., et al., *Phosphodiesterase profile of human B lymphocytes from normal and atopic donors and the effects of PDE inhibition on B cell proliferation.* Br J Pharmacol, 1998. **123**(6): p. 1031-8.
348. Roos, E.O., et al., *OMIP-085: Cattle B-cell phenotyping by an 8-color panel.* Cytometry A, 2023. **103**(1): p. 12-15.
349. Stabel, J.R., J.P. Bannantine, and S. Humphrey, *B cell phenotypes and maturation states in cows naturally infected with Mycobacterium avium subsp. Paratuberculosis.* PLoS One, 2022. **17**(12): p. e0278313.
350. Bonasio, R., E. Lecona, and D. Reinberg, *MBT domain proteins in development and disease.* Semin Cell Dev Biol, 2010. **21**(2): p. 221-30.
351. Gwak, J., et al., *SFMBT2 (Scm-like with four mbt domains 2) negatively regulates cell migration and invasion in prostate cancer cells.* Oncotarget, 2016. **7**(30): p. 48250-48264.
352. Xie, Q., B. Hu, and H. Li, *Acetylation- and ubiquitination-regulated SFMBT2 acts as a tumor suppressor in clear cell renal cell carcinoma.* Biol Direct, 2024. **19**(1): p. 37.
353. Yin, J., et al., *ARHGEF18 can promote BVDV NS5B activation of the host NF-kappaB signaling pathway by combining with the NS5B-palm domain.* Vet Microbiol, 2024. **291**: p. 109911.
354. Rossman, K.L., C.J. Der, and J. Sondek, *GEF means go: turning on RHO GTPases with guanine nucleotide-exchange factors.* Nat Rev Mol Cell Biol, 2005. **6**(2): p. 167-80.
355. van Helden, S.F. and P.L. Hordijk, *Podosome regulation by Rho GTPases in myeloid cells.* Eur J Cell Biol, 2011. **90**(2-3): p. 189-97.
356. Thirunavukkarasu, S., et al., *Macrophage polarization in cattle experimentally exposed to Mycobacterium avium subsp. paratuberculosis.* Pathog Dis, 2015. **73**(9): p. ftv085.
357. Trombetta, A.C., et al., *A circulating cell population showing both M1 and M2 monocyte/macrophage surface markers characterizes systemic sclerosis patients with lung involvement.* Respir Res, 2018. **19**(1): p. 186.
358. Liu, Y., et al., *Metabolic reprogramming in macrophage responses.* Biomark Res, 2021. **9**(1): p. 1.

359. Yabas, M., et al., *Differential requirement for the CD45 splicing regulator hnRNPLL for accumulation of NKT and conventional T cells.* PLoS One, 2011. **6**(11): p. e26440.
360. van den Buuse, M., P. Halley, and G.F. Hoyne, *Behavioural phenotyping of thunder mice with a hypomorphic mutation of heterogeneous nuclear ribonuclear protein L-like (hnRNPLL) and reduced T cell function.* Neurosci Lett, 2021. **740**: p. 135469.
361. Harris, N.L., et al., *Differential T cell function and fate in lymph node and nonlymphoid tissues.* J Exp Med, 2002. **195**(3): p. 317-26.
362. Gao, Y., et al., *Single-cell transcriptomic and chromatin accessibility analyses of dairy cattle peripheral blood mononuclear cells and their responses to lipopolysaccharide.* BMC Genomics, 2022. **23**(1): p. 338.
363. Wang, Y., et al., *The meiotic TERB1-TERB2-MAJIN complex tethers telomeres to the nuclear envelope.* Nat Commun, 2019. **10**(1): p. 564.
364. Musio, A., *The multiple facets of the SMC1A gene.* Gene, 2020. **743**: p. 144612.
365. Kogo, H., et al., *HORMAD2 is essential for synapsis surveillance during meiotic prophase via the recruitment of ATR activity.* Genes Cells, 2012. **17**(11): p. 897-912.
366. Yue, W., et al., *CtIP regulates G2/M transition and bipolar spindle assembly during mouse oocyte meiosis.* J Genet Genomics, 2024. **51**(12): p. 1435-1446.
367. Pohland, R., J. Vanselow, and F.M. Sterza, *Translocation of Oocytic HES1 into Surrounding Cumulus Cells in Bovine: Mechanism of Cellular Interaction during IVM?* Int J Mol Sci, 2023. **24**(15).
368. Wu, X., *Maternal depletion of NLRP5 blocks early embryogenesis in rhesus macaque monkeys (Macaca mulatta).* Hum Reprod, 2009. **24**(2): p. 415-24.
369. Varlakhanova, N.V., et al., *myc maintains embryonic stem cell pluripotency and self-renewal.* Differentiation, 2010. **80**(1): p. 9-19.
370. Okamura, E., et al., *Esrrb function is required for proper primordial germ cell development in presomite stage mouse embryos.* Dev Biol, 2019. **455**(2): p. 382-392.
371. Keramari, M., et al., *Sox2 is essential for formation of trophectoderm in the preimplantation embryo.* PLoS One, 2010. **5**(11): p. e13952.
372. Salleh, N. and N. Giribabu, *Leukemia inhibitory factor: roles in embryo implantation and in nonhormonal contraception.* ScientificWorldJournal, 2014. **2014**: p. 201514.
373. Seo, L., et al., *Discovery of Klf2 interactors in mouse embryonic stem cells by immunoprecipitation-mass spectrometry utilizing exogenously expressed bait.* Biochim Biophys Acta Proteins Proteom, 2021. **1869**(9): p. 140672.
374. Festuccia, N., et al., *Nr5a2 is dispensable for zygotic genome activation but essential for morula development.* Science, 2024. **386**(6717): p. eadg7325.
375. Chiu, C.F., et al., *The Mechanism of the Zika Virus Crossing the Placental Barrier and the Blood-Brain Barrier.* Front Microbiol, 2020. **11**: p. 214.
376. Robbins, J.R. and A.I. Bakardjiev, *Pathogens and the placental fortress.* Curr Opin Microbiol, 2012. **15**(1): p. 36-43.
377. Pradhan, J., et al., *Pregnancy, infection, and epigenetic regulation: A complex scenario.* Biochim Biophys Acta Mol Basis Dis, 2023. **1869**(7): p. 166768.

378. Shimizu, Y., et al., *Influence of Immune System Abnormalities Caused by Maternal Immune Activation in the Postnatal Period.* Cells, 2023. **12**(5).
379. Pereira, L., M. Petitt, and T. Tabata, *Cytomegalovirus infection and antibody protection of the developing placenta.* Clin Infect Dis, 2013. **57 Suppl 4**(Suppl 4): p. S174-7.
380. Walker, C.L., et al., *Ultrasound prediction of Zika virus-associated congenital injury using the profile of fetal growth.* PLoS One, 2020. **15**(5): p. e0233023.
381. Yue, Y., et al., *Maternal infection during pregnancy and type 1 diabetes mellitus in offspring: a systematic review and meta-analysis.* Epidemiol Infect, 2018. **146**(16): p. 2131-2138.
382. Corley, M.J., et al., *Genome-wide DNA methylation profiling of peripheral blood reveals an epigenetic signature associated with severe COVID-19.* J Leukoc Biol, 2021. **110**(1): p. 21-26.
383. Viana, J.H.M., Dode, M. A. N., Basso, A. C. , *General sanitary procedures associated with in vitro production of embryos* in *Manual of the International Embryo Transfer Society* 2020. p. 1-11.
384. Barfield, J., Demetrio, Daniela, *Appendix 3. Considerations for evaluating in vitro-produced bovine embryos*. 5th ed. Manual of the International Embryo Transfer Society. Vol. 2. 2021.

SUPPLEMENTARY CHAPTER: ABATTOIR DERIVED IVP EMBRYOS ARE RENDERED CLEAN OF POTENTIALLY PATHOGENIC BACTERIAL CONTAMINANTS VIA IETS RECOMMENDED WASHING PROCEDURES

Short Summary

Since 2016, the quantity of *in vitro* produced (IVP) bovine embryos has surpassed the number of *in vivo* derived (IVD) bovine embryos. Most IVP embryos are generated from oocytes collected posthumously from ovaries sourced from local abattoirs. As the health of the cow from which the IVP embryos are generated is unknown, there is just cause for the concern of pathogenic contamination. The recommended washing procedures for IVD embryos have subsequently been adapted and applied to IVP embryos. The recommendations indicate that embryos at the blastocyst stage should be washed 5 times through culture medium containing antibodies and bovine serum albumin (BSA), washed twice in balanced salt solution containing 0.25% trypsin, and washed another 5 times in antibiotic treated medium [383]. While the efficacy of these methods has been tested in IVD embryos, they have not yet been examined in IVP embryos. It was hypothesized that these washing procedures would be sufficient in removing any bacterial contaminants contained in the follicular fluid or attached to abattoir derived embryos. To this end, oocytes were aspirated from abattoir ovaries sourced from beef cattle twice monthly for 12 months. Oocytes were aspirated from abattoir ovaries sourced from dairy cattle twice monthly for approximately 6 months. Follicular fluid was plated on brain, heart, infusion agar and any resulting bacterial colonies were identified using 16S. Following *in vitro* fertilization

and culture to day 7 blastocysts, half of the generated embryos were washed in phosphate buffered saline (PBS) and half were washed according to IETS recommendations. Potentially pathogenic bacteria were cultured from follicular fluid of abattoir derived beef and dairy ovaries. However, most bacterial contaminants were removed from day 7 blastocysts by a single wash in PBS. Nearly all contamination was removed from blastocysts when IETS recommendations were utilized. These findings have implications for the evaluation of disease transmission risk due to global import and export of IVP embryos.

Introduction

Since 2016 the world has produced more *in vitro* produced (IVP) embryos than *in vivo* derived embryos (IVD). Each following year has demonstrated a drastic increase in the use of IVP embryos. The most recent report of statistics from the International Embryo Technology Society (IETS) showed the production of approximately 1.6 million IVP embryos in 2022 (a 6% increase from 2021). The IVD embryos are fertilized within the animal and collected using flushing methods, while IVP embryos result from the culture and fertilization of oocytes within a laboratory setting.

The generation of IVP embryos begins with oocytes, often collected posthumously in collaboration with local abattoirs. Because bovine oocytes are frequently derived from animals of unknown health status, the cow's follicular fluid could contain pathogens associated with infection that pose a threat to the success of IVF. For instance, bacterial contamination within the in vitro fertilization (IVF) system can lead to developmental halt and degeneration of embryos that would have otherwise been

utilized for embryo transfer and the generation of pregnancy. In human IVF the addition of semen for fertilization of oocytes serves as the primary source of bacterial contamination, but the follicular fluid bathing oocytes in vivo is also frequently contaminated [1-4]. Several bacteria genera have been detected in human follicular fluid, including Lactobacillus, Actinomyces, Peptostreptococcus, Staphylococcus, Corynebacterium, Peptinophilus, Propionibacterium, Prevotella, and Fusobacterium [5, 6]. The fungus Candida albicans has also been isolated from human follicular fluid [5, 6]. Similarly, bovine follicular fluid has been found to contain Escherichia coli, Staphylococcus, Pasteurella, Corynebacterium, Streptococcus, Klebsiella, Citrobacter, and Micrococcus [7]. In addition to bacterial and fungal organisms, viral pathogens have also been isolated from follicular fluid. Both hepatitis C virus (HCV) and human immunodeficiency virus (HIV) have been isolated from human follicular fluid, while bovine viral diarrhea virus (BVDV) and bovine alphaherpesvirus 1 (BHV-1) have been isolated from bovine follicular fluid [8-11].

The pathogenic risk associated with bovine oocytes and embryos has birthed the necessity for procedures that render the cells ‘clean’ and free of contaminants. The washing procedures published in 1985 by E. L. Singh remain the adopted recommendation for bovine IVF systems by IETS for IVD embryos [12]. This protocol indicates that day 7 embryos at the blastocyst stage should be washed five times through a culture medium containing antibiotics and bovine serum albumin (BSA), washed twice in a balanced salt solution containing 0.25% trypsin (T-4424; Sigma-Aldrich, St. Louis, MO, USA), and washed another five times in medium containing antibiotics and either BSA or FBS [13]. The protocol was proven efficacious in removing

pathogens responsible for BVDV, bluetongue, akabane, infectious bovine rhinotracheitis, and vesicular stomatitis from IVD embryos [12, 14, 15]. These recommendations have been extended to application in IVP embryos. It has been shown that the IETS standard washing procedures are not effective in removing all BHV or BVDV contamination from IVP embryos [16-18], but the washings do significantly reduce the viral load [19]. However, the efficacy of the serial washes in removing other potentially pathogenic contaminants from IVP embryos has not yet been assessed. We hypothesized that bacteria present in follicular fluid of abattoir-derived ovaries would be removed from IVP embryos by the IETS-recommended serial washings (including trypsin in two washes). To this end, ovaries were obtained from a local abattoir for oocyte aspiration and standard IVF and standard washing procedures evaluated for their ability to remove microbial contaminants.

Results

Embryo Production

Abattoir derived ovaries from beef cattle yielded 3,670 oocytes from a total of 24 collections with an average collection of 153 oocytes per ‘round’ of aspiration. Cells were classified based on the number of blastomeres 56 hours post fertilization. On average, 19.7% of the oocytes exposed to sperm remained unfertilized, 8.5% developed 2 to 3 blastomeres, 20.7% of cells developed 4 to 6 blastomeres, and 51.1% of zygotes developed 6 or more blastomeres. The average overall cleavage rate for beef embryos was 80.3%. On day 7 of incubation post fertilization, embryos were assessed for blastocyst formation according to IETS stages of development [384]. An

average of 4.27% of zygotes had developed to the morula stage. Of the morula stage embryos identified, 56% were classified as grade 2 and 44% were classified as grade 3 according to the IETS grading standards [384]. An average of 23.18% of zygotes had developed to a blastocyst stage. Of the cells that developed to a blastocyst stage, 19.9% were classified as early blastocysts, 28% were true blastocysts, 43.6% were expanded blastocysts, 5.8% were hatching blastocysts, and 5.8% were hatched blastocysts. The early blastocysts consisted of 11.5% grade 1, 42.3% grade 2, and 46.2% grade 3 . The true blastocysts were 26.4% grade 1, 55.3% grade 2, and 18.3% grade 3 . Expanded blastocysts were 63.9% grade 1, 31.6% grade 2, and 4.5% grade 3 (Table S1).

Abattoir derived ovaries from dairy cattle yielded 1,084 oocytes from a total of 12 collections with an average collection of 120 oocytes. Cells were classified based on the number of blastomeres 56 hours post fertilization. On average, 17.1% of cells were not fertilized, 10.4% of zygotes developed 2 to 3 blastomeres, 25.3% developed 4 to 6 blastomeres, and 47.2% developed 6 or more blastomeres. The average cleavage rate for dairy embryos was 82.9%. Seven days after fertilization, embryos were assessed for blastocyst formation. An average of 3% of zygotes developed to the morula stage. Of the morula stage embryos identified, 21.4% were grade 1, 39.3% were grade 2, and 39.3% were grade 3. On average, 18% of zygotes developed to a blastocyst stage. Of the embryos that developed to a blastocyst stage, 25.3% were early blastocysts, 30.7% were true blastocysts, 41.2% were expanded blastocysts, 2% were hatching blastocysts, and 0.9% were hatched blastocysts. Of the early blastocysts, 22% were grade 1, 41.5% were grade 2, and 36.5% were grade 3. Identified blastocysts consisted

of 20.4% grade 1, 63% grade 2, and 16.6% grade 3. Expanded blastocysts were 54.4% grade 1, 39.2% grade 2, and 6.4% grade 3 (Table S1).

Table S1 – Abattoir derived embryo development and blastocyst rates.
The percentage of cleaved embryos was determined in respect to the total number of COCs subjected to maturation and IVF. The percentage of blastocysts was determined at day 7 of maturation in respect to the total number of COCs matured and subjected to IVF.

Beef			
Round	**Oocyte Collection**	**Cleavage Rate**	**Blastocyst Rate**
1	300	84.59%	11.99%
2	150	77.22%	21.52%
3	150	89.73%	21.92%
4	150	79.73%	31.76%
5	150	83.89%	13.42%
6	150	80.67%	13.33%
7	150	81.76%	10.14%
8	110	84.87%	28.57%
9	125	81.45%	37.10%
10	150	85.91%	38.26%
11	171	77.19%	24.56%
12	111	75.45%	19.09%
13	114	72.17%	18.26%
14	200	80.81%	33.84%
15	163	68.71%	14.11%
16	150	62.07%	20.69%
17	105	72.12%	26.92%
18	200	82.41%	27.14%
19	200	92.59%	34.92%
20	90	77.65%	12.94%
21	151	83.45%	24.14%
22	175	88.95%	18.60%
23	151	82.24%	17.11%
24	104	81.55%	35.92%
Total/Avg	3670	80.30%	23.18%

Dairy			
Round	**Oocyte Collection**	**Cleavage Rate**	**Blastocyst Rate**
1	101	72.00%	15.00%
2	51	76.47%	15.69%
3	93	85.56%	7.78%
4	78	81.33%	8.00%
5	90	83.33%	26.67%
6	73	83.33%	7.58%
7	70	87.32%	39.44%
8	102	89.90%	10.10%
9	72	87.32%	28.17%
10	125	85.37%	17.89%
11	61	81.67%	18.33%
12	108	81.37%	21.57%
Total/Avg	1024	82.91%	18.02%

Contamination

All follicular fluid samples were negative for bovine viral diarrhea virus per IDEXX snap test and PCR [20].

Various bacterial contaminants were identified in follicular fluid collected from abattoir derived beef ovaries. Bacterial contaminants identified include *Acinetobacter, Aestuariimicrobium, Arthrobacter, Bacillus, Bordetella, Burkholderia, Dermatophilus, Enterobacter, Enterococcus, Escherichia coli* (*E. coli*), *Klebsiella, Kocuria, Lactococcus, Macrococcus, Microbacterium, Mobillicoccus, Moraxella, Pectobacterium, Salmonella, Shigella,* and *Staphylococcus*. Six rounds of follicular fluid contained an unknown contaminant unidentifiable by 16S sequencing. Bacteria cultured from unwashed embryos include E. coli. Two rounds of washed embryos contained a contaminant that was unidentifiable by 16S. No bacteria were cultured from washed embryos.

Bacterial contaminants identified in follicular fluid collected from abattoir derived ovaries of dairy cattle include *Acinetobacter, Cupriavidus, Dietzia, Histophilus somni*, *Microbacterium, Mycolicbacterium, Oceanbacillus, Ralstonia, Rothia, Truperella Pyogenes,* and *Virgibacillus*. Follicular fluid from five rounds contained an unknown contaminant unidentifiable by 16S. Bacteria cultured from unwashed embryos derived from abattoir derived dairy cattle oocytes include *Actinomycetia, Dietzia,* and *Ralstonia*. No bacteria were cultured from washed embryos.

Table S2 – Bacterial contaminants cultured from beef cattle IVP embryo production.

Bacterial contaminants were cultured on brain heart infusion agar for a maximum of 5 days. Resulting colonies were picked, heat inactivated for removal from the BSL3 facility as required, and the 16S portion of the genome was amplified for identification by sequencing. Some colonies could not be heat inactivated, others did not return conclusive identification through 16S sequencing. These contaminants may be fungal in origin.

Beef			
Round	**Follicular Fluid**	**Unwashed Embryos**	**Washed Embryos**
1	Clean	Clean	Clean
2	Unknown Contaminant	Clean	Clean
3	Arthrobacter, Bordetella	Clean	Clean
4	Unknown Contaminant	Clean	Clean
5	E. Coli	Clean	Clean
6	Clean	Clean	Clean
7	E. Coli	Clean	Clean
8	Macrococcus	Clean	Clean
9	E. Coli	E. Coli	Clean
10	Lactococcus	Clean	Clean
11	E. Coli, Shigella	Clean	Clean
12	Acinetobacter	Clean	Clean
13	Mobilicoccus, Dermatophilus	Clean	Clean
14	E. Coli, Mobilicoccus, Klebsiella, Shigella, Salmonella	Clean	Clean
15	Microbacterium, Lactococcus, Kocuria	Clean	Clean
16	Aestuariimicrobium, Mobilicoccus, Burkholderia, Macrococcus	Clean	Clean
17	Macrococcus	Clean	Clean
18	Bacillus	Clean	Clean
19	Unknown Contaminant	Unknown Contaminant	Clean
20	Staphylococcus, Lactococcus, Enterococcus, Enterobacter, Pectobacterium, Klebsiella,	Clean	Clean
21	Micrococcus, Mobilicoccus, Dermatophilus	Clean	Clean
22	Moraxella	Clean	Clean
23	Unknown contaminant	Clean	Clean
24	Unknown Contaminant	Unknown Contaminant	Unknown Contaminant
25	Unknown Contaminant	Clean	Clean

Table S3 – Bacterial contaminants cultured from dairy cattle IVP embryo production.

Bacterial contaminants were cultured on brain heart infusion agar for a maximum of 5 days. Resulting colonies were picked, heat inactivated, and the 16S portion of the genome was amplified for identification by sequencing. Some colonies could not be inactivated or did not return conclusive identification; these contaminants may be fungal in origin.

Dairy			
Round	**Follicular Fluid**	**Unwashed Embryos**	**Washed Embryos**
1	Unknown Contaminant	Ralstonia	Clean
2	Unknown Contaminant	Clean	Clean
3	Unknown Contaminant	Clean	Clean
4	Dietzia, Mycolicibacterium, Mycobacterium, Ralstonia, Cupriavidus, Truperella Pyogenes	Clean	Clean
5	Truperella Pyogenes, Histophilus Somni†	Actinomycetia, Dietzia	Clean
6	Microbacterium, Virgibacillus, Oceanobacillus	Clean	Clean
7	Truperella Pyogenes†	Clean	Clean
8	Unknown Contaminant	Clean	Clean
9	Acinetobacter	Clean	Clean
10	Clean	Clean	Clean
11	Unknown Contaminant	Clean	Clean
12	Rothia	Clean	Clean

Discussion

Biosafety concerns are associated with embryos generated from abattoir derived ovaries due to lack of knowledge concerning the donor health status. Currently, washing standards established in IVD embryos are recommended for IVP embryos but have not yet been verified. To this end, follicular fluid, unwashed, and washed embryos were analyzed for bacterial contaminants. Bacterial contaminants were identified in follicular fluid from both beef and dairy ovaries. Most of the bacterial contaminants identified are ubiquitous and non-pathogenic, but opportunistically pathogenic bacterial contaminants were also identified. Interestingly, there was only one bacterial genus in common

between those identified in follicular fluid and embryos of beef cattle and dairy cattle: Acinetobacter, which clearly demonstrates bacterial diversity between environments. Nearly all bacterial contaminants were removed from embryos washed in PBS. All bacterial contaminants were removed from embryos that were washed according to IETS standards.

Two of the bacteria identified in follicular fluid were non-pathogenic in nature, including the genus *Aestuariimicrobium* and *Bacillus safensis*. *Aestuariimicrobium* is a gram-positive bacterium that was first identified from a diesel contaminated tidal flat in 2007 and is often associated with decomposition of organic materials [21]. Identification of bacteria through sequencing of the 16S region revealed the presence of bacteria within the Bacillus genus. The species of bacteria sequenced was most similar to *Bacillus safensis* or *B. pumilus*. *Bacillus safensis* is a gram-positive spore forming bacterium and was first isolated as a contaminant of a spacecraft assembly facility [23]. Both *Bacillus safensis* and *Bacillus pumilus* are relatively common bacteria that can survive even in the excrement of humans and animals as well as the gut of insects [24]. *Bacillus safensis* has no proven pathogenicity; rather, it can produce an antifungal, antibacterial, or antiviral effect in crops [25-27]. *Bacillus pumilus* is considered an opportunistic pathogen in cattle and is associated both with endometritis and mastitis [28-30]. However, *Bacillus pumilus* has also been used in combination with other similar bacteria as probiotic support of hindgut digestion in cattle [31].

The remainder of the contaminants identified in follicular fluid can be considered opportunistic pathogens. Several bacteria identified herein have previously been isolated from the environment within dairy facilities [32]. Moreover, many of the

identified bacteria are associated with clinical or subclinical mastitis [33]. Species within Acinetobacter can be isolated from bovine feces and have been detected in milk from dairy cattle with subclinical mastitis [34, 35]. These bacteria are specifically associated with persistent mastitis due to their ability to form a hardy biofilm which makes the infection difficult to treat [36, 37]. *Burkholderia multivorans* was identified in the follicular fluid of a single collection of beef follicular fluid. *Burkholderia multivorans* is often isolated from soil and water [38]. An increase in *Burkholderia* has been identified in the milk of cattle displaying clinical signs for mastitis [33]. *E. coli*, *Enterobacter, Enterococcus,* and *Klebsiella* can be found in the intestinal tract of warm-blooded animals but are also commonly isolated from contaminated soil and water [39, 40]. These bacteria are commensal within mammalian intestines but can cause infection if introduced inappropriately. In North America, coliform bacteria including *E. Coli, Enterobacter,* and *Klebsiella*, as well as *Streptococci* are most often to blame for environmentally contracted cases of mastitis in dairy cattle [41]. *E. coli* is the most common cause of mastitis worldwide [42-45]. *Enterococcus* has been shown to be a significant cause of both subclinical and clinical mastitis in cattle [46]. Species of *Enterobacter* have been associated with respiratory illness of calves in China [47]. *Kocuria* bacteria are extremely ubiquitous. As *Kocuria* is part of the normal flora of human skin [48], it is possible that this bacterium was introduced through human contamination during the IVF process. However, *Kocuria* has also been isolated from the vagina of healthy cattle in the Czech Republic [49] and has recently been associated with mastitis infections in cattle [52]. *Truperella pyogenes* and *Staphylococcus* bacteria are often found on the skin and mucous membranes of both

humans and cattle. *Truperella pyogenes* has been isolated from the rumen and reproductive tract of cattle [53, 54]. As such, *Truperella pyogenes* is closely related to mastitis and reproductive disease in cattle [55]. *Lactococcus lactis* is often used in the fermentation process of dairy products and is considered safe for consumption [56], while other species are assumed causative agents of mastitis [57]. *Lactococcus* bacterium have been detected in numerous environments including soil, water, bulk milk tanks, and milking equipment [57]. *Macrococcus* bacteria are a commensal that has been identified on the skin of cattle, raw milk, and dairy products [58-61]. These bacteria are generally regarded as safe but have recently been identified in the milk of cattle with mastitis [62]. *Microbacterium* has also been identified in the milk of cattle with mastitis and may serve as an early indicator of infection [63, 64]. *Mycolicbacteria* have been associated with mastitis and have been identified in the rumen of cattle [65, 66]. Bacterium belonging to this genus have also been identified in eutrophic water and alfalfa rhizospheres in soil contaminated with petroleum hydrocarbon [67, 68].

Other bacteria identified in the follicular fluid of cattle are associated with various diseases in cattle ranging from skin, respiratory, and reproductive tract infections. *Dermatophilus* is associated with exudative dermatitis, also known as ‘rain rot’ or ‘streptothricosis’, which occurs in both equids and bovids. *Dermatophilus* infections can also present as ‘lumpy wool disease’ or ‘strawberry foot rot’ in sheep [69]. *Cupriavidus* contains ubiquitous bacteria that has been isolated from both soil and water, among other extraneous environments [71-74]. Species of *Cupriavidus* rarely cause infection, most of which occur in immunocompromised humans, but it can cause diarrhea in cattle as well [75-78]. *Histophilus somni* is a commensal bacterium commonly found in the

upper respiratory tract and genital tracts of healthy cattle but can opportunistically lead to disease [79]. The bacteria *H. somni* is often related to bovine respiratory disease (BRD) and is considered a primary bacterial agent of such [80, 81]. However, this bacterium has also been correlated with the occurrence of suppurative vaginitis, cervicitis, and endometriosis in cattle, making its removal from embryos critical [82]. Infections with *Klebsiella* spp. can cause septicemia in calves and have been reported in association with reproductive infection and abortion in equine [83-85]. *Moraxella* spp. can be found on the skin and in the upper respiratory tract, conjunctiva, and mucous membranes of both humans and cattle [86-89]. *Moraxella* spp. are associated with outbreaks of infectious bovine keratoconjunctivitis (IBK), also known as pink eye, in cattle [90-92]. *Mycobacterium*, although famously associated with tuberculosis or paratuberculosis (Johne's disease), are commonly identified in soil, water, sediment, and the feces of infected cattle. In the case of bovine paratuberculosis, the bacterium is ingested, undergo binary fission within the rumen, and can migrate to other tissues to induce what is known as Johne's disease. More recently, species within this genus have been linked to bovine nodular thelitis, a contagious skin infection of cattle [93]. *Salmonella* is commonly identified in fecal samples from cattle herds [94-96]. These bacteria are associated with disease in cattle and can induce diarrhea, fever, anorexia, decrease milk production, and lead to abortion [97, 98]. Cattle have recently been identified as a reservoir for *Shigella* bacteria [99]. These bacteria are often found in water and fecal material and contaminate raw milk products and meat from cattle [100, 101], while causing diarrhea in the animal [102]. *Shigella* spp. have also been identified in the reproductive tract of cattle [55].

Some of the bacteria identified in follicular fluid, although considered opportunistic pathogens, have weak relationships to disease in cattle. Bacteria classified within *Arthrobacter* are extremely common in the environment. Although these bacteria are considered opportunistic pathogens, infections in immunocompromised individuals are rare [103]. Commonly found as a contaminant of bulk milk tanks [104], these bacteria are often found contributing to the spoilage of raw food products including milk, meat, and fish, among others [105]. However, bacteria in this genus also have an implicit role in the creation of fermented dairy products including yoghurt and cheese [106]. Bacteria belonging to the genus *Bordetella* were also identified herein. This genus contains opportunistic pathogens that are most often associated with respiratory illness in pigs, dogs (kennel cough), and humans (whooping cough) [107-109]. These bacteria have been found in a variety of environments including soil, water, and plants [110] Research linking *Bordetella* to disease in cattle remains sparse. The *Dietzia* genus is relatively new, with several new species being isolated in the 21st century from various sites associated with soil or water [111]. Some *Dietzia* species have found novel use as a probiotic in treating cattle with paratuberculosis or Johne's disease [112, 113]. *Dietzia* bacteria maintain the ability to cause infrequent infections in those who are immunocompromised [114-116]. *Mobilicoccus* bacteria have been detected in aerosol samples collected from areas used for cattle shelter as well as for feed treatment and collection [117]. However, this genus of bacteria remains vaguely characterized. There are currently no reports of infection with these bacteria, although closely related bacteria within the *Dermatophilus* genus are related to skin infection. *Oceanobacillus* bacteria have been identified in the rumen of cattle, soil high in salt

content, fermented food products, and even in human fecal material [118-121]. *Pectobacteria* are plant pathogens associated with soft rot in food crops and can be found in soil or water [122, 123]. These bacteria are not associated with disease in cattle. *Ralstonia* species can be found in the milk and udders of healthy cattle, with no reported cases of mastitis due to these bacteria [33, 124]. Rothia bacteria are frequently found in the upper respiratory tract of multiple species including humans, pigs, rats, and cattle [125-128]. While these bacteria are opportunistic pathogens capable of infecting the immunocompromised of multiple species, these cases are uncommon [129, 130]. *Virgibacillus* bacteria have been isolated from the rumen of cattle as well as the human gut [131, 132]. While infections due to *Virgibacillus* have not been documented, they appear to opportunistically worsen infections caused by other bacteria [133].

Bacterial contaminants identified by 16S sequencing in this study were classified most often to the level of genus per high sequence homology, to preserve confidence of identification despite the lack of confirmatory testing. In the cases of *Bacillus safensis*, *Burkholderia multivorans*, and *Truperella pyogenes*, species with the highest sequence homology were included for clarity. Contaminants listed as ‘unknown’ were not identifiable per 16S methods. It is possible that these contaminants were fungal in nature, as the 16S sequence is highly conserved in bacteria and archaea, but not in fungi. Conversely, other samples could not be proven inactivated for removal from a biosafety level (BSL) 3 facility and identification by 16S sequencing. This may be due to the formation of bacterial biofilms, which increase tolerance to methods of inactivation including heat.

Conclusions

A majority of abattoir-derived follicular fluid from both beef and dairy cattle was contaminated by bacterial and unknown contaminants. While many of the isolates were classified as contaminants or opportunistic pathogens, it is notable that pathogens of major health concern, including *Brucella abortus* and *Mycobacterium bovis*, were not identified. All samples were negative for BVDV. However, this study did not focus on other viruses and as such cannot rule them out. Multiple bacteria identified could cause disease in cattle, while others were not associated with disease. Embryos generated from abattoir-derived oocytes were mostly free of contamination following washing procedures with PBS. All embryos were rendered free of identifiable bacterial contamination by IETS recommended washing procedures including trypsin. Therefore, it is highly recommended that the IETS washing procedure be used to assure that microbial contaminants are removed from the embryos.

Methods

Ovary Collection and Follicular Fluid Inoculation

Abattoir sourced ovaries were transported to the Animal Reproduction and Biotechnology Laboratory (ARBL) at Colorado State University (CSU) in sterile saline (0.9% NaCl) at ambient temperature. Cumulus oocyte complexes (COCs) were aspirated from small, growing follicles (2-8 mm diameter) with an 18-gauge needle attached to a tubing system and vacuum pump with ~50 mmHg of pressure into two sterile 50 mL conical tubes.

Oocyte Recovery & Incubation

The COCs were collected and washed through CSU chemically defined medium for handling oocytes (HCDM-M) with 10% BSA (A-6003; Sigma) and 10 mg/mL gentamicin (G-1272; Sigma) [1, 2]. Grade 1 COCs with three or more layers of unexpanded cumulus cells and evenly granulated cytoplasm were selected for in vitro maturation. Using a 4 well dish, fifty COCs were incubated in each well containing 1 mL CSU chemically defined medium for in vitro maturation of oocytes (IVM) supplemented with 0.5% BSA and hormones (10 µg/mL estradiol 17β (E-2257; Sigma), 10 µg/mL cysteamine (M6500; Sigma), 1 µg/mL LH (USDA-LH-B-5; USDA, Beltsville, MD, USA), 1 µg/mL FSH (NIH-FSH-S17; NIH, Bethesda, MD, USA) , 1 µg/mL EGF (E-9644; Sigma)). The COCs were incubated at 38.5ºC in 5% CO2 for 23 ± 1h.

In Vitro Fertilization and Culture of Bovine Embryos

After maturation, COCs were transferred to a well in a 4 well plate containing 430 µL of CSU chemically defined medium for in vitro fertilization (FCDM) pre-equilibrated at 38.5ºC for ≥ 5h. Frozen-thawed semen was washed through a 45/90 Percoll® gradient [3] at 800g for 20 minutes. The same bull was used for all five replicates. After removal of the supernatant, semen was washed in 2 ml HCDM-1, a CSU chemically defined medium for early embryo handling and centrifuged for 5 minutes at 300g. Sperm was quantified using a hemocytometer and diluted with FCDM medium to a concentration of 5 x 106 sperm/mL. Sperm were added to each group of 50 COCs at a final concentration of 0.5 x 106 sperm/mL and co-incubated in a final volume of 500 µL FCDM at 38.5ºC in 5% CO2 for 18h.

After 18h of co-incubation, presumptive zygotes were stripped of cumulus cells using a Vortex-Genie® 2 (Scientific Industries, Inc., Bohemia, NY, USA) by transferring into a 0.6 mL Eppendorf tube with approximately 30 µL of media. After vortexing at maximum speed for 75 seconds, HCDM-1 medium was added to the tube to wash zygotes off the sides. Zygotes were washed through multiple drops until all debris was removed. Zygotes with cumulus adhered to the sides were pipetted with a stripper to remove cumulus from the zona pellucida. Once clean, 50 presumptive zygotes per well were transferred to 4-well dishes in wells of 500 µL of CSU chemically defined medium for in vitro culture of early embryos (CDM-1) in 5% CO2 5% O2, 90% N2 at 38.5°C for 56h. After 56h of culture, embryo cleavage was recorded by transferring embryos into warmed CSU chemically defined medium for embryo handling (HCDM-2) for assessment. Embryos containing ≥ 4 blastomeres were separated into groups of 35 embryos per well and transferred into 4-well dishes with wells containing 500 µL of CSU chemically defined medium for in vitro culture of late embryos (CDM-2) and cultured in 5% CO2 5% O2, 90% N2 at 38.5°C for 96h. On day 7 (156h after fertilization), embryos were assessed for blastocyst formation.

Bacterial Identification

On day 7, all embryos were assessed for blastocyst formation and snap-frozen in PBS + 30% glycerol. Samples were transferred to a BSL3 facility and thawed in a biosafety cabinet. Samples containing embryos were homogenized for 5 minutes at a rate of 25 cycles per second (Tissuelyser; Qiagen, Germantown, MD, USA). A volume of 100 µL of each sample was plated on a Brain Heart Infusion (BHI) agar plate and spread using

glass beads. The beads were then discarded, and the plates left to incubate at 37°C. Plates were incubated at 37°C for 5 days. Bacterial colony quantification and qualities were recorded daily. On the 5th day, bacterial colonies were picked and stored in PBS containing 10% glycerol. Suspended bacterial colonies were stored frozen at 4°C until inactivation. Samples were boiled at 100°C for a minimum of 10 minutes, cooled, and replated to confirm inactivation. After being rendered safe to remove from a BSL3 facility, samples were transferred to a BSL2 laboratory for DNA amplification. Samples were thawed and vortexed to ensure homogeneity. Bacterium cultured from the anthrax spore vaccine (Serial #471, Vet License No. 188), which contains B. anthracis Sterne 34F2, was used as a positive control for each round of amplification. Molecular grade water was used as a negative control. A primer mix was created by adding 10µL of 100µM forward and reverse primer, each, to 80µL of 10mM TRIS + HCl at a pH of 8.0. The forward primer (27F) contained the sequence: 5'-AGA-GTT-TGA-TCM-TGG-CTC-AG-3', where M can be either adenine or cytosine (Integrated DNA Technologies, Coralville, IA, USA). The reverse primer (1492R) contained the sequence: 5'-TAC-GGY-TAC-CTT-GTT-ACG-ACT-T-3', where Y can be either cytosine or thymine (Integrated DNA Technologies, Coralville, IA, USA). Each PCR tube contained 1µL of the designated sample, 22.5 µL of PCR Supermix (cat # 10572014, Thermo Fisher Scientific, Waltham, MA, USA), 0.5 µL of the primer mix, and 1µL of molecular grade water. Samples were first heated to 94°C and held for 2 minutes prior to 30 cycles of denaturation at 94°C for 15 seconds, primer annealing at 48°C for 30 seconds, and an extension at 72°C for 90 seconds, before holding at 4°C infinitely. Gel electrophoresis was performed on an ethidium bromide (EtBr) gel with a 1kb ladder and visualized using

a Bio-Rad ChemiDoc XRS+ System (Hercules, CA, USA) to confirm the presence of intact, non-degraded DNA. Amplified samples were then mixed with 8μL of ExoSAP-IT (cat #78200.200.UL, Thermo Fisher Scientific, Waltham, MA, USA). Samples containing ExoSAP-IT were run through a single cycle of 37°C for 15 minutes and 80°C for 15 minutes before being cooled to 4°C and held indefinitely. Concentrations of DNA were measured using a Nanodrop spectrophotometer (Thermo Fisher, Waltham, MA, USA). Samples were diluted to an approximate concentration of 30ng in 10μL, as specified by GeneWiz (Azenta, Burlington, MA, US). Following submission to GeneWiz and sequencing, sample DNA sequences were identified to the genus level using BLAST® (National Center for Biotechnology Information, Bethesda, MD, USA).

References

1. Ricci, S., et al., Impact of asymptomatic genital tract infections on in vitro Fertilization (IVF) outcome. PLoS One, 2018. 13(11): p. e0207684.
2. Cottell, E., et al., Microbial contamination in an in vitro fertilization-embryo transfer system. Fertil Steril, 1996. 66(5): p. 776-80.
3. Stsepetova, J., et al., The complex microbiome from native semen to embryo culture environment in human in vitro fertilization procedure. Reprod Biol Endocrinol, 2020. 18(1): p. 3.
4. Cottell, E., et al., Are seminal fluid microorganisms of significance or merely contaminants? Fertil Steril, 2000. 74(3): p. 465-70.
5. Pelzer, E.S., et al., Microbial colonization of follicular fluid: alterations in cytokine expression and adverse assisted reproduction technology outcomes. Hum Reprod, 2011. 26(7): p. 1799-812.
6. Pelzer, E.S., et al., Microorganisms within human follicular fluid: effects on IVF. PLoS One, 2013. 8(3): p. e59062.
7. Salary, A., et al., Detection of bacteria in bovine ovarian follicular fluid. Lett Appl Microbiol, 2020. 70(3): p. 137-142.
8. Bertrand, E., et al., Presence of HIV-1 in follicular fluids, flushes and cumulus oophorus cells of HIV-1-seropositive women during assisted-reproduction technology. AIDS, 2004. 18(5): p. 823-5.
9. Devaux, A., et al., Hepatitis C virus detection in follicular fluid and culture media from HCV+ women, and viral risk during IVF procedures. Hum Reprod, 2003. 18(11): p. 2342-9.
10. Bielanski, A., T. Sapp, and C. Lutze-Wallace, Association of bovine embryos produced by in vitro fertilization with a noncytopathic strain of bovine viral diarrhea virus type II. Theriogenology, 1998. 49(6): p. 1231-8.
11. Bielanski, A. and C. Dubuc, In vitro fertilization and culture of ova from heifers infected with bovine herpesvirus-1 (BHV-1). Theriogenology, 1994. 41(6): p. 1211-7.
12. Singh, E.L., Disease control : procedures for handling embryos. Rev Sci Tech, 1985. 4(4): p. 867-872.
13. Stringfellow, D.A., Rubessa, M., Perry, G., Lazzari, G., Krisher, R., Galli, C., Recommendations for sanitary handling of oocytes and embryos. 5th ed. International Embryo Technology Society Manual, ed. S. Leelawardana, Perry, G. Vol. 1. 2023.
14. Singh, E.L. and F.C. Thomas, Embryo transfer as a means of controlling the transmission of viral infections. XI. The in vitro exposure of bovine and porcine embryos to vesicular stomatitis virus. Theriogenology, 1987. 28(5): p. 691-7.
15. Singh, E.L., et al., Embryo transfer as a means of controlling the transmission of viral infections. I. The in vitro exposure of preimplantation bovine embryos to akabane, bluetongue and bovine viral diarrhea viruses. Theriogenology, 1982. 17(4): p. 437-44.
16. Lalonde, A. and A. Bielanski, Efficacy of the International Embryo Transfer Society (IETS) washing procedure for rendering oocytes matured in vitro free of bovine viral diarrhea virus (BVDV). Theriogenology, 2011. 76(2): p. 261-6.

17. D'Angelo, M., et al., Evaluation of trypsin treatment on the inactivation of bovine herpesvirus type 1 on in vitro produced pre-implantation embryos. Reprod Domest Anim, 2009. 44(3): p. 536-9.
18. Bielanski, A., et al., The efficacy of trypsin for disinfection of in vitro fertilized bovine embryos exposed to bovine herpesvirus 1. Anim Reprod Sci, 1997. 47(1-2): p. 1-8.
19. Gard, J.A., et al., Bovine viral diarrhea virus (BVDV) associated with single in vivo-derived and in vitro-produced preimplantation bovine embryos following artificial exposure. Theriogenology, 2009. 71(8): p. 1238-44.
20. Monteiro, F.L., et al., Detection of bovine pestiviruses in sera of beef calves by a RT-PCR based on a newly designed set of pan-bovine pestivirus primers. J Vet Diagn Invest, 2019. 31(2): p. 255-258.
21. Jung, S.Y., et al., Aestuariimicrobium kwangyangense gen. nov., sp. nov., an LL-diaminopimelic acid-containing bacterium isolated from tidal flat sediment. Int J Syst Evol Microbiol, 2007. 57(Pt 9): p. 2114-2118.
22. Branquinho, R., et al., Differentiation of Bacillus pumilus and Bacillus safensis using MALDI-TOF-MS. PLoS One, 2014. 9(10): p. e110127.
23. Satomi, M., M.T. La Duc, and K. Venkateswaran, Bacillus safensis sp. nov., isolated from spacecraft and assembly-facility surfaces. Int J Syst Evol Microbiol, 2006. 56(Pt 8): p. 1735-1740.
24. Branquinho, R., et al., Phylogenetic and clonality analysis of Bacillus pumilus isolates uncovered a highly heterogeneous population of different closely related species and clones. FEMS Microbiol Ecol, 2014. 90(3): p. 689-98.
25. Berrada I., B.O., Swings J., Bendaou N. & Amar M. , Selection of halophilic bacteria for biological control of tomato gray mould caused by Botrytis cinerea. Phytopathologia Mediterranea 2012(51): p. 625-630.
26. Sun H., H.Y., Xiao Q., Ye R. & Tian Y., Isolation, characterization, and antimicrobial activity of endophytic bacteria from Polygonum cuspidatum. African Journal of Microbiology Research 2013(7): p. 1496-1504.
27. Weisskopf, L., The potential of bacterial volatiles for crop protection against phytophathogenic fungi. Microbial Pathogens and Strategies for Combating Them: Science, Technology, and Education, 2013: p. 1352-1363.
28. Nieminen, T., et al., Toxinogenic Bacillus pumilus and Bacillus licheniformis from mastitic milk. Vet Microbiol, 2007. 124(3-4): p. 329-39.
29. Ballas, P., et al., Characterization of Bacillus pumilus Strains Isolated from Bovine Uteri. Animals (Basel), 2023. 13(8).
30. Gartner, M.A., et al., Increased mRNA expression of selected pro-inflammatory factors in inflamed bovine endometrium in vivo as well as in endometrial epithelial cells exposed to Bacillus pumilus in vitro. Reprod Fertil Dev, 2016. 28(7): p. 982-994.
31. Fuerniss, L.K., et al., Cecal microbiota of feedlot cattle fed a four-species Bacillus supplement. J Anim Sci, 2022. 100(10).
32. Rodrigues, N.M., et al., The Matrix-Assisted Laser Desorption Ionization-Time of Flight Mass Spectrometry (MALDI-TOF MS) identification versus biochemical tests: a study with enterobacteria from a dairy cattle environment. Braz J Microbiol, 2017. 48(1): p. 132-138.

33. Kuehn, J.S., et al., Bacterial community profiling of milk samples as a means to understand culture-negative bovine clinical mastitis. PLoS One, 2013. 8(4): p. e61959.
34. Shestivska, V., et al., Proposal of Acinetobacter thermotolerans sp. nov. to accommodate bovine feces-dwelling bacteria growing at 47 degrees C. Syst Appl Microbiol, 2024. 47(6): p. 126560.
35. Chen, Q., et al., Four novel Acinetobacter lwoffii strains isolated from the milk of cows in China with subclinical mastitis. BMC Vet Res, 2024. 20(1): p. 274.
36. Avery, T.M., et al., Analysis of Antimicrobial and Antibiofilm Activity of Human Milk Lactoferrin Compared to Bovine Lactoferrin against Multidrug Resistant and Susceptible Acinetobacter baumannii Clinical Isolates. ACS Infect Dis, 2021. 7(8): p. 2116-2126.
37. Ma, C., et al., Effect of baicalin on eradicating biofilms of bovine milk derived Acinetobacter lwoffii. BMC Vet Res, 2024. 20(1): p. 212.
38. Lipuma, J.J., Update on the Burkholderia cepacia complex. Curr Opin Pulm Med, 2005. 11(6): p. 528-33.
39. Smith, H.W., Observations on the Flora of the Alimentary Tract of Animals and Factors Affecting Its Composition. J Pathol Bacteriol, 1965. 89: p. 95-122.
40. Rosebury, T., D. Gale, and D.F. Taylor, An approach to the study of interactive phenomena among microorganisms indigenous to man. J Bacteriol, 1954. 67(2): p. 135-52.
41. Hogan, J. and K.L. Smith, Managing environmental mastitis. Vet Clin North Am Food Anim Pract, 2012. 28(2): p. 217-24.
42. Gao, J., et al., Incidence of clinical mastitis and distribution of pathogens on large Chinese dairy farms. J Dairy Sci, 2017. 100(6): p. 4797-4806.
43. Blum, S.E., et al., Comparison of the immune responses associated with experimental bovine mastitis caused by different strains of Escherichia coli. J Dairy Res, 2017. 84(2): p. 190-197.
44. Shpigel, N.Y., S. Elazar, and I. Rosenshine, Mammary pathogenic Escherichia coli. Curr Opin Microbiol, 2008. 11(1): p. 60-5.
45. Acres, S.D., Enterotoxigenic Escherichia coli infections in newborn calves: a review. J Dairy Sci, 1985. 68(1): p. 229-56.
46. Gao, X., et al., Enterococcal isolates from bovine subclinical and clinical mastitis: Antimicrobial resistance and integron-gene cassette distribution. Microb Pathog, 2019. 129: p. 82-87.
47. Wang, Z., et al., First report of Enterobacter hormaechei with respiratory disease in calves. BMC Vet Res, 2020. 16(1): p. 1.
48. Szczerba, I., [Occurrence and number of bacteria from the Micrococcus, Kocuria, Nesterenkonia, Kytococcus and Dermacoccus genera on skin and mucous membranes in humans]. Med Dosw Mikrobiol, 2003. 55(1): p. 67-74.
49. Stykova, E., et al., Bovine vaginal strain Kocuria kristinae and its characterization. Folia Microbiol (Praha), 2016. 61(3): p. 243-8.
50. Stackebrandt, E., et al., Taxonomic dissection of the genus Micrococcus: Kocuria gen. nov., Nesterenkonia gen. nov., Kytococcus gen. nov., Dermacoccus gen. nov., and Micrococcus Cohn 1872 gen. emend. Int J Syst Bacteriol, 1995. 45(4): p. 682-92.

51. Savini, V., et al., Drug sensitivity and clinical impact of members of the genus Kocuria. J Med Microbiol, 2010. 59(Pt 12): p. 1395-1402.
52. Kenar, B., The New Mastitis Agents Emergend in Cattle in Turkey and An Investigation of Their Antimicrobial Susceptibility. Kocatepe Veterinary Journal 2019.
53. Narayanan, S., et al., Biochemical and ribotypic comparison of Actinomyces pyogenes and A pyogenes-like organisms from liver abscesses, ruminal wall, and ruminal contents of cattle. Am J Vet Res, 1998. 59(3): p. 271-6.
54. Silva, E., et al., Genomic characterization of Arcanobacterium pyogenes isolates recovered from the uterus of dairy cows with normal puerperium or clinical metritis. Vet Microbiol, 2008. 132(1-2): p. 111-8.
55. Pascottini, O.B., et al., Dynamics of uterine microbiota in postpartum dairy cows with clinical or subclinical endometritis. Sci Rep, 2020. 10(1): p. 12353.
56. Casalta, E. and M.C. Montel, Safety assessment of dairy microorganisms: the Lactococcus genus. Int J Food Microbiol, 2008. 126(3): p. 271-3.
57. Rodrigues, M.X., et al., The Lactococcus genus as a potential emerging mastitis pathogen group: A report on an outbreak investigation. J Dairy Sci, 2016. 99(12): p. 9864-9874.
58. Randazzo, C.L., et al., Diversity, dynamics, and activity of bacterial communities during production of an artisanal Sicilian cheese as evaluated by 16S rRNA analysis. Appl Environ Microbiol, 2002. 68(4): p. 1882-92.
59. Giannino, M.L., et al., Study of microbial diversity in raw milk and fresh curd used for Fontina cheese production by culture-independent methods. Int J Food Microbiol, 2009. 130(3): p. 188-95.
60. Fontana, C., et al., Surface microbiota analysis of Taleggio, Gorgonzola, Casera, Scimudin and Formaggio di Fossa Italian cheeses. Int J Food Microbiol, 2010. 138(3): p. 205-11.
61. Kloos, W.E., et al., Delimiting the genus Staphylococcus through description of Macrococcus caseolyticus gen. nov., comb. nov. and Macrococcus equipercicus sp. nov., and Macrococcus bovicus sp. no. and Macrococcus carouselicus sp. nov. Int J Syst Bacteriol, 1998. 48 Pt 3: p. 859-77.
62. Schwendener, S., K. Cotting, and V. Perreten, Novel methicillin resistance gene mecD in clinical Macrococcus caseolyticus strains from bovine and canine sources. Sci Rep, 2017. 7: p. 43797.
63. Watts, J.L., et al., Identification of corynebacterium bovis and other coryneforms isolated from bovine mammary glands. J Dairy Sci, 2000. 83(10): p. 2373-9.
64. Gryaznova, M.V., et al., Microbiota of Cow's Milk with Udder Pathologies. Microorganisms, 2021. 9(9).
65. Peraza, P., et al., Exploring the Linkage Between Ruminal Microbial Communities on Postweaning and Finishing Diets and Their Relation to Residual Feed Intake in Beef Cattle. Microorganisms, 2024. 12(12).
66. Supre, K., et al., Short communication: Mycolicibacterium smegmatis, basonym Mycobacterium smegmatis, causing pyogranulomatous mastitis and its cross-reactivity in bovine (para)tuberculosis testing. J Dairy Sci, 2019. 102(9): p. 8405-8409.

67. Golubev, S.N., et al., Mycolicibacterium sp. strain PAM1, an alfalfa rhizosphere dweller, catabolizes PAHs and promotes partner-plant growth. Microbiol Res, 2021. 253: p. 126885.
68. Xiao, Y., et al., Mycolicibacterium lacusdiani sp. nov., an Attached Bacterium of Microcystis aeruginosa. Front Microbiol, 2022. 13: p. 861291.
69. Zaria, L.T., Dermatophilus congolensis infection (Dermatophilosis) in animals and man! An update. Comp Immunol Microbiol Infect Dis, 1993. 16(3): p. 179-222.
70. Abu-Samra, M.T., The epizootiology of Dermatophilus congolensis infection. Rev Elev Med Vet Pays Trop, 1980. 33(1): p. 23-32.
71. Watanabe, T., et al., Draft Genome Sequence of Cupriavidus pauculus Strain KF709, a Biphenyl-Utilizing Bacterium Isolated from Biphenyl-Contaminated Soil. Genome Announc, 2015. 3(2).
72. Oie, S., et al., Microbial contamination of nebulization solution and its measures. Biol Pharm Bull, 2006. 29(3): p. 503-7.
73. Manaia, C.M., et al., Heterotrophic plate counts and the isolation of bacteria from mineral waters on selective and enrichment media. J Appl Bacteriol, 1990. 69(6): p. 871-6.
74. Wyndham, R.C., et al., Distribution of the catabolic transposon Tn5271 in a groundwater bioremediation system. Appl Environ Microbiol, 1994. 60(1): p. 86-93.
75. Coenye, T., et al., Use of PCR analyses to define the distribution of Ralstonia species recovered from patients with cystic fibrosis. J Clin Microbiol, 2005. 43(7): p. 3463-6.
76. D'Inzeo, T., et al., Catheter-related bacteremia by Cupriavidus metallidurans. Diagn Microbiol Infect Dis, 2015. 81(1): p. 9-12.
77. Karafin, M., et al., Fatal infection caused by Cupriavidus gilardii in a child with aplastic anemia. J Clin Microbiol, 2010. 48(3): p. 1005-7.
78. Papageorgiou, K., et al., First detection of Cupriavidus gilardii in a bovine neonatal diarrhea outbreak. BMC Vet Res, 2024. 20(1): p. 345.
79. Siddaramppa, S. and T.J. Inzana, Haemophilus somnus virulence factors and resistance to host immunity. Anim Health Res Rev, 2004. 5(1): p. 79-93.
80. Angen, O., et al., Proposal of Histophilus somni gen. nov., sp. nov. for the three species incertae sedis 'Haemophilus somnus', 'Haemophilus agni' and 'Histophilus ovis'. Int J Syst Evol Microbiol, 2003. 53(Pt 5): p. 1449-1456.
81. Cirone, F., et al., Prevalence of Pathogens Related to Bovine Respiratory Disease Before and After Transportation in Beef Steers: Preliminary Results. Animals (Basel), 2019. 9(12).
82. Szenci, O., et al., Co-infection with Bovine Herpesvirus 4 and Histophilus somni Significantly Extends the Service Period in Dairy Cattle with Purulent Vaginal Discharge. Reprod Domest Anim, 2016. 51(1): p. 143-9.
83. Szeredi, L., S. Janosi, and M. Tenk, Klebsiella oxytoca as a cause of equine abortion--short communication. Acta Vet Hung, 2008. 56(2): p. 215-20.
84. Fecteau, G., B.P. Smith, and L.W. George, Septicemia and meningitis in the newborn calf. Vet Clin North Am Food Anim Pract, 2009. 25(1): p. 195-208, vii-viii.

85. Roy, M.F., Sepsis in adults and foals. Vet Clin North Am Equine Pract, 2004. 20(1): p. 41-61.
86. Bovre, K., Oxidase positive bacteria in the human nose incidence and species distribution, as diagnosed by genetic transformation. Acta Pathol Microbiol Scand B Microbiol Immunol, 1970. 78(6): p. 780-4.
87. Berger, U. and E. Falsen, [Distribution of species of Moraxella and moraxella-like organisms in the nasopharynx of healthy human adults (author's transl]. Med Microbiol Immunol, 1976. 162(3-4): p. 239-49.
88. Han, X.Y. and J.J. Tarrand, Moraxella osloensis blood and catheter infections during anticancer chemotherapy: clinical and microbiologic studies of 10 cases. Am J Clin Pathol, 2004. 121(4): p. 581-7.
89. Barber, D.M., G.E. Jones, and A. Wood, Microbial flora of the eyes of cattle. Vet Rec, 1986. 118(8): p. 204-6.
90. Angelos, J.A., et al., Moraxella bovoculi sp. nov., isolated from calves with infectious bovine keratoconjunctivitis. Int J Syst Evol Microbiol, 2007. 57(Pt 4): p. 789-795.
91. Henson, J.B. and L.C. Grumbles, Infectious bovine keratoconjunctivitis. I. Etiology. Am J Vet Res, 1960. 21: p. 761-6.
92. Angelos, J.A., Infectious bovine keratoconjunctivitis (pinkeye). Vet Clin North Am Food Anim Pract, 2015. 31(1): p. 61-79, v-vi.
93. Pin, D., et al., Mycobacterium species related to M. leprae and M. lepromatosis from cows with bovine nodular thelitis. Emerg Infect Dis, 2014. 20(12): p. 2111-4.
94. 1996., U.S.D.o.A.U.U.-A.-U.-C.F.C.C., E.coli O157:H7 and Salmonella status on dairy farms.
95. 2007., U.S.D.o.A.U.U.-A.-U.-C.F.C.C., Salmonella, listeria and campylobacter on US dairy operations, 1996-2007.
96. Cummings, K.J., et al., The incidence of salmonellosis among dairy herds in the northeastern United States. J Dairy Sci, 2009. 92(8): p. 3766-74.
97. Hinton, M., Salmonella dublin abortion in cattle: preliminary observations on the serological response. Vet Rec, 1971. 88(18): p. 481.
98. Pender, A.B., Salmonellosis in a herd of beef cows. Can Vet J, 2003. 44(4): p. 319-20.
99. Liang, J., et al., Evolutionary and genomic insights into the long-term colonization of Shigella flexneri in animals. Emerg Microbes Infect, 2022. 11(1): p. 2069-2079.
100. Elkenany, R., et al., Characterization of multi-resistant Shigella species isolated from raw cow milk and milk products. J Vet Med Sci, 2022. 84(7): p. 890-897.
101. Chen, K.T., C.J. Chen, and J.P. Chiu, A school waterborne outbreak involving both Shigella sonnei and Entamoeba histolytica. J Environ Health, 2001. 64(4): p. 9-13, 26.
102. Zhu, Z., et al., Virulence factors and molecular characteristics of Shigella flexneri isolated from calves with diarrhea. BMC Microbiol, 2021. 21(1): p. 214.
103. Li, S.Y., et al., Arthrobacter woluwensis Bacteremia: A Clinical and Genomic Report. Pathogens, 2021. 10(4).
104. Rodrigues, M.X., et al., The microbiome of bulk tank milk: Characterization and associations with somatic cell count and bacterial count. J Dairy Sci, 2017. 100(4): p. 2536-2552.

105. Wauters, G., et al., Identification of Arthrobacter oxydans, Arthrobacter luteolus sp. nov., and Arthrobacter albus sp. nov., isolated from human clinical specimens. J Clin Microbiol, 2000. 38(6): p. 2412-5.
106. Sutthiwong, N., S. Lekavat, and L. Dufosse, Involvement of Versatile Bacteria Belonging to the Genus Arthrobacter in Milk and Dairy Products. Foods, 2023. 12(6).
107. Schulz, B.S., et al., Detection of respiratory viruses and Bordetella bronchiseptica in dogs with acute respiratory tract infections. Vet J, 2014. 201(3): p. 365-9.
108. Zhao, Z., et al., The occurrence of Bordetella bronchiseptica in pigs with clinical respiratory disease. Vet J, 2011. 188(3): p. 337-40.
109. Chomel, B.B., Emerging and Re-Emerging Zoonoses of Dogs and Cats. Animals (Basel), 2014. 4(3): p. 434-45.
110. Hamidou Soumana, I., B. Linz, and E.T. Harvill, Environmental Origin of the Genus Bordetella. Front Microbiol, 2017. 8: p. 28.
111. Koerner, R.J., M. Goodfellow, and A.L. Jones, The genus Dietzia: a new home for some known and emerging opportunist pathogens. FEMS Immunol Med Microbiol, 2009. 55(3): p. 296-305.
112. Click, R.E. and C.L. Van Kampen, Assessment of Dietzia subsp. C79793-74 for treatment of cattle with evidence of paratuberculosis. Virulence, 2010. 1(3): p. 145-55.
113. Click, R.E., Successful treatment of asymptomatic or clinically terminal bovine Mycobacterium avium subspecies paratuberculosis infection (Johne's disease) with the bacterium Dietzia used as a probiotic alone or in combination with dexamethasone: Adaption to chronic human diarrheal diseases. Virulence, 2011. 2(2): p. 131-43.
114. Pilares, L., et al., Identification of atypical Rhodococcus-like clinical isolates as Dietzia spp. by 16S rRNA gene sequencing. J Clin Microbiol, 2010. 48(5): p. 1904-7.
115. Brown, W.D., et al., Dietzia cinnamea: An increasingly recognized human pathogen. IDCases, 2022. 29: p. e01539.
116. Pidoux, O., et al., Molecular identification of a Dietzia maris hip prosthesis infection isolate. J Clin Microbiol, 2001. 39(7): p. 2634-6.
117. Riccardi, C., et al., Comparison of analytical approaches for identifying airborne microorganisms in a livestock facility. Sci Total Environ, 2021. 783: p. 147044.
118. Long, X., et al., Oceanobacillus damuensis sp. nov. and Oceanobacillus rekensis sp. nov., isolated from saline alkali soil samples. Antonie Van Leeuwenhoek, 2015. 108(3): p. 731-9.
119. Whon, T.W., et al., Oceanobacillus kimchii sp. nov. isolated from a traditional Korean fermented food. J Microbiol, 2010. 48(6): p. 862-6.
120. Lagier, J.C., et al., Genome sequence of Oceanobacillus picturae strain S1, an halophilic bacterium first isolated in human gut. Stand Genomic Sci, 2015. 10: p. 91.
121. Gao, Z., et al., Alfalfa hay substitution for wheat straw improves beef quality via rumen microflora alteration. Heliyon, 2023. 9(10): p. e20803.
122. Pedron, J., et al., Pectobacterium aquaticum sp. nov., isolated from waterways. Int J Syst Evol Microbiol, 2019. 69(3): p. 745-751.

123. Zoledowska, S., et al., Population Structure and Biodiversity of Pectobacterium parmentieri Isolated from Potato Fields in Temperate Climate. Plant Dis, 2018. 102(1): p. 154-164.
124. Delbes, C., L. Ali-Mandjee, and M.C. Montel, Monitoring bacterial communities in raw milk and cheese by culture-dependent and -independent 16S rRNA gene-based analyses. Appl Environ Microbiol, 2007. 73(6): p. 1882-91.
125. Holman, D.B., E. Timsit, and T.W. Alexander, The nasopharyngeal microbiota of feedlot cattle. Sci Rep, 2015. 5: p. 15557.
126. Manrique, P., et al., Perturbation of the indigenous rat oral microbiome by ciprofloxacin dosing. Mol Oral Microbiol, 2013. 28(5): p. 404-14.
127. Wilbert, S.A., J.L. Mark Welch, and G.G. Borisy, Spatial Ecology of the Human Tongue Dorsum Microbiome. Cell Rep, 2020. 30(12): p. 4003-4015 e3.
128. Lowe, B.A., et al., Microbial communities in the tonsils of healthy pigs. Vet Microbiol, 2011. 147(3-4): p. 346-57.
129. Haddad, S., et al., Native valve endocarditis complicated by abscess formation caused by Rothia mucilaginosa. IDCases, 2021. 26: p. e01348.
130. Zhang, J., et al., Rothia nasimurium as a Cause of Disease: First Isolation from Farmed Chickens. Vet Sci, 2022. 9(12).
131. Seck, E., et al., Virgibacillus senegalensis sp. nov., a new moderately halophilic bacterium isolated from human gut. New Microbes New Infect, 2015. 8: p. 116-26.
132. Lima, F.S., et al., Prepartum and postpartum rumen fluid microbiomes: characterization and correlation with production traits in dairy cows. Appl Environ Microbiol, 2015. 81(4): p. 1327-37.
133. Galaviz-Silva, L., J.M. Iracheta-Villarreal, and Z.J. Molina-Garza, Bacillus and Virgibacillus strains isolated from three Mexican coasts antagonize Staphylococcus aureus and Vibrio parahaemolyticus. FEMS Microbiol Lett, 2018. 365(19).

Table of Abbreviations

Acronym	Expanded
ABCA2	ATP binding cassette subfamily A member 2
ABCA9	ATP binding cassette subfamily A member 9
ACK	Ammonium-chloride-potassium
ADCY	Adenylate cyclase
ALPL	Alkaline phosphatase, biomineralization associated
AMP	Adenosine monophosphate
ANXA2	Annexin A2
APC	Antigen presenting cell
ARBL	Animal Reproduction and Biotechnology Laboratory
ARDEC	Agricultural Research, Development, and Education Center
ARHGEF18	Rho/Rac guanine nucleotide exchange factor 18
ASZ1	Ankyrin repeat, SAM and basic leucine zipper domain containing 1
ATP12A	ATPase H+/K+ transporting non-gastric alpha 2 subunit
AURKB	Aurora kinase b
BACH2	BTB domain and CNC homolog 2
BAM	Binary alignment map
BAS	Basophil
BCKDK	Branched chain alpha ketoacid dehydrogenase complex
BCL11b	BCL11 transcription factor B
BCOR	BCL6 corepressor
BDNF	Brain derived neurotrophic factor
BMPR1A	Bone morphogenic protein receptor type 1A
BOC	BOC cell adhesion associated, oncogene regulated
BRD	Bovine respiratory disease
BREH1	Retinyl ester hydrolase type 1
BT	Bovine turbinate
BVDV	Bovine viral diarrhea virus
C	Capsid
C1r	Complement C1r
C2	Complement 2
C8	Complement 8
CA5A	Carbonic anhydrase 5A
CACNG1	Voltage dependent calcium channel gamma 1
CALM1	Calmodulin 1
Cas9	CRISPR-associated protein 9
CASP4	Caspase 4
CASZ1	Castor zinc finger 1
CBC	Complete blood count
CBFA2T3	CBFA2/RUNX1 partner transcriptional corepressor 3
CD	Cluster of differentiation
CDKN1C	Cyclin dependent kinase inhibitor 1C

CELA3B	Chymotrypsin like elastase 3B
COL4A	Collagen type 4 alpha chain
CP	Cytopathic
CpG	Cytosine-phosphate-guanine
CREB	cAMP response element-binding protein
CRISPR	Clustered regularly interspaced short palindromic repeats
CSFV	Classical swine fever virus
CSU	Colorado State University
CTL	Cytotoxic T lymphocyte
CXCL	Chemokine ligand
CXCR	Chemokine receptor
DAG	Diacylglycerol
DC	Dendritic cell
DDIT3	DNA damage inducible transcript 3
DDX58	RNA sensor RIG-I
DICER1	DICER1, ribonuclease III
DMR	Differentially methylated region
DNA	Deoxyribonucleic acid
DNMT	DNA methyltransferase
DOHAD	Developmental origin of health and disease
DPBS	Dulbecco’s phosphate buffered saline
DPP6	Dipeptidyl peptidase like 6
DTX2	Deltex E3 ubiquitin ligase 2
E	Envelope
ECE1	Endothelin converting enzyme 1
EFNA2	Ephrin A2
EFNA5	Ephrin A5
EGLN2	Egl-9 family hypoxia inducible factor 2
EIF2S2	Eukaryotic translation initiation factor 2 subunit 2
ELISA	Enzyme-linked immunosorbent assay
EMH	Extramedullary hematopoiesis
EOS	Eosinophil
EPHB1	EPH receptor B1
EZR	Ezrin
FACS	Fluorescence-activated cell sorting
FAM20C	FAM20C Golgi associated secretory pathway kinase
FBS	Fetal bovine serum
FDR	False discovery rate
FGF	Fibroblast growth factor
FGFR	Fibroblast growth factor receptor
FOXC1	Forkhead box C1
FOXS1	Forehead box S1
GATA3	GATA binding protein 3
GATD3	Glutamine amidotransferase class 1 domain containing 3
GBP4	Guanylate binding protein 4

GBP4	Guanylate binding protein 4
GEO	Gene Expression Omnibus
GFIC	Global Food and Innovation Center
GLI1	Glioma associated oncogene homolog 1
GP6	Glycoprotein 6
GP9	Glycoprotein 9
GSN	Gelsolin
GSTK1	Glutathione S-transferase kappa 1
HCT	Hematocrit
HGB	Hemoglobin
HIV	Human immunodeficiency virus
HNRNPLL	Heterogeneous nuclear ribonucleoprotein L like
IFI	Interferon inducible protein
IFN	Interferon
IGF2R	Insulin like growth factor 2 receptor
IGSF22	Immunoglobulin superfamily member 22
IHC	Immunohistochemistry
IL	Interleukin
INHBA	Inhibin subunit Beta A
INPP5A	Inositol polyphosphate-5-phosphatase A
IPA	Ingenuity pathway analysis
IRF	Interferon regulatory factor
ISG	Interferon stimulated gene
JNK	c-Jun N-terminal kinase
KCNA1	Potassium voltage gated channel subfamily A member 1
KCNB1	Potassium voltage gated channel subfamily B member 1
KCNQ1	Potassium voltage gated channel subfamily Q member 1
KIF1B	Kinesin family member 1B
KIFC3	Kinesin family member C3
KLF	KLF transcription factor
KV	Killed vaccine
L1CAM	L1 cell adhesion molecule
LAMP2	Lysosome associated membrane glycoprotein 2
LIF	Leukemia inhibitory factor
LOC101904842	Uncharacterized LOC101904842
LOC101906717	Zinc finger protein 182
LOC101907140	Uncharacterized LOC101907140
LOC104972957	KH domain containing 1
LOC104974744	Uncharacterized LOC104974744
LOC104976302	Uncharacterized LOC104976302
LOC107131765	Uncharacterized LOC107131765
LOC107131849	Uncharacterized LOC107131849
LOC107131849	Uncharacterized LOC107131849
LOC107131967	Uncharacterized LOC107131967

LOC112443431	Uncharacterized LOC112443431
LOC112443852	Uncharacterized LOC112443852
LOC112444767	Uncharacterized LOC112444767
LOC112444931	Uncharacterized LOC112444931
LOC112444931	Uncharacterized LOC112444931
LOC112447841	Uncharacterized LOC112447841
LOC112448077	Uncharacterized LOC112448077
LOC112448161	Small nucleaolar RNA SNORA70
LOC112448374	U6 spliceosomal RNA
LOC112448374	U6 spliceosomal RNA
LOC1124485325	Uncharacterized LOC1124485325
LOC112449090	Uncharacterized LOC112449090
LOC112449328	Uncharacterized LOC112449328
LOC112449328	Uncharacterized LOC112449328
LOC112449597	Uncharacterized LOC112449597
LOC520626	Myeloid associated differentiation marker
LOC522763	Uncharacterized LOC522763
LOC613282	Beta galactosidase 1 like protein 2
LPL	Lipoprotein lipase
LRIG1	Leucine rich repeats and immunoglobulin like domains 1
LYM	Lymphocyte
MADIL1	Mitotic arrest deficient 1 like 1
MAFB	MAF BZIP transcription factor B
MAFK	MAF BZIP Transcription factor K
MAN2B1	Mannosidase alpha class 2B member 2
MAVS	Mitochondrial antiviral signaling protein
MCF2L	MCF.2 Cell line derived transforming sequencing like
MCH	Mean corpuscular hemoglobin
MCHC	Mean corpuscular hemoglobin concentration
MCM4	Minichromosome maintenance complex component 4
MD	Mucosal disease
MDA5	Melanoma differentiation-associated protein 5
MDBK	Madin-Darby bovine kidney
MEF2A	Myocyte enhancer factor 2A
Meth.diff	Methylation difference
MHC	Major histocompatibility complex
MIF	Macrophage migration inhibitor factor
ML	Machine learning
MLV	Modified live vaccine
MMP9	Matrix metalloproteinase 9
MOA	Months of age
MONO	Monocyte
MPEG1	Macrophage expressed 1
MPV	Mean platelet volume
MUC2	Mucin 2

MX1	MX dynamin like GTPase 1
MX1	MX Dynamin Like GTPase 1
MYBPC3	Myosin binding protein C3
MYE	Myeloid
NCBI	National Center for Biotechnology Information
NCP	Non-cytopathic
NDOR1	NADPH dependent diflavin oxidoreductase 1
NEDD4L	NEDD4 like E3 ubiquitin protein ligase
NEK7	NIMA related kinase 7
NEU	Neutrophil
NFAT	Nuclear factor of activated T cells
NFκB	Nuclear factor kappa B subunit 1
NK	Natural killer
NLR	NOD-like receptor
NLRP6	NLR family pyrin domain containing 6
NOD	Nucleotide oligomerization domain
NS	Non-structural
ORF	Open reading frame
P2RY11	Purinergic receptor P2Y11
PAMP	Pathogen associated molecular pattern
PANX1	Pannexin 1
PBS	Phosphate buffered saline
PCR	Polymerase chain reaction
PDE4D	Phosphodiesterase 4D
PDXK	Pyridoxal kinase
PES1	Pescadillo ribosomal biogenesis factor 1
PGC1A	PPARG coactivator 1 alpha
PGKD	Protein kinase, DNA activated, catalytic subunit
PI	Persistent infection
PITPNA	Phosphatidylinositol transfer protein alpha
PKNOX2	PBX/Knotted 1 homeobox 2
PLA2G2A	Phospholipase A2 group IIA
PLD4	Phospholipase D family member 4
PLT	Platelet
PODNL1	Podocin like 1
POMC	Proopiomelanocortin
PPP3R2	Protein phosphatase 3 regulatory subunit B, Beta
PRDM	PR/SET domain
PROZ	Protein Z, vitamin K dependent plasma glycoprotein
PRR	Pattern recognition receptor
PRR18	Proline rich 18
PSMB9	Proteasome 20S subunit beta 9
PTH	Parathyroid hormone
PTPRE	Protein tyrosine phosphatase receptor Type E
RAB20	RAB20, Member RAS Oncogene family

RANBP3	RAN binding protein 3
RBC	Red blood cell
RBM20	RNA binding motif protein 20
RBM38	RNA binding motif protein 38
RDW	Red cell distribution width
RIG-I	Retinoic acid-inducible gene I
RIPOR2	Rho family interacting cell polarization regulator 2
RLR	RIG-I like receptor
RNA	Ribonucleic acid
ROS	Reactive oxygen species
ROUT	Robust outlier under testing
RRBS	Reduced representation bisulfite sequencing
RT	Reverse transcription
RUSC1	RUN and SH3 domain containing 1
RXRA	Retinoid acid receptor alpha
SAMD8	Sterile alpha motif domain containing 8
SARS-CoV	Severe acute respiratory syndrome – coronavirus
SDHB	Succinate dehydrogenase complex iron sulfur subunit B
SEM	Standard error of mean
SFMBT2	Scm like with four Mbt domains 2
SH3GL1	SH3 domain containing GRB2 like 1, endophilin A2
SMYD2	SET and MYND domain containing 2
SNTG2	Syntrophin gamma 2
SOD1	Superoxide dismutase 1
SORBS1	Sorbin andSH3 domain containing 1
SOX	SRY-Box transcription factor
SPNS2	SPNS lysolipid transporter 2, sphingosine-1-phosphate
SPP1	Secreted phosphoprotein 1
SPTBN4	Spectrin beta, non-erythrocytic 4
STAT	Signal transducer and activator of transcription
TBX21	T-box expressed in T cells
TENM4	Teneurin transmembrane protein 4
THBS2	Thrombospondin 2
TI	Transient infection
TKDP4	Trophoblast Kunitz domain protein 4
TLR	Toll like receptor
TMEM91	Transmembrane protein 91
TNF	Tumor necrosis factor
TNNC1	Troponin C1
TRMU	TRNA mitochondrial 2-thiouridylase
TRPC3	Transient receptor potential cation channel subfamily C member 3
UBAC1	Ubiquitin associated domain containing protein 1
UBE2T	Ubiquitin conjugating enzyme E2 T
UBXN11	UBX domain protein 11
UCSC	University of California, Santa Cruz

USDA	United States Department of Agriculture
VAV2	Vav guanine nucleotide exchange factor 2
VD	Viral diarrhea
VWA3B	Von Willebrand factor A domain containing 3B
WBC	White blood cell
WNT	WNT family member
ZAP70	Zeta chain associated protein kinase 70